AEOLIAN FEATURES OF SOUTHERN CALIFORNIA:

A Comparative Planetary Geology Guidebook

Arizona State University, College of the Desert,
and NASA-Ames Research Center

Sponsored by Planetary Geology Program,
National Aeronautics and Space Administration

PREFACE

Recent spacecraft results, coupled with Earth-based observations and theoretical considerations, show that the surfaces of several terrestrial planets are subjected to aeolian, or wind, processes. Active dust storms are observed on Mars, along with a host of landforms related to wind, including dune fields and yardangs. Wind measurements on the surface of Venus suggest the possibility of wind transported particles. Titan, one of the satellites of Saturn, may have sufficient atmosphere for aeolian processes.

The Planetary Geology Field Conference on Aeolian Processes was organized to bring together geologists working on aeolian problems on Earth, and planetologists concerned with the modification of planetary surfaces by wind. The setting for the conference was chosen to afford the opportunity to visit several sites where problems in aeolian geology could be discussed in a field context.

This guidebook and the conference are part of a continuing program sponsored by the Office of Planetary Geology, National Aeronautics and Space Administration, Washington, D. C., to show the differences and similarities among the terrestrial planets. The guidebook is the result of the efforts of many individuals. The editors thank the contributors who generally provided their sections on time; we also acknowledge with thanks C. Greeley (typesetting), D. Stroud (graphics), P. Fry (photography), and L. Loftus (manuscript typing).

R. Greeley
Arizona State University
Tempe, Arizona 85281

TABLE OF CONTENTS

Chapter		Page
1.	GEOLOGICAL ASPECTS OF THE EASTERN MOJAVE DESERT AND SALTON TROUGH, *Robert P. Sharp*	1
2.	AEOLIAN ACTIVITY IN WESTERNMOST COACHELLA VALLEY AND AT GARNET HILL, *Robert P. Sharp and R. Stephen Saunders*	9
3.	FIELD GUIDE TO AMBOY LAVA FLOW, SAN BERNARDINO COUNTY, CALIFORNIA, *Ronald Greeley and James D. Iversen*	23
4.	THE KELSO DUNE COMPLEX, *Robert P. Sharp*	53
5.	FIELD TRIP TO DUNES AT SUPERSTITION MOUNTAIN, *Roger S. U. Smith*	65
6.	GUIDE TO SELECTED FEATURES OF AEOLIAN GEOMORPHOLOGY IN THE ALGODONES DUNE CHAIN, IMPERIAN COUNTY, CALIFORNIA, *Roger S. U. Smith*	73
7.	GEOLOGICAL FIELD GUIDE TO THE SALTON TROUGH, *Eilene Theilig, Michael Womer, Ronald Papson*	99
8.	GEOLOGICAL FIELD GUIDE TO THE SOUTHEASTERN MOJAVE DESERT, *Eilene Theilig, Ronald Papson, Michael Womer*	161
9.	AERIAL GUIDE TO GEOLOGICAL FEATURES OF SOUTHERN CALIFORNIA, *John S. Shelton, Ronald P. Papson and Michael Womer*	215
10.	COACHELLA VALLEY AREA GENERAL GEOLOGY FIELD TRIP, *George L. Meyer*	251

1. GEOLOGICAL ASPECTS OF THE EASTERN MOJAVE DESERT AND SALTON TROUGH

Robert P. Sharp
Division of Geological and Planetary Science
California Institute of Technology
Pasadena, California 91125

1. GEOLOGICAL ASPECTS OF THE EASTERN MOJAVE DESERT AND SALTON TROUGH

Robert P. Sharp
Division of Geological and Planetary Science
California Institute of Technology
Pasadena, California 91125

Mojave Desert is divided into eastern and western parts of contrasting topographic character by the northward flowing reach of Mojave River between the San Bernardino Mountains and Barstow (Figs. 1-1 and 1-2). The western Mojave is a triangular-shaped wedge of relatively low relief and generally modest elevation (600 - 750 m) lying between the westward converging traces of San Andreas (south) and Garlock (north) faults. The eastern Mojave is much more rugged, especially in its easternmost part, featuring mountain ranges rising to 1500 m above alluvium-filled valleys and basins. Our concern will be with the eastern Mojave Desert.

FIGURE 1-1. Physiographic diagram of part of western United States showing setting of Mojave Desert (arrow) (from U.S. Geological Survey, 1968).

FIGURE 1-2. LANDSAT mosaic of Mojave Desert.

Garlock fault provides a well-defined northern border for the eastern Mojave as far as the south end of Death Valley, beyond which the region begins to assume characteristics of ranges of the Great Basin. The south border is defined by the contrast of an east-west structural grain in the Transverse Ranges and the generally northwest grain of much of the eastern Mojave. An argument could be made on geological and topographic grounds that the eastern limit should be along a line running north-northwest and south-southeast through Baker, but in practice the Mojave Desert province is generally regarded as extending approximately to the California-Nevada border. The following comments concerning the eastern Mojave pertain to this more extended area.

Crystalline rocks exposed within this region are pre-Cretaceous metamorphics, partly Paleozoic and partly Mesozoic, intruded by late Mesozoic coarse-grained plutonic rocks. These pre-Tertiary rocks are overlain by varied, extensive, and locally thick accumulations of volcanics ranging in age from Miocene to Pleistocene. Relatively thick deposits (many thousands of meters of Miocene and Pliocene land-laid sedimentary strata) have accumulated in local basins. These beds are now deformed, uplifted and dissected. Structures within the eastern Mojave are generally complex and include warps, folds, and faults, both high- and low-angle, of several different ages and trends, with tectonic activity extending up to the present time.

In times past, some of the more highly deformed and coarsely recrystallized metamorphic rocks have been regarded as Precambrian, but direct proof of such a designation within the eastern Mojave, except for the section east of Baker, has not been forthcoming. The oldest metamorphics west of Baker may be largely upper Paleozoic, and locally they include marble units containing traces of fossils supporting that conclusion. However, most of this complex west of Baker is known to consist of Triassic metavolcanics. Both the Paleozoic and Mesozoic rocks are extensively intruded by late Mesozoic (Jurassic to Cretaceous) coarse-grained plutonic igneous rocks of predominantly silicic composition.

One of the notable features of that part of the eastern Mojave west of Baker is the scarcity of Paleozoic sedimentary rock which is surprising in view of the relatively thick Paleozoic sections in the Mojave east of Baker and in the Great Basin ranges to the north. It seems likely that these Paleozoic rocks once covered the area in view of scattered Paleozoic metamorphic pendants preserved within granitic intrusive bodies. The removal of the Paleozoic strata by erosion largely during early Tertiary time was no trivial task, as a conservative estimate places the thickness of rock at 4500 - 6000 m which implies an uplift of the Mojave block west of Baker of roughly corresponding magnitude.

It is clear that erosion reigned during the early Tertiary and by Miocene time had produced a surface of gentle relief onto which great thicknesses of heterogeneous volcanics were extruded. At about the same time, and also in subsequent periods, warping or faulting created local basins in which coarse to fine fluvial and lacustrine sediments, some rich in vertebrate animal remains and fragmental volcanic debris, accumulated.

Following volcanism and the upper Tertiary sedimentation, further warping, folding, and faulting created a terrain of varied relief which has been strongly modified by erosion of uplifted blocks and deposition of the resulting detritus as alluvial fill in broad intervening basins and valleys. The surface area of alluvial valley fill exceeds the area of exposed bedrock throughout the province. Tectonic activity and volcanism have continued into recent times. Eastern Mojave is not a region of high seismicity, but historical earthquakes and related ground disruption are on record. Volcanism

at Pisgah, Amboy, and in an extensive volcanic field southeast of Baker certainly extended well into the Pleistocene, and almost certainly into the Holocene at Amboy and Pisgah. The Lenwood anticline just south of Barstow is, at oldest, a Pleistocene feature, and even more recent deformation may have played a role in the disruption of drainages within this desert region. The western part of the region was affected by the Palmdale bulge of the early 1960's.

The southwestern part of the eastern Mojave has a strong northwest structural grain reflecting the influence of a series of parallel, subequally spaced northwest trending faults, some 20 in all, that cut the country like a loaf of sliced bread. Along some of these faults fresh scarps in alluvium indicate recent activity, and evidences of right-lateral displacement are found on some. The structural grain in much of the rest of the eastern Mojave is more haphazard, except to the north approaching Garlock fault where an east-west trend is discernible. East of Baker northerly trends suggestive of a Great Basin influence are perceptible but hardly dominant.

Two large, wide topographic troughs with an anomalous southeasterly trend cross part of the eastern Mojave. The first, and larger, extends from Barstow to Bristol Playa and the second from Victorville to Dale Playa, east of Twentynine Palms. This latter trough ends in a *cul de sac* at Dale Playa. Although regarded by some workers as the product of former drainage to the Colorado River, these troughs may well be largely structural in nature.

Many playa lakes dot the alluvial surfaces of this region. Most are dry playas with hard, smooth surfaces, except when temporarily wetted by rain or flood. A few are so-called wet playas with a punky, soft, hummocky surface created by crystallization of alkali salts through evaporation from the capillary fringe of a near-surface water table.

Mojave River drains north out of the relatively well-watered San Bernardino Mountains and then flows east to Soda Playa and Cronese lakes. It is the only through-flowing stream course of any consequence. In wet years its floods can reach as far as Silver Lake Playa, north of Baker, and given enough sustenance, floods could reach Death Valley along the course of pluvial Mojave River. Lake Manix with its shoreline features, including a huge and spectacular beach ridge near Afton, was formed by ponding of Mojave River waters in a pluvial epoch. Lake Mojave occupied the now separate basins of Soda and Silver lakes, respectively south and north of Baker, in at least late pluvial times.

SOME GEOLOGICAL ASPECTS OF THE SALTON TROUGH

Salton Trough is one of the more unusual geological provinces of southern California, more because of its substructure than its surface characteristics and configuration. However, even the latter are distinctive as the trough includes the largest land area below sea level in the Western Hemisphere, covering 5200 km^2. Death Valley is a bit lower, −86.3 m compared to −83.5 m but is not comparable in area.

As viewed from the southeast by satellite, Salton Trough is clearly a landward extension of the narrow depression of the Gulf of California, and it continues as a well-defined topographic and structural feature 225 km northwest from the Gulf to San Gorgonio Pass at the west end of Coachella Valley. It is now recognized from the principles of plate tectonics, as well as from geophysical

and geological relationships, that the peninsula of Baja California has been split from the west coast of Mexico and shifted west-northwest by the processes of sea-floor spreading and transform faulting. Salton Trough presumably represents the landward effects of these same processes, and it displays characteristics compatible with that interpretation.

The continental crust is abnormally thin under the southern part of Salton Trough, and the underlying mantle displays a corresponding upward bulge. The area is riven with faults, many of which are currently active. The trough is one of the most active seismic areas in North America with several historical quakes of notable size, a high flux of current micro-seismic activity, and secular creep occurring on several faults. It is also the site of relatively recent volcanic activity, as expressed by the volcanic buttes at the southeast corner of Salton Sea, and by high temperature geothermal brines. The Salton Trough has been active in the immediate geological past, and there is every reason to believe such activity will continue into the future, perhaps ultimately resulting in the separation of coastal southern California from mainland North America.

Salton Trough is bounded on both sides by relatively high rugged mountain masses composed principally of Precambrian to Mesozoic crystalline igneous and metamorphic rocks. The trough itself is filled with over 6000 m of soft, relatively unconsolidated Cenozoic sedimentary materials, mostly non-marine, but containing interfingerings of marine beds, and impressively coarse deposits near the margins. The most notable marine unit is the late Miocene (10-12 m.y.) Imperial Formation, which contains abundant marine fossils more closely related to Gulf of California fauna than to the open Pacific coastal assemblages. These Cenozoic beds are deformed, both by faulting and folding, and locally the deformation is severe. An example can be seen in Painted Canyon in the Mecca Hills along the central eastern edge of Salton Trough, where sharp anticlines within late Cenozoic beds have cores of old metamorphic rocks squeezed up into the folds.

Three of the largest strike-slip fault zones of southern California, the San Andreas, San Jacinto, and Elsinore, extend southeast into the Salton Trough where they splay out into a sequence of parallel and *en echelon* fractures. Imperial Fault, of the San Jacinto family, has been particularly active, causing large earthquakes in 1915 and 1940 and offsetting the U. S. – Mexican border by about 15 feet in 1940. It also displays signs of current creep; geodetic measurements suggest a right lateral drift of 3 to 5 cm per year along this structure.

The floor of Salton Trough is thinly mantled by lacustrine clays deposited by predecessors of the present Salton Sea. Just as the present sea is known to be the product of diversion of the Colorado River into the Salton Trough, some of these earlier and much larger water bodies are regarded as probably of a similar origin. Marine waters from the Gulf of California are currently barred from Salton Trough by the Colorado River delta with a crest 12 to 13 m above sea level, but in earlier times, marine waters from the Gulf also invaded Salton Trough.

Shorelines of some of these older water bodies are prominent around the edges of the trough, like rings on a bath tub, particularly on the northwest side near the north end of the current Salton Sea. The most recent high water level with the strongest shoreline features, at about 12 to 13 m above sea level, is thought to have been attained within the last few hundred years.

Three areas of noteworthy aeolian-sand accumulation lie within Salton Trough. By far, the largest is Algodones Dunes along the southeast margin of Imperial Valley. This remarkably linear mass of dunes, 6 to 13 km wide, extends for more than 70 km to south of the Mexican border.

Large, subequally spaced intradune flats are a notable feature within the southern one-third of the chain. Owing to sand accumulation on a steep lee face on the northwest edge and sand removal from a gentler slope along the southeast edge, these flats show apparent motion along the axis of the dune chain at a rate of 15 to 25 cm per year. The All American Canal and Interstate 8 use one of these flats to cross the dune chain.

Farther north along the west shore of Salton Sea, some 16 km south of Salton City, is a group of about 50 active barchan (crescent-shaped) dunes moving eastward into Salton Sea at rates averaging about 20 m per year. The third area of sand accumulation is in northern Coachella Valley between Palm Springs and Indio. The dunes found here are not particularly large or unusual, as considerable vegetation and works of man obscure their pattern, but economically and socially, they are the most disruptive of all Salton Trough sand accumulations.

2. AEOLIAN ACTIVITY IN WESTERNMOST COACHELLA VALLEY AND AT GARNET HILL

Robert P. Sharp and R. Stephen Saunders

Division of Geological and Planetary Science
California Institute of Technology
Pasadena, California 91125

Jet Propulsion Laboratory
Pasadena, California 91103

2. AEOLIAN ACTIVITY IN WESTERNMOST COACHELLA VALLEY AND AT GARNET HILL

Robert P. Sharp and R. Stephen Saunders
Division of Geological and Planetary Science, California Institute of Technology, Pasadena, California 91125
Jet Propulsion Laboratory, Pasadena, California 91103

COACHELLA VALLEY

The westernmost end of Coachella Valley (Fig. 2-1), north and west of Palm Springs, provides a splendid natural laboratory for observations of and experiments with the behavior of sand moving by traction and saltation under a powerful unidirectional wind regime of high frequency. Ancient ventifacts (sand blasted rocks) on Garnet Hill (Fig. 2-2), just east of Indian Avenue and south of Interstate Highway I-10, indicate that similar activity has characterized this area in past millennia. Current conditions will be treated before the spectacular sand blasting of stones of Garnet Hill is described.

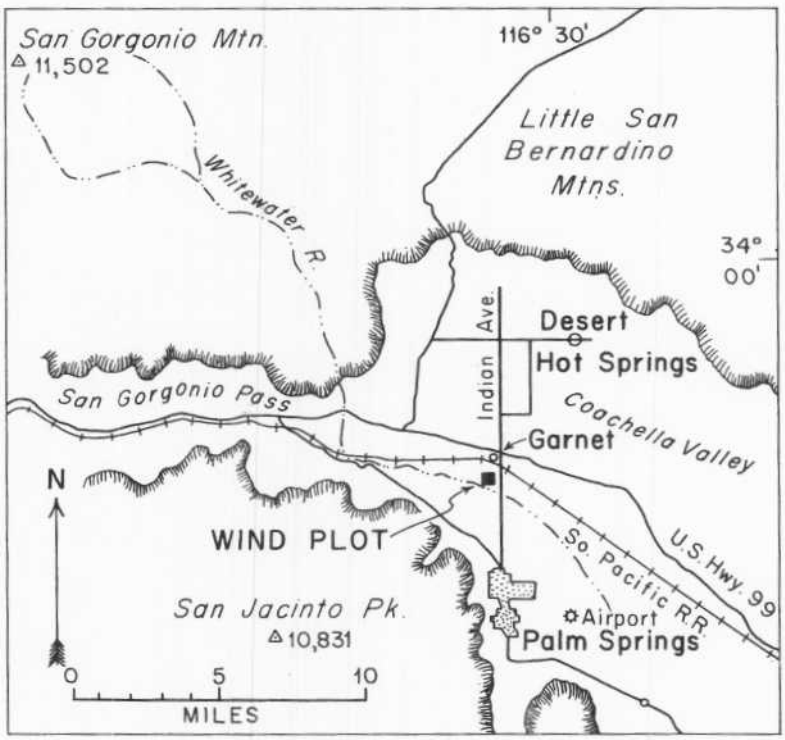

FIGURE 2-1. Location map of Garnet and aeolian erosion study area (from Sharp, 1964).

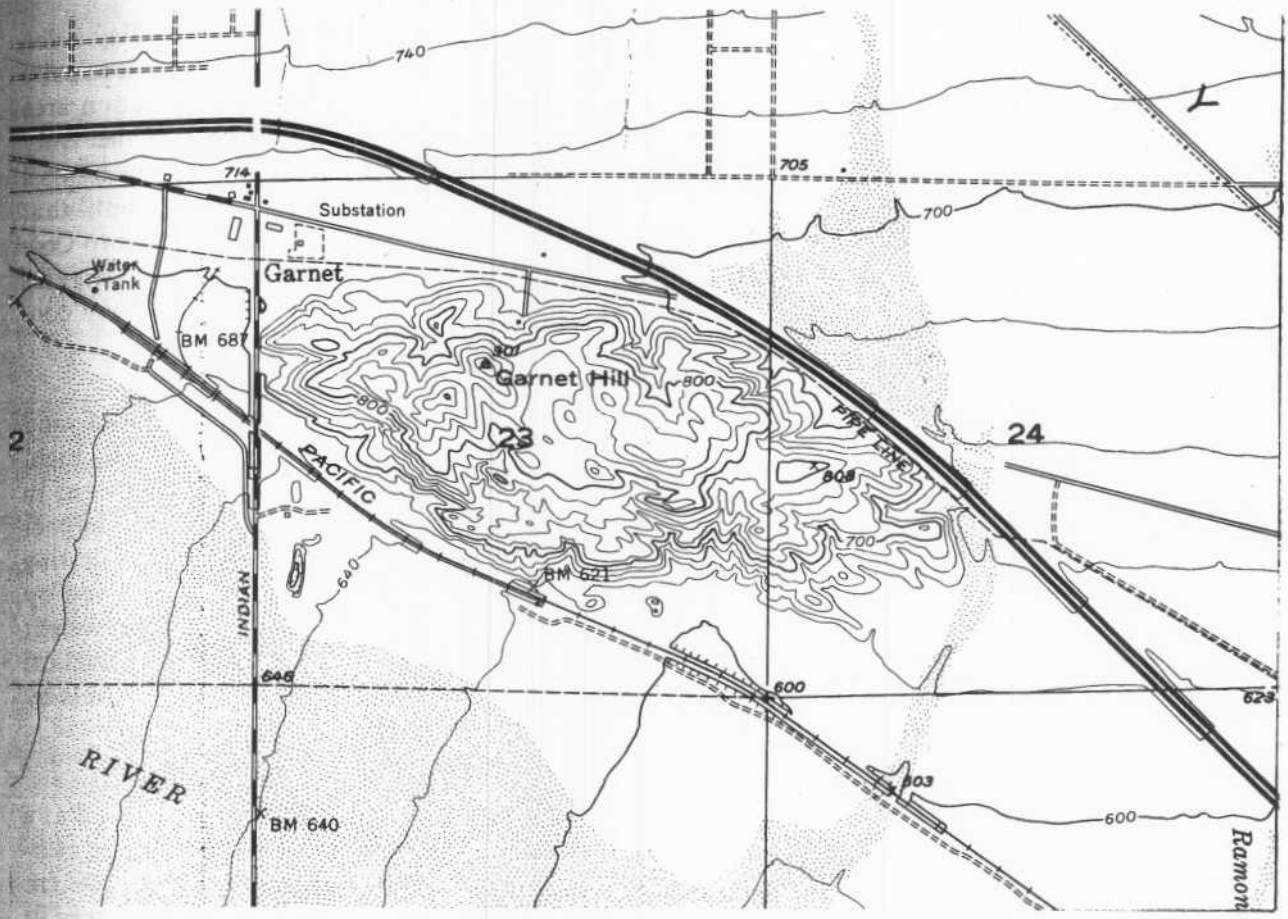

FIGURE 2-2. Enlargement of U. S. Geological Survey topographic map showing location of Garnet Hill.

The area currently has a high flux of aeolian sand transport derived from the barren active alluvial plain of Whitewater River. This stream, and its principal tributary, San Gorgonio wash, are ephemeral and only occasionally inundate the alluvial plain during wet winters. The plain slopes less than 1° eastward, is scarred by braided channels mostly 0.3 to 0.6 m deep, consists largely of coarse sand and gravel with largest boulders at 0.5 to 1 m, and in its active parts, is only sparsely dotted with low perennial bushes. Most stones on the surface of this plain, except those in recently active channels, show evidence of sand blasting as do other materials such as beer cans and chunks of wood.

The orographic setting is unusual in being at the east end of narrow San Gorgonio Pass between the two highest peaks in southern California, San Gorgonio (3508 m) to the north and San Jacinto (3303 m) to the south (Fig. 2-1). The pass serves as a funnel through which winds of high velocity blow from the coastal region to the Colorado Desert. Wind frequency is high in all seasons, becoming almost daily from May through July. These winds are almost entirely from N 75° W; only occasionally does air move from other directions and then only as gentle breezes with the exception of very rare strong storm winds from the north.

The alluvial plain created by the Whitewater River at the west end of Coachella Valley is the source for the windblown sand that inundates parts of the valley floor farther east, principally between Palm Springs and Indio. The flux of windborne sand carried into this accumulation area varies in direct relation to the amount of flooding of the alluvial plain west of Indian Avenue. Only a year or two is required for the wind to remove most of the transportable grains from the alluvial plain, leaving a residual armor of coarse material that prevents further significant removal until that armor is disturbed, or a new supply of debris is brought by flood waters. The flux of sand into Coachella Valley thus varies with fluctuations in climatic conditions, being greater following wet years than in time of drought. The solution to control of windblown sand here lies more with flood control than with wind control, as now attempted by means of hedges and other barriers.

When sand has been made available by floods, and wind action is strong, the flux of sand moving across the barren westernmost part of the Coachella Valley alluvial plain is extremely high. Sand movement occurs by traction, saltation, and impact creep. Traction refers to movement in which the particle is continuously on the ground surface, saltation is a hopping process, and impact creep is a form of traction in which material is moved by the impact of fast traveling saltating grains. Impact creep results in transport of grains many diameters larger than could be moved by wind drag alone, and its effects are probably underrated. However, the greatest volume and weight of sand moves by saltation, and it is the saltating grains which produce much of the mechanical wear on fixed objects and also launch into the air much of the material that ultimately travels by suspension.

Collection and mechanical analysis of the saltating sand curtain over an eleven year period at a station 1070 m west of Indian Avenue not far from Garnet Hill (Fig. 2-1) shows that, on the average, 50 percent by weight of the saltating grains travel within 13 cm and 90 percent within 64 cm of the ground surface. Saltating grains up to 2 mm diameter occasionally rebound to heights of at least 6 m in this environment. Both the amount of saltating material and mean grain size decrease with height, as would be expected, but many departures from this generalization occur within the saltation curtain with respect to materials of specific grain diameter, as expressed in terms of weight percentages. Particles smaller than 0.062 mm are essentially universally distributed, indicating they probably move in suspension, and particles up to 0.125 mm behave in a manner suggesting that they are strongly influenced by wind turbulence. The amount of larger grains, expressed in weight percentage relative to other grain sizes, peak at heights increasing with grain size under some wind regimes (Fig. 2-3).

Erosion of objects by windblown particles was also studied in the field (Sharp, 1964). Wear was measured largely on objects artifically placed in the wind plot, but a recording of cutting on natural rocks was also attempted. Maximum wear on a vertical lucite rod anchored in the experimental plot occurred at a level 23 cm above the ground (Fig. 2-4). This is thought to represent the level at which grain size, grain number, and grain velocity combine to give the greatest impact energy, and hence erosion, upon the rod. The amount of wear was essentially 1 mm in ten years. Cutting on common red bricks and cubes of hydrocal (a gypsum compound) of various dimensions and orientations was impressive (Figs. 2-5 and 2-6). Nearly 1 mm of cutting occurred in fifteen years on the face of a gneissic granitic boulder in the plot, most of it within the last two or three years of the experiment, when sand flux was abnormally heavy, owing to extensive and repeated floodings of the alluvial plain farther west. The station was destroyed in its fifteenth year by a flood of unusual magnitude.

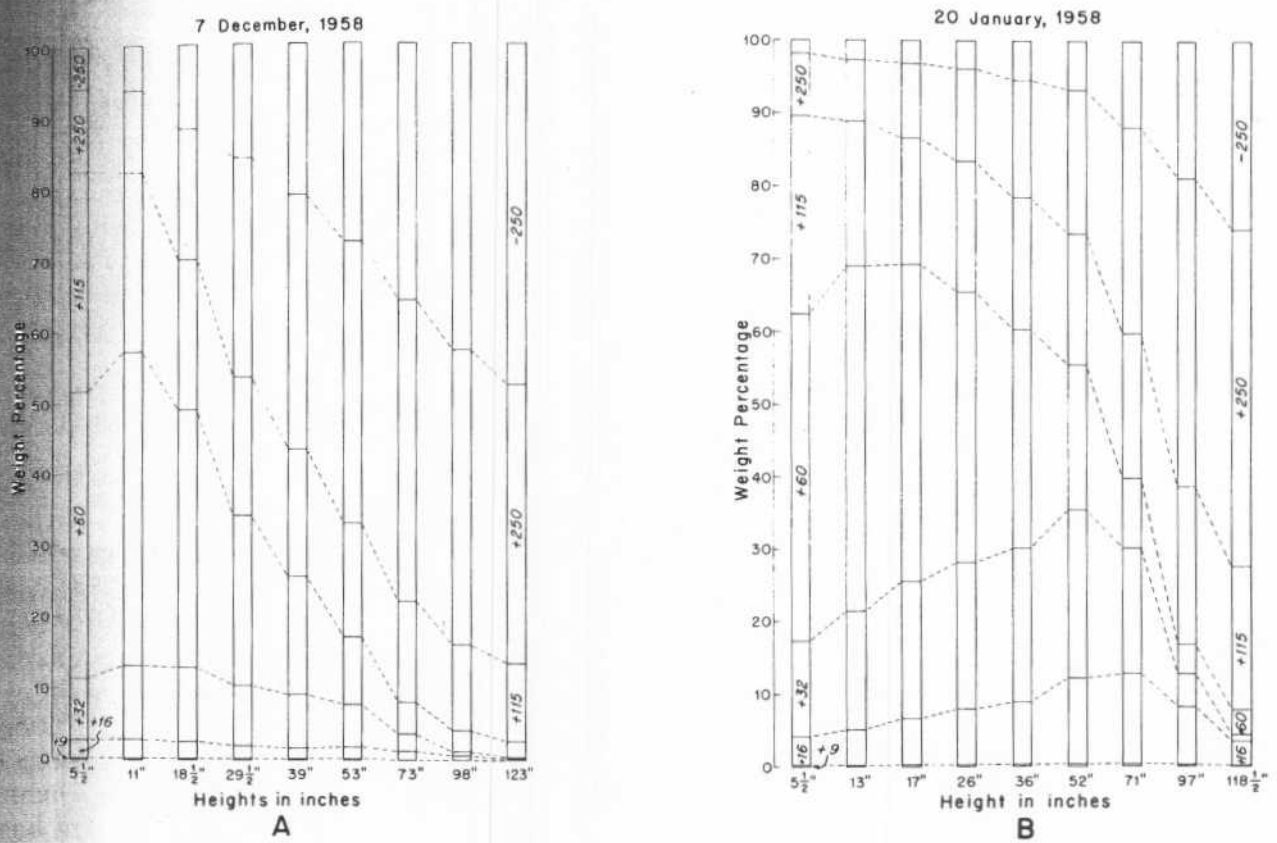

FIGURE 2-3. Histograms showing relative weight percentages of different grain-size fractions collected at various heights. A–collection of 7 December 1958; B–collection of 20 January 1958 (from Sharp, 1964).

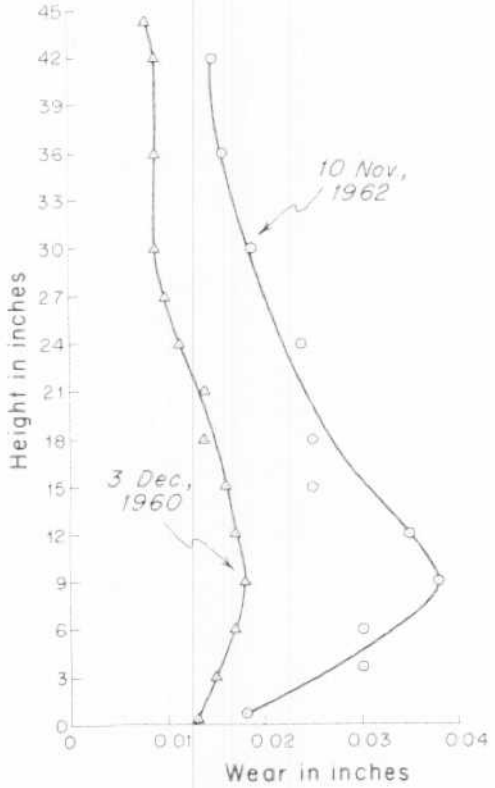

FIGURE 2-4. Wear by sand blast on a lucite rod anchored in the experimental plot (from Sharp, 1964).

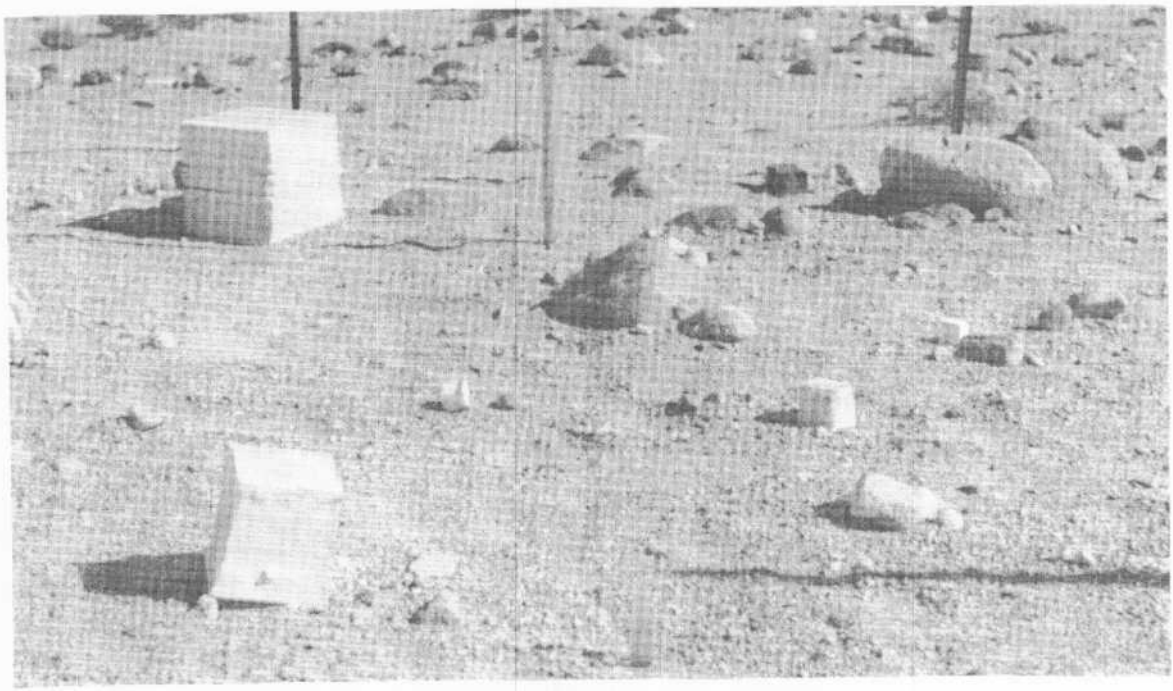

FIGURE 2-5. Stub of broken lucite rod center foreground. Overturned 6-inch cube to left and overturned 2-inch cubes right and left center. Three-inch cube (right) and 12-inch cube (left rear) undisturbed but worn. View northeasterly, 25 January 1964 (from Sharp, 1964).

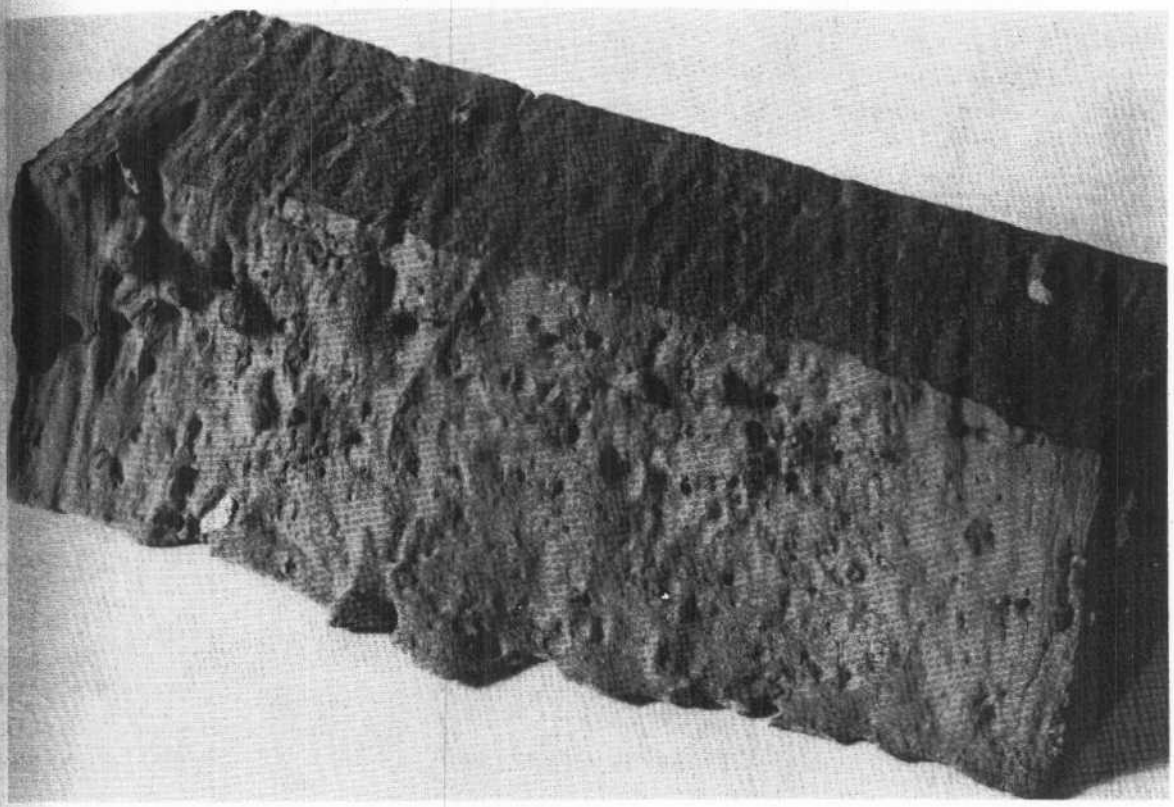

FIGURE 2-6. Common brick after six years of sand blasting (from Sharpe, 1964).

AEOLIAN PROCESSES AT GARNET HILL

Garnet Hill (Figs. 2-2 and 2-7) is about 2.5 km long, parallel to Interstate Highway I-10 on the north and Southern Pacific Railroad on the south. The hill is formed from an eroded anticline in Cenozoic sedimentary rocks and is bounded on the south by Garnet Hill fault. The uppermost stratigraphic unit, the Cabezon Fanglomerate, is of late Pleistocene age, deposited between 100,000 and 1 million years ago. This unit consists of poorly sorted pebbly and bouldery arkosic sandstone with about fifty percent gneiss clasts, forty-five percent granitic and pegmatitic rocks, and a minor amount of basalt. The lithologic character of the clasts indicates the sediment source was the San Bernardino Mountains, drained by the ancestral Whitewater River. On Garnet Hill, however, there are boulders of siliceous limestone and a predominance of diorite and granodiorite. These are rock types found in the San Jacinto Mountains and suggest this area as a contributing sediment source. The Cabezon Fanglomerate has been exposed at Garnet Hill by upwarping and subsequent erosion of overlying alluvium. The fanglomerate is the source of the abundant cobbles and boulders, some up to 3 m across, that dot the hillslopes.

Underlying the Cabezon Fanglomerate, and revealed primarily in scattered exposures on the south margin of Garnet Hill, is the marine Imperial Formation of late Pliocene age (more than two million years old). The Cabezon Fanglomerate rests unconformably on the Imperial Formation at Garnet Hill; elsewhere this gap is occupied by terrestrial conglomerates in which early horse and

FIGURE 2-7. Oblique aerial view of Garnet Hill (left side) looking west. Trace of San Andreas fault is visible in middle foreground. (Photograph by J.S. Shelton).

camel teeth have been found. The Imperial Formation records an early invasion of the Salton Trough by the Gulf of California. This marine transgression filled the area with warm shallow water in which oysters and scallops thrived, evidenced by fossils that are common in the sandy facies. Garnet Hill has been discussed briefly by several authors that are referred to in Sharp (1964, 1972) and additional details of the local stratigraphy and structure may be found in Proctor (1968).

There are few places in the United States where large ventifacts deeply scoured, polished, faceted, and engraved by wind blasting are better displayed than on the slopes of Garnet Hill. These are fossil ventifacts in the sense that active blasting no longer occurs on most of them. Their antiquity is demonstrated by fractured and displaced wind-cut facets on individual stones, by shifting of wind-cut features on large, usually immobile stones, to an orientation incompatible with the local unidirectional wind regime, and by extensive solution of wind-cut facets on carbonate stones as well as oxidation and staining of wind-cut surfaces on stones of other compositions.

Why the slopes of Garnet Hill should have at one time, presumably centuries to millennia ago, have been subject to such intensive wind blasting, but now are almost totally spared such activity, is a matter of inference and interpretation. The area currently upwind from Garnet Hill is largely stabilized by armoring and a cover of creosote bushes. At earlier times and under possibly different climatic conditions, the area may have been barren alluvium and hence a rich source of windblown sand for Garnet Hill. This seems the most likely explanation, but the lithology of the fanglomerates composing Garnet Hill indicates that they have been derived from the north face of San Jacinto Mountain 6 to 8 km to the west. From this relationship, an argument could be made for several km of right-lateral displacement along Garnet Hill fault. The ventifacts are clearly fossil with respect to the present relationships controlling sandblasting. Active cutting is currently limited to the west end and to the lowermost flanks of Garnet Hill. Although the rocks of Garnet Hill may have been laterally displaced by strike-slip faulting, fault movement has probably not played a role in determining the effectiveness of sand blasting on Garnet Hill ventifacts. It may be that the Whitewater River was dumping alluvial material more directly upwind from Garnet Hill at some time than at present. At such a time, the hill may have lain directly in the path of maximum sand flux and climatic conditions may have created both a greater flux and stronger winds.

The ventifacts merit brief description. Stones of all sizes from pebbles only a few centimeters in diameter to huge boulders several meters across bear evidence of severe wind blasting (Figs. 2-8 and 2-9). Those of fine grain and relatively high silica content show a considerable degree of polish. Nearly all display pitting, fluting, and grooving on wind-cut faces and facets. Small stones susceptible to shifting may be cut on several sides (Fig. 2-10), but larger, stable stones show only the effects of wind blasting from the N 75°W direction. Some large boulders with a semi-radial arrangement of deep grooves look like they have been blasted by a permanently set fire hose (Fig. 2-11). Grooving often transects structure (foliation or lamination) in a stone (Figs. 2-12, 2-13, and 2-14)

FIGURE 2-8. Large ventifact on Garnet Hill. Note smaller ventifact in foreground. (Photograph by W. A. Hunter, 1977.)

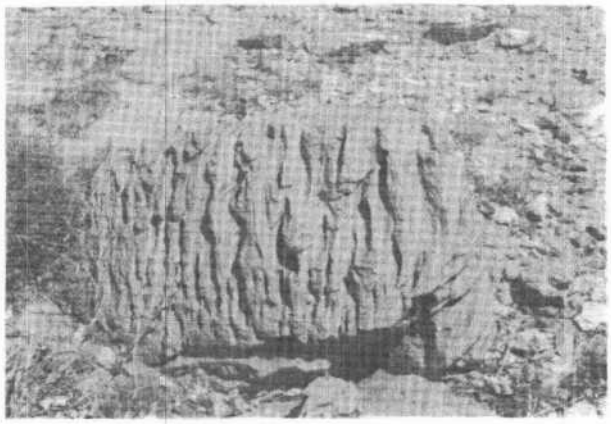

FIGURE 2-9. Multiple fluted ventifact on Garnet Hill. (Photograph by W. A. Hunter, 1977.)

FIGURE 2-10. Ventifact on Garnet Hill. (Photograph by R. Greeley.)

FIGURE 2-11. Large grooved ventifact on Garnet Hill displaying radial arrangement of pits, grooves, and flutes. Rock is a coarse, crystalline igneous variety, and cutting is old. (Photograph by R. P. Sharp.)

FIGURE 2-12. Grooved ventifact with foliation perpendicular to grooving. (Photograph by R. Greeley.)

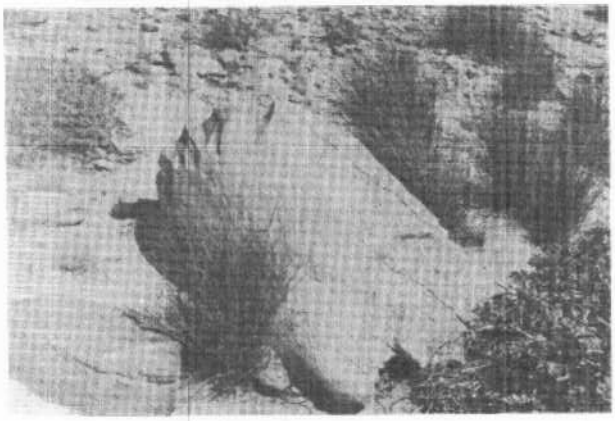

FIGURE 2-13. Fluted ventifact boulder on Garnet Hill. (Photograph by W. A. Hunter, 1977.)

FIGURE 2-14. Close-up view of grooves cutting rock structure on Garnet Hill ventifact.

unless the structure happens to be parallel to wind direction (Fig. 2-15). Hard parts or resistant mineral grains stand in positive relief (Fig. 2-16), spectacularly so in the instance of carbonate stones. In some instances, the shape and, roughly, the size of the original unmodified stone can be inferred from the wind blasted remnant, and it is apparent that up to 70 to 80 percent of some rocks have been worn away. One can easily spend many hours wandering over the slopes of Garnet Hill admiring the surprising variety and character of wind blasted rocks.

FIGURE 2-15. Ventifact grooving parallel to rock foliation. (Photograph by R. Greeley.)

FIGURE 2-16. Differential aeolian erosion in Garnet Hill ventifact. (Photograph by R. Greeley.)

REFERENCES

Proctor, R. J., 1968. Geology of the Desert Hot Springs–Upper Coachella Valley Area, California: Special Report 94, Calif. Div. Mines and Geology.

Sharp, R. P., 1964. Wind-driven sand in Coachella Valley, California: Bull. Geol. Soc. Am., vol. 75, pp. 785-804.

Sharp, R. P., 1972. Geology Field Guide to Southern California: Wm. C. Brown Co., Publishers, Dubuque, Iowa, 181 p.

3. FIELD GUIDE TO AMBOY LAVA FLOW, SAN BERNARDINO COUNTY, CALIFORNIA

Ronald Greeley and James D. Iversen
Department of Geology and Center for Meteorite Studies
Arizona State University
Tempe, Arizona 85281

Department of Aerospace Engineering
Iowa State University
Ames, Iowa 50010

3. FIELD GUIDE TO AMBOY LAVA FLOW, SAN BERNARDINO COUNTY, CALIFORNIA

Ronald Greeley and James D. Iversen
Department of Geology and Department of Aerospace Engineering
Center for Meteorite Studies Iowa State University
Arizona State University Ames, Iowa 50010
Tempe, Arizona 85281

The Amboy lava field (Figs. 3-1 and 3-2) is of interest to planetologists for several reasons. First, it is a young basaltic area that may be analogous to some of the small volcanic surface features observed on the Moon and Mars. In addition, it has an overprint of aeolian features, including large scale "streaks" (Fig. 3-3), sand drifts, and ventifacts. The wind-eroded vesicular basalt and general surface bear a striking resemblance to the views of the martian plains obtained by the Viking landers (Fig. 3-4). The Amboy lava field has been the site for two planetary geology field programs: the first was a study of the micrometeorology and related aeolian geology for a wind-swept basaltic lava field (Greeley and Iversen, 1977); the second study involved "drop" tests for penetrators, devices that are being considered as a potential mission option for post-Viking Mars exploration. The objective of this study (Blanchard and others, 1977) was to determine if penetrators and instruments could survive impact in vesicular basalts.

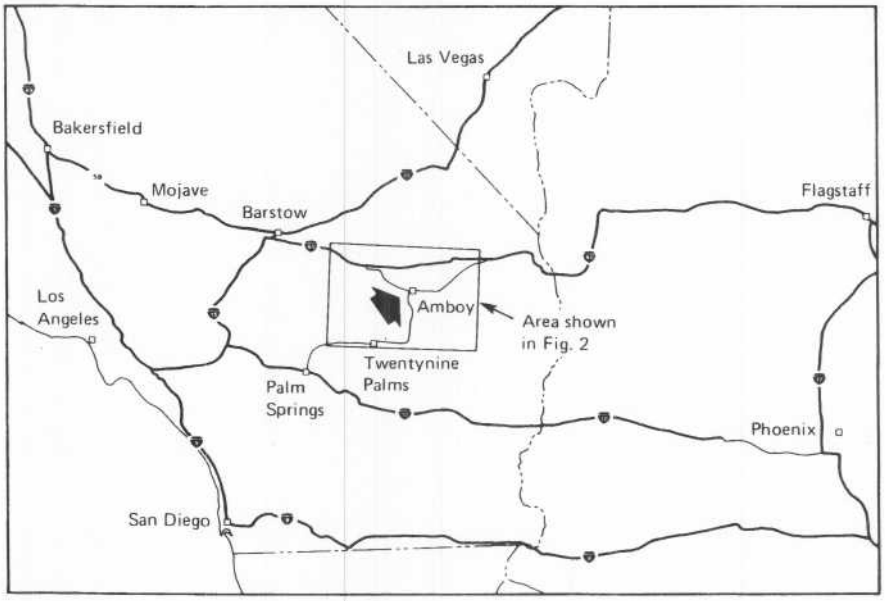

FIGURE 3-1. Location of Amboy, San Bernardino County, California.

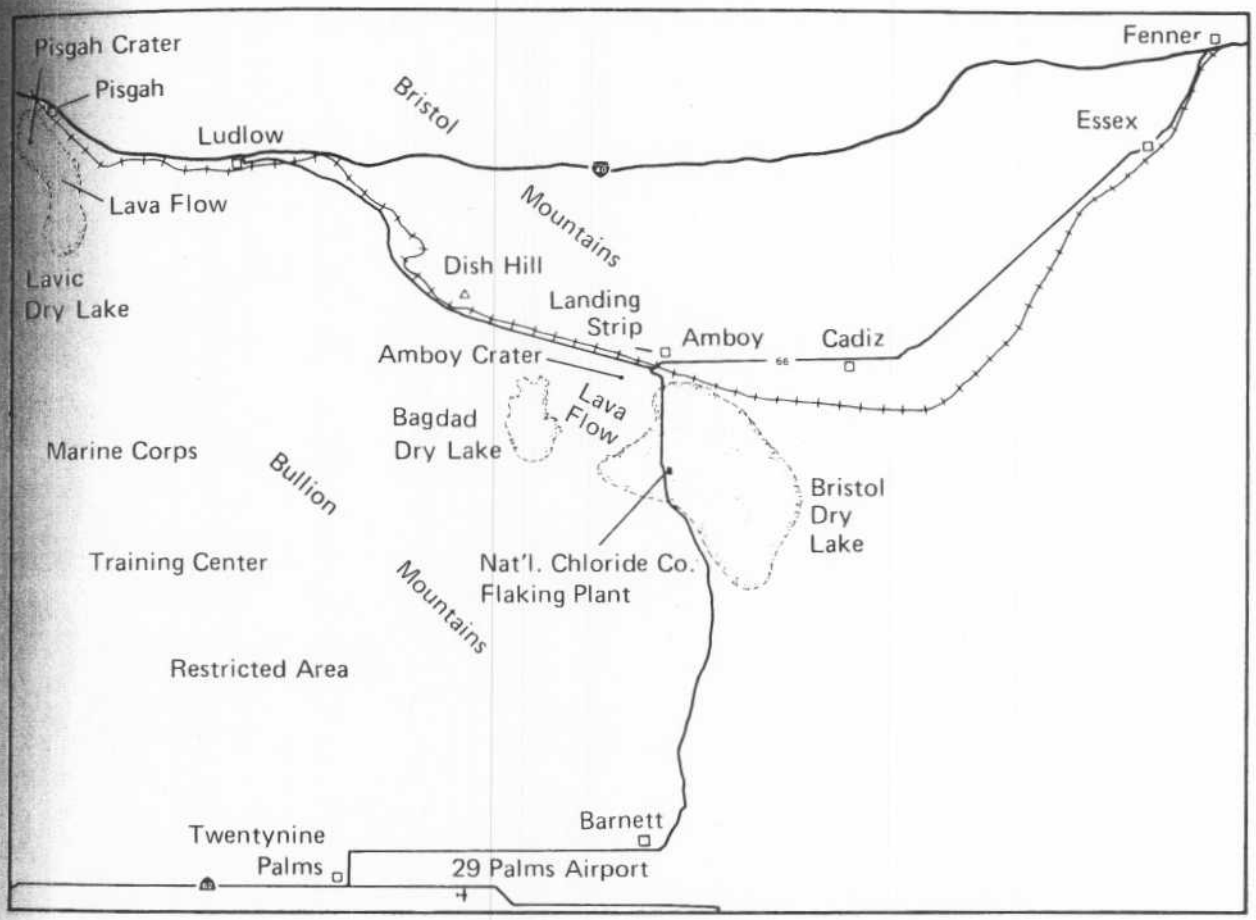

FIGURE 3-2. Detail of the Amboy area.

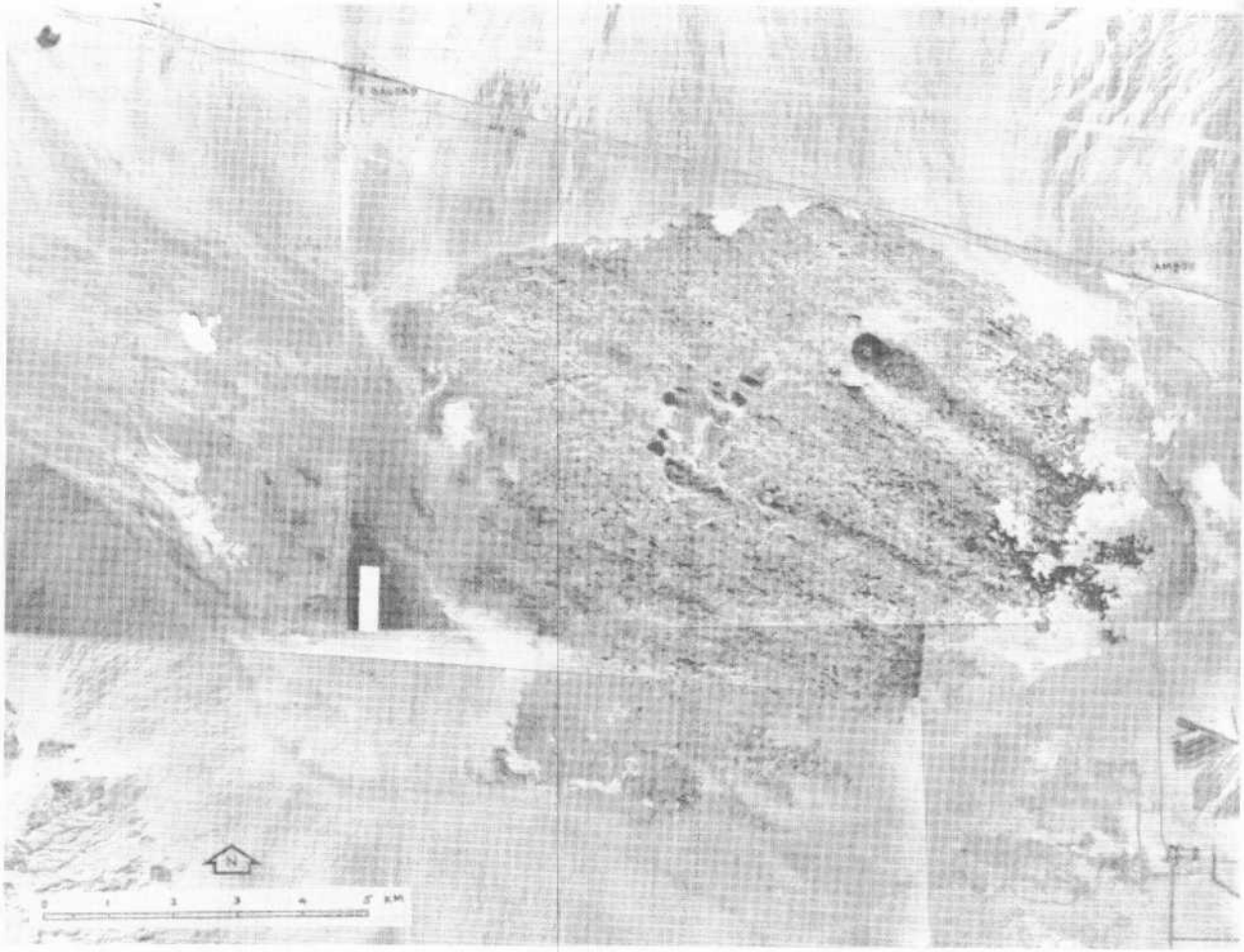

FIGURE 3-3. Mosaic of vertical aerial photographs showing the Amboy lava field. Dark streaks are parts of the lava flows that have not been covered by windblown sediments. (U.S. Geological Survey photographs VV FS 5737, 5738, 6524, 6525, 1954-1955.)

FIGURE 3-4. View of the martian surface obtained by the Viking 2 lander in the Utopia Planitia region showing rocks that may be vesicular basalt and drifts of windblown particles; the surface on Amboy lava field may be analogous. (NASA photograph P-17689; Viking 2-14.)

GENERAL GEOLOGY

The Amboy lava field covers about 70 km^2 and consists primarily of vesicular pahoehoe lava (Greeley and Bunch, 1976). The field (Figs. 3-2 and 3-5) is situated in an alluvial-fill valley between the Bullion Mountains to the southwest and the Bristol Mountains to the northeast; within the valley, it lies between Bagdad Dry Lake to the west and Bristol Dry Lake to the east – both are playa lakes typical of the Mojave Desert.

Previous geological studies include those of Bassett and Kupfer (1964) who provide a geological reconnaissance of the southeastern Mojave desert and the playas, Parker (1963) who studies volcanism at Amboy Crater, and Hatheway (1971) who included the Amboy lava field in part of an extensive study of basalt "collapse" depressions. A series of open file reports (Watkins, 1965, 1966a,b) of the U. S. Geological Survey include data on Amboy Crater. Studies of aeolian processes in the general area are summarized by Smith (1967).

Amboy Crater and Cone

Amboy Crater (Parker, 1963) is a prominent undissected cinder cone (Fig. 3-6) in the northeastern quadrant of the lava field. The volcano erupted along the northern border of Bristol Dry Lake and poured lava out onto its surface, dividing it into the two present playas. The cone rises 75 m above the surrounding lava flows and is about 460 m in basal diameter. It is composed of a loose accumulation of volcanic ejecta with secondary amounts of agglutinated ejecta and flows. The ejecta include angular scoriaceous tephra plus ropy, ribbon- and almond-shaped bombs. Some lithic nonvesicular accessory basaltic ejecta are present, but included xenolithic fragments are absent.

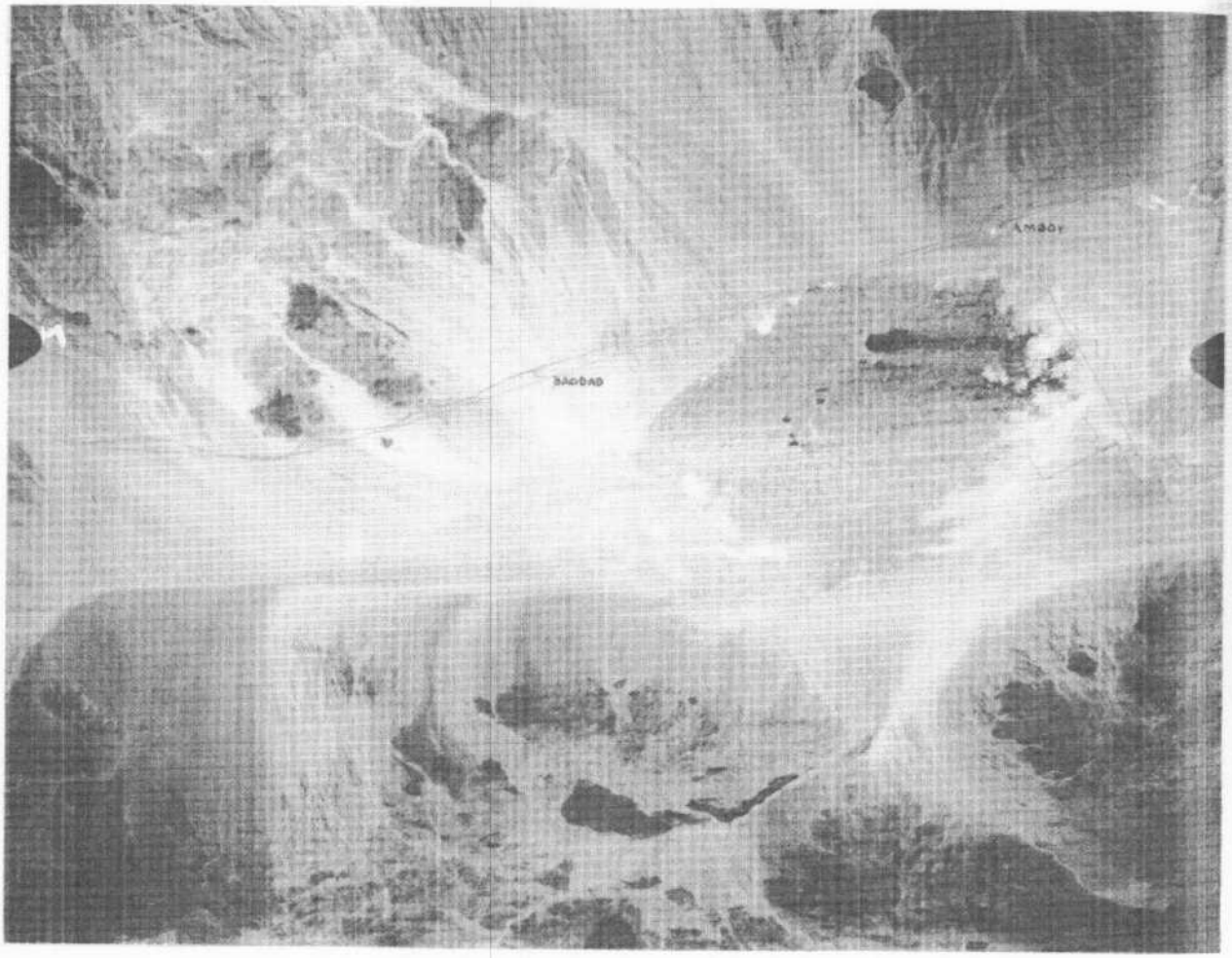

FIGURE 3-5. High altitude vertical photograph of the Amboy lava field (north is to the top). (NASA-Ames photograph.)

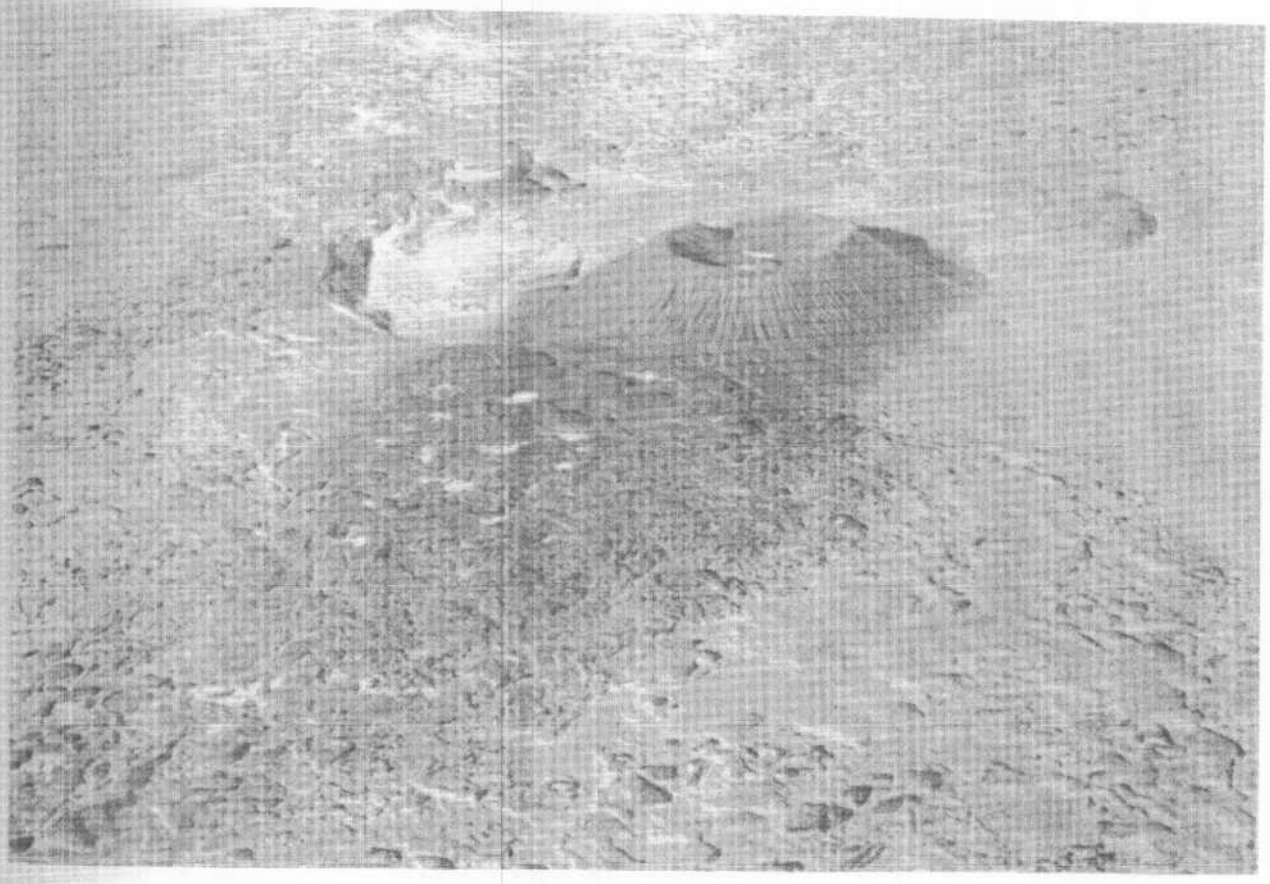

FIGURE 3-6. Low oblique aerial photograph westward of Amboy crater showing the dark "streak." (Photograph by James Iversen, 1976.)

Amboy Crater is not a single cone but is composed of at least four nearly coaxial nested cones (Parker, 1963). The outer slopes of the main cone are gullied by erosion. Within the main outer cone, there is a remnant of a second cone on the west side; both cones are breached on the west side. In addition to the two main cones, there are two relatively undisturbed cone walls within the main crater. These innermost conelets are composed almost entirely of angular scoriaceous cinders.

The sequence of events at the main vent of Amboy Crater has been synthesized by Parker (1963) as follows:

1. Early eruptions were explosive, and many fluid bombs were ejected. The main cone was formed at this time. A period of inactivity followed, during which the outer slopes of the cone were gullied by erosion or by avalanching volcanic material.

2. A second phase of eruptive activity resulted in the deposition of an agglutinated aggregate of basaltic blocks on the rim and western flank of the cone. This was probably accompanied by the eruption of pasty bombs.

3. Formation of an inner conelet by a mild explosive phase.

4. The two cone walls were then breached on the western side by a sideways-directed explosion or by the flow which now occupies this breach.

5. Activity was renewed with the formation of another inner conelet.

6. Formation of the innermost conelet terminated the explosive eruptions at the volcanic center now occupied by Amboy Crater.

7. Subsequent eruptions, if any, from this central vent took the form of quiet outpourings of fluid lava from the base of the main outer cone.

Thus, a minimum of six distinct periods of eruption at Amboy cone can be derived from field evidence at Amboy Crater. Petrographic evidence which supports this sequence of events is discussed by Parker (1959).

Flow Descriptions

Figure 3-7 is a geological map after Hatheway (1971), showing the main flow units of the Amboy lava field. Most of the field is composed of undifferentiated flow units of relatively dense, "degassed" pahoehoe lavas that form a hummocky terrain (see Swanson, 1973, for discussion of types of pahoehoe). The surface relief on this unit ranges from 2 to 5 m. The flow is characterized by abundant tumuli (small mounds) and pressure ridges and, as typical for this type of flow, a fractured surface. Lava tubes are not present in any of the flows, nor are blisters or shelly-type pahoehoe; only a few lava channels are present. Low-lying areas on the flow are filled with aeolian (windblown) sediments which range from a few centimeters to more than 1 m thick. Thickness of aeolian deposits increase toward the southwest part of the field. Sand-blasting is prevalent over the entire flow and wind-faceted pebbles of basalt are common.

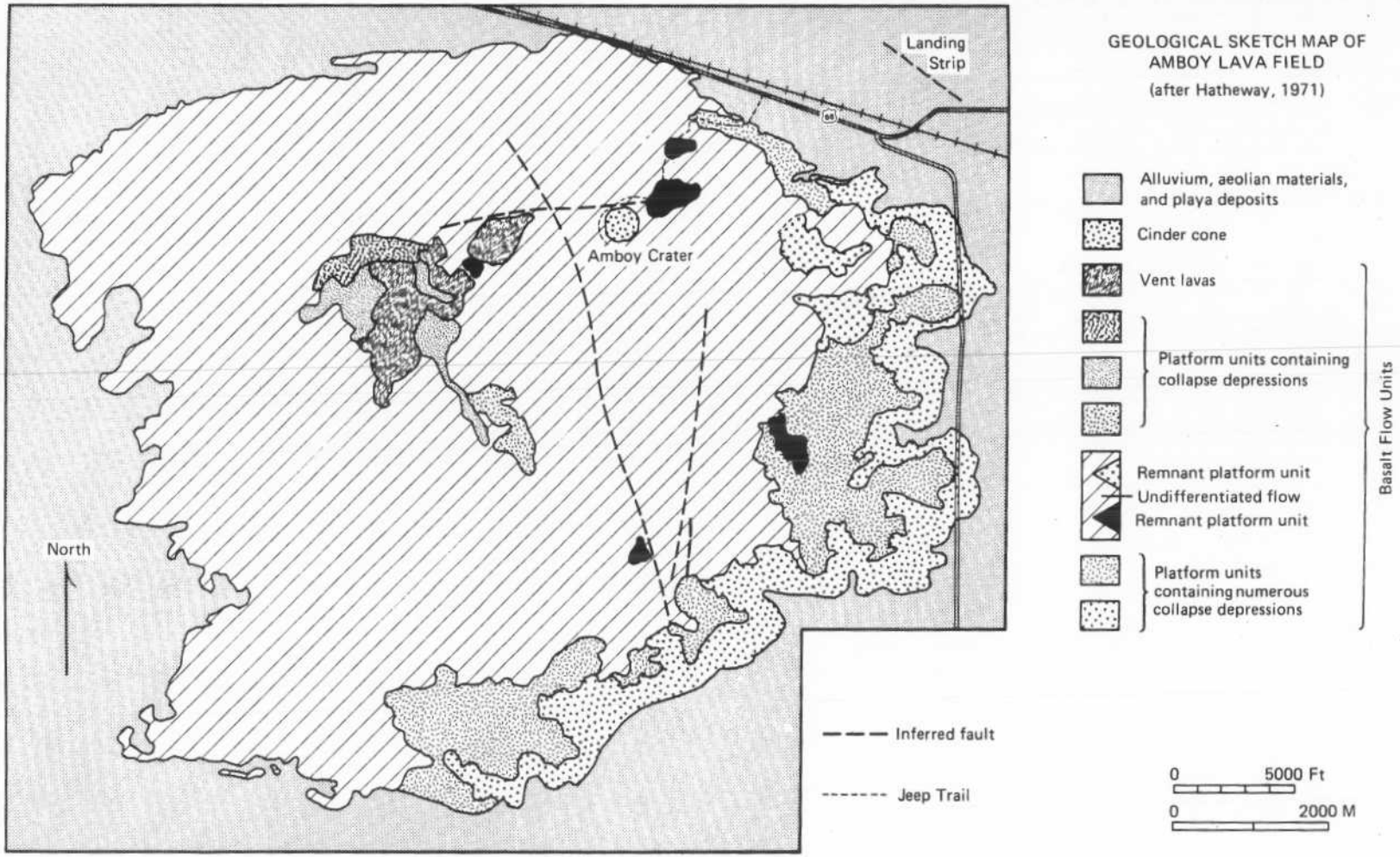

FIGURE 3-7. Geological sketch map of the Amboy lava field showing main lava flows by geomorphic type and their apparent relative age (after Hatheway, 1971).

The oldest flows occur in the eastern and southeastern part of the field. They are characterized by numerous "collapse" depressions (circular pits) up to about 10 m in diameter and several meters deep (Fig. 3-8). Although the name would imply that "collapse" depressions formed by the collapse of a crust over fluid lava, recent observations by Holcomb (personal communication) of active lava flows in Hawaii suggest that at least some depressions may form as a result of *inflation* of an emplaced, but still plastic, crust by molten lava around a general void in the flow. This mechanism would be more in concert with the general degassed nature of the hummocky pahoehoe.

Two other types of flows occur in the field: platform units and vent lavas (Fig. 3-9). Platform units are isolated zones of uniform basalt that have relatively flat surfaces. These areas appear to represent stagnant parts of basalt flows that solidified in place with relatively little lateral movement after emplacement. The surfaces of the platform units consist of a layer of fist-sized cobbles and smaller fragments of basalt weathered *in situ* and windblown sediments. Vent lavas (Fig. 3-10) are so named because they appear to be situated over some of the vents for the Amboy lava field. Vent lavas are topographically raised areas about 10 m high that consist of relatively dense pahoehoe. The flows appear to have cooled in relatively stagnant ponds which either drained back down the vent, causing slight crustal collapse on the surface, or broke out through subsequent flows around the edges of the pond. The surfaces are relatively flat and unfractured except around the edges of the pond. Individual collapse craters (Figs. 3-11 and 3-12) which could represent drain-back in the vents occur in the middle of the ponds. Like the platform areas, the surfaces of the vent lavas have weathered basalt fragments and aeolian particles to a depth of several centimeters.

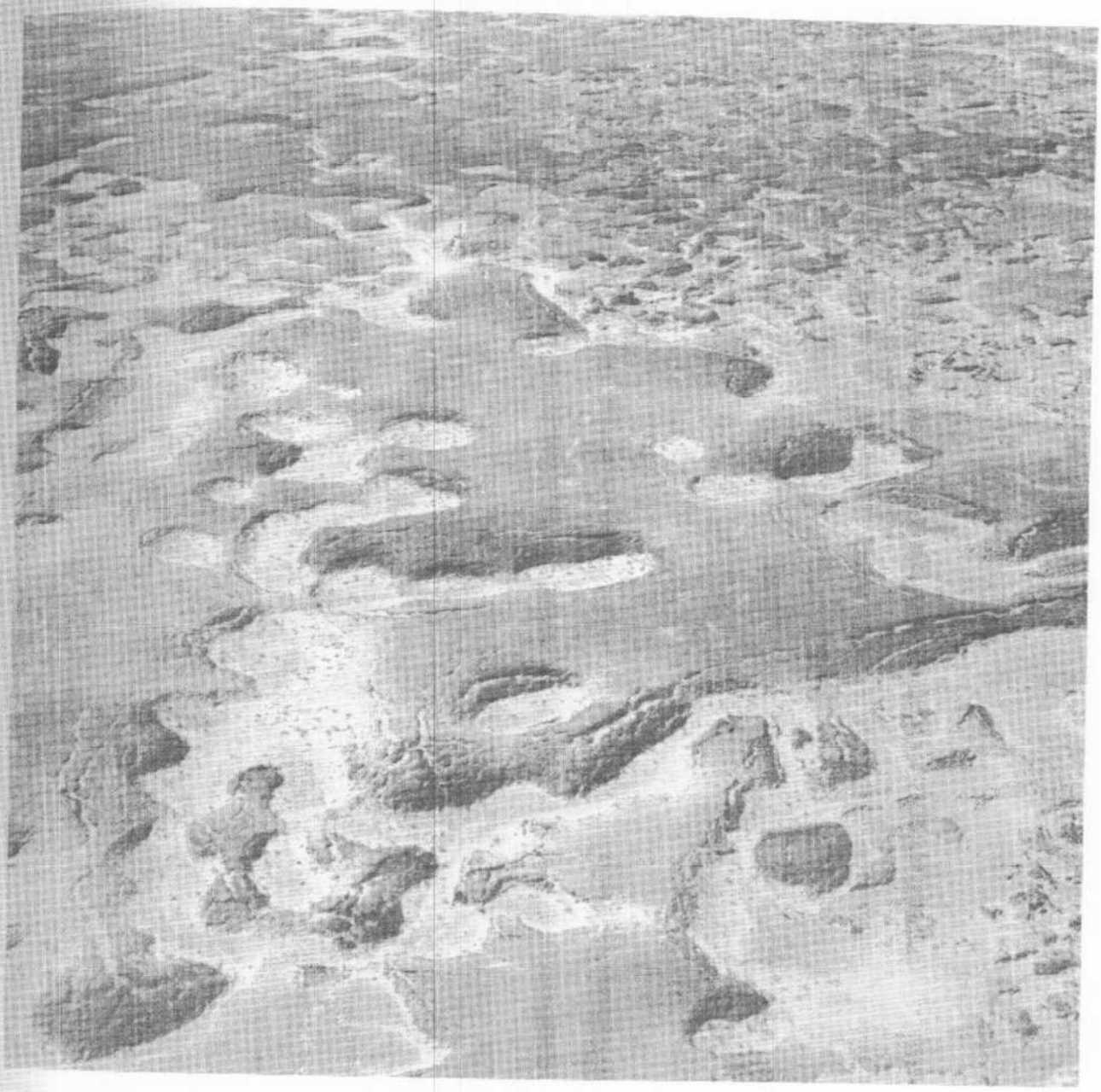

FIGURE 3-8. Oblique aerial view of the east end of the Amboy lava field showing the typical "platform" units with collapse depressions. (Photograph by Ronald Greeley, 1976.)

FIGURE 3-9. Oblique aerial view showing "platform" units (smooth areas) and rough, hummocky surface of the undifferentiated flows that make up most of the field. White line is the jeep trail from the highway (lower right) to the base of Amboy cone (upper left). Numbers correspond to stations in the field guide. (Photograph by Ronald Greeley, 1976.)

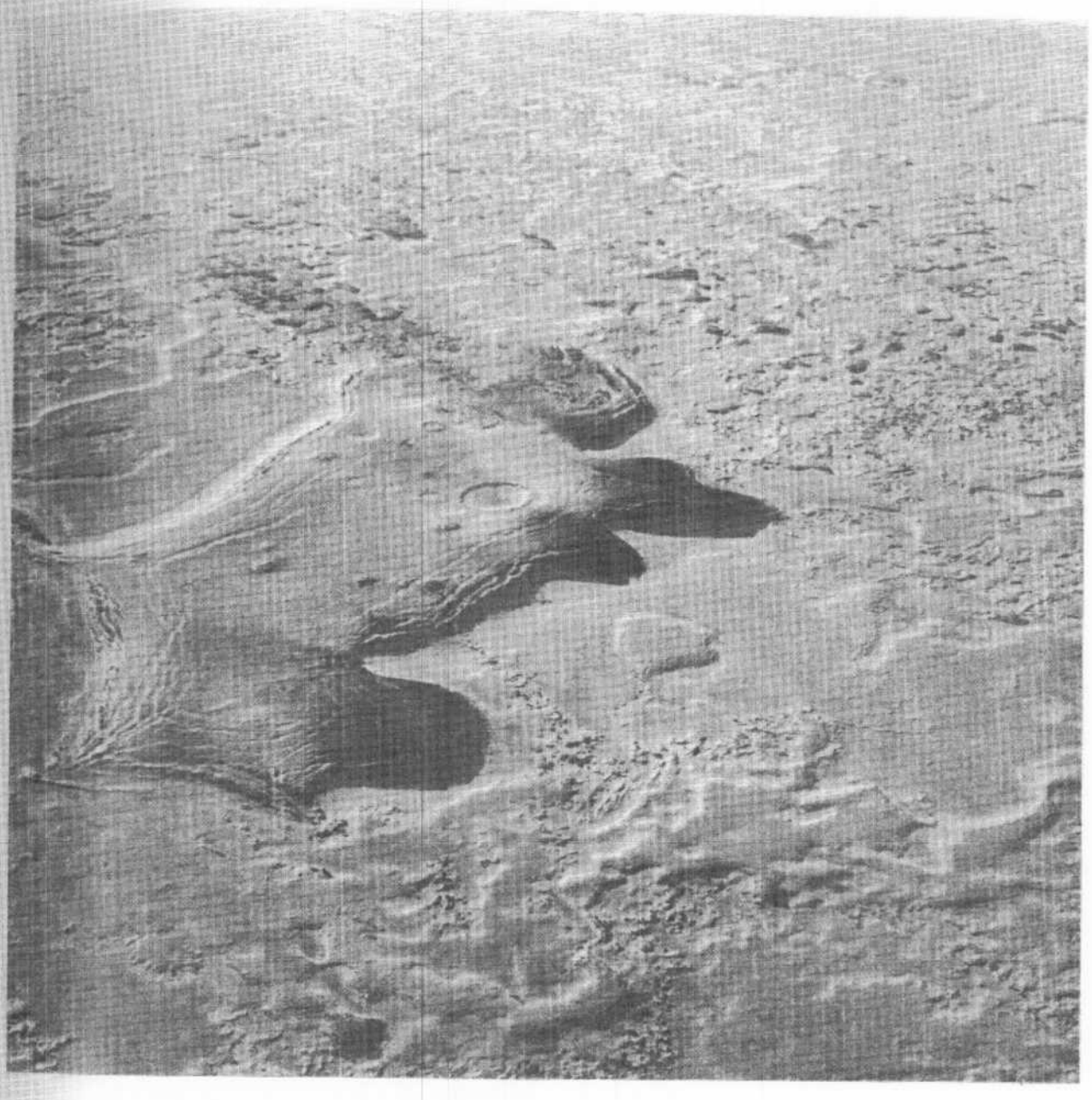

FIGURE 3-10. "Vent" lava area (Station 7). Dark areas on the right face the prevailing wind and are swept free of deposited particles. Large crater to the right is same as shown in Figure 3-11. (Photograph by Jim Iversen, 1976.)

FIGURE 3-11. Panoramic view of the prominent crater on the "vent" lava lake shown in Figure 3-10. Crater is about 40 m across. (Photograph by Ronald Greeley, 1976.)

FIGURE 3-12. Low altitude oblique aerial view of a small crater on a "vent" lava and the tensional fractures that bound the "vent" lavas. (Photograph by Ronald Greeley, 1976.)

AEOLIAN FEATURES

Aeolian aspects of Amboy lava field include basaltic ventifacts, desert pavement, the micrometeorological effects resulting from winds blowing across the rough lava flow surface, and the patterns of aeolian erosion and deposition that develop around the cinder cone and other features on the flow.

Micrometeorology

It is a well known fact that surface roughness (the relief of a given surface and the spacing of the roughness elements) affects the ability of a given wind to move particles because of the influence of roughness on the structure of the lower part of the planetary boundary layer. Surface roughness has been studied in boundary layer wind tunnels and in field experiments for agricultural applications, but full-scale quantitative tests in geological environments are mostly lacking. The evaluation of the roughness parameter is of first-order importance in determining aeolian erosion rates, zones of preferential erosion versus deposition, and in the general expressions for threshold speeds for particle movement. Knowledge of these factors is critical for understanding the geology of all surfaces subject to aeolian processes.

In order to assess the affect of surface roughness under field conditions, an experiment was carried out at Amboy Crater in January and February, 1976. The prevailing strong winds are from the northwest, across the smooth, alluvial-fill valley between the Bristol Mountains and the Bullion Mountains. As the wind passes across the rough lava flow, the wind velocity structure near the surface should change significantly. To measure this effect, two 50-foot towers (Fig. 3-13), each with an array of five cup anemometers and a wind vane were aligned with the dominant wind direction. Tower No. 1 was established upwind of the lava field (Fig. 3-7) to measure the wind velocity profile for winds blowing across the smooth plain. Tower No. 2 was placed about 4 km downwind on the rough lava field. Concurrent measurements by the two towers were made of wind velocity and direction to determine the effect of the lava surface on the wind velocity profile. Details of the results are given in Greeley and Iversen (1977); in general, the results show that there is a substantial drop in *effective* wind velocity, as evidenced by the deposition of sands in the lava field, which are otherwise transported across the smooth plains. These field measurements, coupled with wind tunnel simulations, permit quantification of roughness effects on winds blowing across basaltic terrains.

Wind Flow Patterns

When viewed from the air (Figs. 3-3 and 3-6), one of the most striking aspects of the Amboy lava field is the dark streak that extends more than 3 km downwind from Amboy cinder cone. Hypotheses for the origin of the streak include: 1) the cone-and-crater forms an obstruction that blocks particles from reaching the leeward area, leaving the basalt uncovered by particles; 2) the dark zone is composed of basaltic particles ablated from the cone and deposited downwind; or 3) the cone-and-crater causes a turbulent wind flow in the wake zone, creating an area of erosion which keeps the lavas swept free of particles.

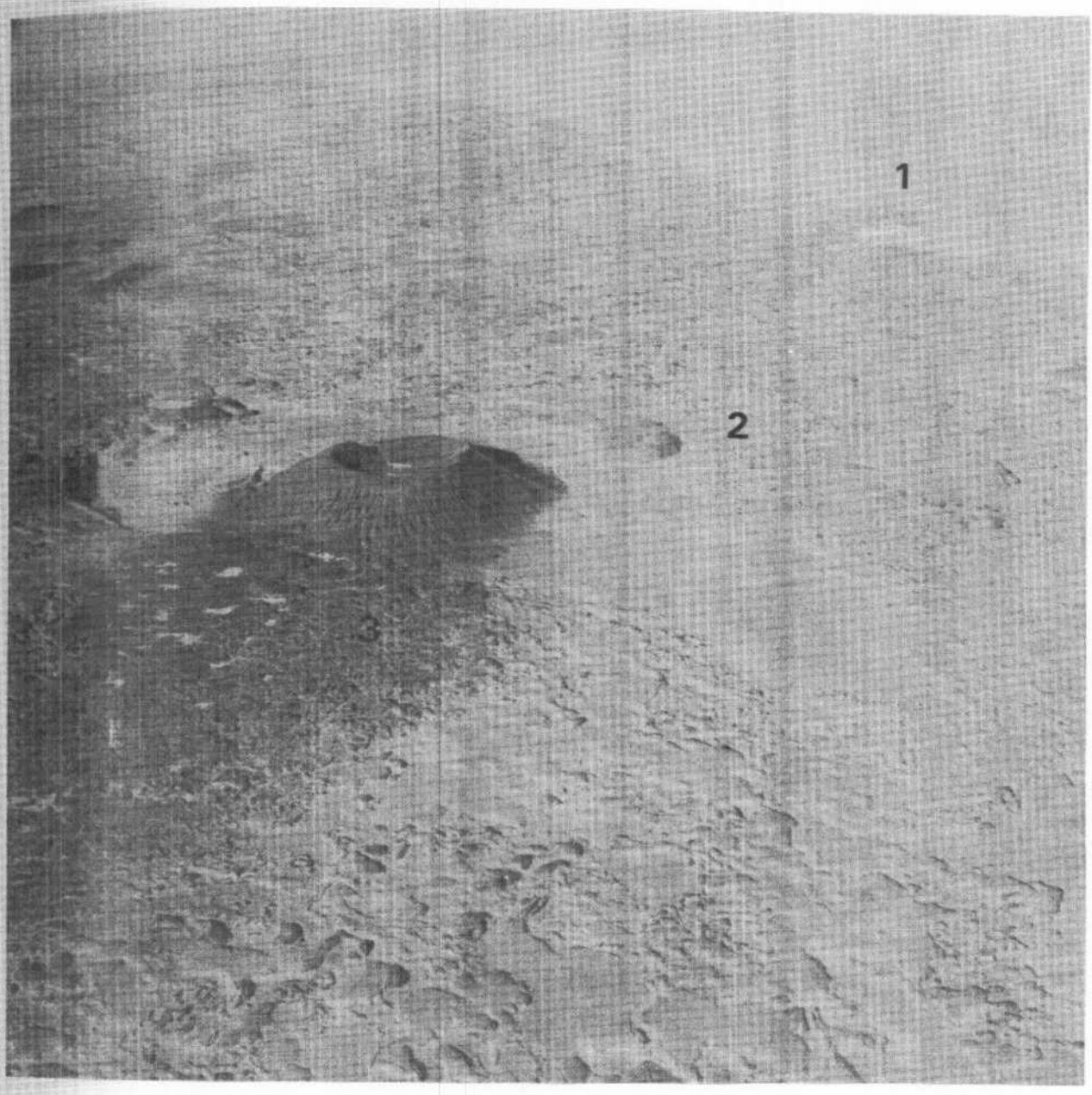

FIGURE 3-13. Oblique aerial view "upwind" (northwest) showing the location of meteorological Tower No. 1 (to obtain wind velocity profile for winds blowing over smooth plain), Tower No. 2 (to measure winds over the rough lava flow) and Tower No. 3 (to measure winds in the wake of Amboy cone). (Photograph by Ronald Greeley, 1976.)

During the field experiments, a third meteorological tower was established in the wake of the cone (Fig. 3-13), and measurements of the winds were taken concurrently with Tower No. 2. In addition, a scale model of part of the Amboy field, including the cone, was placed in a wind tunnel and measurements of the winds in the vicinity of the cone were taken. Results from both the field measurements and the wind tunnel simulations support the hypothesis that the winds are turbulent in the cone wake and prevent deposition of most aeolian particles.

Patterns of aeolian erosion and deposition on a smaller scale than the dark streak associated with the cinder cone are also displayed on the lava field. These include dark streaks emanating from basalt prominences where turbulent flow is generated (Fig. 3-14), deposition and scour patterns around knobs (Fig. 3-15), and depressions that act as depositional traps for sand.

Small-Scale Aeolian Features

Basalt ventifacts occur throughout the Amboy lava field. It is particularly interesting to observe the wind fluting generated in vesicular basalt (Figs. 3-16 and 3-17). In addition, a type of desert pavement often develops in which the find sand is removed by winnowing, leaving a surface of coarse basalt fargments (Figs. 3-18 and 3-19). Walking across this surface pushes the basalt into the underlying sand and leaves a white trail. A few episodes of strong winds quickly remove the exposed sand and reestablish the dark surface.

FIGURE 3-14. Oblique aerial view "downwind" showing a "vent" lava lake (left), a "plateau" lava (arrow) and pyramidal structures (1, 2). Arrow also indicates the prevailing wind direction. Note that a faint dark streak is visible trailing from structure 1, possibly a result of turbulence generated from the structure which is topographically elevated. (Photograph by Ronald Greeley, 1976.)

FIGURE 3-15. Oblique aerial view of a small lava knob and the wind shadow deposition of sand in the wake of the knob. Arrow indicates prevailing wind direction, as do the white deposits of sand in the lee of small bushes. (Photograph by Jim Iversen, 1976.)

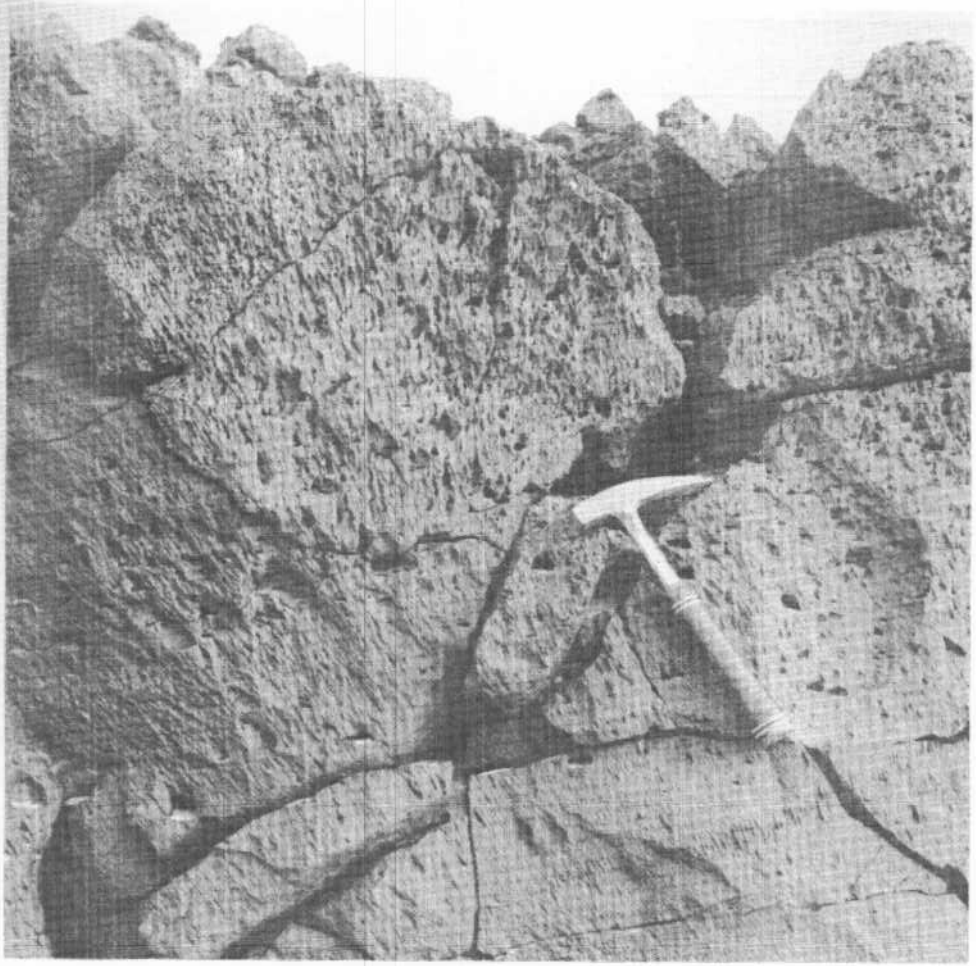

FIGURE 3-16. Wind-fluted vesicular basalt at Station 5.

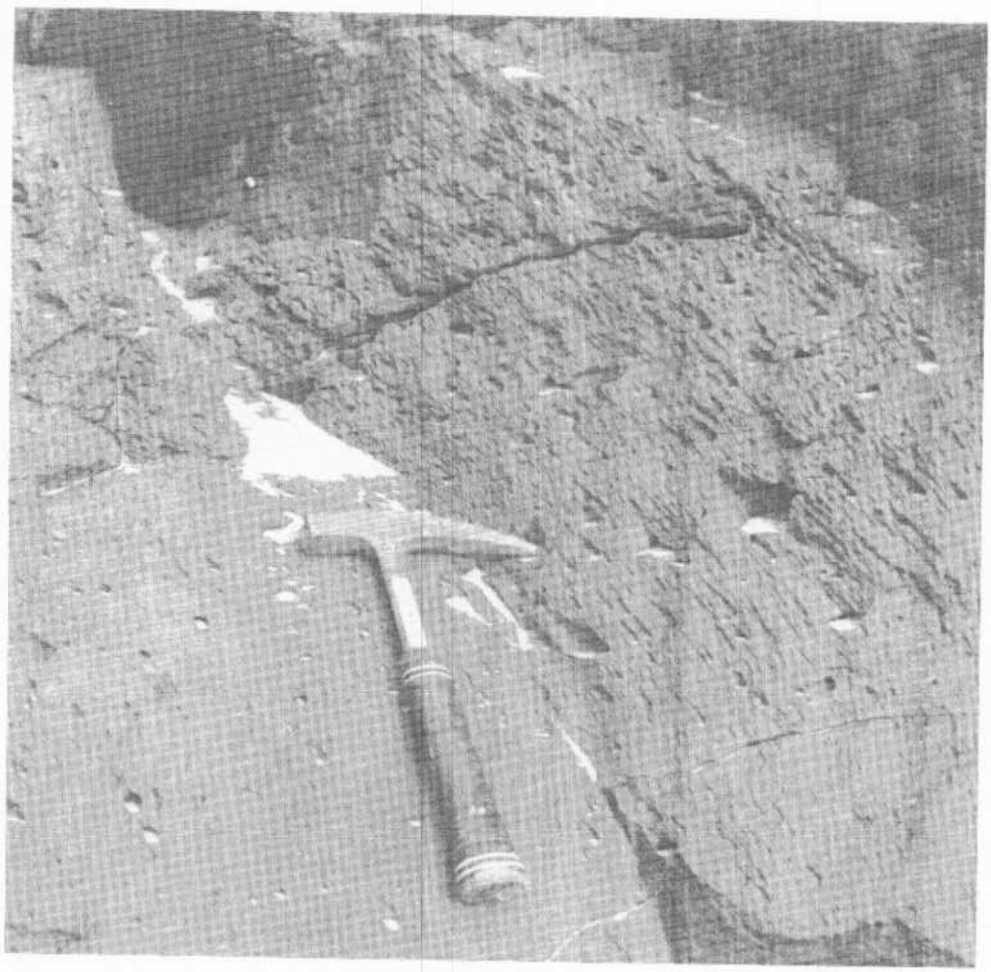

FIGURE 3-17. Wind-fluted vesicular basalt at Station 5.

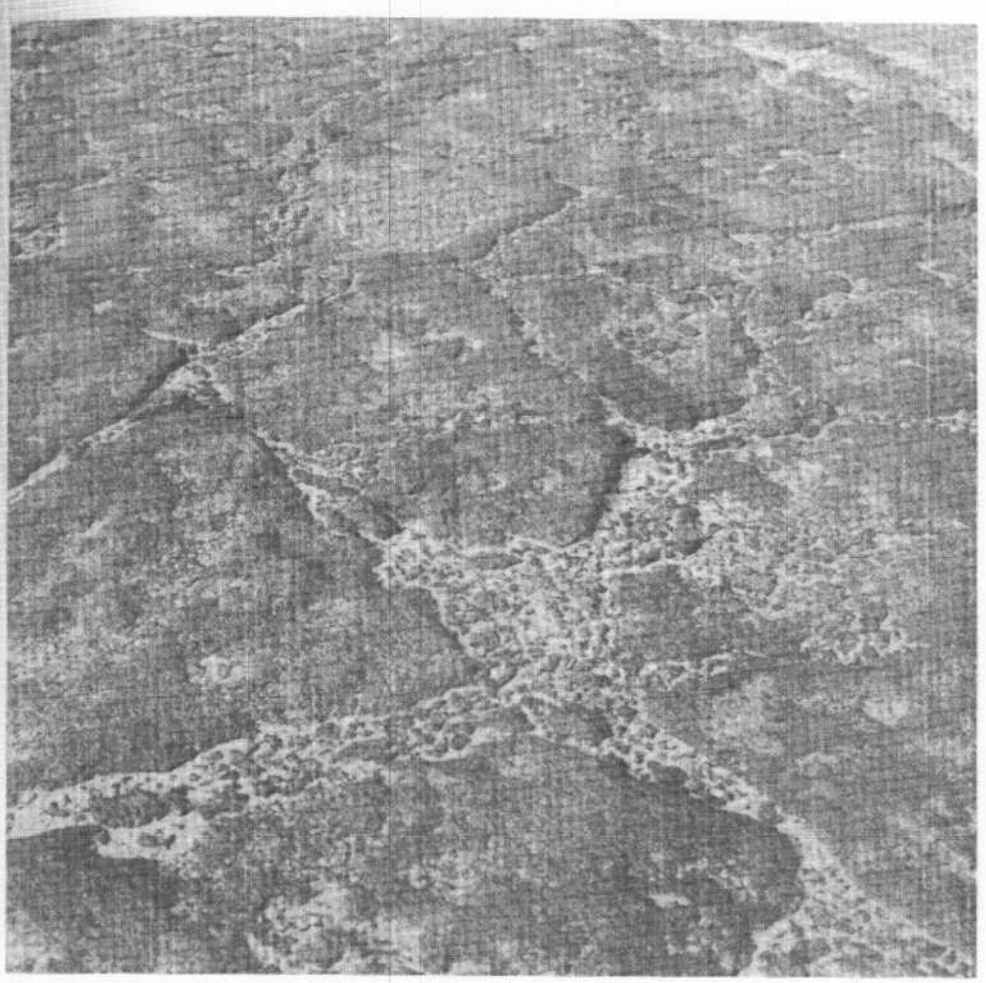

FIGURE 3-18. Desert pavement of bedrock (polygonal pattern) and gravel-sized basalt fragments. Width of picture at bottom is about 1 m.

FIGURE 3-19. Desert pavement of gravel-sized basalt fragments that form an armored surface. Footprints have disturbed the surface; however, an episode or two of strong winds would re-establish the surface.

FIELD TRIP TO AMBOY LAVA FIELD

The field excursion outlined here (Fig. 3-20) requires about six hours to complete and involves a hike of about 8 km. Time and distance can be cut in half by returning after the visit to the cone summit.

Amboy is the nearest community to the field area and contains a post office, gas station, motel, and cafe. The field trip begins by traveling west on old U. S. Highway 66, across the railroad, to the junction with the Amboy-Twentynine Palms Road. Continue west on old U. S. Highway 66 for one mile and turn south toward the cone on a desert track. With reasonable driving care, it is possible to continue on the dirt track onto the "platform" unit to Station 1 (Fig. 3-20).

STATION 1

Park vehicles here. The rest of the trip will be on foot. The surface exposed here is characteristic of the "platform" areas on the lava field and has a relatively flat surface. Follow the road to Station 2.

STATION 2

This station is also on a "platform" area and was the site of one of the penetrator drop tests. The penetrator (Fig. 3-21) was dropped as a free-fall projectile from an altitude of 2590 m and impacted into basalt with a velocity of 213 m/sec, penetrating about 120 cm. A small collapse depression just east of the road gives a good cross sectional exposure of the basalt.

Continue along the road to Station 3. Note the hummocky lava flow terrain characteristic of the "undifferentiated" flows shown on the geological map (Fig. 3-7). Note also that windblown sands collect more readily on the rougher surface.

STATION 3

This area was the site of the second penetrator drop test. The western end of the area includes a block and bomb field from Amboy Crater (Parker, 1963). Continue along the road around the north side of the cone to Station 4. Although there is a "trail" on the north flank of the cone, the easiest approach to the summit is via Station 4.

STATION 4

This station marks the breach in the cinder cone by late-stage lava flows. Continue up the trail to the rim and summit of the cone, where a good perspective can be gained of the lava field and the surrounding area. The view northwest is upwind; note the smooth alluvial fill valley and playa surface, and the abrupt change to the rough-surfaced lava flow. This increase in surface roughness causes a drop in the wind velocity near the surface, resulting in deposition of windblown particles.

Continue clockwise around the rim. Note that parts of the cone are composed of agglutinate, or loosely welded spatter.

If time is short, return to Station 1; otherwise, continue to Station 5.

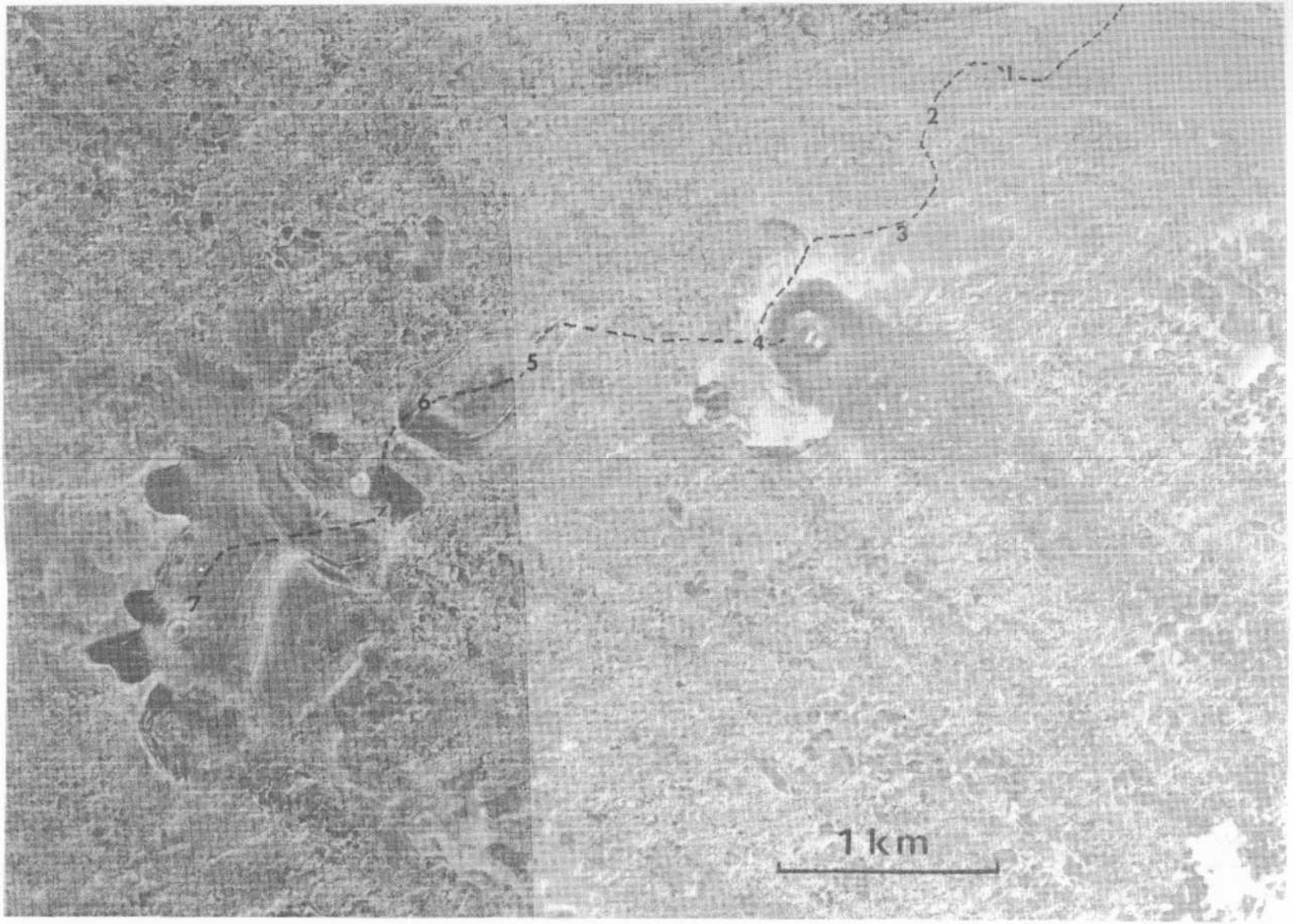

FIGURE 3-20. Mosaic of vertical aerial photographs showing the field trip path and station numbers. (U.S. Department of Agriculture photographs AXL-1K-73, AXL-26K-36, October, 1952.)

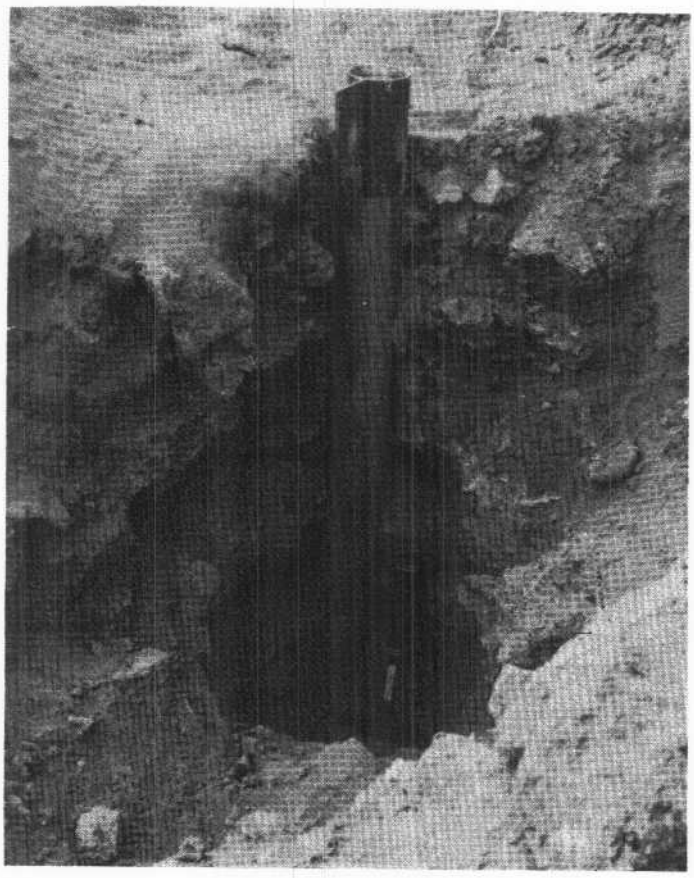

FIGURE 3-21. View of a penetrator that was dropped from an altitude of 2590 m to impact the basalt at Station 2. Basalt on near side has been removed to expose the meter-long penetrator (from Blanchard and others, 1977).

STATION 5

This station marks the north end of one of the vent-lava areas. The tensional fracture in the lava in this area displays numerous wind-fluted basalt exposures (Figs. 3-16 and 3-17) and wind-polished surfaces.

Continue down the fracture to the main vent area. The large flat surface appears to be a former lava lake that was ponded, then sagged slightly in the middle, perhaps in response to withdrawal of magma down the vent, by outflows along the edges, by degassing, or by some combination of these processes. The sagging in the middle evidently was responsible for the formation of the ring fracture on the margin of the lake (Fig. 3-10).

Continue across the surface to Station 6. Note the desert pavement.

STATION 6

The view southwest from the rim of the lava lake shows a small "platform" lava flow (Fig. 3-14), and a pyramidal structure that may have formed in response to up-doming. Continue across the flows to the pyramidal feature, following the path shown on Figure 3-20. Note the desert pavement on the surface between the tensional cracks of the pyramidal feature. Continue to Station 7.

STATION 7

The surface here appears to be another vent lava flow that was ponded as a lava lake. Tensional fractures outline the edge of the feature. Several craters on the surface may represent collapse of the lava lake surface. Note the patterns of aeolian erosion and deposition formed around the craters, knobs (Fig. 3-15), and other small topographic features. Many of these are similar in morphology (but not size) to aeolian patterns observed on Mars (Fig. 3-22).

Retrace the path to Station 1. The cinder cone makes a good landmark for the return across the flow.

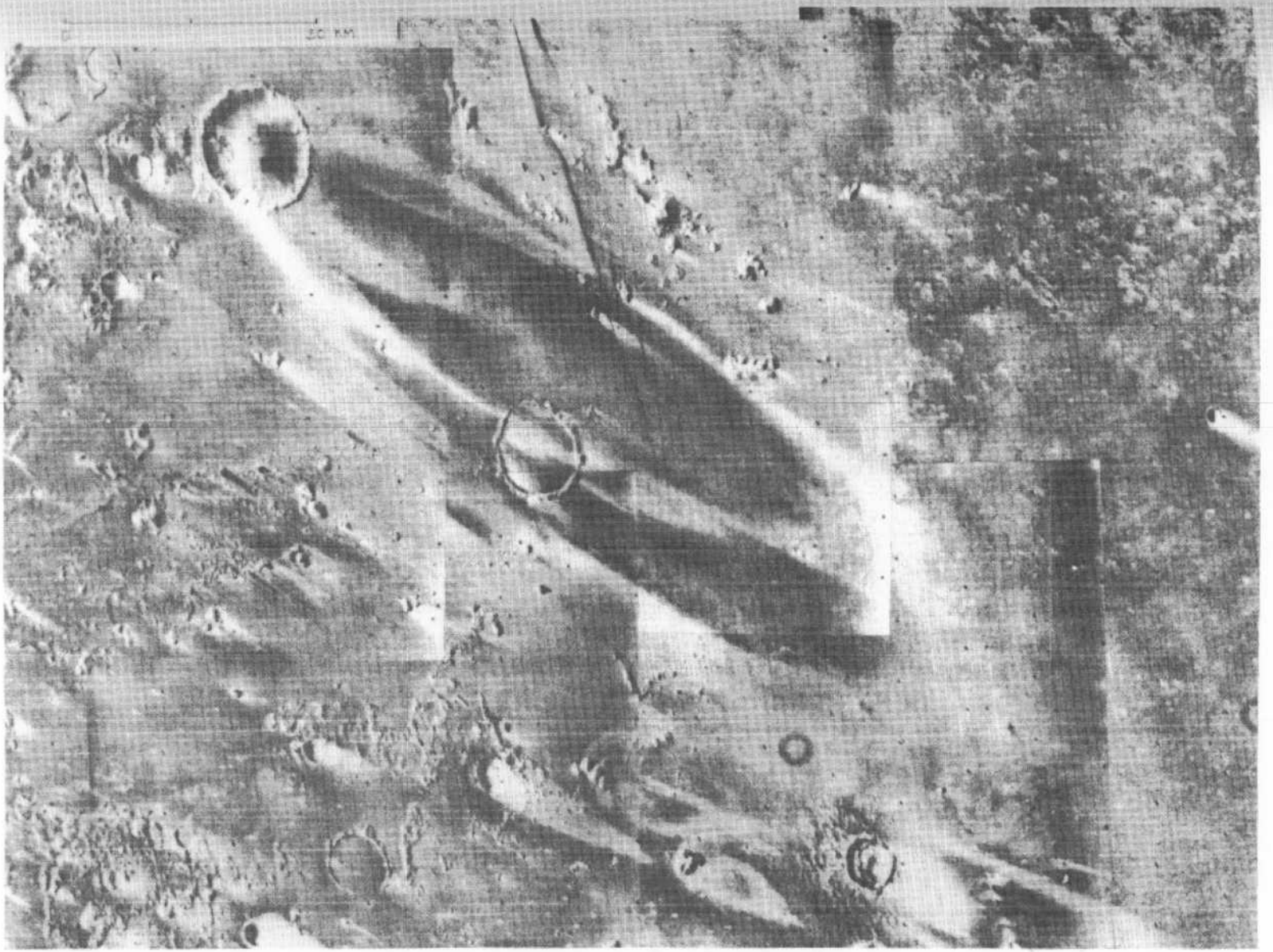

FIGURE 3-22. Mosaic of Viking Orbiter images of the Mesogaea region of Mars showing various streaks that are the result of aeolian processes.

REFERENCES

Bassett, A. M. and D. H. Kupfer, 1964. A Geologic Reconnaissance in the Southeastern Mojave Desert: Special Report 83, California Div. Mines and Geology.

Blanchard, M., T. Bunch, A. Davis, H. Shade, J. Erlichman, and G. Polkowski, 1977. Results of analyses performed on basalt adjacent to penetrators emplaced into volcanic rock at Amboy, California, April, 1976: NASA Tech. Paper 1026, 15 p.

Greeley, R. and T. E. Bunch, 1976. Basalt models for the Mars penetrator mission: Geology of the Amboy lava field, California: NASA TM X-73,125, 53 p.

Greeley, R. and J. D. Iversen, 1977. Aeolian processes at Amboy Crater, California, as martian analogs. (In preparation.)

Hatheway, A. W., 1971. Lava Tubes and Collapse Depressions: Univ. Arizona, Ph.D. Thesis.

Parker, R. B., 1959. Magmatic differentiation at Amboy Crater, California: Am. Mineralogist, vol. 44, pp. 656-658.

Parker, R. B., 1963. Recent Volcanism at Amboy Crater, San Bernardino County, California: Special Report 76, California Div. Mines and Geology.

Smith, H. T. U., 1967. Past versus present wind action in the Mojave Desert region, California: Rep. 67-0683, Air Force Cambridge Research Lab.

Swanson, D. A. , 1973. Pahoehoe flows from the 1969-1971 Mauna Ulu eruption, Kilauea Volcano, Hawaii: Geol. Soc. Amer. Bull., vol. 84, pp. 615-626.

Watkins, J. S., ed., 1965. Investigation of *in situ* physical properties of surface and subsurface site materials by engineering geophysical techniques: U. S. Geol. Survey Project Rep. to NASA for fiscal year 1965.

Watkins, J. S., ed., 1966a. Investigation of *in situ* physical properties of surface and subsurface site materials by engineering geophysical techniques: U. S. Geol. Survey Quarterly Rep., 1 Oct 1965 to 31 Dec 1965.

Watkins, J. S., ed., 1966b. Investigation of *in situ* physical properties of surface and subsurface site materials by engineering geophysical techniques: U. S. Geol. Project Rep. to NASA for Fiscal Year 1966.

4. THE KELSO DUNE COMPLEX

Robert P. Sharp
Division of Geological and Planetary Science
California Institute of Technology
Pasadena, California 91125

4. THE KELSO DUNE COMPLEX

Robert P. Sharp
Division of Geological and Planetary Science
California Institute of Technology
Pasadena, California 91125

Study of Kelso Dunes was undertaken for the purpose of learning something about the fundamentals of dune behavior through measurements of sand movement and changes in dune shape, orientation, and position. In the process, other information concerning the origin, nature, and behavior of this relatively large complex of dunes was obtained.

Kelso Dunes lie in the eastern part of Mojave Desert, 80 km west of the Nevada border and in the middle of the triangular region bounded by the Barstow-Las Vegas highway (I-15) on the north and the Barstow-Needles highway (I-40) on the south (Fig. 4-1). The dunes are approximately 48 airline km southeast of Baker and roughly 25 airline km north of Interstate Highway 40. They are intermittently visible to travelers on I-15 between Rasor Road and Baker. The dunes can be reached from either the north or south via the Kel-Baker road, a well graded, partly paved, back-country desert route. Located at 34°48′ latitude and 115°43′ W longitude, they are shown on U. S. G. S. 15-minute quadrangles, Flynn and Kerrens.

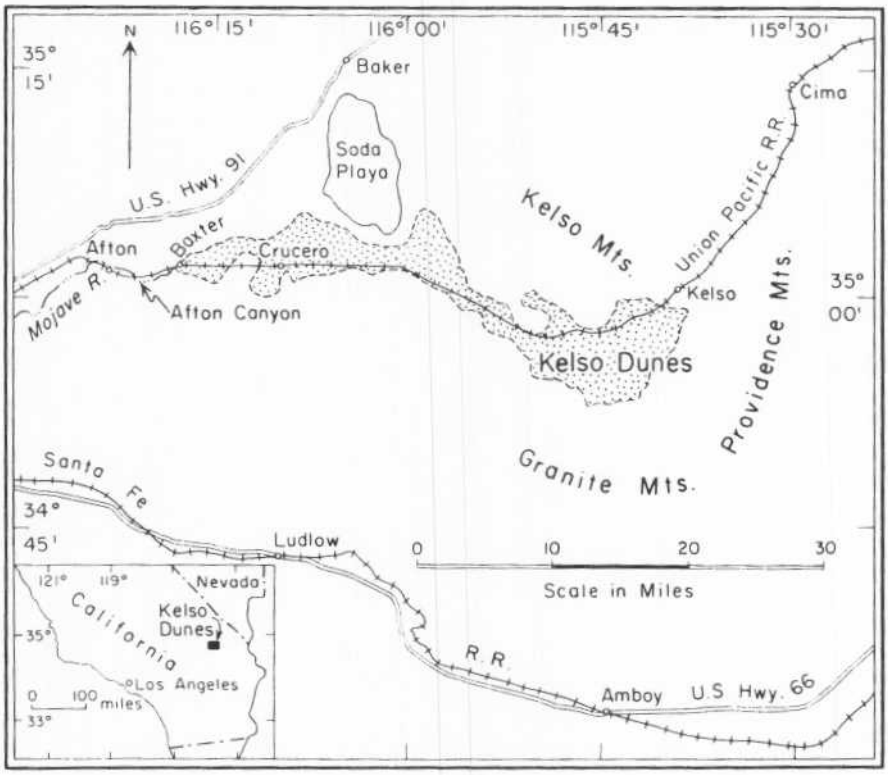

FIGURE 4-1. Location map for Kelso Dunes, Mojave Desert, California (from Sharp, 1966).

The dunes comprise an elliptically-shaped mass, with its long axis bearing northeasterly, covering 175 km^2 and consisting of a rather irregular complex of modest-sized transverse dunes surrounding and partly superimposed upon several larger, irregular, linear ridges bearing N 65° E (Figs. 4-2, 4-3). The crest of the southernmost of these linear ridges is the highest part of the complex. It rises nearly 170 m above the alluvial apron to the south and is judged to be underlain by

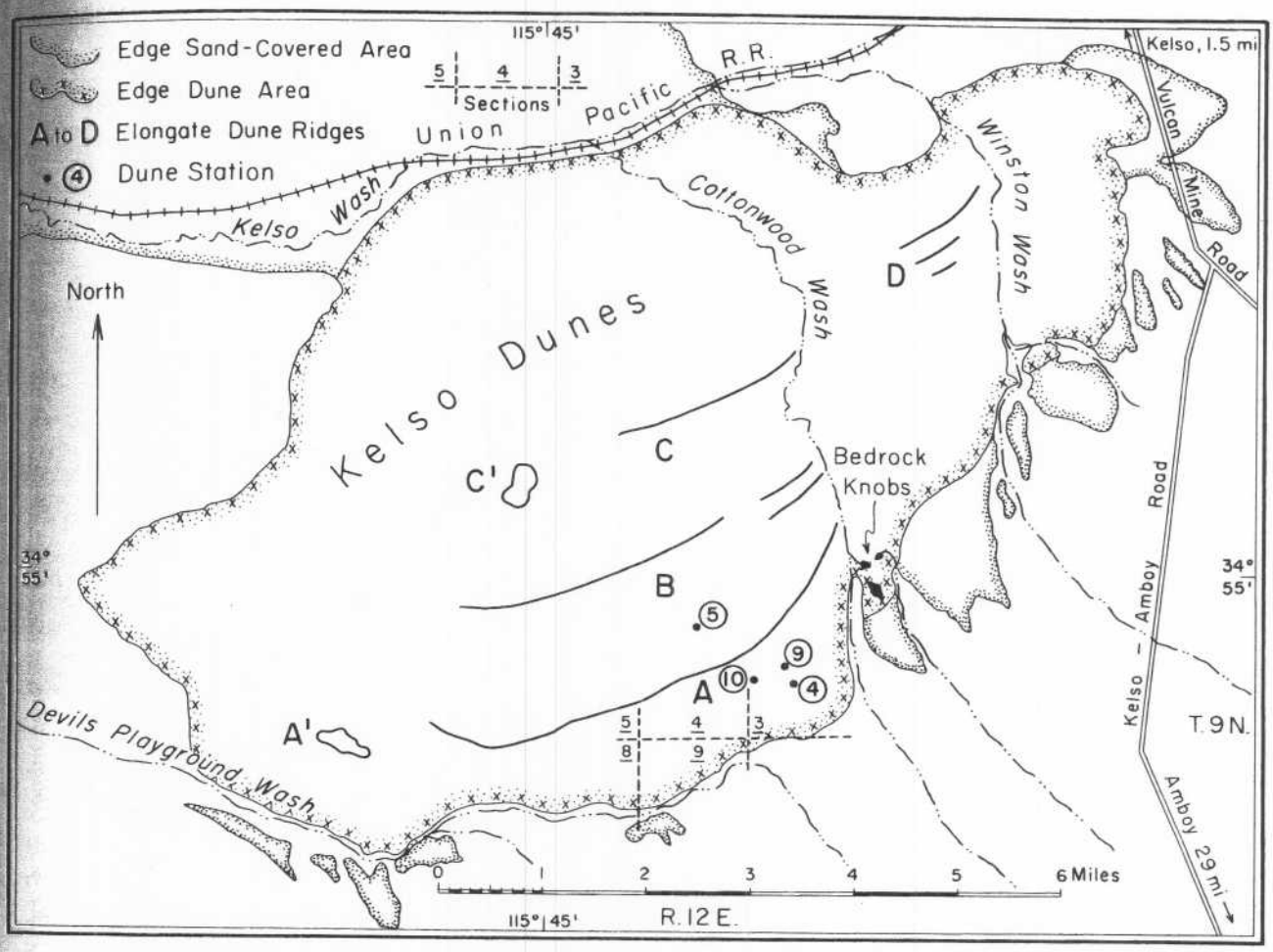

FIGURE 4-2. Geographic details of Kelso Dunes and location of dune stations (from Sharp, 1966).

FIGURE 4.3. Oblique aerial view of Kelso Dunes. (Photograph by J. S. Shelton.)

aeolian sand roughly 215 m thick (Fig. 4-4). The dunes lie well out on the floor of Kelso Valley, which is enclosed by mountainous terrain to the south, east, and north with openings to the west and northeast. Prevailing winds are from the west-northwest, but strong storm winds blow from other directions with modest frequency.

FIGURE 4-4. Highest (170 m) peak in Kelso Dunes viewed from south (from Sharp, 1966).

Sand for the dunes is clearly derived from the west, and the principal source is judged to be the plain of active alluviation created by the Mojave River where it debouches from Afton Canyon, roughly 55 km to the west. The last 37 km of the sand movement is on an uphill gradient rising 300 m. Changes in size, rounding, and sorting of sand during aeolian transport over the 55 km reach have been recorded but are not a focus of interest here. Kelso dune sand is well rounded, well sorted, and somewhat coarser than typical dune sand with 90 percent of the grains between 0.25 and 0.50 mm in diameter; the mean grain size at most localities within the dunes is close to 0.30 mm. Aside from a coarsening of grain size in deflated hollows and toward the base of avalanche slopes, no consistent variation in grain size with location on dune ridges was found in this complex (Fig. 4-5).

One surprising aspect of Kelso Dunes is their location well into Kelso Valley on the north sloping alluvial apron of Granite Mountains, rather than plastered up against one of the bordering mountain ranges. Although a cluster of small rock knobs lie near the southeast edge of the dunes (Fig. 4-2), there is little other evidence to suggest they were initiated by a major bedrock prominence or are presently anchored on one. Instead, their location is attributed to a multi-directional wind regime strongly influenced by the local orographic configuration. The work of prevailing

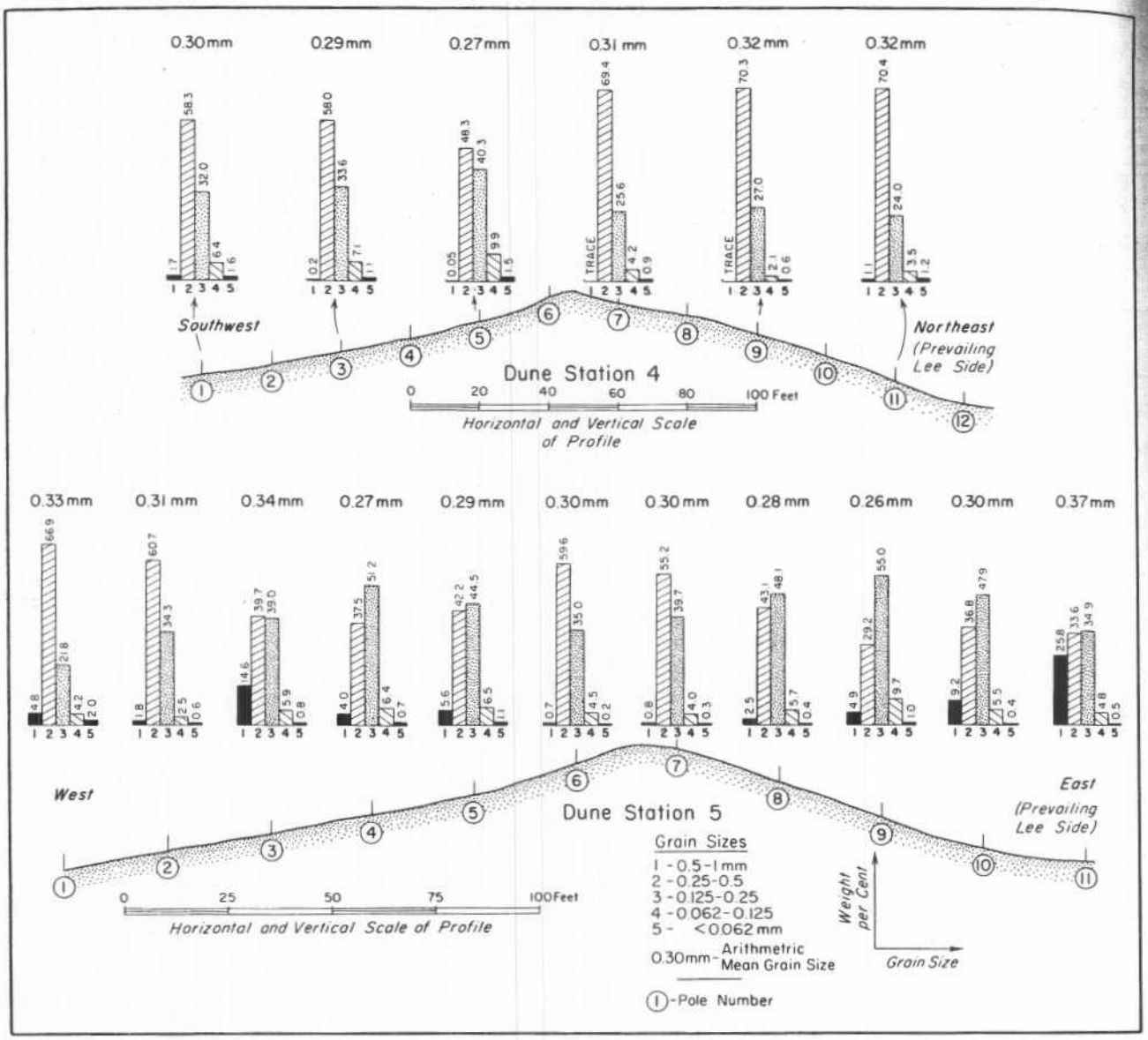

FIGURE 4-5. Grain-size distribution on dunes at stations 4 and 5 (from Sharp, 1966).

westerly winds is judged to be balanced by occasional more effective strong storm winds from other directions, principally from the east, southeast, north, and northeast. Winds from the southwest are less frequent and less effective. It has long been recognized that strong winds, blowing only occasionally, can effectively counterbalance the work of more pervasive, but gentler, prevailing winds from other directions. This interpretation is supported by measurements over a 15-year interval of the behavior of individual dune ridges within the complex.

Measurements made on dune ridges of different orientations in different locations within the dune complex show that, under the variable wind regime of this locality, the sand composing a dune ridge is shifted back and forth from one flank to the other with corresponding changes in crestal symmetry, location, and height. This is not to say that any single dune ridge does not lose or gain

sand from neighboring dune ridges, but most of the sand moved during any particular episode of activity is sand already in the dune. Dune crests moved back and forth within a zone 10 - 12 m wide, making a total journey of perhaps 150 m in 10 to 12 years and ending up within a meter or two of the position initially marked (Fig. 4-6). Large volumes of sand were involved in such changes

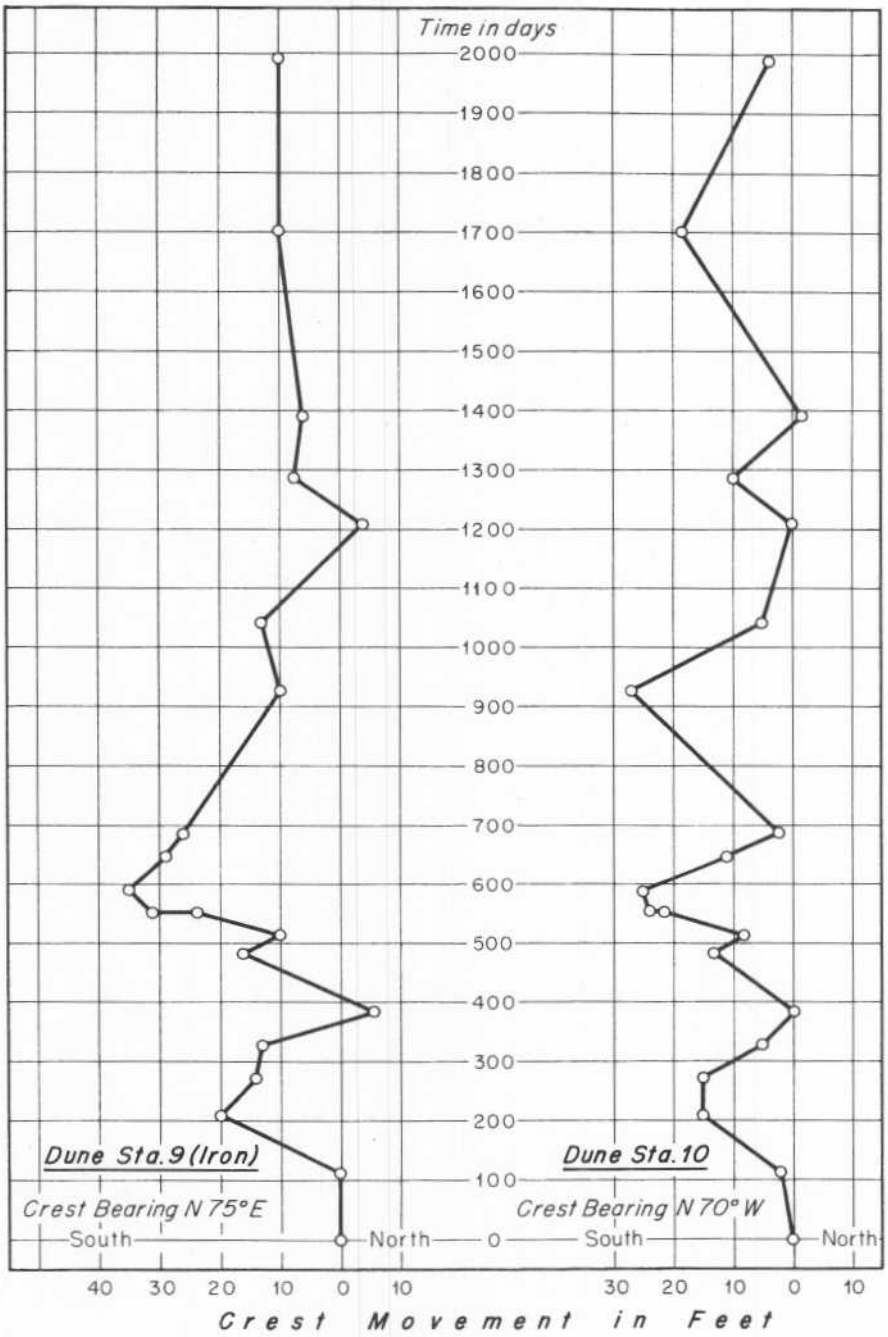

FIGURE 4-6. Plots of shifts in position of dune crests at stations 9 and 10 (from Sharp, 1966).

but the dune was merely passing the sand back and forth from its left hand to its right hand and vice versa. The greatest changes of removal or accumulation of sand in Kelso Dunes, occurred within the crestal zone of a dune ridge accompanied by marked changes in asymmetry and crestal morphology. The cumulative changes in sand level at a point may be as great as 20 m in a decade with a resultant change in level of a meter or less (Figs. 4-7, 4-8).

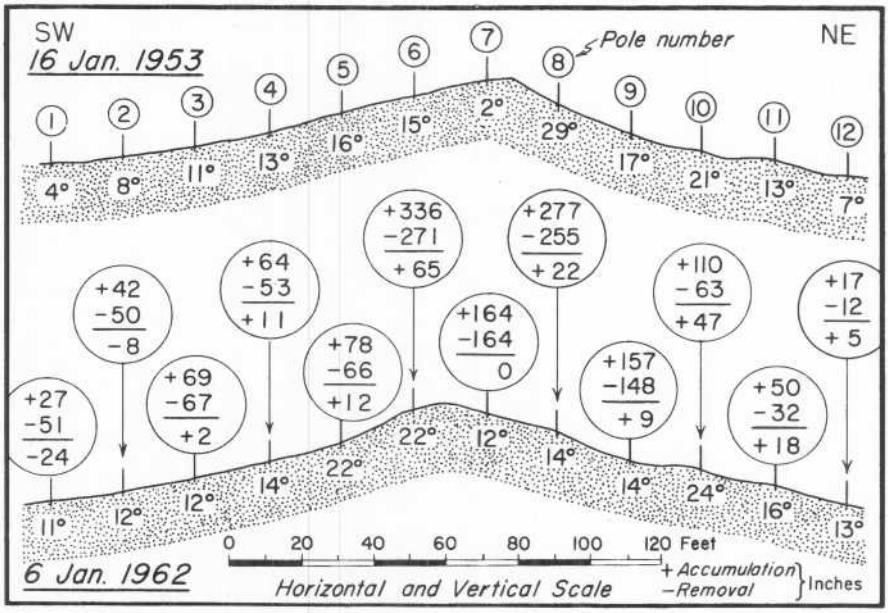

FIGURE 4-7. Summation of changes in inches recorded at poles of dune station 4 over a 9-year period. Because of intervals between measurements, gross changes recorded are probably only one-third to one-fourth of the absolute changes (from Sharp, 1966).

Sand-flow avalanches (Fig. 4-9) are rampant on the lee side of active dune ridges, and it is something of a wonder that any lee-slope bedding at an inclination around 30° is preserved in dune deposits of this type. Lee-side longitudinal wind currents following strong avalanche activity may create the plane surfaces seen on steeply dipping cross beds in ancient aeolian sands. Excavated pits in Kelso Dunes (when wet) have revealed very little lee-side bedding with dips over 30° (Fig. 4-10). If Kelso Dunes were to be lithified and subsequently exposed in the stratigraphic section, the dip of most cross bedding seen would be at angles between 10° and 20°.

One learns from the Kelso Dunes that surface morphology strongly influences the direction of winds at the ground surface. It is possible to stand on a transverse dune ridge with a strong wind blowing directly up the gentler windward side of the ridge and see a longitudinal wind moving in an orthogonal direction along the lee face of the dune. If the transverse ridge has peaks and swales (domes and saddles) along its crest, these variations can cause as much as a 30° divergence from the prevailing wind direction as the ground wind approaches the crest. It is a startling experience to stand on a dune crest during a strong prevailing wind aloft and observe the different directions of wind current at ground level created by variations in surface topography.

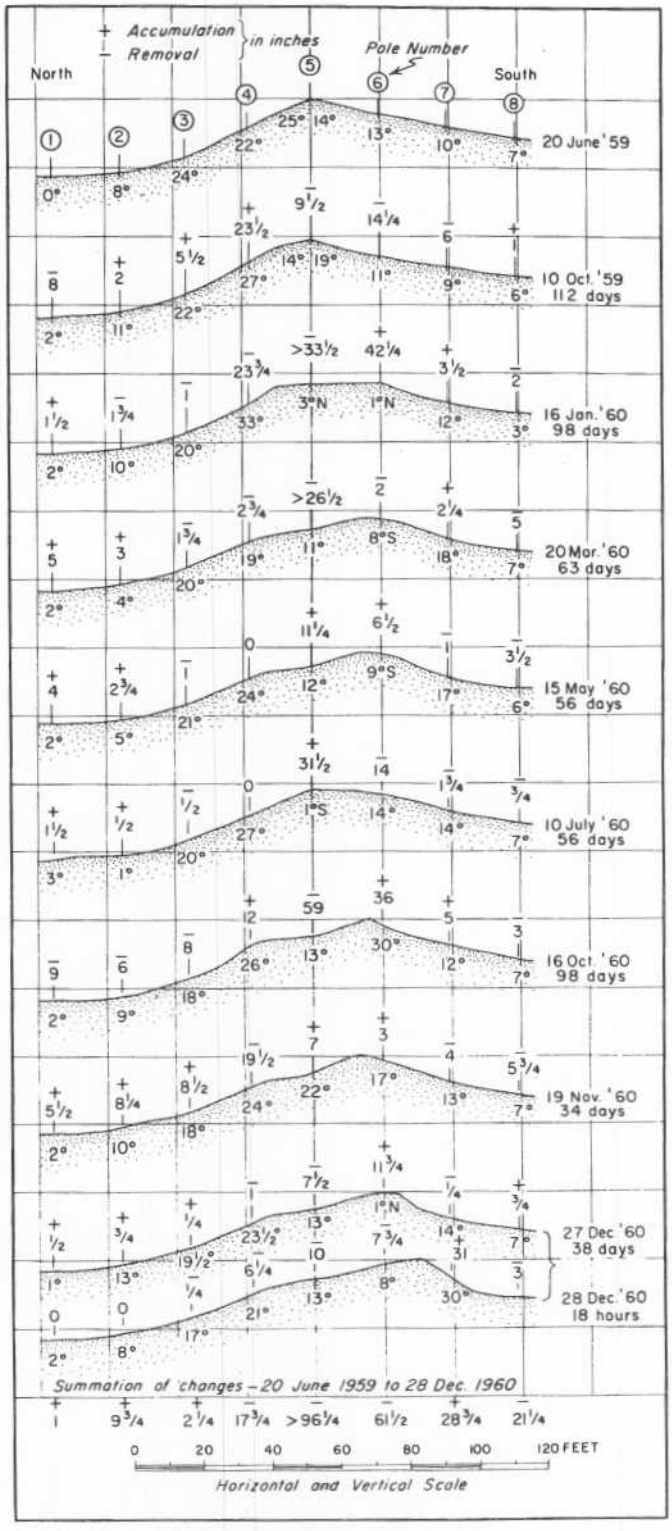

FIGURE 4-8. Changes at poles of station 9 (iron) for 1.5 years. Plus and minus figures above each profile indicate change in inches since preceding observation (from Sharp, 1966).

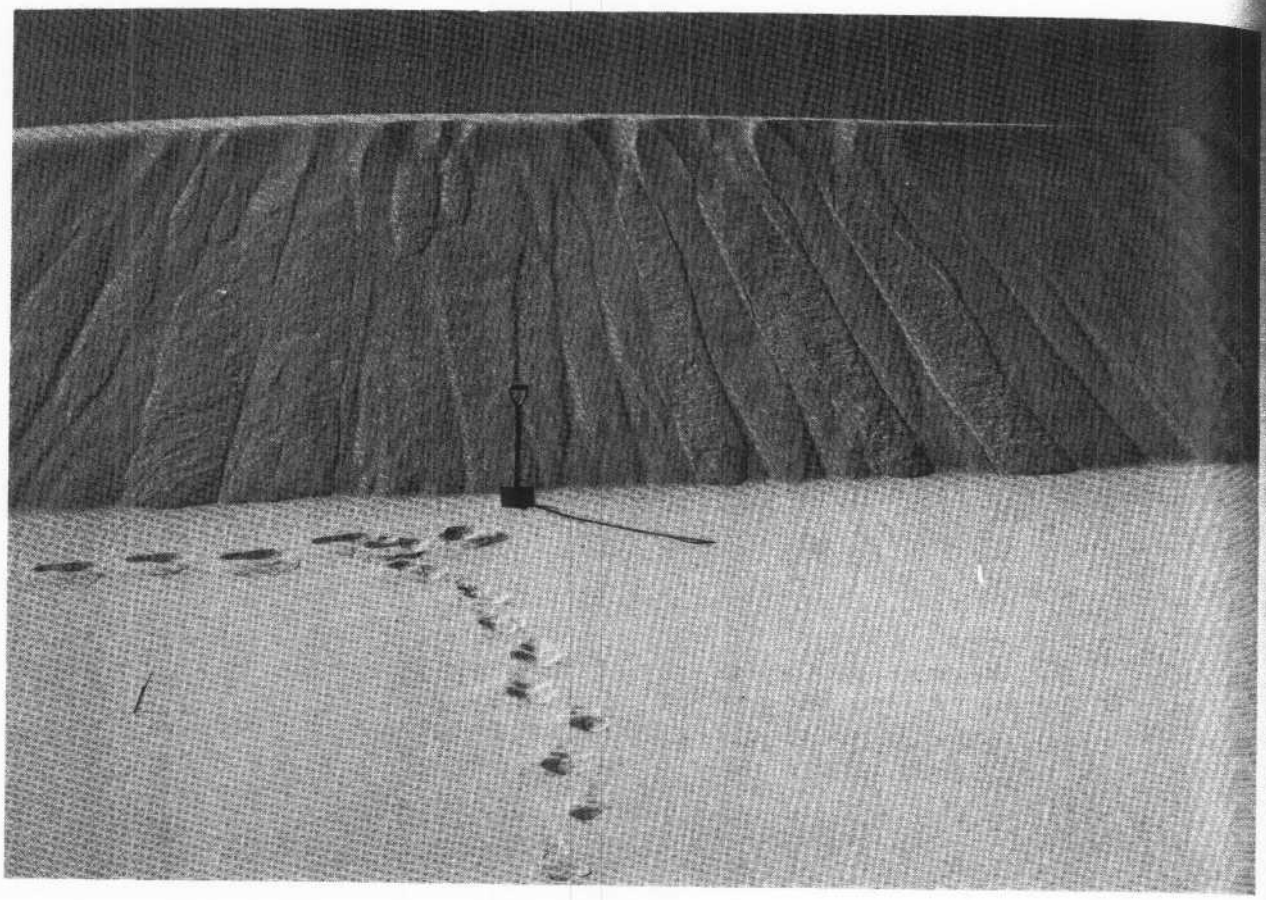

FIGURE 4-9. Slumps on recently active slip face (from Sharp, 1966).

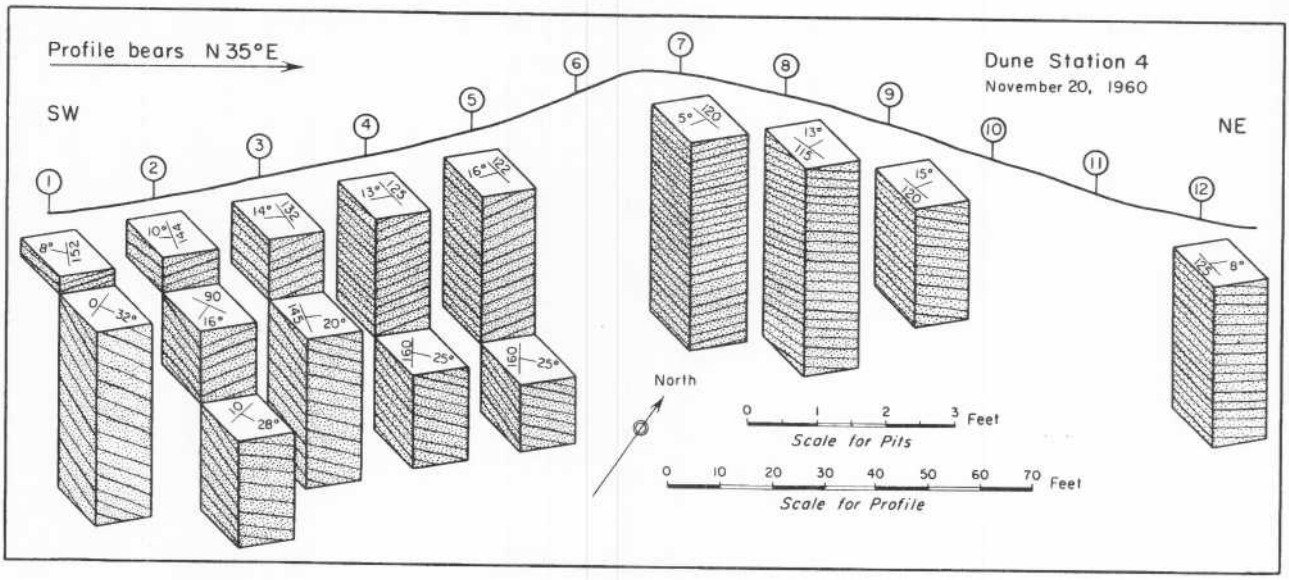

FIGURE 4-10. Bedding attitudes in pits across dune at station 4 (from Sharp, 1966).

The pattern of transverse dune ridges within the Kelso complex varies in different places because of the local topographic setting, but some of these differences also probably reflect antecedent conditions with different effective wind regimes. It is not known how long Kelso Dunes have existed as a discrete dune mass, but a figure of many thousands of years is probable. Some 22 separate clumps of large desert willow (catalpa) trees growing well up in the dune mass, with trunk diameters up to 35 cm, show that the dunes were once more stable than at present. Some of these trees are being buried, and others have been buried and are now partly or wholly re-exposed under the current regime with which they are clearly out of phase. Within any period of several thousand years, the dunes have inevitably experienced significant environmental changes, presumably including some change in the relative effectiveness of the wind pattern. Winds from the southwest are currently few and weak, yet a pattern of ridges in the southwest part of the dune mass suggests an effective wind from the southwest quadrant. This may be an inherited, essentially fossil pattern. Once a transverse ridge is established, its orientation can, to limited degree, influence and control the effects of winds from somewhat oblique directions without a significant change in its own orientation. Eventually, it is probably doomed, but for a while the melody lingers on, and the original transverse ridge maintains its orientation, although with probably some change in transverse symmetry.

Studies with smoke pots on Kelso Dunes and a host of other observations confirm an earlier conclusion of other workers that the fixed lee-side eddy concept of dune mechanics is largely falacious. It certainly does not operate in the classically conceived manner in Kelso Dunes.

The long, high linear ridges within the Kelso complex are not understood. They basically have the form of linear dune ridges, but are not linear to any currently dominating wind direction. Their crestal symmetry, in fact, is controlled by transverse winds. They are possibly a product of some antecedent condition and are large enough to preserve themselves under the present regime of winds from oblique or transverse directions.

Kelso Dunes are extremely active, but they are not going anywhere at any perceptible pace. Like all dune masses, they are lovely when viewed in low-angle light and are fascinating because of their dynamic behavior. It is always satisfying to work with an earth process that proceeds at a rate susceptible to short-term measurement.

REFERENCE

Sharp, R. P., 1966. Kelso dunes, Mojave Desert, California: Geol. Soc. Amer. Bull., v. 77, p. 1045-1074.

5. FIELD TRIP TO DUNES AT SUPERSTITION MOUNTAIN

Roger S. U. Smith
Department of Geology
University of Houston
Houston, Texas 77004

5. FIELD TRIP TO DUNES AT SUPERSTITION MOUNTAIN

Roger S. U. Smith
Department of Geology
University of Houston
Houston, Texas 77004

Spectacular longitudinal dune ridges cover much of the southern part of Superstition Mountain which lies on the west side of the Salton basin about 25 km west of Brawley, California (Figs. 5-1 and 5-2). Superstition Mountain is a hill of crystalline rocks two kilometers wide by ten kilometers long and rises 70 to 150 meters above the surrounding desert floor. Its irregular knobby surface has been overrun by numerous longitudinal dune ridges, some of which climb the hill from the west, but most of which extend 0.5 to 1.5 km eastward from bedrock knobs (Figs. 5-2 and 5-3). These dune ridges, five to ten meters tall, were briefly noted by Brown (1923) and by Eymann (1953). Most of these dunes now lie within a U. S. Navy test area, but the southernmost ones can be reached easily from a gravel road which enters the area from the southeast. The wind regime of the dunes is not precisely known, but long-term wind records from the El Centro Naval Air Station, 20 km to the southeast, suggest a regime of nearly unidirectional winds from the west-southwest to west.

ROAD LOG

Mileage		
Cumulative	Difference	
0.0	0.0	Brawley, intersection of California Highways 78 and 86. Turn south onto Highway 86.
5.3	5.3	Turn west (right) onto Imperial County Rt. 27.
8.3	3.0	Turn north (right) onto Imperial County Rt. 30.
9.2	0.9	Turn west (left) onto Imler Road.
13.7	4.5	Entrance to U. S. Navy test area on right. Stay on Imler Road.
15.0	1.3	Turn west (right) onto gravel road. Proceed with caution because this road is poorly maintained and may be sandy, rutted, and/or washed out.
20.0	5.0	The southernmost dune ridge is about a quarter mile to the north and numerous jeep tracks lead to it. Passenger cars should park here; pickups and jeeps can drive to the dune ridge or follow the sandy road ahead to a burned-out stone building about 0.4 miles ahead. Climb to the top of the bedrock knob just north of the building and walk down the dune ridge's crest (this route is shown as dotted line on Figure 5-1). Note that the steepness of the ridge is comparable on its north and south sides and that only the upper part of the slope on one side is a slip face at the angle of repose of sand. The slip

Mileage

Cumulative Difference

face may be on either the north or south side of the ridge, depending on which way sand-moving winds blew most recently. As the distal end of the ridge is reached, numerous tire tracks perpendicular to the ridge seem to have been covered by eastward advance of the ridge, but examination of aerial photographs taken in 1934, 1953, and 1973 suggests that the position of the eastern tip and the overall shape of the dune ridge have changed little during the last 40 years (compare Figs. 5-2a and 5-2b). A field of poorly-developed barchan and transverse dunes extends about 2 km eastward from the tips of the dune ridges, from which they may have been spawned (Figs. 5-2b and 5-4).

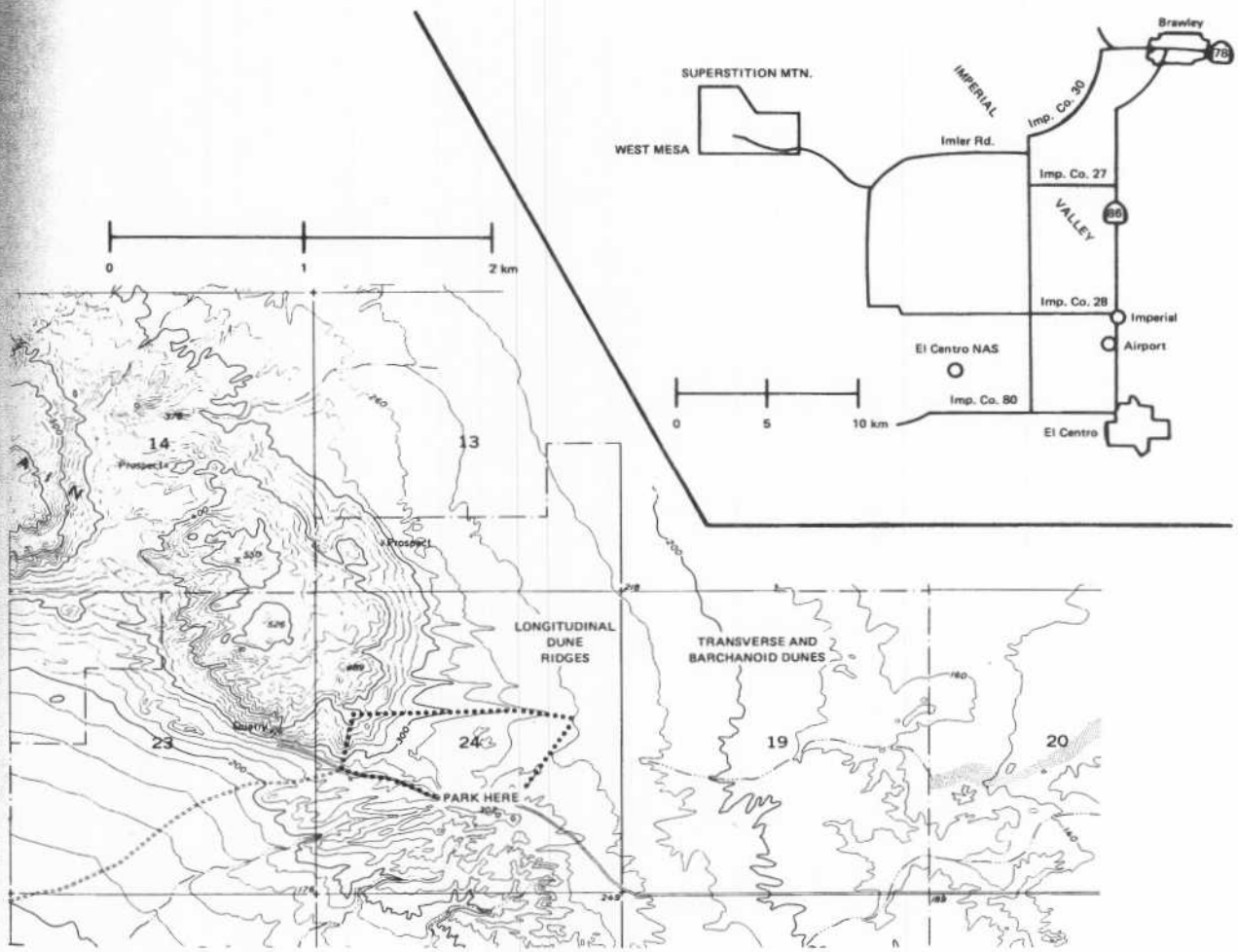

FIGURE 5-1. Location map of Superstition Mountain dunes.

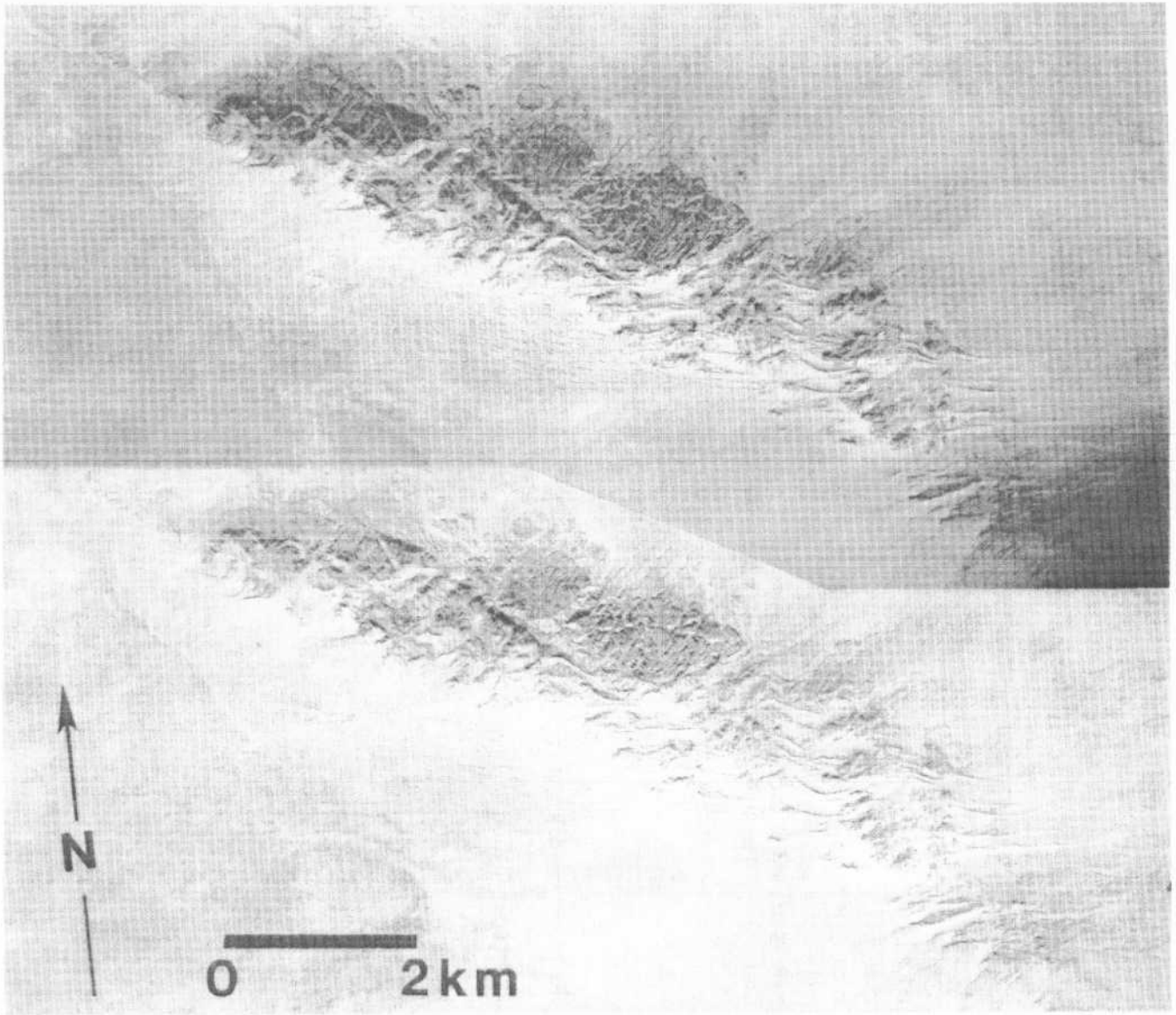

FIGURE 5-2a. Air photo stereogram of dunes at Superstition Mountain (USGS/AMS VV FS M73 145 5852 and 5853, Dec. 1954).

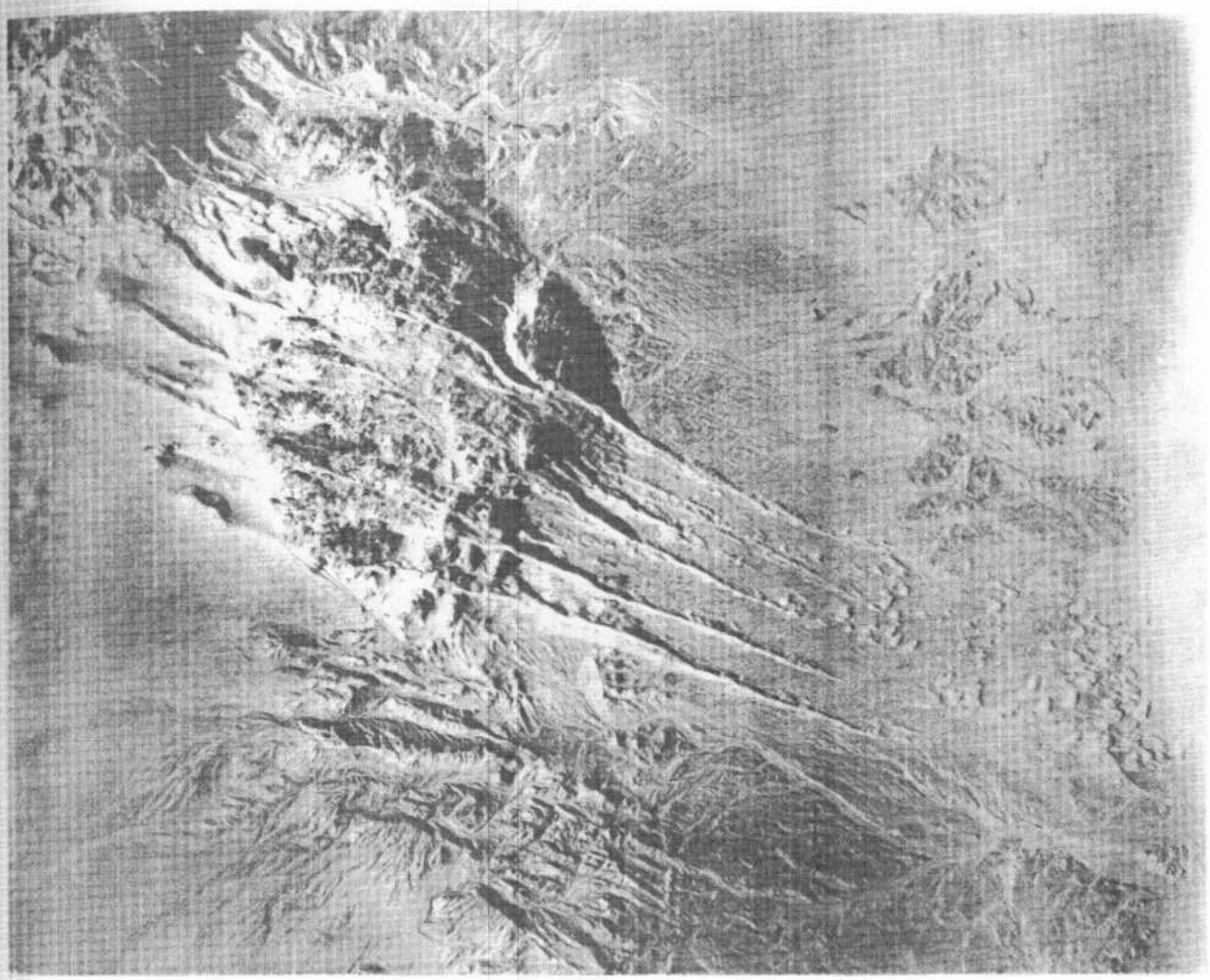

FIGURE 5-2b. Large-scale air photo of Superstition Mountain dunes. Note how the longitudinal dune ridges break up downwind into individual barchanoid dunes (Spence Air Photos, no. AA 672-133, Jan. 1934).

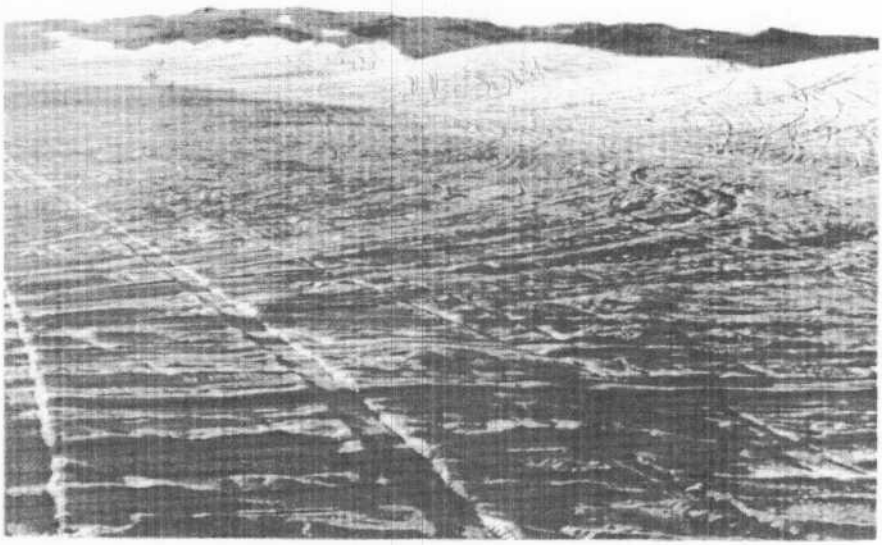

FIGURE 5-3. View to northwest across southernmost dune ridge at Superstition Mountain. Note the irregular, sinuous crest (Jan. 1976).

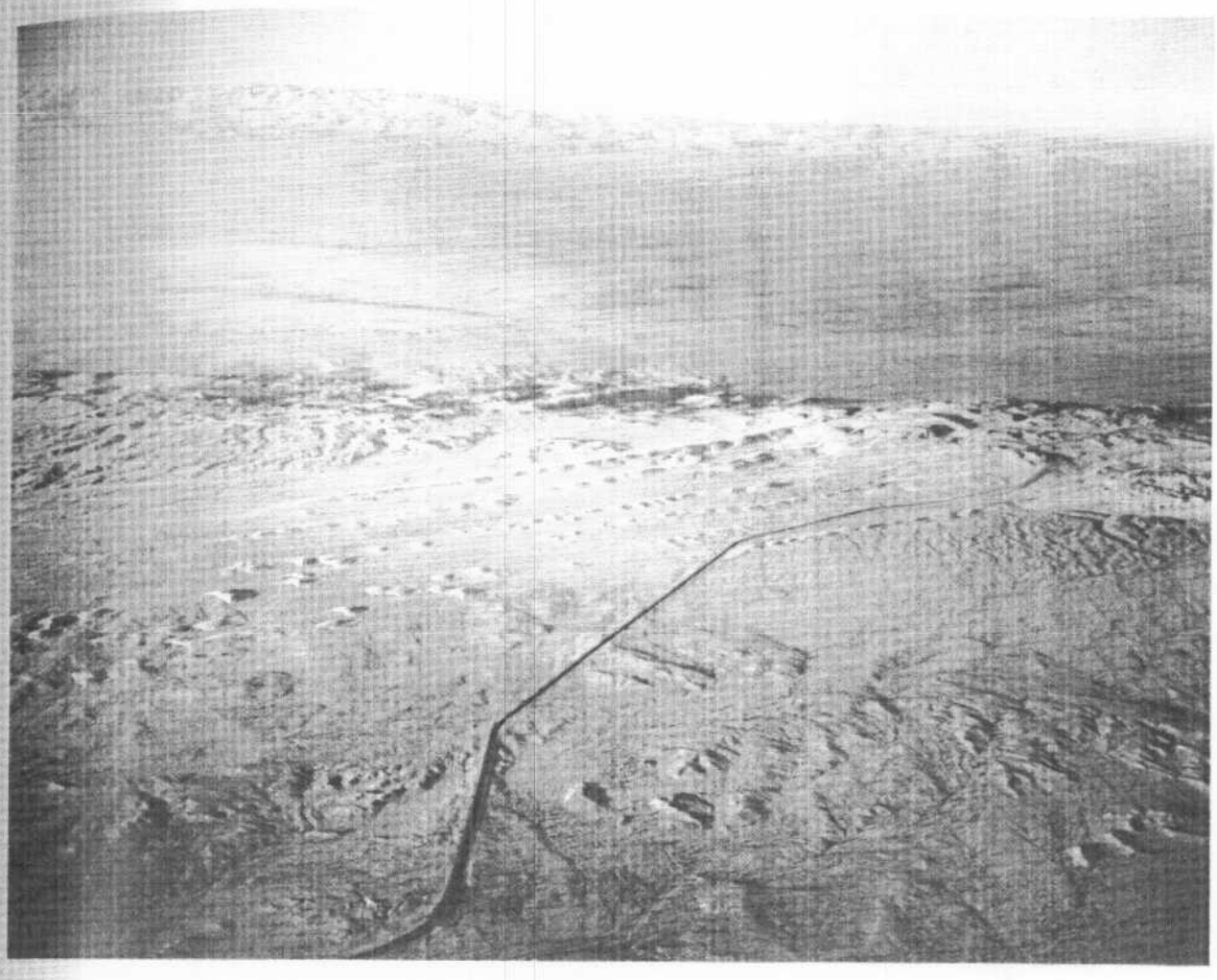

FIGURE 5-4. Poorly-developed barchans spawned from dune ridges at Superstition Mountain. (Aerial oblique photograph by John S. Shelton, No. 67-201, September, 1977.)

REFERENCES

Brown, J. S., 1923. The Salton Sea region, California: U. S. Geol. Survey Water Supply Paper 497, 290 p.

Eymann, J. E., 1953. A study of sand dunes in the Colorado and Mojave deserts: Univ. Southern California, unpub. M.S. Thesis.

6. GUIDE TO SELECTED FEATURES OF AEOLIAN GEOMORPHOLOGY IN THE ALGODONES DUNE CHAIN, IMPERIAL COUNTY, CALIFORNIA

Roger S. U. Smith
Department of Geology
University of Houston
Houston, Texas 77004

6. GUIDE TO SELECTED FEATURES OF AEOLIAN GEOMORPHOLOGY IN THE ALGODONES DUNE CHAIN, IMPERIAL COUNTY, CALIFORNIA

Roger S. U. Smith
Department of Geology
University of Houston
Houston, Texas 77004

The Algodones dune chain represents one of the largest and most accessible fields of unstabilized dunes in the United States. Its variety of forms and ease of access from two major highways render it well suited to both casual and serious study of the aeolian phenomena of sand transport and the development, migration, and destruction of sand dunes (Figs. 6-1 and 6-2). It is of particular and continuing interest to planetologists because the various aeolian landforms may provide analogs for martian landforms. Cutts and Smith (1973) and Breed (1977) have compared the Algodones dune chain with the Hellespontus dune field on Mars.

The Algodones dune chain has been described by Norris and Norris (1961), who also summarized earlier studies. Small-scale forms found within the dune chain range from small sand ripples to large granule ripples and include sand streamers anchored by bushes (Figs. 6-3 and 6-4). Intermediate-scale forms include "longitudinal" dune ridges, barchans and transverse dunes, both free and stabilized by vegetation (Figs. 6-5 and 6-6). Large-scale forms include "longitudinal" dunes tens of kilometers long, complex coalesced domical dunes, hybrid forms and the "megabarchans" of Norris and Norris (Figs. 6-7, 6-8, 6-9, 6-10, and 6-11). The surface of most large forms is extensively modified by "peak-and-hollow" topography.

The Algodones dunes overlie eroded Cenozoic sediments along the eastern margin of the tectonically-active Salton basin (Fig. 6-1). Kovach and others (1962) postulated an extension of the San Andreas fault beneath the length of the dune chain on the basis of seismic and gravity studies, but faulting is poorly expressed at the surface.

During Quaternary time, the Colorado River sometimes drained into the Salton basin, producing a succession of lakes whose highest level was stabilized by overflow across the Colorado River delta into the Gulf of California. The oldest known lake stand is represented by a warped shoreline which lies at 43 to 49 meters elevation along part of the basin's west side but which descends southward to disappear beneath the modern delta in Mexico (Stanley, 1962, 1965; Thomas, 1963). Along the basin's east side, this shoreline descends northward from an elevation of 49 meters at the south end of the dune chain to 30 meters at the north end and meets the 13 to 15 meter Holocene shoreline north of Niland (Loeltz and others, 1975; Robison, 1965). Nearshore deposits of this lake stand contain fresh-water shells whose radiocarbon age is about 37,000 years (Hubbs and others, 1963, 1965). A prominent Holocene shoreline at 13 to 15 meters elevation represents repeated filling of the Salton basin during the last 1900 years; several earlier stands have also been noted (Stanley, 1962; Hubbs and others, 1963, 1965). These Holocene stands are collectively called Lake Cahuilla, whose shoreline lies along the western margin of East Mesa, well west of the dune chain except at the chain's north end. East Mesa is a triange-shaped gravel plain, 40 to 60 kilometers on a side, which lies between the dune chain and the Imperial Valley (Fig. 6-2). The older, 37,000 year shoreline follows directly along the southwest margin of the dune chain.

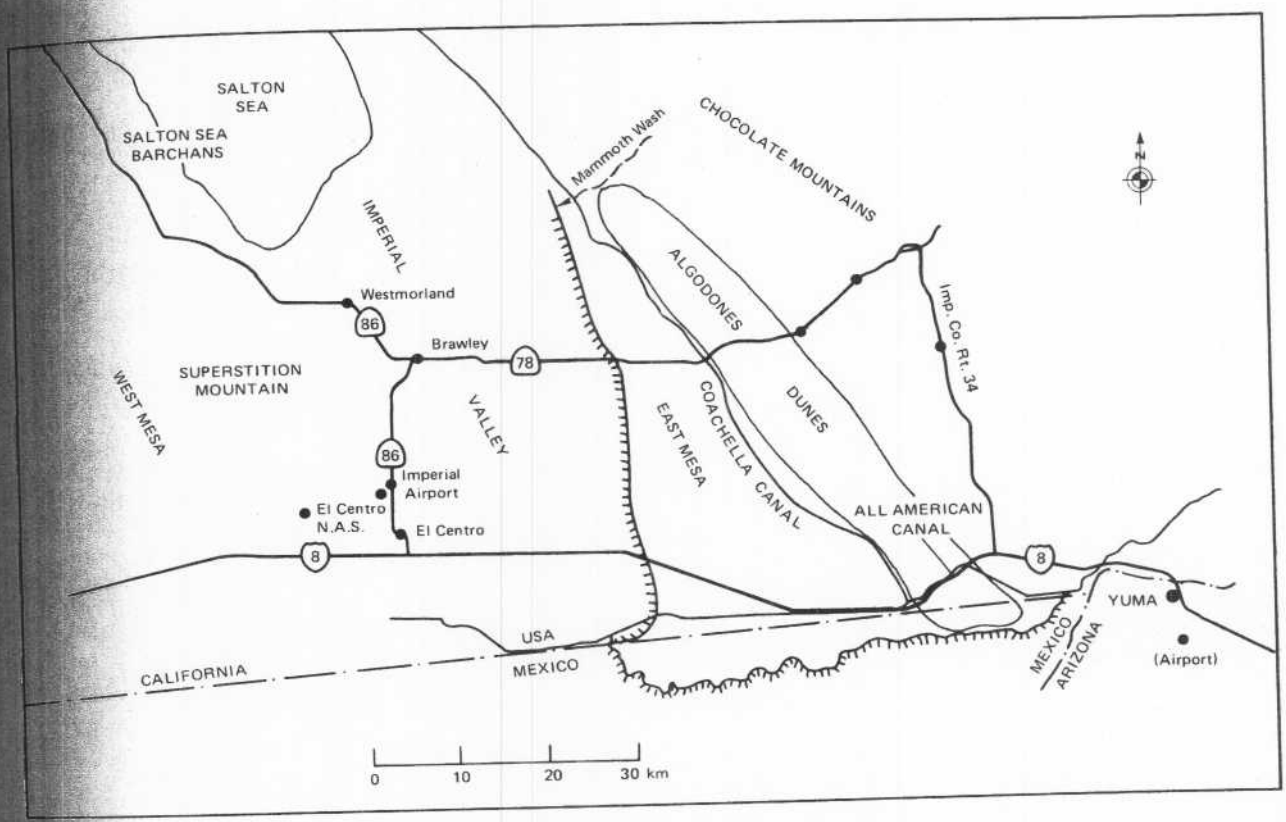

FIGURE 6-1. Index map of dune areas in the Imperial Valley, California.

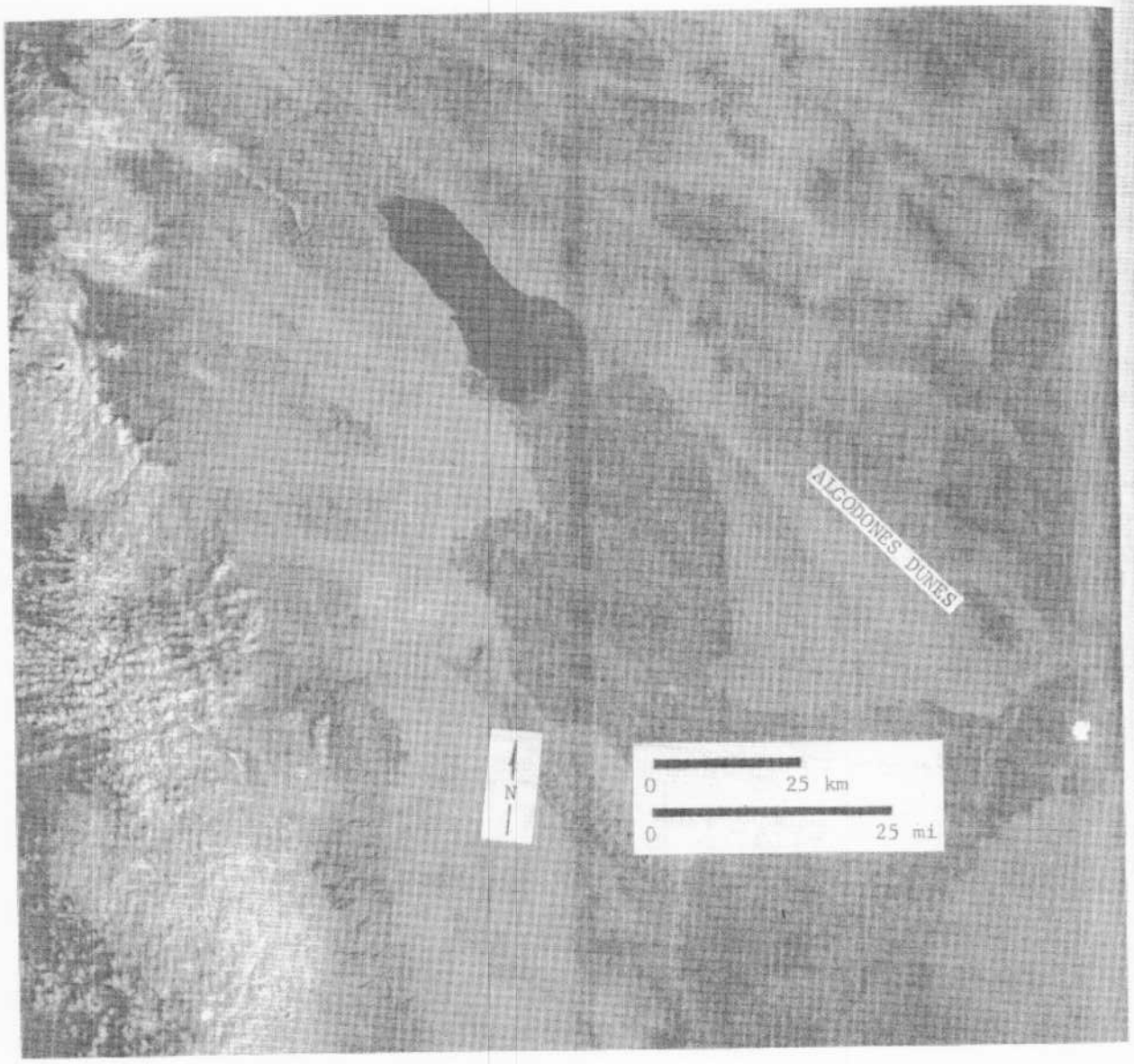

FIGURE 6-2. Orbital view of the Salton basin from Apollo spacecraft.

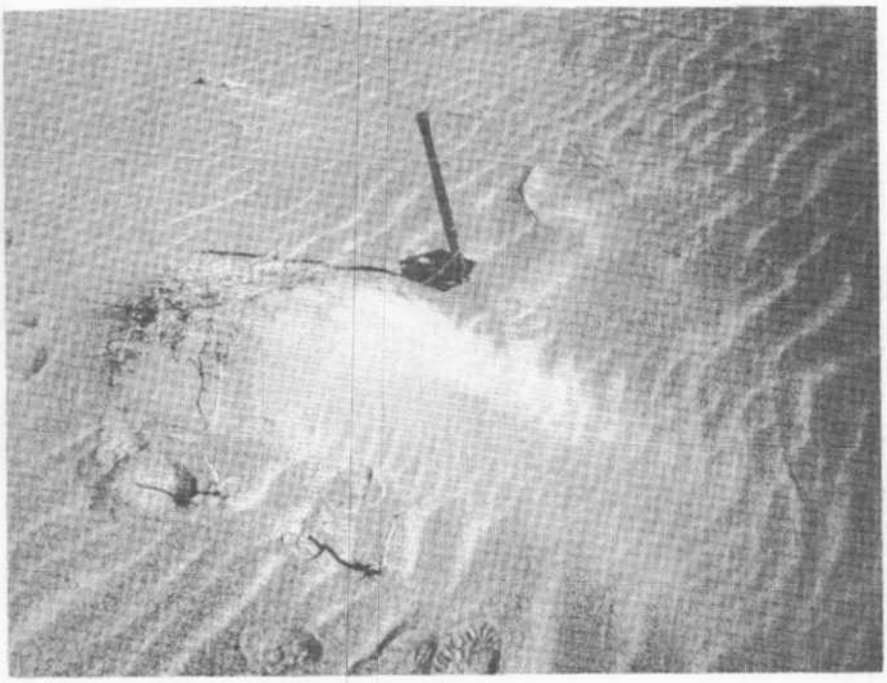

FIGURE 6-3. Sand streamer anchored by bush. Note that the ripple spacing in the fine sand of the streamer is much closer than in the coarse granule surface beneath the streamer. (West margin of dune chain, 8 km north of U. S. Interstate 8; January, 1976.)

FIGURE 6-4. Broadly-spaced granule ripples. Note that the trend of small ripples is oblique to the trend of large ones. (View to northeast along west margin of dune chain, 8 km north of U. S. Interstate 8; January, 1976.)

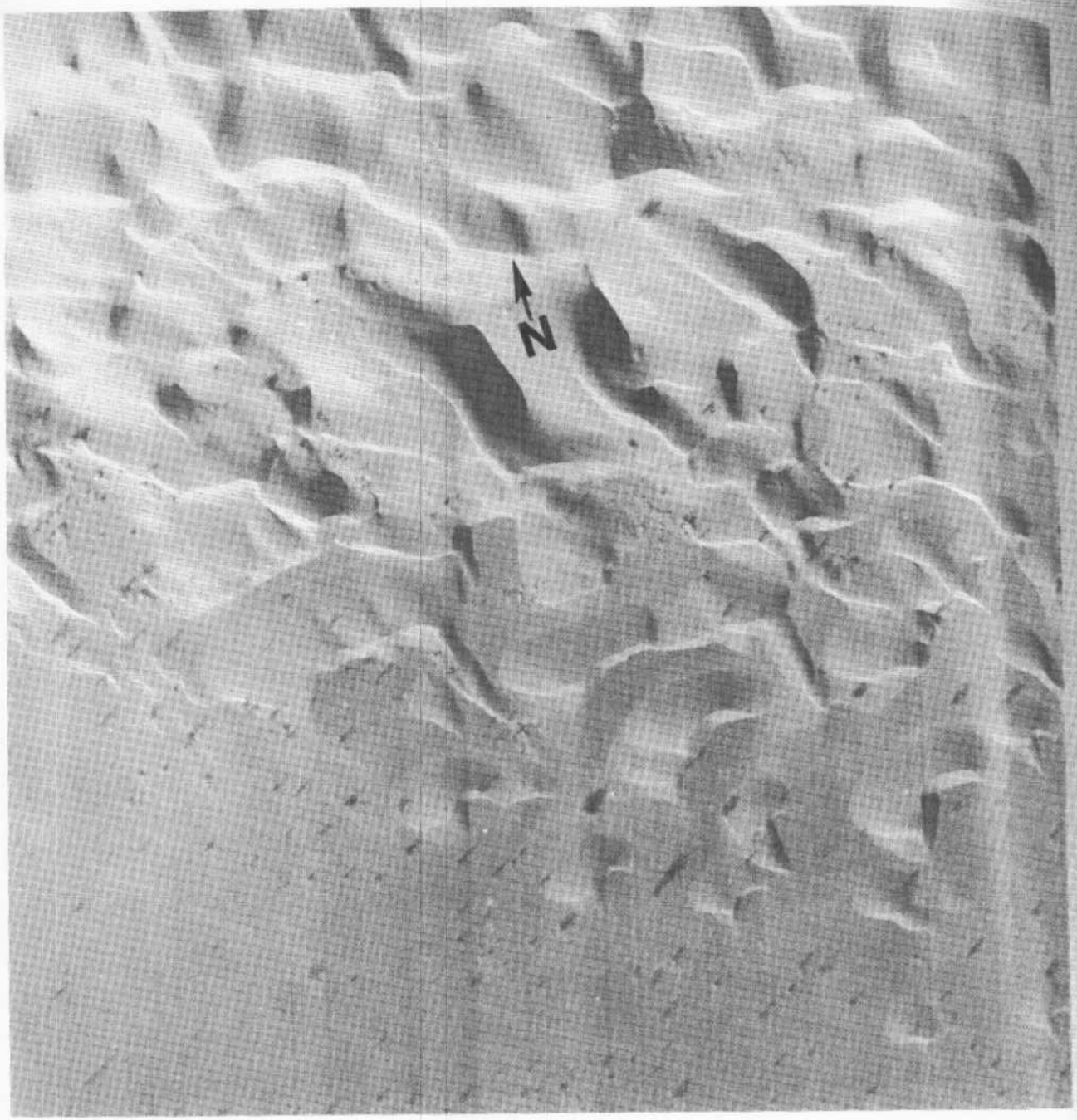

FIGURE 6-5. Vertical air photograph of barchans and longitudinal ridges. Recent north winds have modified the barchans' form. (Three km southeast of rest area on U.S. Interstate 8; January, 1976; tire tracks give scale.)

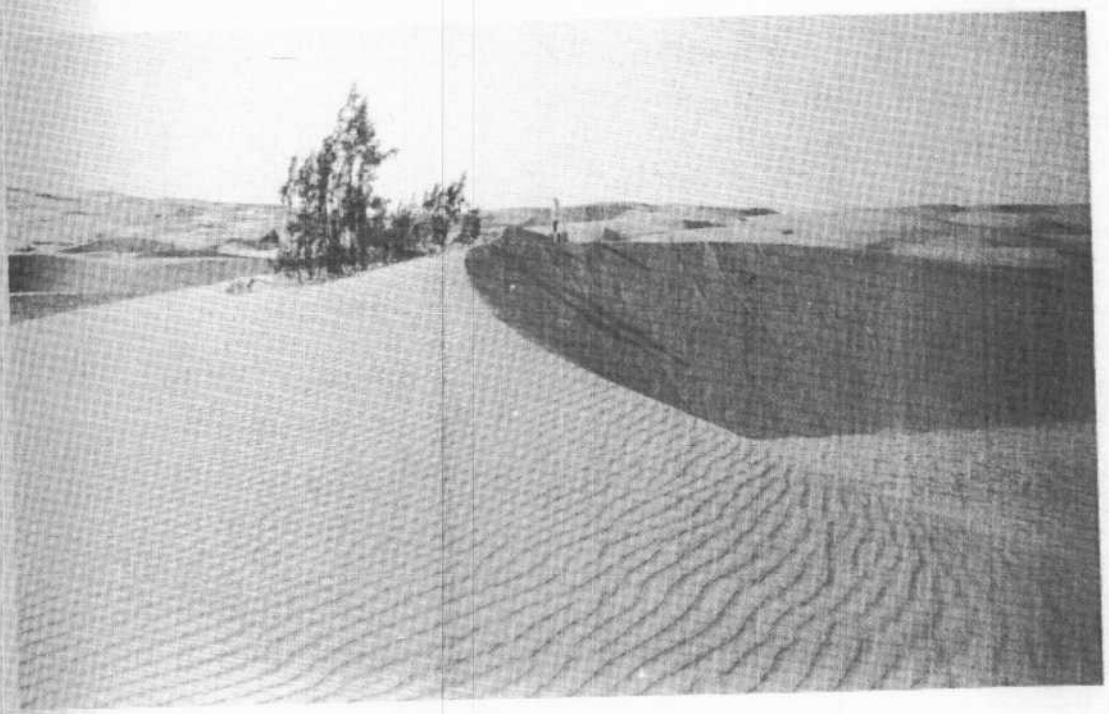

FIGURE 6-6. Ground view of barchans in vicinity of Figure 6-5. Looking east at barchan about 2 m tall; note that its form seems little affected by the creosote bush that it has overriden. (May, 1968.)

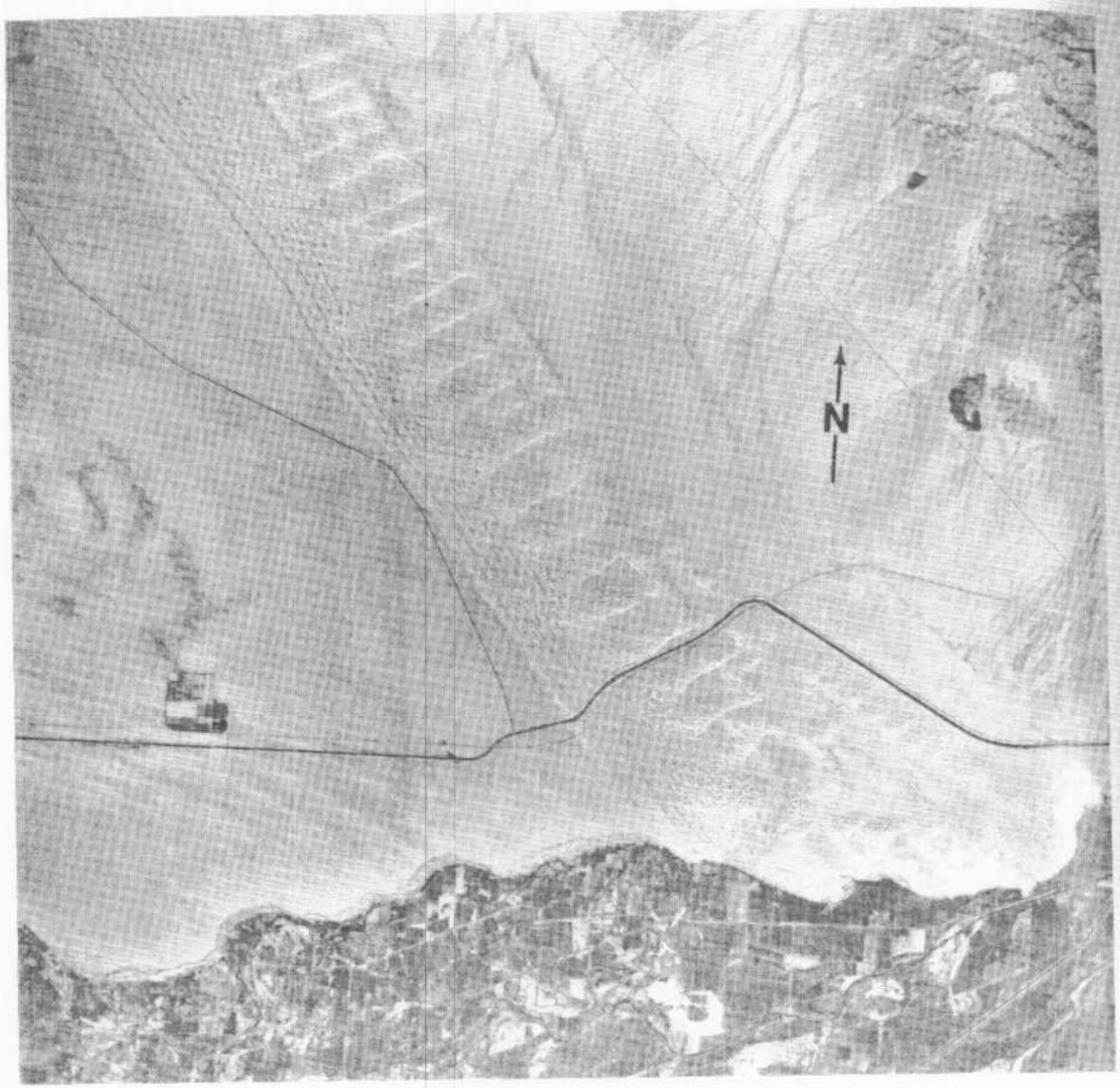

FIGURE 6-7. U-2 vertical air photo of the southern Algodones dune chain. Note: 1) Parallel dune ridges along the southwest margin of the dune chain; 2) Difference in trend between these ridges and those to the west; 3) Regular spacing of large domical dunes; and 4) Southeastward breakup of connected dunes into individual forms. (U.S. Geological Survey high-altitude Photo 665 V 049, November, 1967.)

FIGURE 6-8. Oblique aerial view to northwest across the southern Algodones dune chain. Note intradune hollows, floored by gravel, and sinuous dune ridges along the southwestern margin of the dune chain. (January, 1976.)

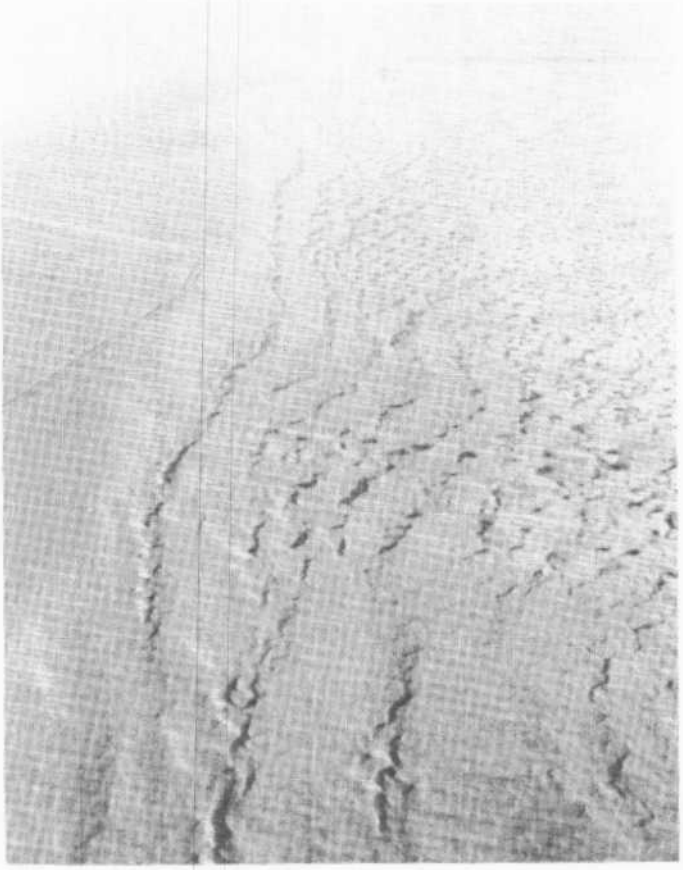

FIGURE 6-9. Oblique aerial view to the north-northwest along the southwestern margin of the dune chain. Note the continuity, sinuosity and parallelism of the dune ridges. (January, 1976.)

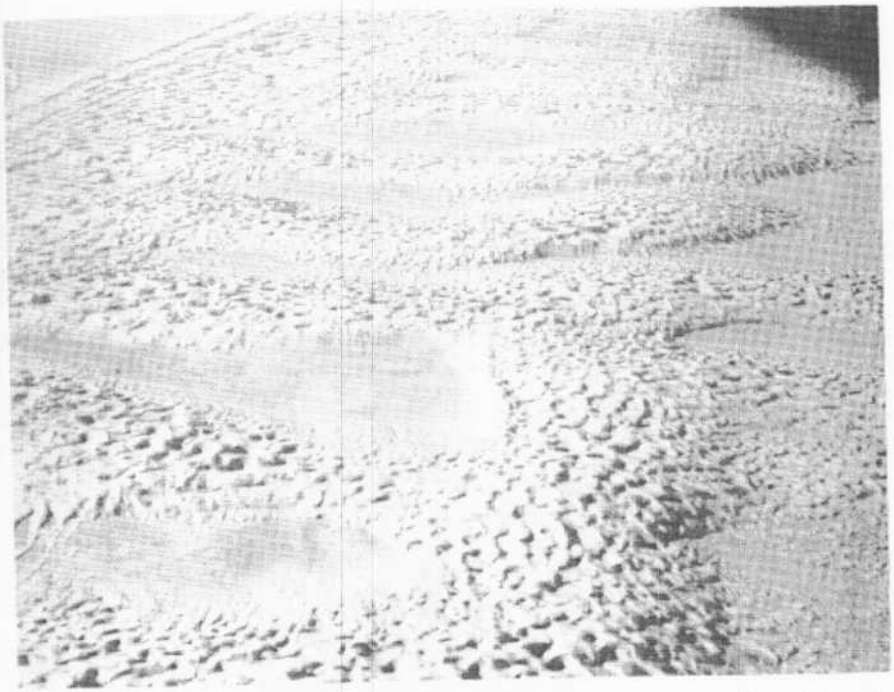

FIGURE 6-10. Oblique aerial view to the northwest across coalesced domal dunes, with tall, straight slip faces on the southeast margins of the saddles between them. (January, 1976.)

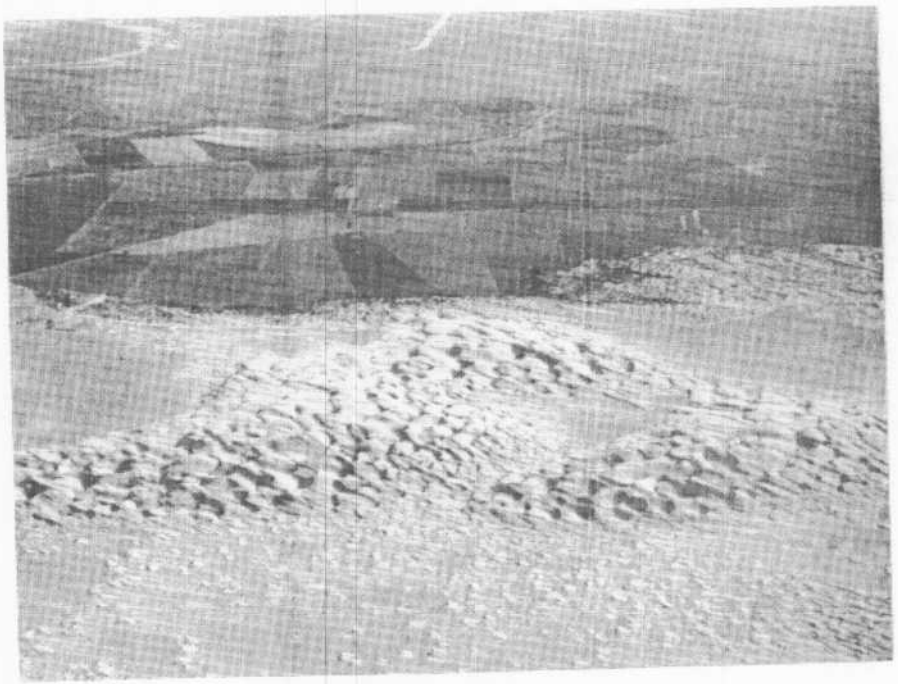

FIGURE 6-11. Oblique aerial view to the south across large, barchanoid dunes at the south end of the dune chain. These are the "megabarchans" of Norris and Norris (1961). Note the swarms of small barchans in the foreground. (January, 1976.)

DESCRIPTION OF THE DUNES

The Algodones dunes extend about 70 kilometers southeast from Mammoth Wash to the flood plain of the Colorado River just south of the Mexican border (Fig. 6-1). From north to south, the dune chain widens from about one kilometer to eight kilometers. Its total volume of sand is on the order of six to 11 billion cubic meters (Eymann, 1953; McCoy, Nockelberg and Norris, 1967). The dune chain consists primarily of complex, coalesced domal dunes 30 to 90 meters tall arranged in two to three sets parallel to the long axis of the dune chain. Domal dunes of adjacent sets are commonly joined into dumbbell-like forms by broad, northeast-trending saddles 0.3 to 1.2 kilometers long whose southeast margins commonly exhibit remarkably linear slip faces about 30 meters tall (Figs. 6-7 and 6-10). These "dumbbells" separate south of the All American Canal into *en echelon* sets of barchanoid dunes about one kilometer across (Figs. 6-7, 6-11, and 6-12). These intradune hollows are floored by lag gravel (Fig. 6-13).

Fields of barchan dunes occupy most of the intradune flats in the southern end of the dune chain (Norris, 1966). Within a representative field, these barchans are one-half to six meters tall and have migrated towards S 60-65°E at average rates of about five meters per year for large dunes and 20 meters per year for small dunes (Smith, 1970, 1972; Figs. 6-5, 6-6, 6-14, and 6-15). Despite seasonal reversal both of wind direction and the orientation of some small barchans, these dunes have not shrunk but continue to develop and prosper (Smith, 1977).

The southwestern margin of the dune chain is marked by a series of sinuous "longitudinal" dune ridges which parallel the edge of the chain and locally attain lengths of more than 20 kilometers (Figs. 6-7 and 6-9). These dune ridges are only approximately symmetrical in cross section. The orientation of slip faces along their crests alternates between northeast- to southwest-facing, depending on the latest direction of sustained sand-moving wind (Figs. 6-16 and 6-17). Typically, the ridges rise five to 25 meters above elongate troughs on their northeast margins, but only five to ten meters above a smooth, granule-covered surface on their southwest margins (Fig. 6-17). This granule surface seems to represent a lag deposit on fine-grained dune sand, and a comparable surface is found locally in swales along the dune ridges (Fig. 6-18). The granule surface slopes gently down to the desert floor to the southwest, 25 to 50 meters below. The surface is locally formed into low, gentle-sided, southeast-trending ridges arranged *en echelon* to the south-southeast trend of the margin of the dune chain. These ridges are typically steepest on their southwest sides. Remarkably, little dune sand is found on these ridges, but the granules themselves are formed into coarsely-spaced ripples (Figs. 6-3 and 6-4).

Dunes on East Mesa and along the northeast margin of the dune chain are mostly stabilized by vegetation. The northeast margin of the dune chain is a zone about two to three kilometers wide of choked transverse dunes and vegetation-shadow dunes less than six meters tall and some low, southeast-trending ridges (Figs. 6-7 and 6-12). Dunes on East Mesa are mostly low, broad east-southeast trending ridges, with some small local fields of transverse dunes and poorly-developed barchans (Figs. 6-7, 6-19, and 6-20).

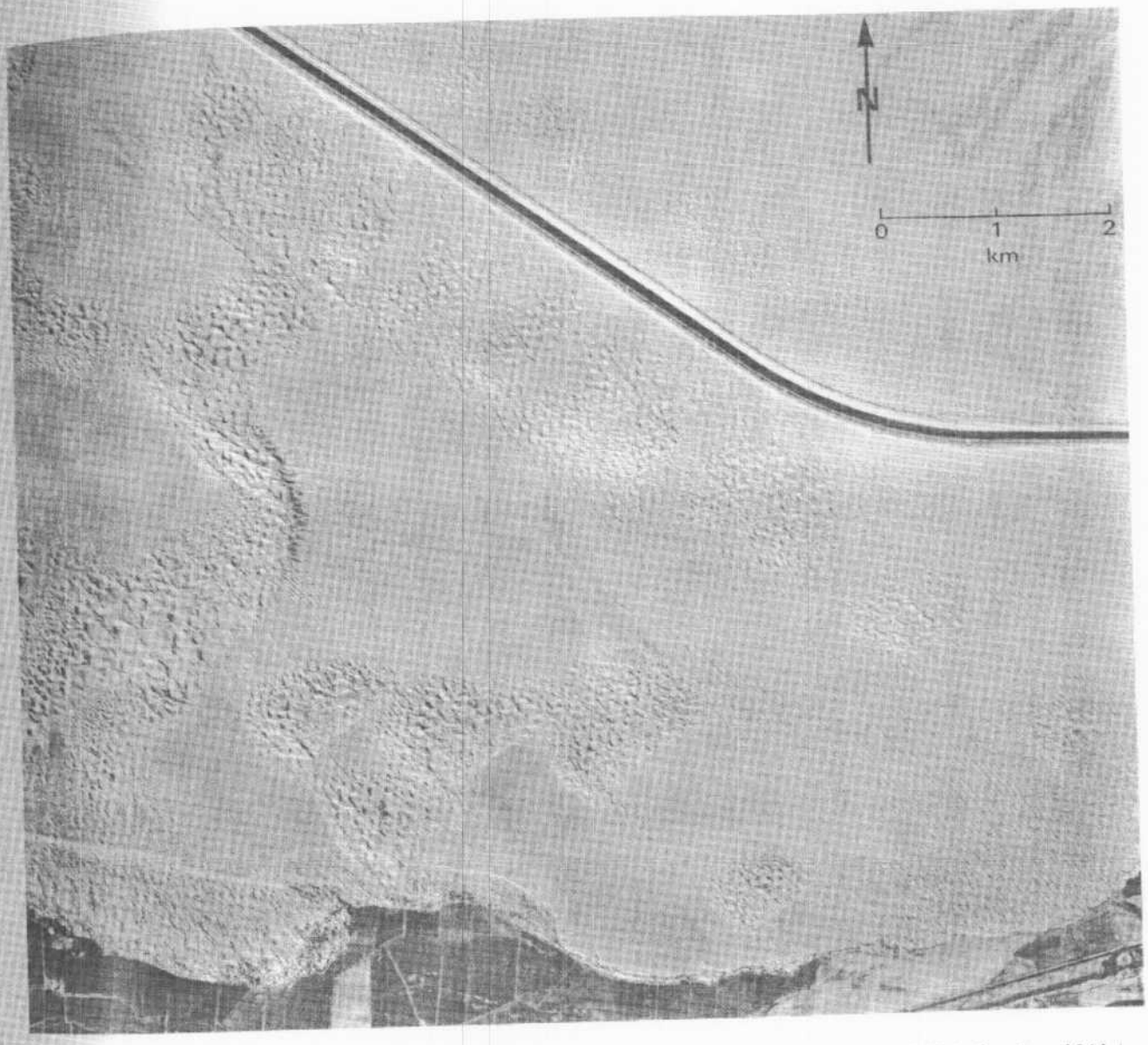

FIGURE 6-12. Vertical aerial photograph of the south end of the dune chain. (NOS 61 S7273A, October, 1961.)

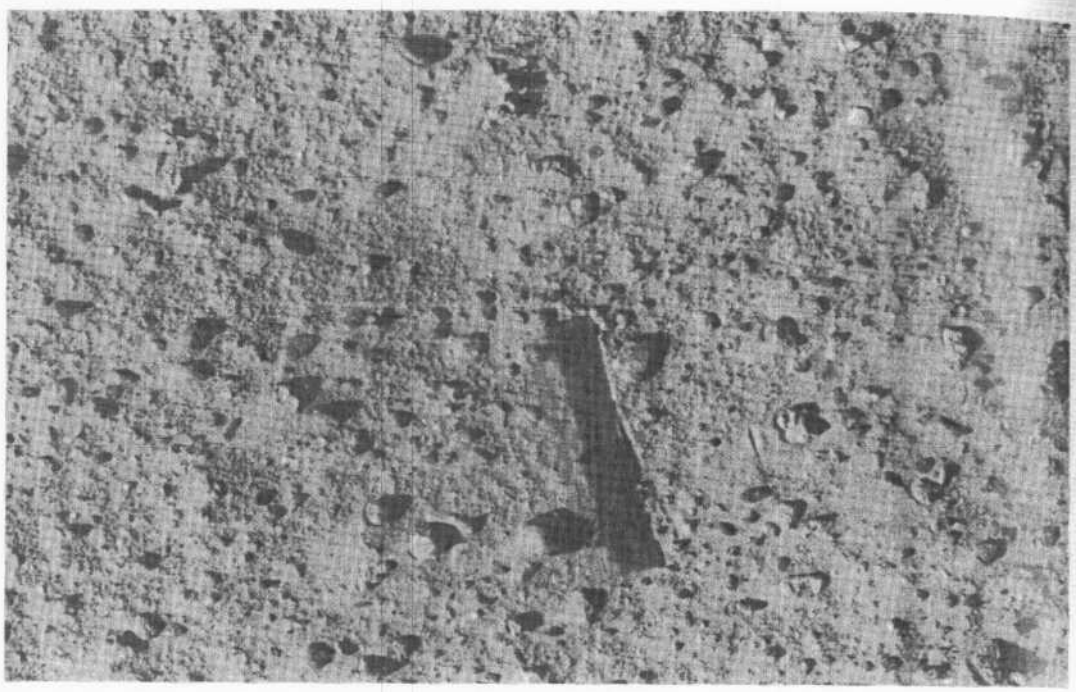

FIGURE 6-13. Lag gravel on floor of intradune hollow, 3 km southeast of rest area on U. S. Interstate 8. Scale is six inches long. (November, 1968.)

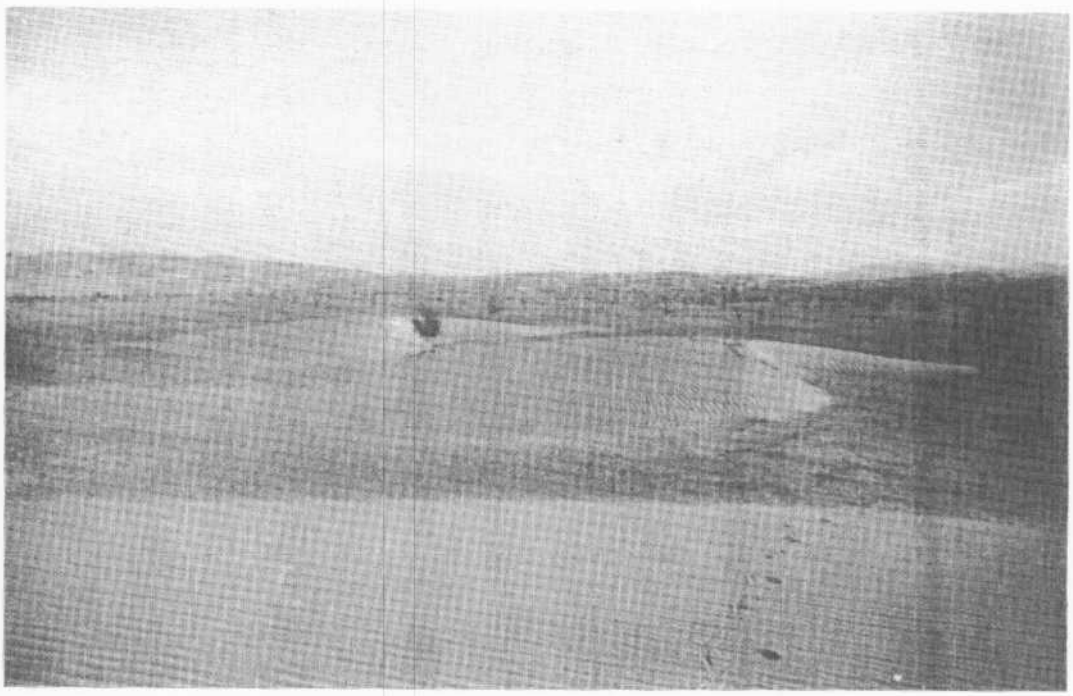

FIGURE 6-14. View to north across small barchan dunes 4 km southeast of rest area on U.S. Interstate 8. Note the rippled dune surface, the gravel pavement beneath the dunes and the stubby horns of these barchans. (June, 1968.)

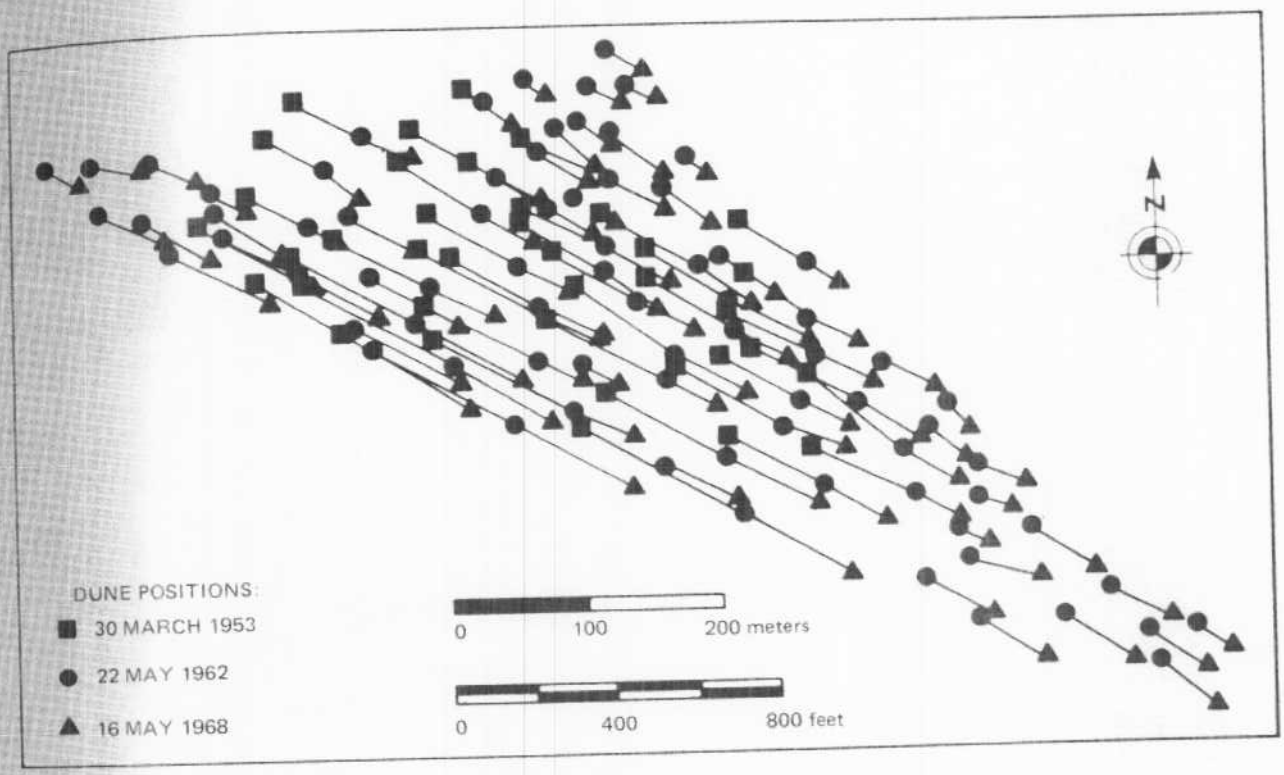

FIGURE 6-15. Map of 1953-1968 barchan migration within a field 3 km southeast of rest area on U.S. Interstate 8 (after Smith, 1970).

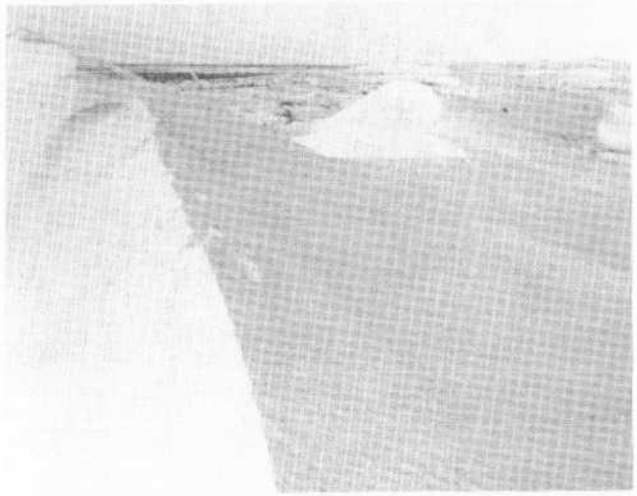

FIGURE 6-16. View to the northwest along dune ridge near west margin of dune chain, 8 km north of U.S. Interstate 8. Note the irregular crest of the dune, whose steeper side faces southwest. This is the westernmost dune ridge on Figure 6-9. (January, 1976.)

FIGURE 6-17. View to the southeast along dune ridge of Figure 6-16. Note the broad trough to the left and slip faces dropping down to a smooth, granule-covered surface. (January, 1976.)

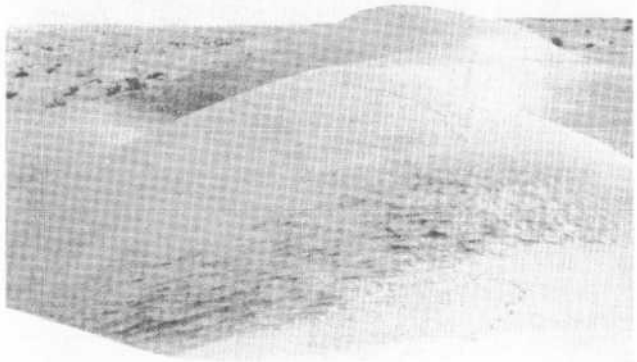

FIGURE 6-18. View to the southeast along dune ridge of Figure 6-16. Note the granule ripples in the lag surface in the saddle in the foreground. (January, 1976.)

FIGURE 6-19. Sand drifts and creosote bushes on East Mesa, 16 km southwest of western margin of Algodones dune chain and 5 km north of U.S. Interstate 8. (January, 1976.)

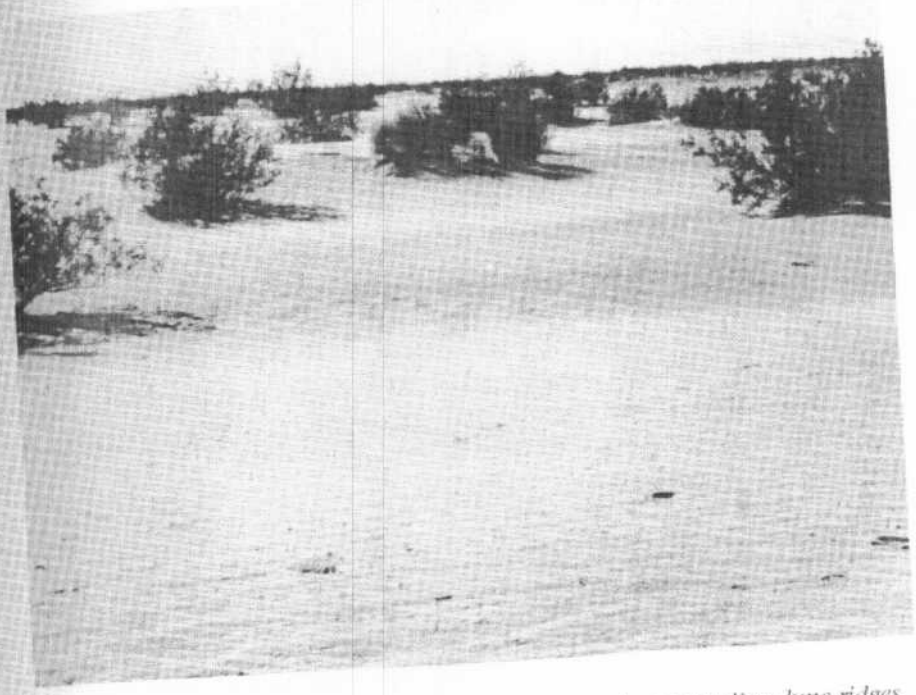

FIGURE 6-20. View to northeast across low, southeast-trending dune ridges on East Mesa. Location is 8 km southwest of western margin of Algodones dune chain and 10 km north of U. S. Interstate 8. (January, 1976.)

WIND REGIME

The regime of sand-blowing winds within the Algodones dune chain is imperfectly known because no weather station lies within the dunes and the wind regime to the west of the dunes differs from the wind regime to the east. Long-term wind records are available from airport stations at Yuma, Arizona, 20 to 80 kilometers to the southeast of the dunes, at Imperial, and El Centro Naval Air Station, 40 to 80 kilometers southwest of the dunes (Fig. 6-1). The wind regime at Imperial and El Centro is much stronger and more unidirectional than at Yuma, with winter winds blowing almost exclusively from the west-southwest to west sector (Figs. 6-21 and 6-22). As summer approaches, this pattern weakens as the direction shifts to the southwest to south-southwest sector with gentle opposing easterly winds. Winds at Yuma blow from a north-to-northwest sector from October through February, shifting to a west-to-northwest sector during March through May. As summer approaches, incursion of winds from the south-southeast sector become increasingly frequent, and winds from this sector prevail from late June through early September to the virtual exclusion of winds from other directions. Winds from this sector diminish through September and October during restoration of the northwesterly wind pattern. At all stations, winds tend to be strongest during the spring and weakest during the fall.

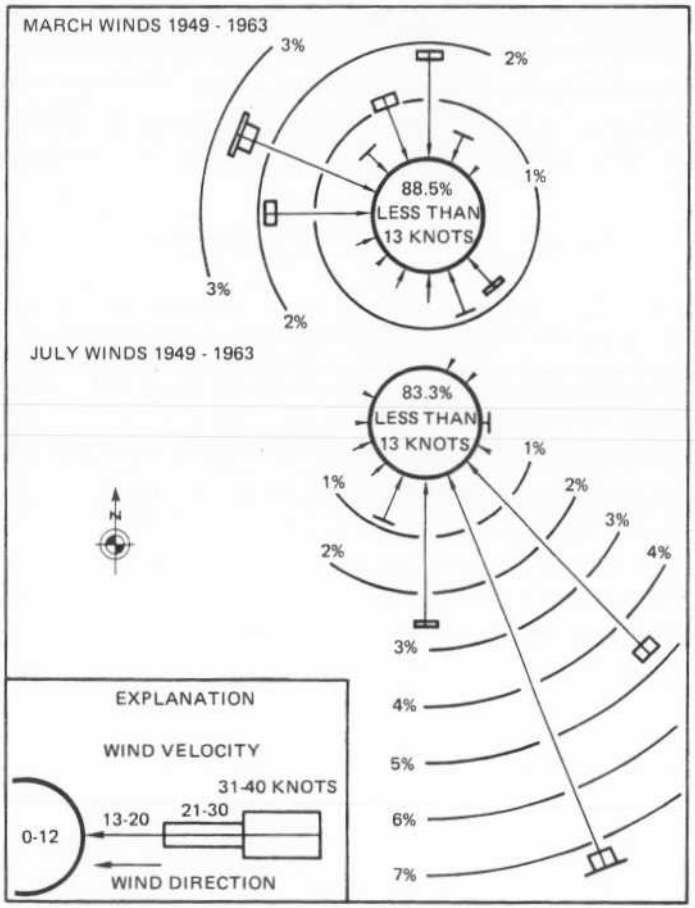

FIGURE 6-21. March and July wind roses for Yuma, Arizona, airport (after Smith, 1970).

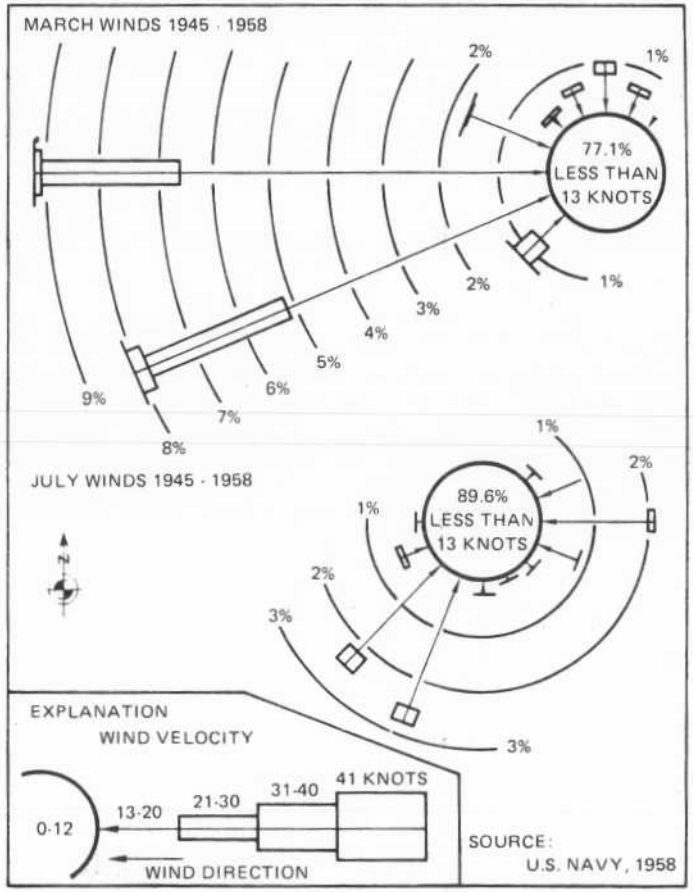

FIGURE 6-22. March and July wind roses for El Centro Naval Air Station, California (after Smith, 1970).

ORIGIN OF THE DUNE CHAIN

The origin of the Algodones dune chain is uncertain, but its sand is commonly thought to have been reworked from shorelines of the Quaternary lakes which intermittently filled the Salton basin. Brown (1923) inferred that southwest, west, and northwest winds pushed the dunes eastward from the shoreline of Lake Cahuilla five to thirty kilometers across East Mesa to their present position. Norris and Norris (1961) suggested that the dunes represent a chain of "megabarchans" formed near Mammoth Wash during lake recession, then extended into a dune chain by northwest winds. Using this hypothesis, McCoy and others (1967) computed the age of the dune chain to be 160,000 years by calculating the amount of sand which would be supplied to the source area by currents in Lake Cahuilla driven by five days per year of winds exceeding 31 knots; such a wind regime remains completely unsubstantiated by modern wind data from stations in the Salton basin (Figs. 6-21 and 6-22). Both Norris and Norris (1961) and McCoy and others (1967) assumed that the dune sand was ultimately derived from the mountains adjoining the Salton basin.

Loeltz and others (1975) argued that the dune sand was ultimately derived from the Colorado River delta, then blown directly east from the higher shoreline of Lake Cahuilla's Pleistocene predecessors, thus explaining the parallelism between this shoreline and the western margin of the dunes. Merriam (1969) and van de Kamp (1973) have confirmed that the dune sand resembles Colorado River sand more closely than it does sand derived from mountains bordering the Salton basin.

ROAD LOG

Mileage		
Cumulative	Difference	
0.0	0.0	Brawley, Intersection of California Highways 78 and 86. Turn east onto Highway 78.
14.3	14.3	Cross East Highline Canal and ascend across beach ridges of Lake Cahuilla onto East Mesa. The route across East Mesa and the Algodones dune chain is shown on three air-photo stereograms (Figs. 6-23, 6-24, and 6-25). The East Highline Canal marks the boundary between cultivated and uncultivated land on the west margin of Figure 6-23. Beach ridges of Lake Cahuilla trend parallel to the canal and are pocked by pits from which sand and gravel have been removed. The road ahead is elevated to prevent encroachment by drifting sand.
15.0	0.7	Road straightens. A series of broad, low, creosote-bush covered dune ridges trends subparallel to the road on both its south and north sides (Fig. 6-23). Most lack slip faces and are approximately symmetrical in cross section. Taller dunes, two to six kilometers to the south, are steeper and may have slip faces on either their north or south sides. Their height reaches 20 meters.

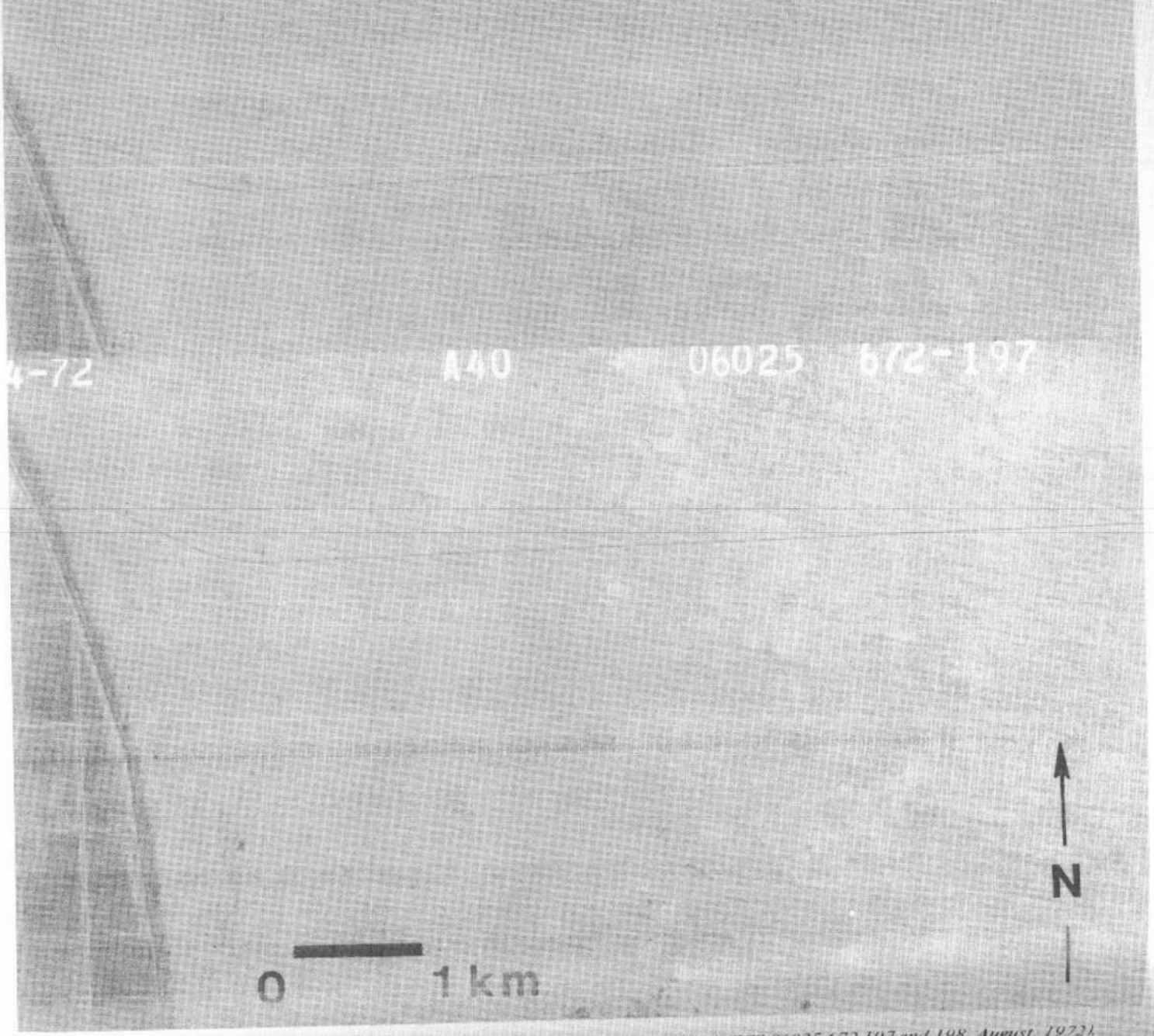

FIGURE 6-23. Air-photo stereogram of field trip route, western third. (USDA/ASCS 06025 672-197 and 198, August, 1972).

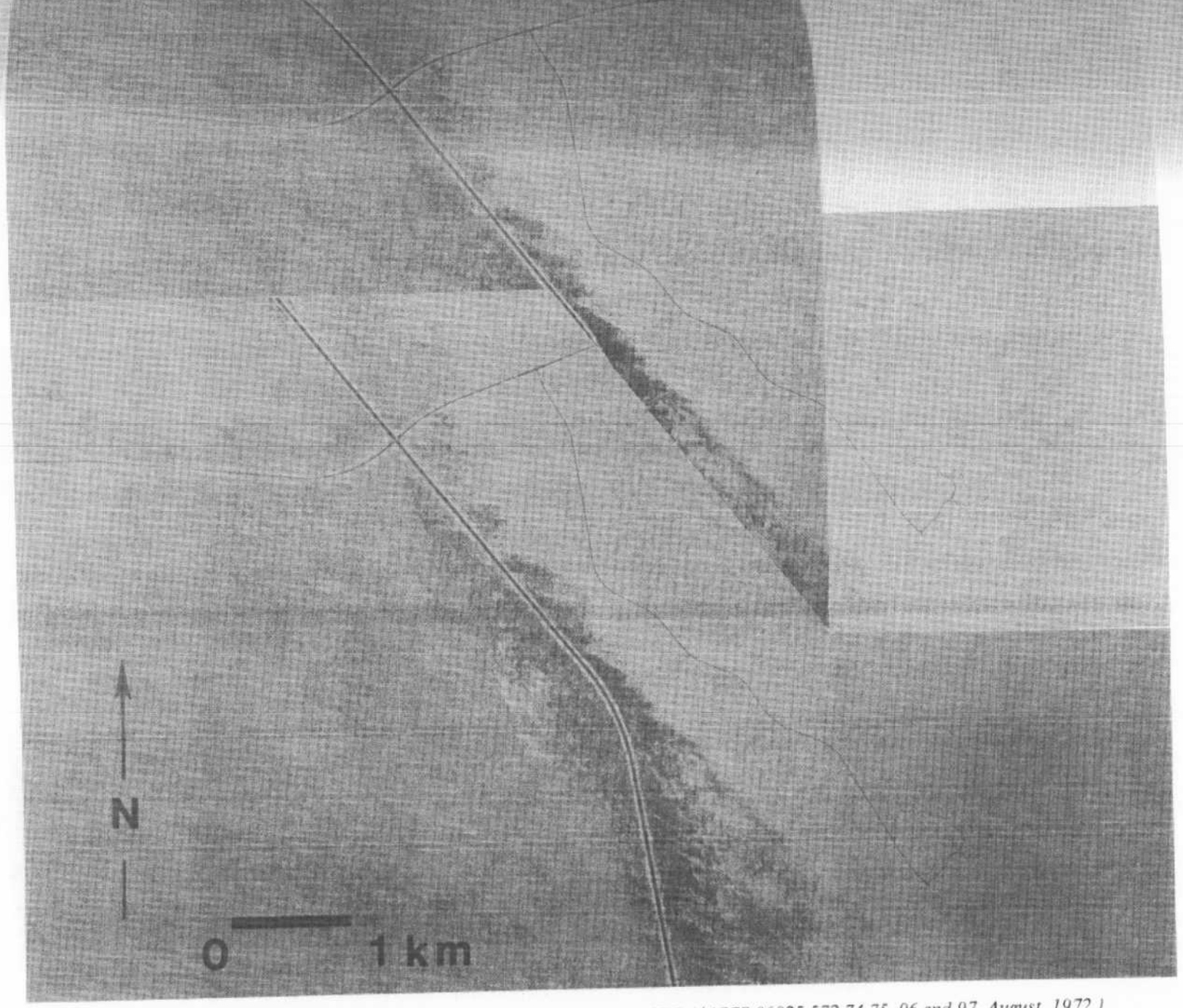

FIGURE 6-24. Air-photo stereogram of field trip route, middle third. (USDA/ASCS 06025 572-74 75, 96 and 97, August, 1972.)

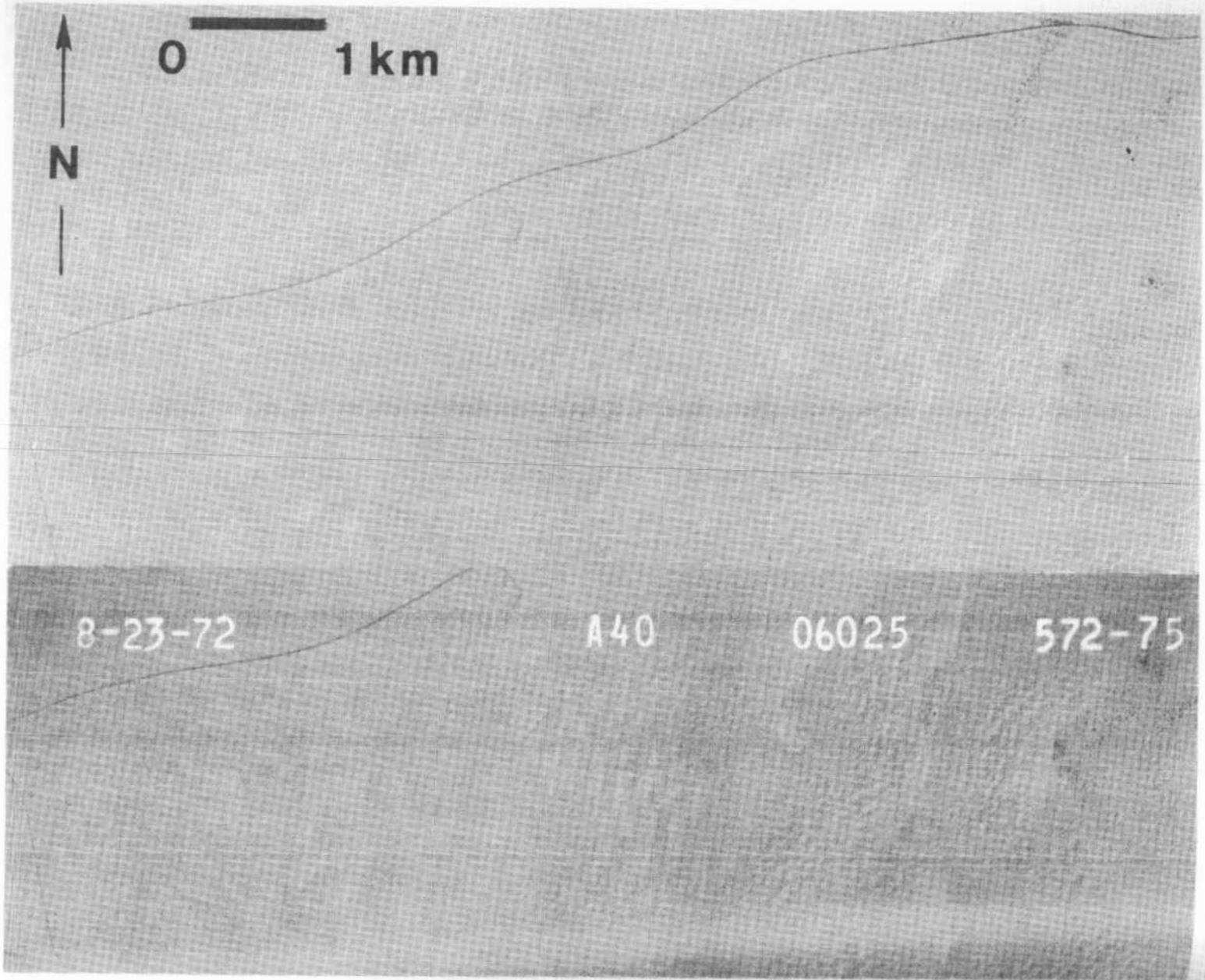

FIGURE 6-25. Air-photo stereogram of field trip route, eastern third. (USDA/ASCS 06025 572-74 and 75, August, 1972.)

Mileage Cumulative	Difference	
21.2	6.2	Cross Coachella Canal. This canal, trending northwest on Figure 6-24, here marks the approximate position of the southwestern margin of the Algodones dune chain. Note the sparseness of vegetation on the dunes ahead compared to the abundance of vegetation on the dune ridges of East Mesa behind. Ahead, the road climbs a gentle slope of subdued topography; this surface is armored by a surficial layer of granules. Broad ridges, arranged *en echelon* to the margin of the dune chain, are steepest on their south sides (Fig. 6-24).
22.0	0.8	Turn right onto paved road to Bureau of Land Management campground. This road traverses the granule surface at an elevation about 25 meters higher than the eastern margin of East Mesa. At about 23.7 miles, the road passes just to the right of a short longitudinal dune ridge.
25.3	3.3	Entrance to campground. Park wherever convenient; mileage will resume at this point upon leaving campground.
		STOP 1. Proceed northeastward from paved campground roads to low dune ridge about one-fourth kilometer northeast of last campground road. Climb to top of ridge and walk along it. Note that the symmetry of this feature is only approximate in cross section, and that troughs separate it from adjacent dune ridges to the northeast, particularly at its north and south ends. A slip face may be present on either the northeast or southwest side of the crest, depending on the latest direction of sand-blowing winds. Note also that swales interrupt the continuity of the dune ridge. Proceed along crest for about one-half kilometer before returning to vehicles, then retrace route to Highway 78.
28.6	3.3	Turn right onto Highway 78. This intersection is just west of the western margin of Figure 6-25. At about 28.9 miles, a longitudinal dune ridge lies just north of the road and resembles the dune ridge at Stop 1 (Fig. 6-26). Ahead, the road crosses several more similar ridges, a broad swale and ascends the north flank of a domical dune.
31.0	2.4	Turn right on paved road to Hugh Osborn County Park. Proceed up hill.
31.3	0.3	STOP 2. Park at lookout. Parking space may be quite limited, particularly on weekends. This lookout is on the crest of the dune chain at an elevation of about 100 meters above the eastern edge of East Mesa. Still taller dunes can be seen to the southeast (Fig. 6-27). The lookout is on a domical dune which has a slip face at its eastern base (Fig. 6-25). To the east and southeast, domical dunes are less congested, lower, and may assume a barchanoid form (Fig. 6-26). Note the extensive development of peak-and-hollow topography on the domical dunes (Fig. 6-27). To the west is a series of low "longitudinal" dunes, separated by swales from the domical dunes along the axis of the dune chain. To the northwest, domical dunes die out into a series of tall "longitudinal" dune ridges at the north end of the dune chain.

FIGURE 6-26. View to northwest along "longitudinal" dune ridge north of Highway 78, about 1.1 miles east of Coachella Canal. Note that the southwest side is steeper than the northeast side and that the crest is sinuous in plan and varies in height. (January, 1976.)

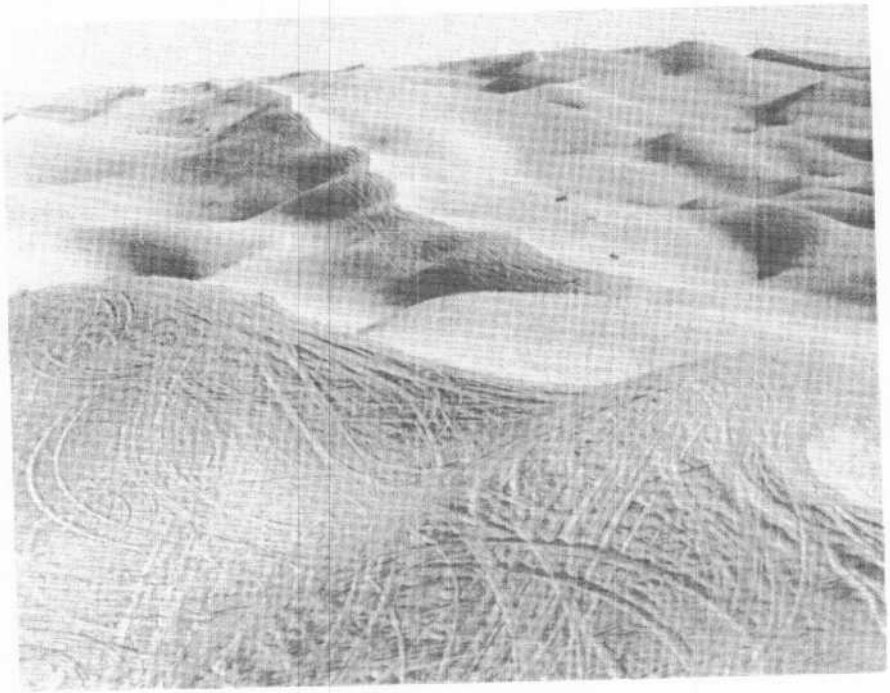

FIGURE 6-27. View to southeast from Hugh Osborn County Park. Note the broad, domical nature of dunes along the axis of the dune chain and the extensive development of peak-and-hollow topography, here somewhat defaced by dune-buggy tracks. (January, 1976.)

The morphology of features here suggests that west and northwest winds predominate over winds from other directions. However, winds from the south to southeast are sometimes very effective in moving sand. Figure 6-28 shows a well-formed barchan formed by such winds during the summer of 1964 on the pavement of this parking lot.

Retrace route to Highway 78.

31.6 0.3 Turn right onto Highway 78 and proceed down east flank of dune chain. Note that the east margin of the dune chain is much less distinct than the west margin and the small dunes here are different, being mostly low transverse dunes, some stabilized or influenced by vegetation.

35.6 4.0 Railroad tracks. Cross tracks and turn around at old railroad station at Glamis, following Highway 78 back to Brawley. As an alternative, follow Highway 78 eastward across scenic desert mountains to Blythe, about 60 miles distant.

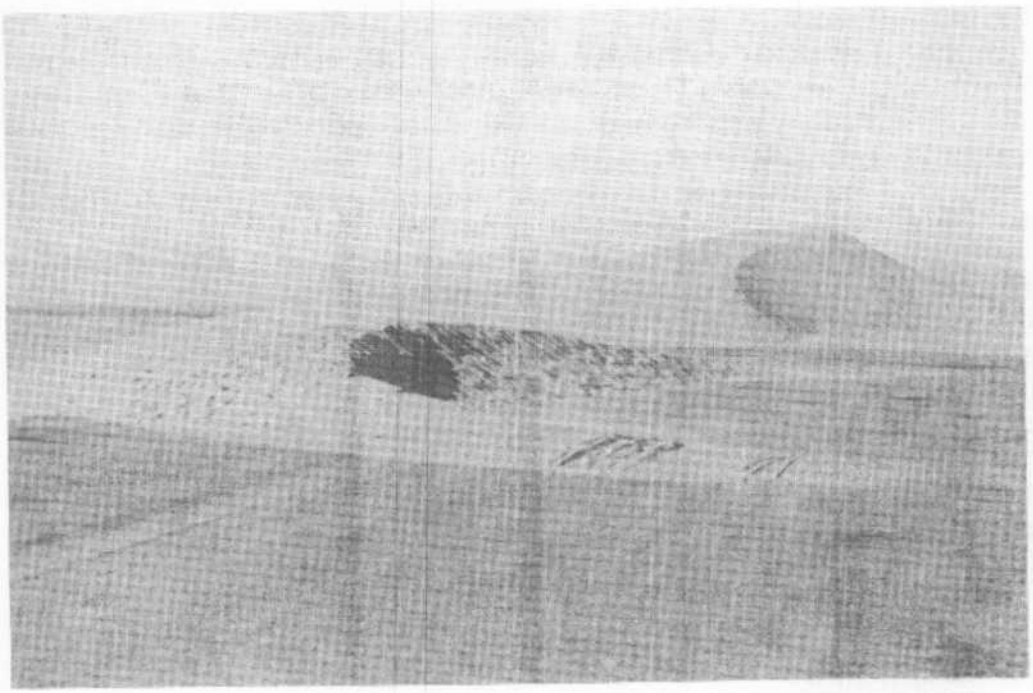

FIGURE 6-28. Small barchan on parking lot at Hugh Osborn County Park. This dune is about 1 m tall and opens to the north and northwest. It was probably formed by southeast and south-southeast summer winds. (August, 1964.)

REFERENCES

Breed, C. S., 1977. Terrestrial analogs of the Hellespontus dunes, Mars: Icarus, vol. 30, pp. 326-340.

Brown, J. S., 1923. The Salton Sea region, California: U. S. Geol. Survey Water-Supply Paper 497, 290 p.

Cutts, J. A. and R. S. U. Smith, 1973. Aeolian deposits and dunes on Mars: Jour. Geophys. Res., vol. 78, pp. 4139-4154.

Eymann, J. E., 1953. A study of sand dunes in the Colorado and Mojave deserts: unpub. M.S. thesis, Univ. Southern California.

Hubbs, C. L., G. S. Bien, and H. E. Suess, 1963. La Jolla natural radiocarbon measurements III: Radiocarbon, vol. 5, pp. 254-272.

Hubbs, C. L., G. S. Bien, and H. E. Suess, 1965. La Jolla natural radiocarbon measurements IV: Radiocarbon, vol. 7, pp. 66-117.

van de Kamp, P. C., 1973. Holocene continental sedimentation in the Salton basin, California: A reconnaissance: Geol. Soc. America Bull., vol. 84, pp. 827-848.

Kovach, R. L., C. R. Allen, and F. Press, 1962. Geophysical investigations in the Colorado delta region: Jour. Geophys. Res., vol. 67, pp. 2845-2871.

Loeltz, O. J., B. Irelan, J. H. Robison, and F. H. Olmsted, 1975. Geohydrologic reconnaissance of the Imperial Valley, California: U. S. Geol. Survey Prof. Paper 486-K.

McCoy, F. M., Jr., W. J. Nokleberg, and R. M. Norris, 1967. Speculations on the origin of the Algodones dunes, California: Geol. Soc. America Bull., vol. 78, no. 8, pp. 1039-1044.

Merriam, R., 1969. Source of sand dunes of southeastern California and northwestern Sonora, Mexico: Geol. Soc. America Bull., vol. 80, pp. 531-534.

Norris, R. M., 1966. Barchan dunes of Imperial County, California: Jour. Geology, vol. 74, no. 3, pp. 292-306.

Norris, R. M. and K. S. Norris, 1961. Algodones dunes of southeastern California: Geol. Soc. America Bull., vol. 72, no. 4, pp. 605-620.

Robison, J. H., 1965. Environment of the Imperial trough, California, during the Quaternary: A paleogeographic problem (abs.): Geol. Soc. America Special Paper 87 (Abs. for 1965), p. 227.

Smith, R. S. U., 1970. Migration and wind regime of small barchan dunes within the Algodones dune chain, southeastern Imperial County, California: Univ. Arizona, unpub. M.S. thesis, 125 p.

Smith, R. S. U., 1972. Barchan dunes in a seasonally-reversing wind regime, southeastern Imperial County, California: Geol. Soc. America, Abs. Programs, vol. 4, pp. 240-241.

Smith, R. S. U., 1977. Barchan dunes: Development, persistence and growth in a multi-directional wind regime, southeastern Imperial County, California: Geol. Soc. America, Abs. Programs, vol. 9, p. 502.

Stanley, G. M., 1962. Prehistoric lakes in the Salton Sea basin (abs): Geol. Soc. America Special Paper 73 (Abs. for 1962), pp. 249-250.

Stanley, G. M., 1965. Deformation of Pleistocene Lake Cahuilla shoreline, Salton basin, California (abs.): Geol. Soc. America Special Paper 87 (Abs. for 1965), p. 165.

Thomas, R. G., 1963. The late Pleistocene 150 foot fresh water shoreline of the Salton Sea area: Southern California Acad. Sci. Bull., vol. 62, pt. 1, pp. 9-18.

U. S. Navy, Office of Chief of Naval Operations, National Weather Service Division, 1958. Summary of monthly aerological records no. 23199: El Centro, California, 2/45-2/58: Asheville, N. C., Office of Navy Representative, National Weather Records Center, 71 p. (unpub.).

7. GEOLOGICAL FIELD GUIDE TO THE SALTON TROUGH

Eilene Theilig, Michael Womer, Ronald Papson
Department of Geology and
Center for Meteorite Studies
Arizona State University
Tempe, Arizona 85281

7. GEOLOGICAL FIELD GUIDE TO THE SALTON TROUGH

Eilene Theilig, Michael Womer, Ronald Papson
Department of Geology and
Center for Meteorite Studies
Arizona State University
Tempe, Arizona 85281

A geological survey of the Salton Trough province in southern California is possible with the four field trips included here. A short trip (4.8 miles) from Palm Desert to Dead Indian Canyon Vista Point provides an excellent overview of Coachella Valley. From Palm Desert to Brawley (100.0 miles) many aeolian features will be identified and discussed. Major interests are the Martinez rock slide, Tule Wash dune, Travertine Point, and Salton Sea barchan dunes. A side trip westward to Clark Dry Lake (16.5 miles) will allow investigation of silt-clay dunes. The Brawley to Palm Desert trip (258.1 miles) includes aeolian features (Algodones dune field), volcanic features (Salton Domes), and fault structures (Mecca fault, Orocopia fault, and Indio Hills).

PALM DESERT TO DEAD INDIAN CANYON VISTA POINT

Mileage		
Cumulative	Difference	
0.0	0.0	Junction State Highway 111 and State Highway 74; turn south onto State Highway 74. Dead Indian Canyon is one of several canyons cut by intermittent streams draining the northeastern Santa Rosa Mountains. It is bounded on the east by Indio Mountain, composed of the late Jurassic Bradley Granodiorite and locally varies from quartz diorite to quartz monzonite (Miller, 1944). To the west is Haystack Mountain, consisting of both Bradley Granodiorite and the Palm Canyon Complex.
2.6	2.6	On the left is the intrusive contact between the Palm Canyon Complex and Bradley Granodiorite.
4.0	1.4	Sandy road into Dead Indian Creek Wash before the bridge. The Palm Canyon Complex is exposed in the canyon wall and consists of granite injected into well-bedded metasediments, with subordinate diorite. Most of the unit is well-banded gneiss, migmatite, impure foliated granite, pegmatite granite, quartzfels, interbedded limestone, quartzite, and mica schist (Miller, 1944) (Figs. 7-1, 7-2). From here the road is narrow and winding and provides little opportunity to stop. Road cuts expose Bradley Granodiorite, Palm Canyon Complex, and Chuckwalla Complex. It also crosses a fault which thrusts granodiorite southward over the Palm Canyon Complex. As the highway winds up Seven-level Hill, vegetation changes from low desert cacti to yucca, agave, mesquite, and ocotillo, to scrub oak and mountain mahogany, and to ponderosa pine near the top.

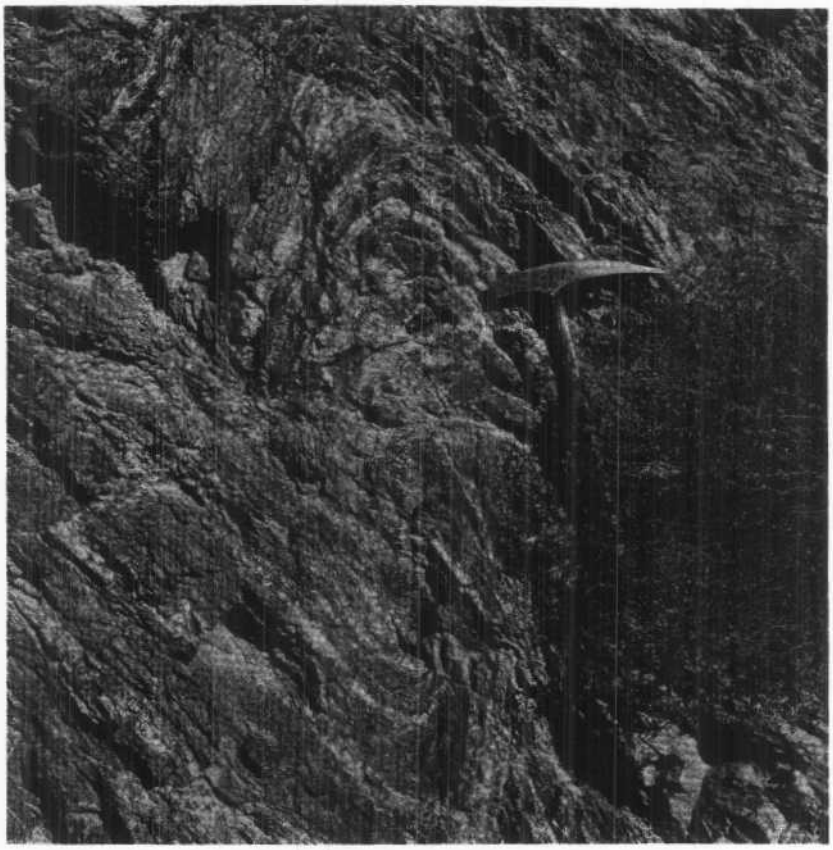

FIGURE 7-1. Highly deformed metamorphic rocks of the Palm Canyon Complex. (Photograph by Ronald Papson, University of Santa Clara, May, 1977.)

Mileage	
Cumulative	Difference
8.8	4.8

STOP 1. DEAD INDIAN CANYON VISTA POINT. View of the north central portion of Coachella Valley, the northwestern-most extension of the Salton Trough (Fig. 7-3). Coachella Valley is bordered on the southwest by the San Jacinto and Santa Rosa Mountains of the Peninsular Ranges and on the northeast by both the Little San Bernardino Mountains and the Orocopia Mountains of the Transverse Ranges. Late Cenozoic sediments, representing almost continual deposition since the Miocene, attain a maximum exposed thickness of 2621 m in this area but may elsewhere fill the basin to a greater depth (Dibblee, 1954). Part of the valley fill can be seen in the Indio Hills at the base of the Little San Bernardino Mountains. These hills were formed by deformation of sediments along the Banning and Mission Creek faults.

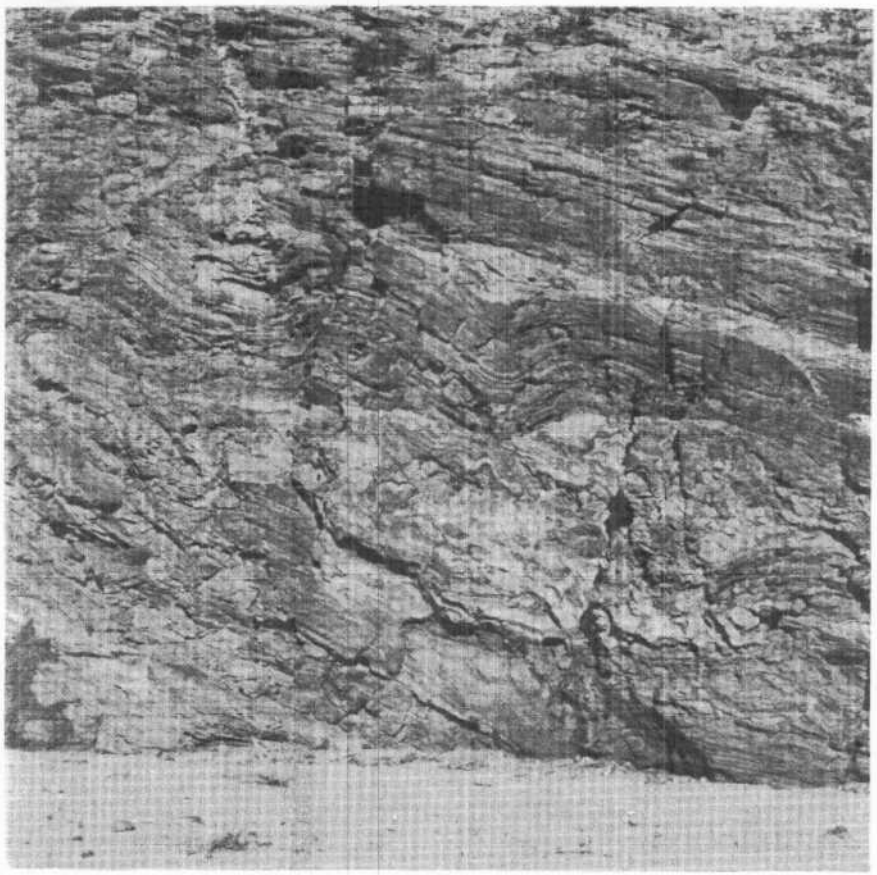

FIGURE 7-2. Palm Canyon Complex, composed of well-bedded metasediments, intruded by granite with subordinate diorite. Portion of outcrop is about 5 m high. (Photograph by Ronald Papson, University of Santa Clara, May, 1977.)

Mileage
Cumulative Difference

The large light tan area in the central valley floor is Palm Springs Sand Ridge. It consists of windblown sand carried through San Gorgonio Pass and deposited as wind velocity decreased through the valley. Depositional features range from small wind shadow dunes near Palm Springs to sand hills 1.5 to 9 m high near the southeastern end of the ridge. Barchan and transverse dunes are present on the ridge margins.

Near the mouth of Dead Indian Canyon at the base of the western wall are the dark metasediments of the Palm Canyon Complex. The contact with Bradley Granodiorite is traceable along the wall and around the end of the point.

From this vantage point the effects of irrigation are clearly visible. The developed areas markedly contrast with the natural desert landscape.

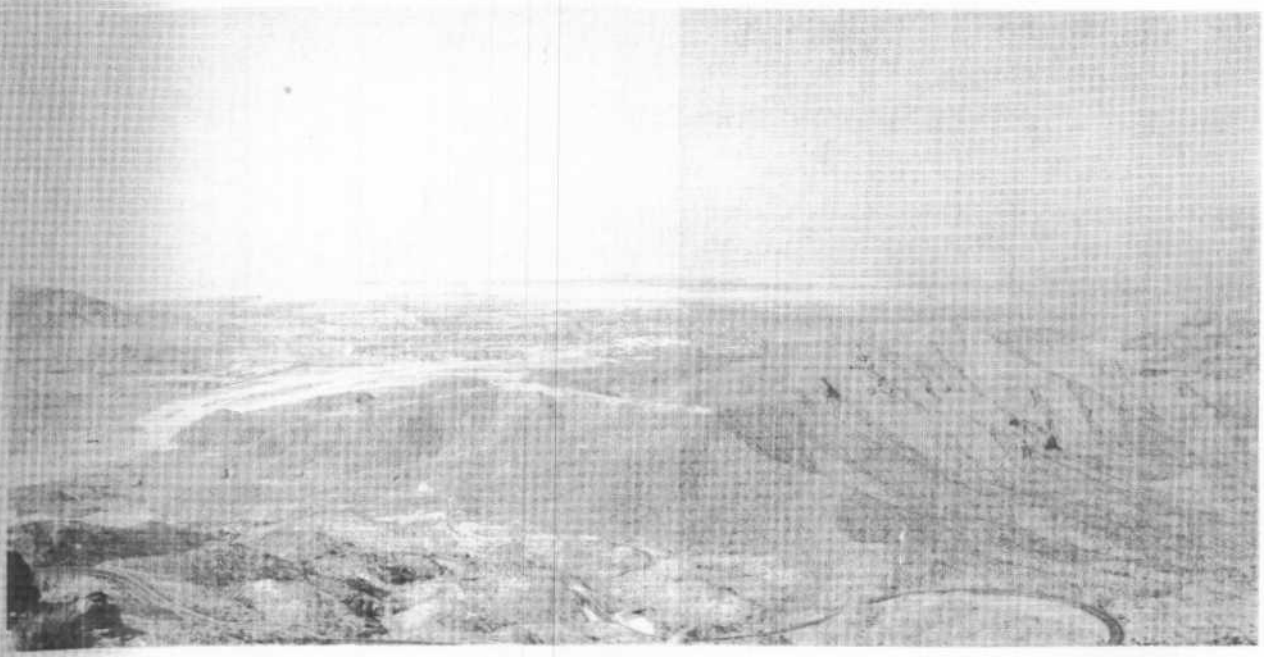

FIGURE 7-3. Panoramic view from Dead Indian Canyon Vista Point. A. Little San Bernardino Mountains; B. Indio Hills; C. Palm Springs Sand Ridge; D. Patches of wave-like transverse dunes; and E. Palm Desert. (Photograph by Ronald Papson, University of Santa Clara, May, 1977.)

PALM DESERT TO BRAWLEY

This trip will follow the western margin of the Salton Trough from Palm Desert to Brawley. The Salton Trough is the landward extension of the Gulf of California and consists of four units: Coachella Valley, Salton Sea, Imperial Valley, and the Colorado River Delta (Fig. 7-4). The trough is a broad, flat, alluviated valley bounded by mountains of pre-Quaternary rock. The most narrow segment, Coachella Valley, has an average width of less than 24 km and is bounded on the northeast by the Little San Bernardino and Orocopia Mountains, and on the southwest by the San Jacinto and Santa Rosa Mounatins.

The Salton Sea forms the transition zone between Coachella Valley and the broader Imperial Valley. Salton Sea is a large manmade lake, formed from 1905 to 1907, which occupies the lowest elevations within the trough. Imperial Valley lies south of the Salton Sea and is bounded on the northeast by the Cargo Muchacho and Chocolate Mountains, and on the southwest by the Peninsular Ranges.

Southward near the International Border, Cenozoic sediments reach a maximum thickness of 6400 m (Biehler and others, 1964). Dibblee (1954) describes the sedimentary deposits in Coachella Valley and western Imperial Valley (Figs. 7-5 and 7-6).

FIGURE 7-4. Index map of the Salton Trough (from Muffler and White, 1969).

Pre-Tertiary rocks include Chuckwalla Complex, Orocopia Schist, Palm Canyon Complex, and Bradley Granodiorite, all of which are described by Miller (1944).

This trip passes a variety of aeolian features, including sand veneers, fixed dunes, and shadow dunes (Eymann, 1953). The many types of dunes in Coachella Valley have been reported by Beheiry (1965). West of Salton Sea are the Salton barchan dunes and the Tule Wash dune, described by Long and Sharp (1964) and Norris (1966). A side trip to Clark Dry Lake is included in order to see the silt-clay shadow dunes (Roth, 1960) on the playa.

Other interesting features seen are the Martinez Rockslide, and San Jacinto fault zone near Clark Dry Lake (Bartholomew, 1970), and the western high shoreline of Lake Cahuilla, recorded by Blake (1854) and Norris and Norris (1961). Lake Cahuilla once covered most of the Salton Basin as a result of a temporary channel shift in the Colorado River. After the water supply was halted by a subsequent channel shift, the lake eventually evaporated, leaving beach deposits, tufa deposits, wave-cut cliffs and other shoreline features. Cultural and historical background are from Shields Date Garden (1957), de Stanley (1966), Leadabrand (1972), and Pepper (1973).

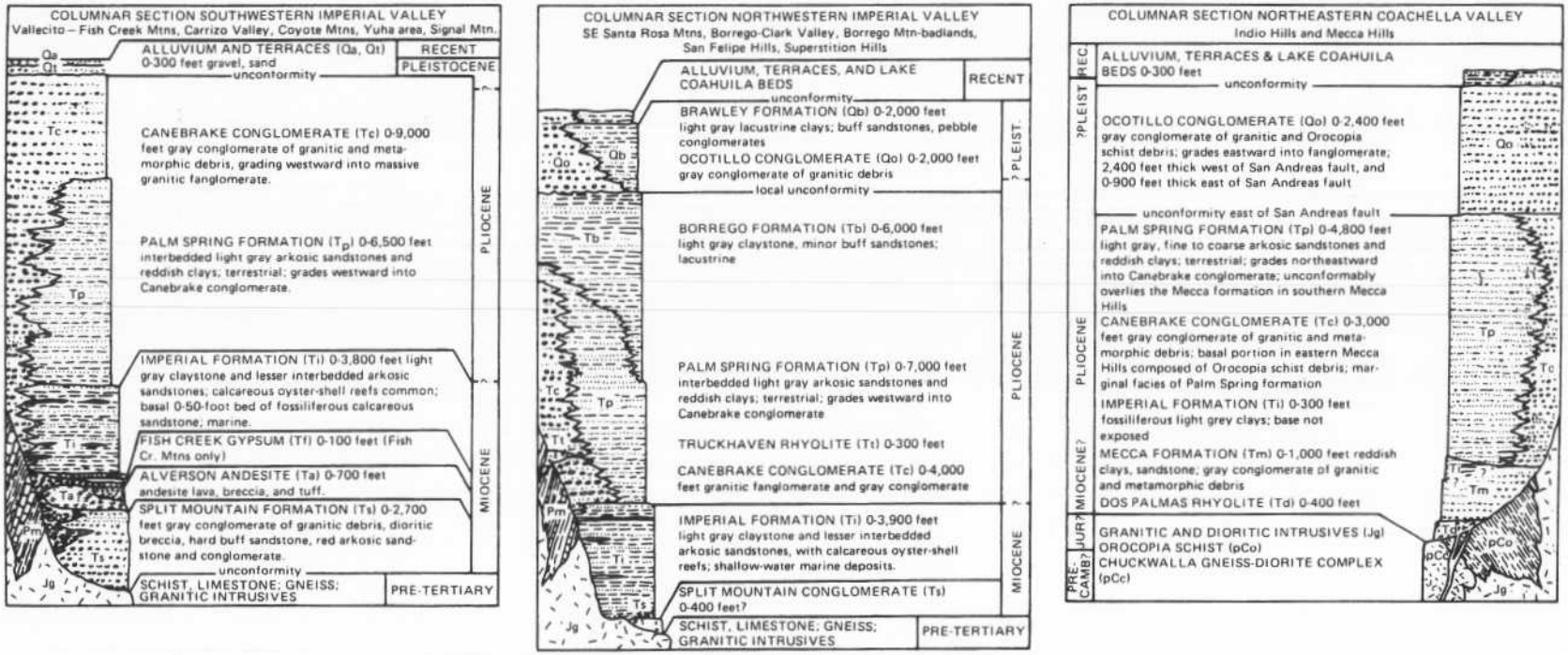

FIGURE 7-5a,b,c. Columnar sections in Salton Trough (from Dibblee, 1954).

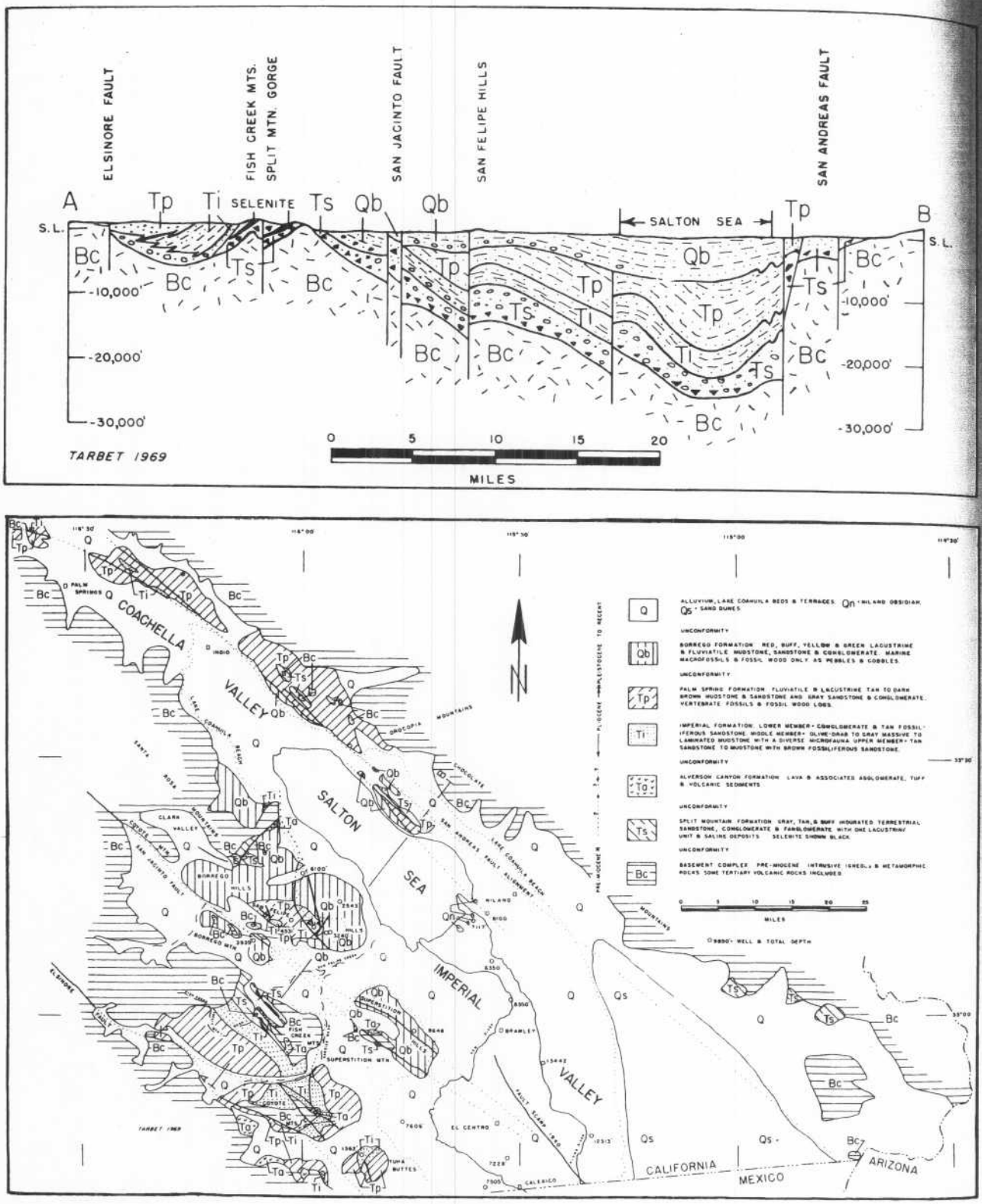

FIGURE 7-6. Schematic cross section across Salton Sea from southwest to northeast (from Tarbet, 1971).

Mileage		
Cumulative	Difference	
0.0	0.0	Junction of Portola Road and State Highway 111 in Palm Desert, located on an alluvial fan at the mouth of Dead Indian Canyon. The new Living Desert Reserve, a division of the Palm Springs Desert Museum, Inc., is located on Portola Road, less than two miles south of State Highway 111. This natural park consists of 162 ha (400 acres) along Dead Indian Creek and encompasses six different desert habitats – a wash bed, sand dunes, rock bajadas, barren hillsides, creosote bush flats, and an ephemeral lake. Other points of interest in Palm Desert are the Desert Southwest Art Gallery, specializing in the work of western artists, and the College of the Desert. Turn north on Portola Road.
1.5	1.5	STOP 2. DUNE FIELD. A sand field approximately 5.12 km^2 in area is accessible where Portola Road ends next to the Sun King Country Club. The field consists of a series of coalescing transverse and barchan-like dunes (Beheiry, 1965), located on the southern margin of the Palm Springs Sand Ridge. The dunes are closely spaced and lee surfaces of adjacent dunes join and form undulating wave-like ridges transverse to the wind direction. Individual dunes within the ridge, however, are longitudinal. After coalescing, the dunes move as a unit until they eventually fragment. At depressions in the ridge crests, increased wind velocity advances the lee sides faster than elsewhere (Fig. 7-7) and causes the lee surfaces to be concave downwind. This sand field is described as a belt of modified barchans whose forms result from unlimited sand supply, urban development of nearby land, and comparative abundance of vegetation. These dunes grow rapidly, often overtaking each other, and result in vague dune forms. Changes in wind patterns lead to reoriented dunes. As dunes merge downwind, the interdune areas close and form a fuljis. Fuljis is a north Arabian term for a depression between barchans, occurring especially where dunes are closely spaced; it has a steep windward slope and a gentle lee slope (Gary and others, 1972). Man-made barriers and vegetation retard dune development by stabilization of potentially active dunes. The dunes in this area are among the largest in upper Coachella Valley; mature dunes average 9 m in height, 30 m in length, and 18 m in width. The sands which comprise this field are sorted. The most recent sand movement on the slip face is marked by concentrations of biotite flakes. Several interdune areas are composed of clay and silt and resemble lake bed deposits.
3.0	1.5	Return to State Highway 111, turn left.
4.0	1.0	Indian Wells is the valley's newest city, incorporated in 1968. Legend has a lost treasure associated with Indian Wells. In 1906 a shipment of $9000 in gold in transit to Fort Yuma was stolen by five men. Four of the men were apprehended, but the fifth, a sharp-shooting gambler known as "Endless Ed," escaped, leaving the gold stashed somewhere in the area. It has never been found.

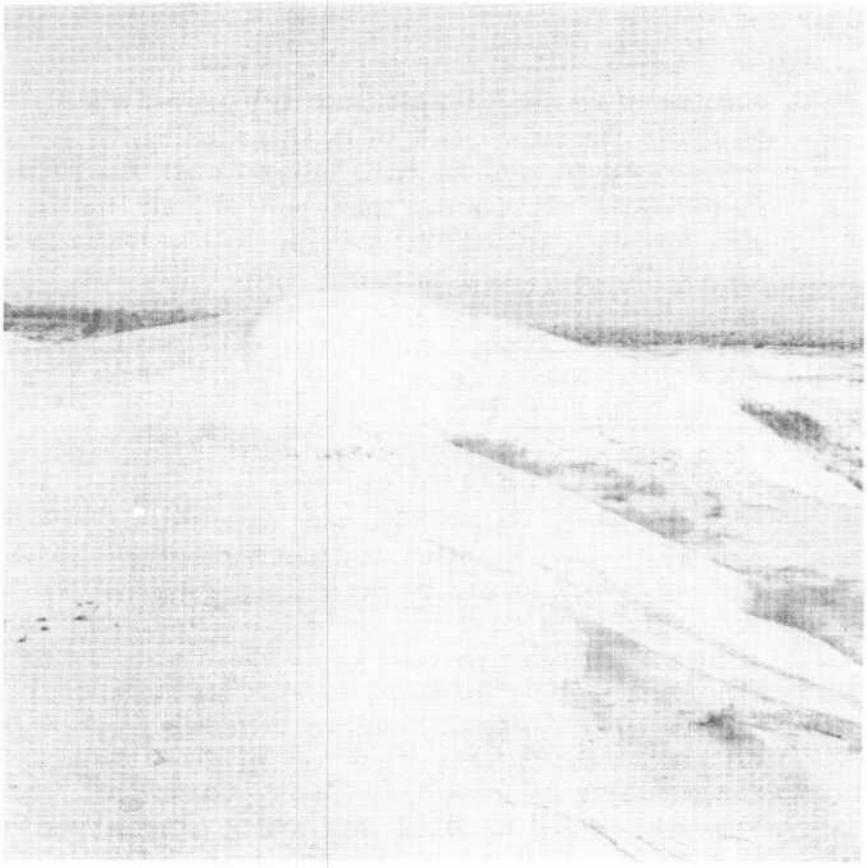

FIGURE 7-7. Slip face at depression along ridge of transverse dune is advancing faster than elsewhere due to increased wind speed in the low area. (Photograph by Ronald Papson, University of Santa Clara, May, 1977.)

Mileage		
Cumulative	Difference	
7.2	3.2	Indio Mountian, composed of Bradley Granodiorite, is to the right. Sand accumulations against the spur of Indio Mountain have been stabilized by vegetation.
7.4	0.2	Road cuts in Bradley Granodiorite. This formation varies from quartz diorite to quartz monzonite and is locally foliated and granulated. It varies from light to dark gray, where fresh, and weathers to a brown to dark brown color.
7.7	0.3	Turn right onto Washington Street.
8.6	0.9	Sand accumulations are also found on this side of the Indio Mountain spur (Fig. 7-8); however, these dune-forms are larger and less vegetated than those on the west side. The sand forms ridges and fan-like features that rise half way up the hillside. The silt and clay beds of Lake Cahuilla crop out below the dunes.

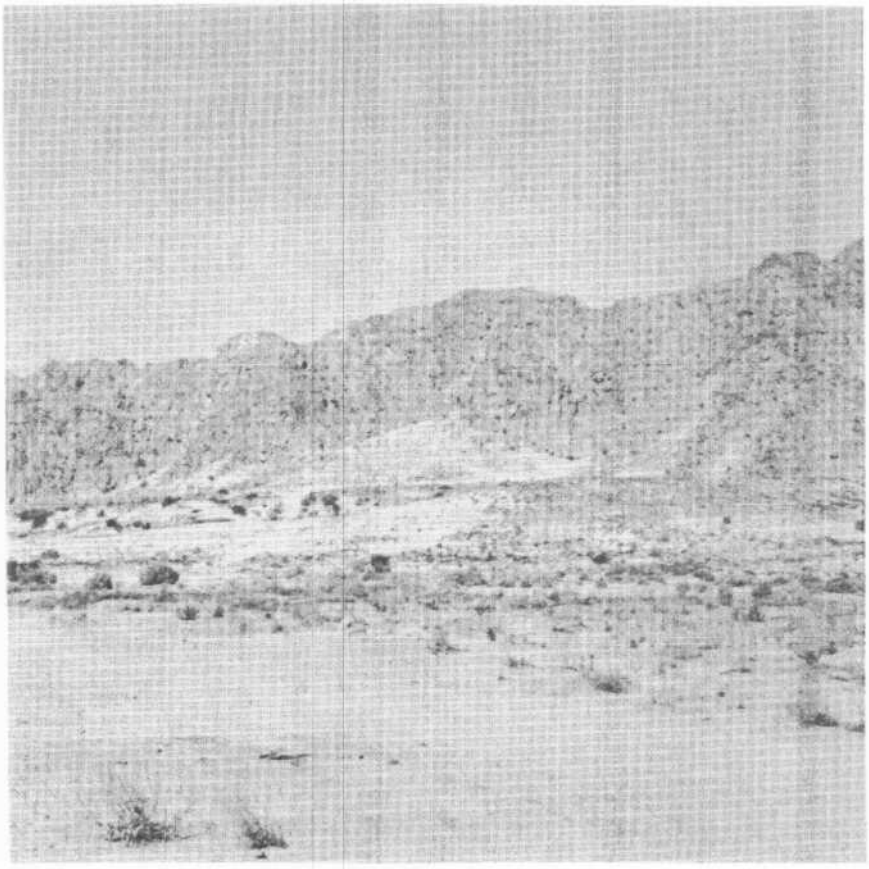

FIGURE 7-8. Sand accumulations on the east side of Indio Mountain with the silt-clay bed of Lake Cahuilla in foreground. (Photograph by Ronald Papson, May, 1977.)

Mileage		
Cumulative	Difference	
10.7	2.1	Turn left at junction of Washington Street and 52nd Avenue. The hill to the right is composed of Bradley Granodiorite.
12.2	1.5	Citrus and date orchards. Citrus fruit produced in Coachella and Imperial Valleys includes grapefruit, tangerines, and navel oranges.

The lower portion of Coachella Valley is one of the leading date producing areas of the world. Ninety percent of all dates grown in the United States are from California and of these, 95 percent are raised in Coachella Valley. Even though the date palm is a desert plant, it requires large quantities of water. In its natural habitat around desert oases, its root system, often 6 to 12 m long, is always in contact with groundwater. In Coachella Valley, however, the date palms must be irrigated every seven to ten days.

Mileage		
Cumulative	Difference	
		Spanish Franciscan and Jesuit missionaries brought the first date palms into California. Unfortunately, the damp coastal climate, where many were planted, was unsuitable and the seedling varieties were of poor quality. Commercial production of dates was first considered after the Civil War when many palms planted in Coachella Valley began fruiting. In 1890, the U. S. Department of Agriculture established experimental stations in the valley and imported 68 offshoots from Algeria and Egypt. These date palms were allowed to propagate and then were released to private growers, thereby beginning successful commercial date production. The *Deglet Neer* variety from Algeria comprised most of the early importations and is the common commercial variety produced today (Shields Date Garden, 1957).
12.5	0.3	Turn right onto Jefferson Street.
12.8	0.3	Tufa deposits mark the high shoreline of ancient Lake Cahuilla at the base of the Santa Rosa Mountains to the right.
15.2	2.4	STOP 3. LAKE CAHUILLA COUNTY PARK at the foot of the Santa Rosa Mountains. Beach sand and tufa deposits are found along the western shoreline of Lake Cahuilla, an ancient lake discovered by Blake (1854). It had a maximum length of 161 km, a width of 56 km and covered about 5,376 km^2. Radiocarbon dating of fish bones indicates that this lake existed until approximately 300 years ago and that another high stand of the lake occurred about 1600 B.P. (Hubbs and others, 1960). Present elevation of the old shoreline averages about 12 m above sea level and ranges from 8 m to almost 18 m. The variation probably indicates slumping on cliff faces, differences in wave intensity, and recent diastrophism with subsequent warping of the shoreline (Norris and Norris, 1961). Fresh water mollusks in lake deposits indicate that Lake Cahuilla was not a marine incursion. The Colorado River Delta formed an effective barrier between the lake and the Gulf of California. The present delta extends southwestward from Yuma, Arizona, to Cerro Prieto Volcano and Sierra de los Cucapas, Mexico, and slopes northward into the Salton Basin and southward to the Gulf of California. Today the minimum elevation of the delta is about 9 m, which is not adequate to contain a 12 m lake level; therefore, the delta must have been higher during the high stand of the lake. The elevation variation of the delta has probably resulted from deposition on a subsiding basement (Longwell, 1954) and eustatic sea level changes (Thomas, 1963). The development of the delta is characterized by shifting river channels. Periodic diversion of the Colorado River northward into the Salton Basin created temporary fresh water lakes such as Lake Cahuilla. Thomas (1963) has reported fresh water beach lines in this area at an elevation of approximately 46 m. The water level of Lake Cahuilla fluctuated with course

changes in the Colorado River and occasional breaches and erosion of the delta southward. Eventually the long term loss by evaporation exceeded the influx of water and the lake disappeared, leaving sandy beaches, tufa deposits, wave cut beaches, strand plains, and evaporite deposits.

The tan tufa deposits coat the base of the mountains (Fig. 7-9) and indicate where water was in contact with the rocks. Rocks above the tufa have been darkened by desert varnish.

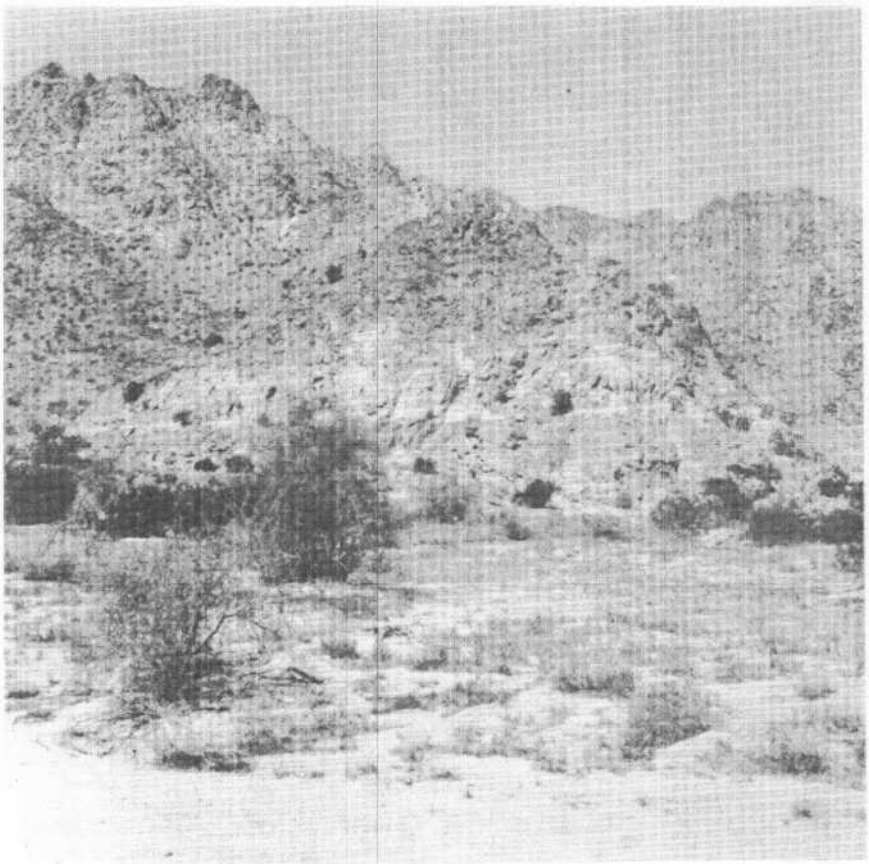

FIGURE 7-9. Tan tufa deposits of Lake Cahuilla can be seen at the base of the hill. A light intermediate zone divides the tufa from the overlying darker rocks which are covered by desert varnish. The top of the tufa deposits is about 2 to 3 m above the valley floor. (Photograph by Ronald Papson, University of Santa Clara, May, 1977.)

Mileage
Cumulative Difference

Beach sand deposits are locally found on the north side of small mountain spurs and in numerous re-entrants. Dissected beach sand deposits reveal interbedded clay, silt and conglomeritic sand layers (Figs. 7-10 and 7-11). The clay beds are relatively resistant and form thin shelves projecting slightly from the gully wall. Silt layers contain abundant biotite flakes and some fossils. These beds are less resistant than the clay beds and vary from 1 to 5 cm in thickness. The least resistant conglomeritic sand layers are poorly sorted and immature, with grain size ranging from fines to cobbles. The main components of the sand layers are feldspar, quartz, and lithic fragments which, along with the biotite flakes in the silt layers indicate local provenance for these sediments.

Nearby, recent alluvial fan material has partially covered the lake bed deposits. These fan areas may have been active during the existence of Lake Cahuilla and delivered sediment to the lake margins. A good cross section of an alluvial fan may be seen in the gravel pit near the park entrance. Leave Lake Cahuilla County Park and go east on 58th Avenue.

17.2 2.0 Turn right onto Monroe Street.

FIGURE 7-10. Unconsolidated Lake Cahuilla beach deposits dissected by intermittent runoff from the Santa Rosa Mountains. The exposure displays bedded clay, silt, and conglomeritic sand. Thin, more resistant clay beds stand out slightly from the coarser beds. The conglomeritic sands are easily eroded to form benches or pockets in the wall. (Photograph by Ronald Papson, University of Santa Clara, May, 1977.)

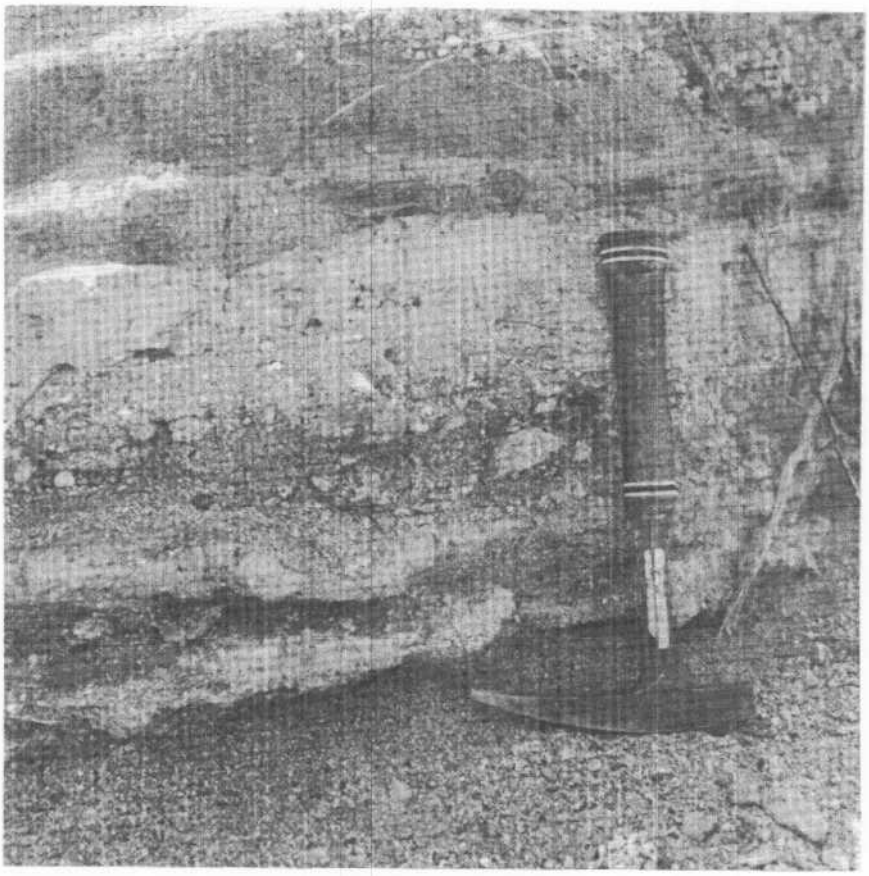

FIGURE 7-11. Bedded Lake Cahuilla beach deposits. Whole and fragmented shells can be seen in the conglomeritic sand layers. Pebbles in these layers may have been derived locally during periods of runoff from the mountains. The lighter units are composed of clay and silt. (Photograph by Ronald Papson, University of Santa Clara, May, 1977.)

Mileage		
Cumulative	Difference	
19.2	2.0	Turn right onto 62nd Avenue.
20.0	0.8	Martinez rock slide (Fig. 7-12) visible from the top of the levee. The slide is about 8 km long and averages approximately 2 km wide.
20.8	0.8	Junction of 62nd Avenue and Monroe Street. Continue straight on 62nd Avenue.
21.8	1.0	Turn right onto Jackson Street.

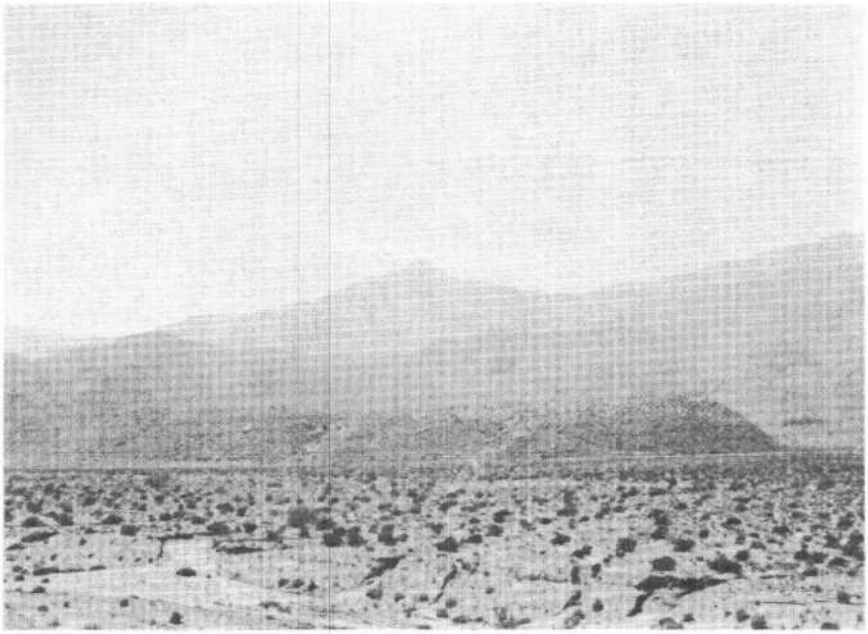

FIGURE 7-12. Distal lobe of Martinez rock slide. Slide debris covers approximately 16 km^2. (Photograph by Ronald Papson, University of Santa Clara, May, 1977.)

Mileage		
Cumulative	Difference	
23.7	1.9	Dirt road on private land to the right leads to fish traps and an old village of the Cahuilla Indians. This land belongs to the Torres Martinez Indian Reservation and permission to enter must be obtained. The Cahuilla Indians have occupied this portion of the Colorado Desert since Lake Cahuilla times. They consisted of many small independent villages with definite boundaries marking hunting and food gathering territories. The scarcity of food in this region caused numerous boundary disputes and was apparently the major reason behind the few wars between Cahuilla villages. However, the Cahuilla seem to have been a peaceful people despite their reputation for independence and rugged integrity (Wilke and Lawton, 1975).

Cahuilla villages extended from San Gorgonio Pass to the Anza-Borrego Desert and were divided into three geographic sections. The western Cahuilla occupied San Gorgonio Pass and northern Coachella Valley, Mountain Cahuilla inhabited the Santa Rosa Mountains, and Desert Cahuilla occupied the rest of Coachella Valley. Slight differences in language and customs often existed between villages.

Mileage
Cumulative Difference

Since availability of water and food were the prime factors in establishing a village, most were located at springs or perennial streams in the mountains and desert canyons. Several villages were developed around seeps where wells similar to the one at Indian Wells could be dug. Protection from wind, warmth in the winter, shade in the summer, and natural beauty were also factors considered before selecting a village site.

Cahuilla legends tell of a time when there was a great lake with abundant fish and aquatic birds which provided most of their food. Villages were located on the lake shores and in the mountains, from which trips to the lake were made to hunt and fish. Fish traps were widely used where the water reached the mountains and many may still be found along the base of the Santa Rosa Mountains. The legends also tell of slow recession of the lake, the fish dying, and of the appearance of mesquite around the disappearing lake. One legend documents occupation of the valley before the lake appeared, the village retreating before the rising waters, settlement on the shore of the lake, and the reoccupation of the valley behind the receding water. It is believed that the legends actually refer to the rise and fall of Lake Cahuilla. Follow road around turn to left. Tufa deposits now extend approximately 20 m up the mountain slopes.

24.3 0.6 Mecca Hills in the distance to the east. Mecca Hills, like Indio Hills, were formed by deformation and uplift along the San Andreas fault system.

25.8 1.5 Turn right onto State Highway 86.

27.3 1.5 The road is now crossing over the alluvial fan from Martinez Canyon to the right. This fan was apparently active both before and after Lake Cahuilla existed. Fan material surrounds a granitic knob near the mouth of the canyon.

30.3 0.3 First view of the Salton Sea, a large inland lake approximately 56 km long, 20 km wide and 11 m deep. The Salton Sea (Fig. 7-13) is the modern equivalent of Lake Cahuilla; however, man rather than nature is responsible for this lake.

In the early 1900's canals were constructed to irrigate Imperial Valley. All canals were finished by 1904; however, the canals soon began having serious siltation problems. When the main canal became totally blocked, a new canal was cut, against the better judgment of the engineers working on the project, between the Colorado River and the canal system in Mexico. In the spring of 1905, several large floods on the Colorado widened the artificial breaches and destroyed a dam built to regulate flow. The steeper gradient into the Salton Basin became the preferred course for the flooding waters and inundated the floor of the Imperial Valley.

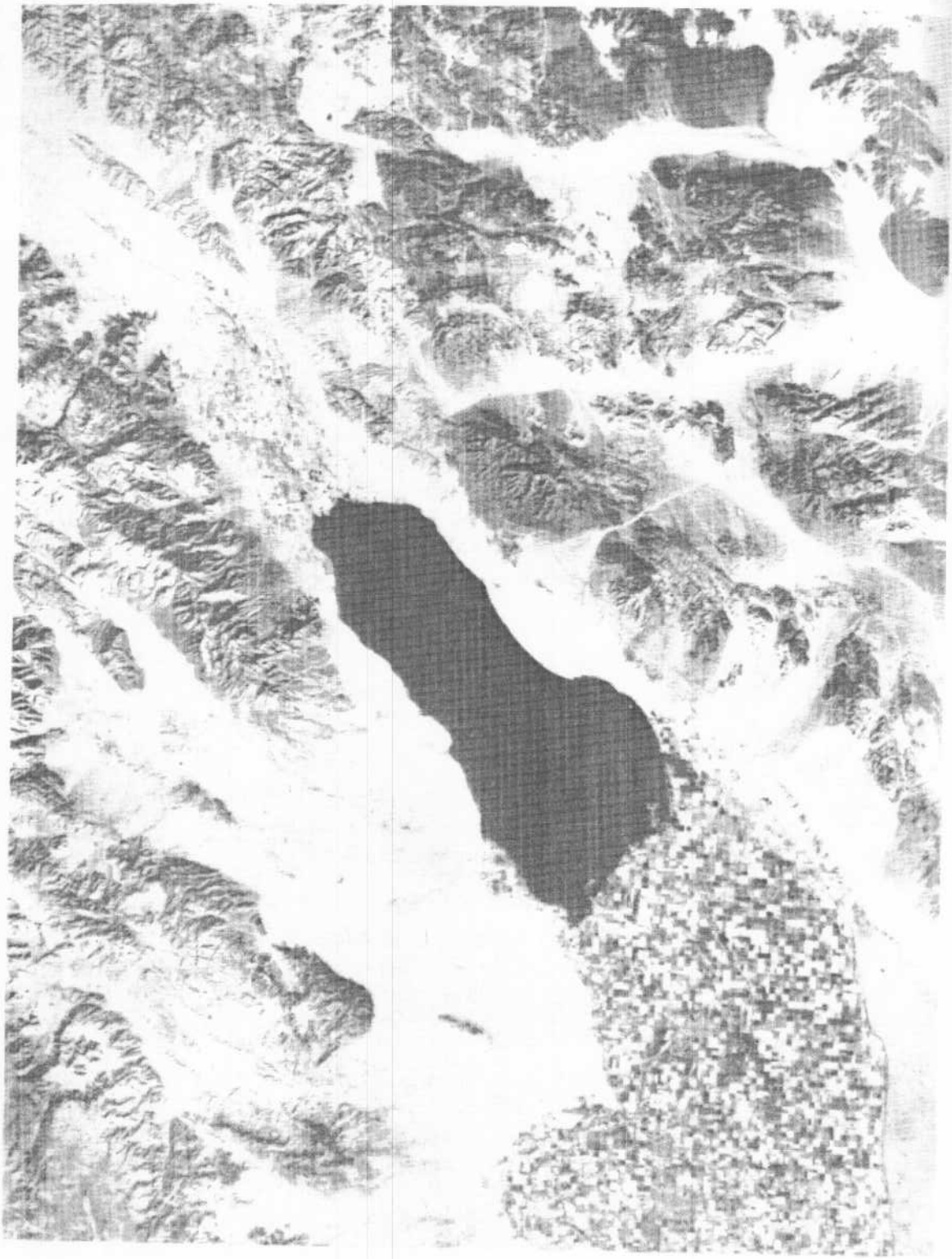

FIGURE 7-13. Vertical ERTS photomosaic, showing the Salton Sea area (from USDA-SCS, Sheet 44, 1973).

Mileage
Cumulative Difference

The California Development Company, responsible for the canals, made several unsuccessful attempts to stop the flow but soon turned the project over to Southern Pacific Railroad. After two years of repeated efforts to halt uncontrolled intake into the canals and flooding of the Basin, the river was reverted to its original course. One result of the flood was a government project to build another dam further upstream of the break and to construct the All-American Canal system through the valley.

The level of the Salton Sea has been quite variable in the past in response to the amount of drainage and leach water that has flowed into it, but today maintains an average elevation of 71.3 m. The level varies approximately 0.3 m annually; being highest in April and lowest in October. The influx by drainage and loss by evaporation has stabilized the lake level.

34.6 4.3 Oasis Station. To the right is a series of coalescing alluvial fans comprising Oasis Piedmont Slope which extends from Martinez Rock Slide to Travertine Point. In the upper reaches of the piedmont, drainage systems dissect the Pleistocene and Pliocene sediments, indicating an eastward migration of the transition between erosion and deposition. The upper fan slopes exhibit tilted Pliocene beds that have been uplifted by faulting.

35.9 1.3 Dissected alluvial fan material to the right.

38.2 2.3 STOP 4. TRAVERTINE ROCK is a small outlier of metasediments isolated from the Santa Rosa Mountains. From the top of Travertine Rock, the narrow Coachella Valley and the Salton Sea area are visible (Fig. 7-4). To the southwest, the Salton Basin widens into the Anza-Borrego Desert.

During the existence of Lake Cahuilla, Travertine Point was a low-lying semicircular group of hills which extended 0.8 km from the mountains. Travertine Rock, the hill farthest from the mountains, was never submerged by the lake but formed a small island rising a few meters above the water. Along the base of the Santa Rosa Mountains, baymouth bars and spits were formed and are still visible (Fig. 7-14). The hills of Travertine Point are connected with the shore by a tombolo. Travertine Rock rises 53 m above the surrounding plain and is covered by a steep talus of large boulders. Below the high water line, the boulders are covered by thick tufa deposits which have an average thickness of 76 cm on the outer surfaces over a vertical range of about 36 m. Both lithoid and dendritic tufas are present, with sand grains and shells occasionally imbedded in the latter.

Calcium carbonate for the tufas was derived from the lake water by algae growing on resistant surfaces (Jones, 1914).

40.7 2.5 Mountain to the right is composed of Palm Canyon Complex and coarsely crystalline limestone. The old shoreline may be traced along the mountainside.

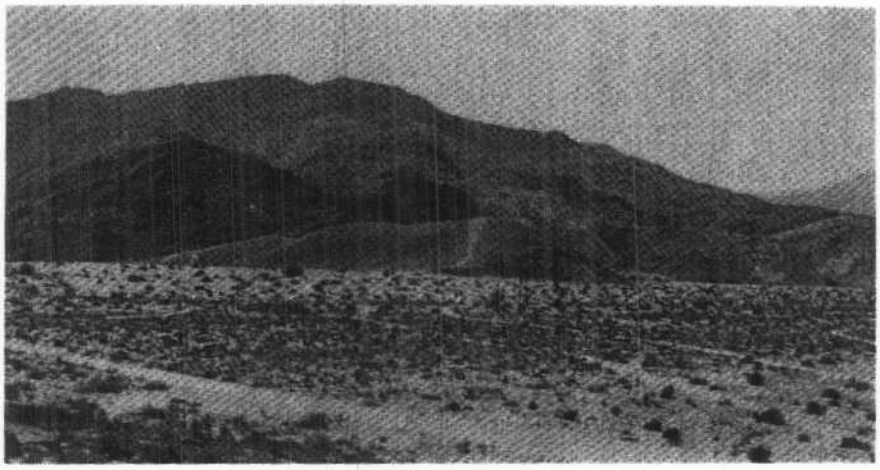

FIGURE 7-14. Lake Cahuilla beach deposit near Travertine Point with bay mouth bars at the base of the Santa Rosa Mountains. (Photograph by Ronald Papson, University of Santa Clara, May, 1977.)

Mileage		
Cumulative	Difference	
43.4	2.7	Fault scarp trending northeast to the right. The scarp divides the granitic Southern California Batholith from the Pliocene Truckhaven Rhyolite. The rhyolite, extruded along the fault, forms a lens of variegated felsitic rock. The lens has a maximum thickness of 30.5 m and wedges out southward into the Canebrake Conglomerate. The dissected alluvial fan visible south of the fault has apparently been inactive since prior to the high level of Lake Cahuilla. Lake beds are continuous up the fan to the estimated high shoreline of Lake Cahuilla. Intermittent streams are present but there are no Quaternary deposits. In this area, the Pliocene non-marine sediments consist of the Palm Spring Formation and the Canebrake Conglomerate.
46.9	3.5	Small hill to the right is composed of the Borrego Formation, a lacustrine facies of the Palm Spring Formation. The Borrego Formation is composed of light gray claystone interbedded with sandstone. Within the claystone layers, lacustrine fauna such as minute mollusks, ostracods, and foraminifera have been found.
50.1	3.2	Salton City. Junction of S22 (Borrego-Salton Seaway) and State Highway 86. Continue south on State Highway 86.
53.1	3.0	Turn right onto Refuse Disposal Road (graded dirt road) before crossing Tule Wash.

Mileage Cumulative	Difference	
56.1	3.0	STOP 5. TULE WASH DUNE is an isolated barchan located on the south bank of Tule Wash (Figs. 7-15 and 7-16). The dune is related to the Salton dunes, 8 km to the east. The sand composing the dunes is more angular and less sorted than elsewhere. Tule Wash dune is moving in the same general direction as the Salton dunes and is fed from the same source. Surface roughness between the Tule and Salton dunes prevents further dune formation.

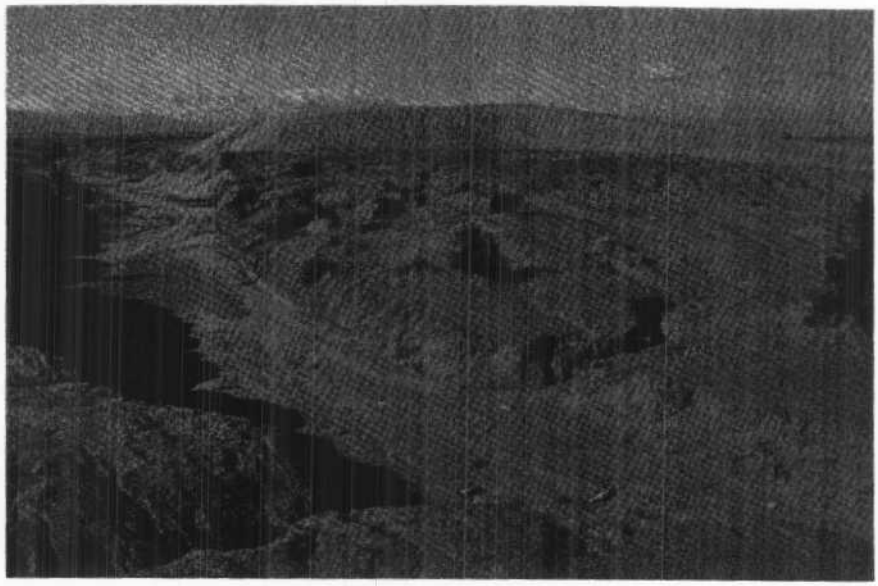

FIGURE 7-15. View of Tule Wash dune looking westward. This asymmetric barchan is an isolated member of the Salton dunes to the east. The south horn of the dune is advancing into the middle fork of Tule Wash, where it will eventually be washed away by floods. Also note the gullied surface around the dune. (Photograph by Ronald Greeley, University of Santa Clara, January, 1977.)

Bedrock in this area consists of poorly indurated, folded and faulted, concretionary sandstones and siltstones of the Pliocene Palm Spring and Borrego Formations. Post-Lake Cahuilla has developed a dendritic system of gullies 1 to 5 m deep and as much as 46 m wide. These gullies are important in the development and destruction of dunes. Inter-gully areas are nearly flat and gently slope about 7.5 m/km toward the Salton Sea. Many wind polished and faceted igneous and metamorphic rocks, deposited by sheetflooding from the west, are scattered about on the inter-gully surfaces.

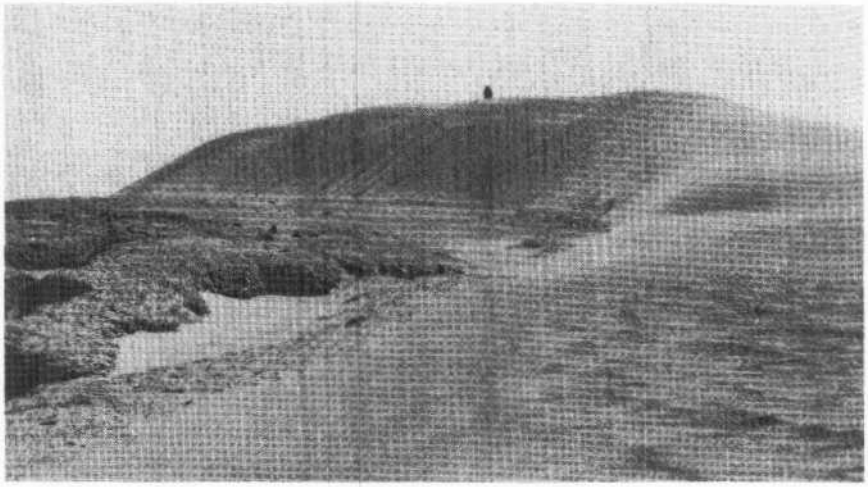

FIGURE 7-16. View of Tule dune from the end of the northern horn. (Photograph by Eilene Theilig, University of Santa Clara, May, 1977.)

Mileage		
Cumulative	Difference	

Three large dunes near McCain Spring were first reported by Mendenhall (1909). Brown (1923) reported only two dunes which had remained almost stationary for 10 to 15 years. Presumably one of Mendenhall's dunes either merged with another or disappeared into one of the washes. In 1932 early aerial photography showed only one remaining dune which has persisted as the present Tule dune. It is the opinion of Norris (1966) that the two dunes merged, probably as a result of unequal size and rate of movement. On its present course, Tule dune will disappear into the middle fork of Tule Wash (Fig. 7-17).

The dune sand is derived from both local sources and Borrego Valley, 32 km to the west. On the windward side rain softened, locally produced silt aggregates form a crust that remains in place with subsequent dune movement (Fig. 7-18). The dune has been asymmetric with the south horn consistently longer than the north horn until recent advancement into Tule Wash.

The absence of new dunes upwind of Tule dune may result from the lack of vegetation.

62.1	4.5	Return to State Highway 86, turn right.
66.6	4.5	Lake bed deposits on the right. Salton barchan dunes to the left.
67.7	1.1	Turn left on road to Salton Sea Naval base.

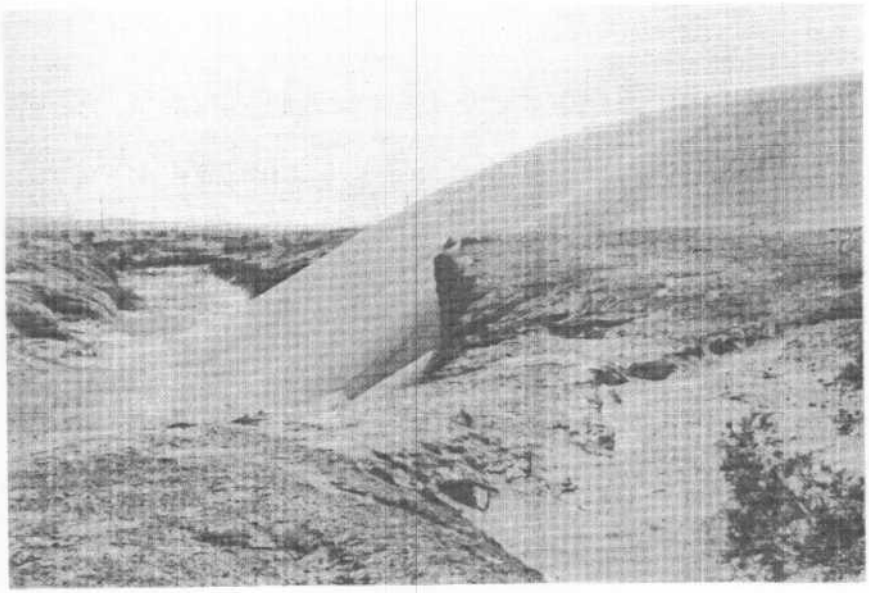

FIGURE 7-17. South horn of Tule dune, forming a fan in the middle fork of Tule Wash in May, 1977. Compare the fan feature with Figure 15, which was taken in January, 1977. (Photograph by Eilene Theilig, University of Santa Clara, May, 1977.)

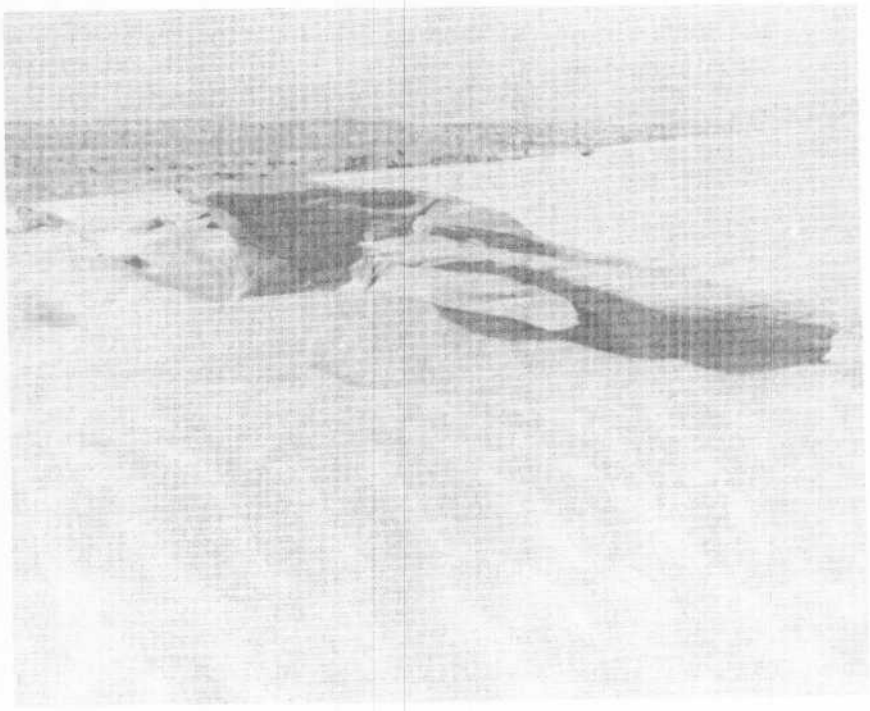

FIGURE 7-18. Resistant portions of the dune sand remain in place while dune advances. This sand is bonded together by cohesion of silt particles. (Photograph by Eilene Theilig, University of Santa Clara, May, 1977.)

Mileage		
Cumulative	Difference	
69.9	2.2	STOP 6. SALTON DUNES. This field consists of closely spaced barchans located between State Highway 86 and the Salton Sea, about 13 km south of Salton City (Fig. 7-19a,b). Since most of the dune field is located on Salton Sea Naval Base, permission is required to inspect dunes. The crescent-shaped dunes are open to the east (Fig. 7-20), although some are distorted with horns of unequal length. Coalescence of dunes has also caused distortion by forming morphologically complex and larger dunes (Fig. 7-21) which obscure barchan characteristics. Individual dunes vary from 9 to 30 m in width and 2 to 12 m in height (Long and Sharp, 1964).

The underlying surface is smooth and slopes approximately 7 to 18 m/km east-northeast. The total elevation ranges from 9 to 70 m below sea level. Bedrock is composed of weakly consolidated clay, mudstone, and sandstone of the deformed and truncated Plio-Pleistocene Brawley Formation, with some Lake Cahuilla deposits. Pebbles, concretions, and cemented sandstone fragments from the underlying material form a patchy veneer on interdune surfaces.

Conditions required for barchan formation are: 1) a moderate sand supply, 2) relatively smooth ground surface, 3) limited vegetation, and 4) consistent prevailing wind direction – all of which are satisfied in the Salton dune area. The dune sand is derived from barren outcrops of Cenozoic sedimentary deposits extending westward to Borrego Valley, Lake Cahuilla beach deposits and fresh alluvium to the west. The local sources result in angular and poorly sorted dune sand and numerous grains of claystone cemented by iron oxide.

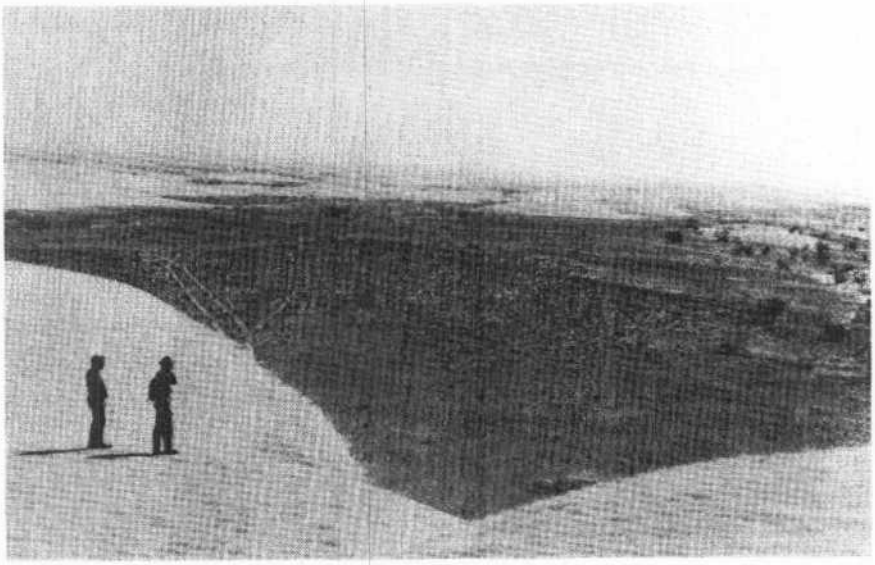

FIGURE 7-19a. Barchan dune field west of Salton Sea, California; view east with sea in background. (Photograph No. 3600 by Troy L. Péwé, April 1, 1973.)

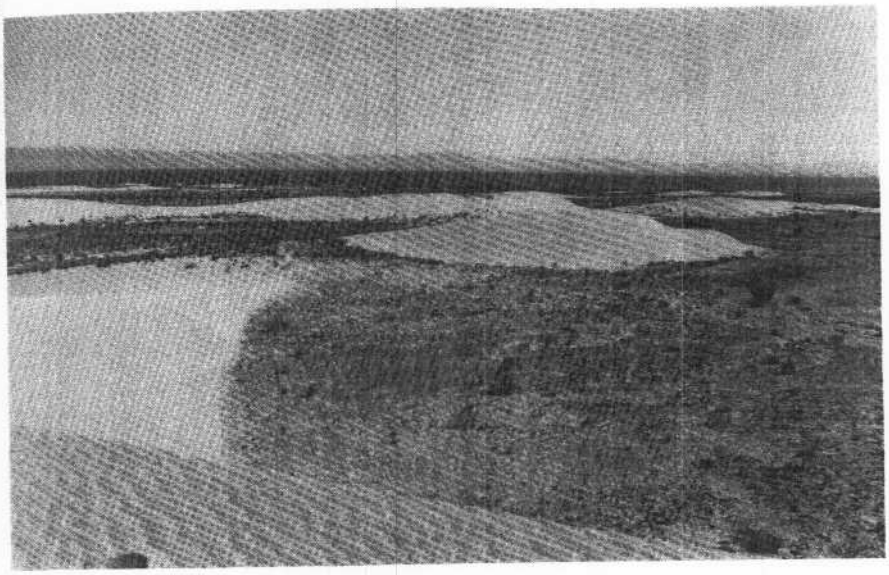

FIGURE 7-19b. Barchan dune field, west side of Salton Sea, California; view east with sea in background. (Photograph No. 3925 by Troy L. Péwé, March 14, 1977.)

Mileage		
Cumulative	Difference	

Factors contributing to the limited extent of the dunes may include supply of sand, smoothness of bedrock, and vegetation. Aeolian sands increase eastward and reach a critical amount for dune formation while local topography funnels large quantities of sand into the area. Growth of vegetation is heavier here than to the west and may be sufficient to begin the accumulation of sand for dune formation (Long and Sharp, 1964).

The Salton dune field may have pre-dated Lake Cahuilla but none of the present dunes are older than 300 years. Dune movement of 18 m/yr would require slightly more than 300 years to pass through the field, which is the approximate time since the area was submerged by Lake Cahuilla. During the formation of the Salton Sea, the lower part of the dune field was flooded by the rising waters.

72.1	2.2	Return to State Highway 86, turn left.
76.3	4.2	Junction State Highway 86 and State Highway 78; continue southward.
76.7	0.4	San Felipe Creek dune field to the right consists of fixed and shadow dunes (Eymann, 1953). Shadow dunes form in the lee of obstacles such as vegetation and usually have a triangular plan view. The crests dividing the windward and leeward sides form either a "T" or a "Y".

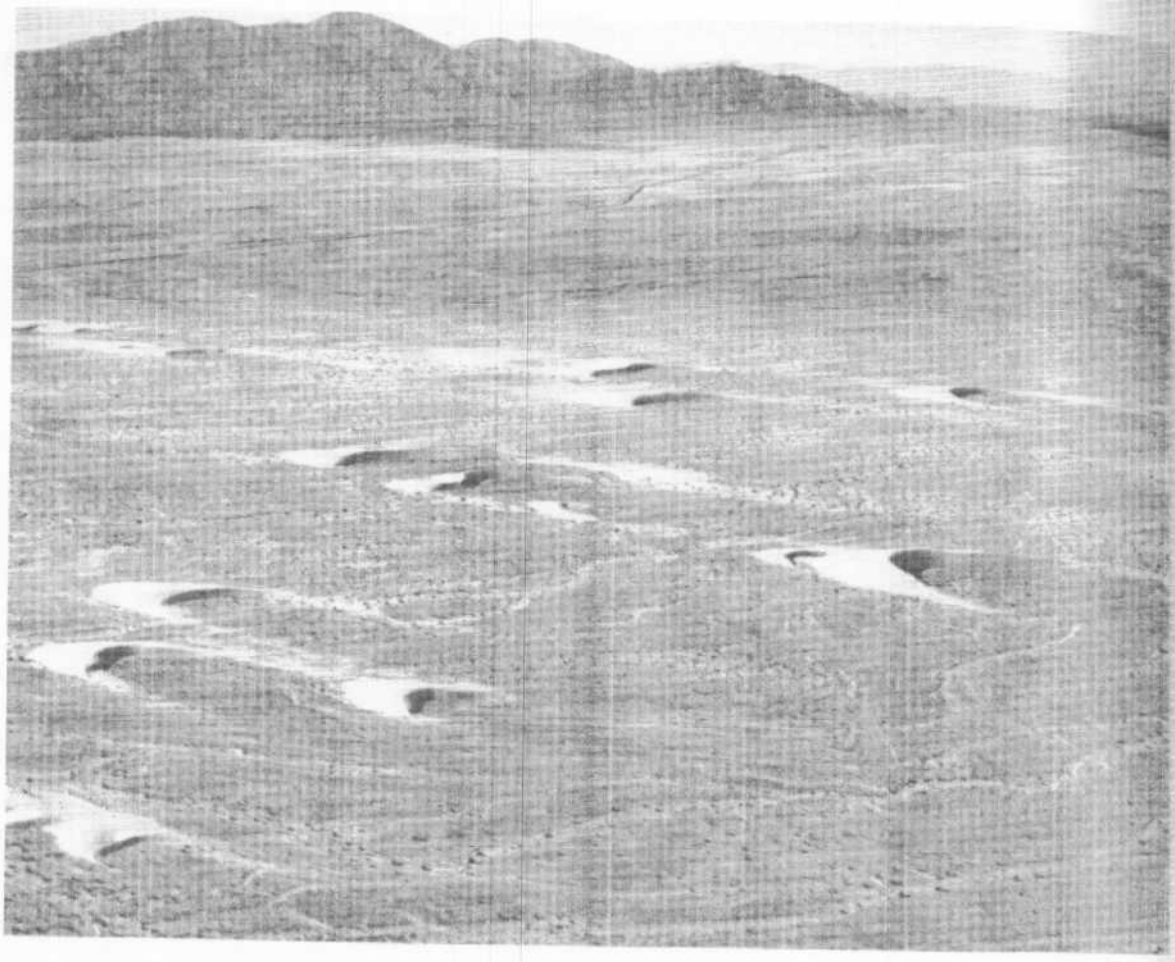

FIGURE 7-20. Typical crescentic-shaped dunes in the Salton dune field. View is northwest towards the Santa Rosa Mountains. (Photograph by John S. Shelton.)

Mileage		
Cumulative	Difference	
		Fixed dunes are dunes stabilized by vegetation or by cementation of the grains (Eymann, 1953) and frequently appear rounded. Stabilized dunes may have increased silt and clay fractions resulting from vegetation entrapment and the breakdown of grains within the dune. Both shadow and fixed dunes are abundant in the Colorado and Mojave Deserts.
93.0	16.3	Junction of State Highway 86 and Forrester Road in Westmoreland. Continue on State Highway 86.
99.0	6.0	Cross New River.
100.0	1.0	Brawley. State Highway 86 turns right and leaves State Highway 78.

FIGURE 7-21. Asymmetric crescent-shaped dune in Salton dune field. Behind the central dune is a complex mass of coalescing dunes in which barchan characteristics are obscured. (Photograph by Ronald Papson, University of Santa Clara, May, 1977.)

SALTON CITY TO CLARK DRY LAKE

The side trip to Clark Dry Lake passes through tilted and faulted beds of Late Cenozoic sedimentary deposits (Dibblee, 1954) (Fig. 7-5a) which have a local maximum exposed thickness of 5700 m. Formations seen include the Palm Spring Formation, Canebrake Conglomerate, Borrego Formation, and Ocotillo Conglomerate. The basal Split Mountain Formation is a red and gray fanglomerate composed of sandstone and dioritic breccia. The Imperial Formation is the only marine sediment of the section and consists of gray to yellow weathering claystone interbedded with buff sandstone and calcareous reef deposits. The Palm Spring Formation, a series of continental arkosic sandstones and red clays, grades upward into the Canebrake Conglomerate, a coarse marginal facies of the Palm Spring Formation. The entire thickness of Palm Spring redbeds exposed west of Salton Sea grades laterally westward into granitic Canebrake facies conglomerate. The latter overlies crystalline rock and extends far up the slopes of the southeastern Santa Rosa Mountains as a fanglomerate. The Palm Spring Formation also grades upward into the Borrego Formation. The Borrego Formation is composed of light gray claystone, containing minute fresh water mollusks, ostracods and rare foraminifera, interbedded with sandstone. Ocotillo Conglomerate, the youngest Cenozoic sediment, overlies the Borrego Formation and consists of a gray granitic pebble conglomerate. The Brawley Formation is the lacustrine equivalent of the Ocotillo conglomerate.

At Clark Dry Lake, part of the playa surface is covered by shadow dunes composed of sand and sand-size aggregates of silt and clay.

Mileage Cumulative	Mileage Difference	
0.0	0.0	Salton City. Junction S22 (Borrego-Salton Seaway) and State Highway 86. Turn right onto S22. The Borrego-Salton Seaway follows parts of the old Truckhaven Trail.
3.3	3.3	Sand mounds on the left. Tilted beds of the Palm Spring Formation are visible on the right.
8.2	4.9	Calcite Canyon. North of here is John Hilton's calcite crystal mining area which was operated during World War II.
9.0	0.8	Drive through a series of arroyos cutting Pleistocene terrace deposits and the Plio-Pleistocene Palm Spring Formation. Most sediments to the north are Canebrake Conglomerate.
11.0	2.0	Tilted beds on both sides of the road; to the left are light colored beds of the Borrego Formation and to the right are red beds of the Palm Spring Formation.
12.0	1.0	Large boulders in wash.
12.6	0.6	Road cuts in Palm Spring Formation and terrace deposits.
14.5	1.9	To the left, sand has accumulated in the lee areas of hills of the Borrego Badlands. The badlands are composed of Ocotillo Conglomerate and Borrego Formation which have been deformed into the Borrego Synclinorium. This feature is a major fold plunging west into Clark Valley which is related to the San Jacinto fault. The Ocotillo Conglomerate was probably deposited in two basins on the downdropped eastern side of the San Jacinto fault. Vertical motion along this fault has been upward on the southwest side.
16.5	2.0	STOP 7. CLARK DRY LAKE RADIO ASTRONOMY STATION of the University of Maryland. Obtain permission from the station personnel before examining dunes on the northeastern surface of the lake bed. When this station is completed, observers will be able to quickly scan the surface of the Sun to study sun spots and flares.

Several types of dunes, including fixed, shadow, and barchan dunes, are found on and around Clark Dry Lake (Eymann, 1953). Our main emphasis will be the shadow dunes described by Roth (1960) as silt-clay dunes. These dunes have formed in the lee of vegetation and range from 15 cm to 2 m in height, 46 cm to 9 m in length, and 2.5 cm to 6 m in width (Fig. 7-22). The dunes are oriented NNW-SSE, roughly parallel to the trend of Clark Valley.

Cross sections of several dunes reveal cross bedding of sand, silt, and clay laminae (Figs. 7-23 and 7-24). Clay and silt layers are the most resistant and

form thin ledges where the wind has etched away sandy layers. Feldspar, biotite, and quartz are abundant with some silt-clay aggregates. Roth (1960) proposed that the silt and clay aggregates originated from decomposition of the surrounding playa floor. During the past 12 years, the water depth has not exceeded 0.6 m (Johanassen, personal comm.) and has not affected the larger dunes.

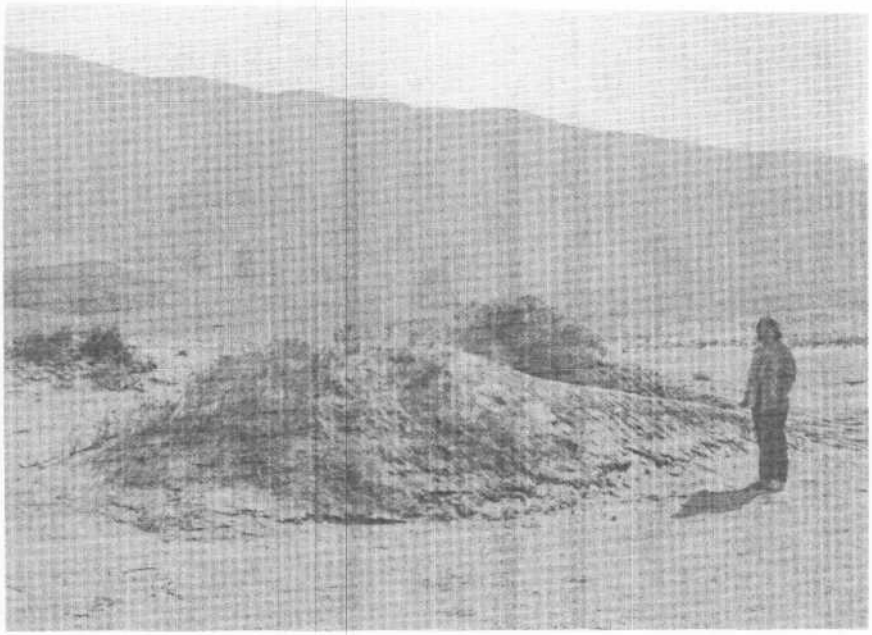

FIGURE 7-22. Silt-clay shadow dune on Clark Dry Lake. The dune is composed of sand and silt-clay aggregates and exhibits the typical vegetation shadow dune form of a blunt windward end with a gently sloping, tapered leeward side. The surface crust, formed by cohesion of silt and clay particles after the last rainfall, has been rilled by surface runoff. (Photograph by Ronald Papson, University of Santa Clara, May, 1977.)

The dunes are covered by a 2 to 5 cm thick crust of silt and clay with some imbedded medium- to coarse-grains formed by coagulation of silt-clay aggregates. The crust is partially detached from the underlying material and exhibits mud cracks and erosional features (Fig. 7-25). In some places the crust has been breached, revealing the internal structure of the dune (Fig. 7-26).

FIGURE 7-23. Cross-section of silt-clay shadow dune on Clark Dry Lake. Cross bedding is illustrated by thin clay layers that stand out in relief. A coarse pebbly, sand layer can be seen near the upper part of the section. The scale is a protective plate from a Hasselblad camera. (Photograph by Ronald Papson, University of Santa Clara, May, 1977.)

Mileage
Cumulative Difference

Scattered patches of sand, composed of quartz, feldspar, biotite and clay aggregates cover the playa surface (Fig. 7-27). The sand increases in quantity towards the edge of the playa and locally forms small shadow dunes behind plants, with grain size increasing with distance from the bush. In the lee of some obstacles, accumulations of loose silt-clay aggregates may be found.

Clark Valley, near the southwestern end of the Santa Rosa Mountains, is interpreted as a graben along the curvilinear San Jacinto fault (Bartholomew, 1970) (Fig. 7-28). This Middle Pleistocene to Holocene fault zone consists of, principally, three right lateral faults with the following displacements: San Jacinto 25 km, Coyote Creek 5 km, and Clark 2 km. Coyote Mountain, immediately west of Clark Valley, is bounded on the southwest by Coyote Creek fault and on the east and northeast by the San Jacinto fault system (Fig. 7-29). The trace of Clark fault passes through Clark Valley and intercepts the northeastern corner of the playa.

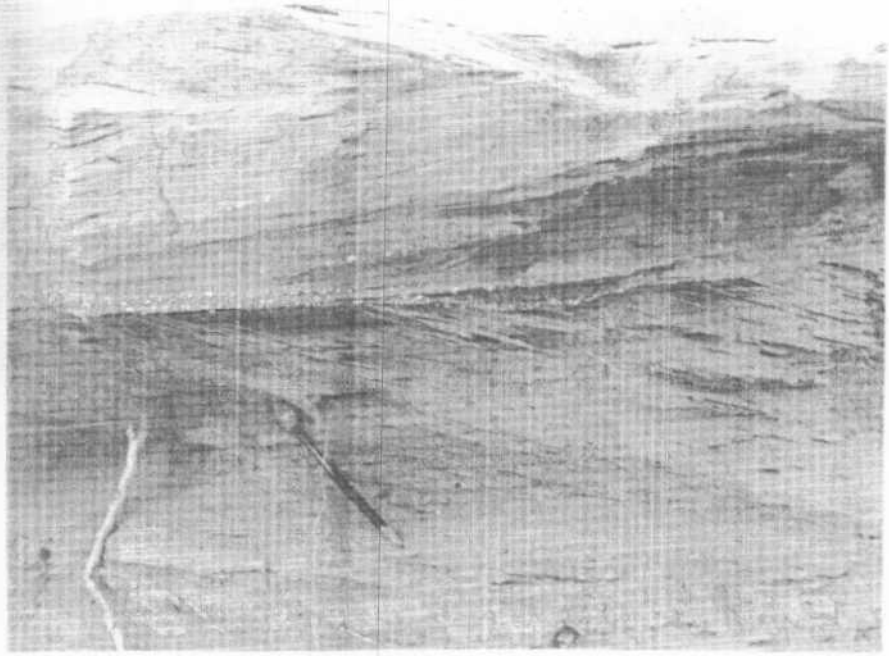

FIGURE 7-24. Close-up view of internal structure within shadow dune. Cross-bedding laminae are cut by a coarse sand layer. (Photograph by Eilene Theilig, University of Santa Clara, May, 1977.)

FIGURE 7-25. Surface crust on dune at Clark Dry Lake. Silt-clay aggregates break down when moistened and tend to coagulate, forming a relatively resistant crust. The crust has subsequently been rilled by rainstorms. (Photograph by Eilene Theilig, University of Santa Clara, May, 1977.)

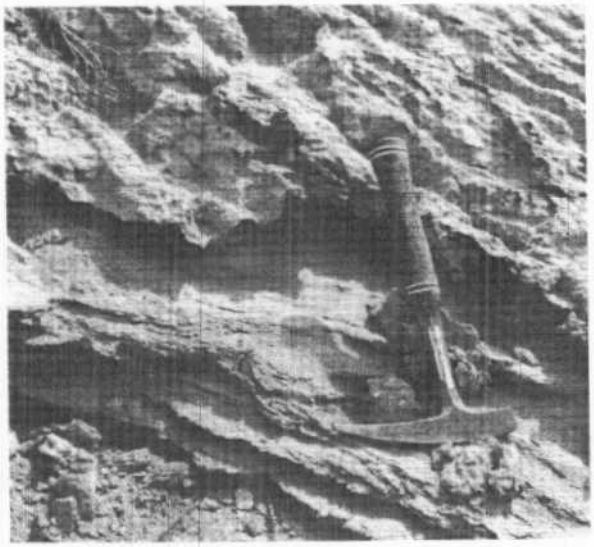

FIGURE 7-26. Portion of surface crust has broken away, revealing interbedded sand, silt, clay. Note how the crust stands in relief from the underlying dune material. (Photograph by Ronald Papson, University of Santa Clara, May 1977.)

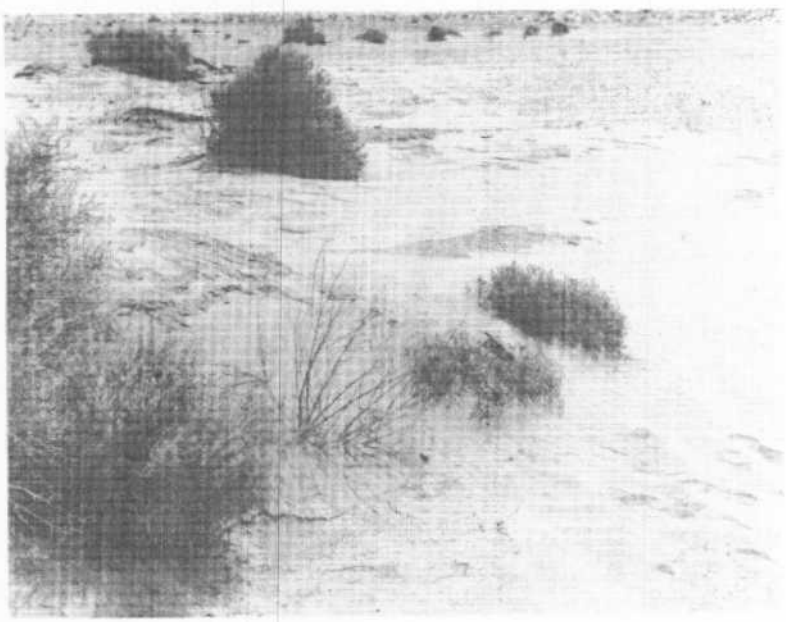

FIGURE 7-27. Aeolian sand sheet covering a silt-clay shadow dune on Clark Dry Lake. Part of this sand may be incorporated into the dune during the next rainfall. (Photograph by Eilene Theilig, University of Santa Clara, May, 1977.)

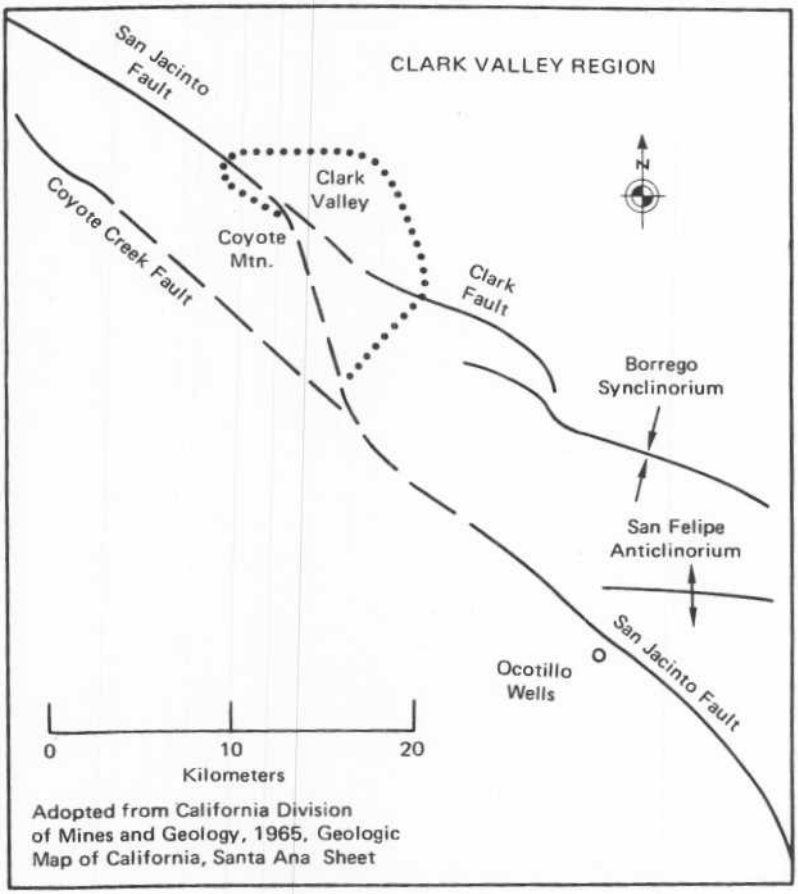

FIGURE 7-28. Generalized fault map of the Clark Valley region. The valley is interpreted as a graben formed along the San Jacinto fault (from Bartholomew, 1970).

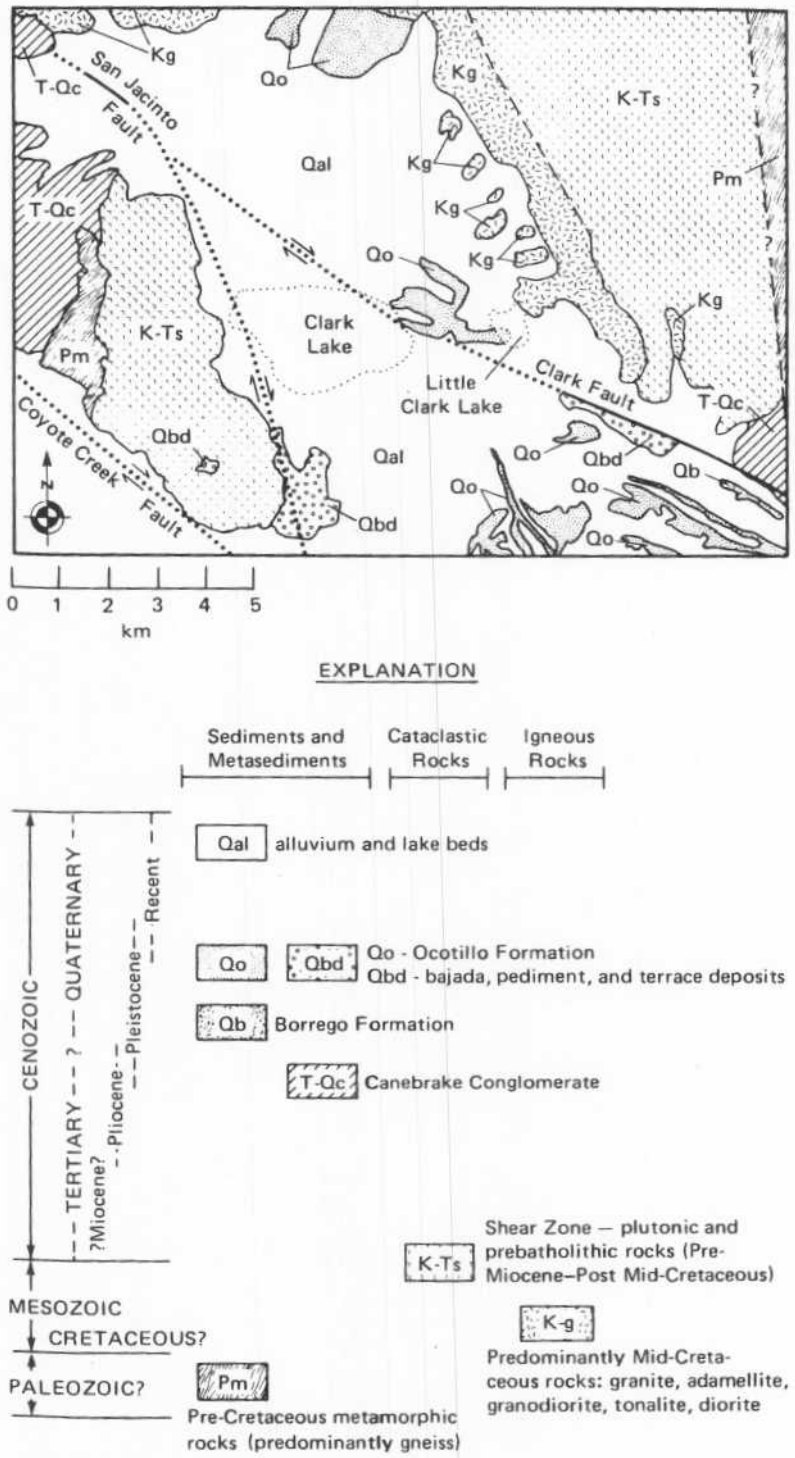

FIGURE 7-29. Generalized geological map of the Clark Valley area. Note the offset of the Late Cretaceous-Early Tertiary shear zone, indicating right lateral displacement along the San Jacinto fault system (after Bartholomew, 1970).

BRAWLEY TO PALM DESERT

This trip traverses the eastern and northeastern margin of the Salton Trough from Brawley to Palm Desert. The subsurface East Pacific Rise extends through Imperial Valley approximately to the southern end of the Salton Sea (Hail and others, 1970). The nearly vertical step faults of the San Andreas fault system structurally bound the trough to the east. Cenozoic sedimentary deposits of the area have been described by Dibblee (1954).

The late Pleistocene Salton Domes, a group of five rhyolitic domes, may be associated with the southern trace of the Banning-Mission Creek fault and lie at an high angle to the fault trace (Kelley and Soske, 1936).

Algodones dunes are a belt of large sand dunes on the southeastern edge of Imperial Valley and may be genetically related to other dune fields in California, Arizona, and Mexico (Merriam, 1969). Algodones dunes have been described by Norris and Norris (1961).

Cultural and historical background is from Brown (1923), Leadabrand (1972), and Pepper (1973).

Mileage		
Cumulative	Difference	
0.0	0.0	Brawley. Junction State Highway 86 and State Highway 78. Follow State Highway 86 south.
9.3	9.3	City of Imperial.
12.8	3.5	State Highway 86 turns left in El Centro.
15.4	2.6	Junction State Highway 86 and Interstate Highway 8. Turn onto Interstate Highway 8 East.
18.4	3.0	Junction State Highway 111 and Interstate Highway 8; continue on Interstate Highway 8.
26.9	8.5	Cross Alamo River.
32.2	5.3	East Highline Canal, part of the All-American Canal system, is located approximately on the high shoreline of Lake Cahuilla. East Mesa, a flat sandy plain, extends eastward from here to Algodones Dunes. Scattered sand dunes cover sections of East Mesa and sand has frequently collected at the base of creosote bushes.
43.4	11.2	Junction of Interstate Highway 8 and State Highway 98. Continue on Interstate Highway 8 East.
47.4	4.0	Cross the All-American Canal. Hoover Dam, Imperial Dam, and the All-American Canal System became possible with the passage of the Boulder

Mileage		
Cumulative	Difference	

Canyon Project Act by Congress in 1928. By 1940 the All-American Canal was providing irrigation water to the valley. The main canal is now 201 km long and the entire system provides irrigation for more than 450,000 acres.

52.5	5.1	Turn off onto Frontage Road to the right. Along Frontage Road is a section of the old plank road (built from 1917 to 1918) which served as the first automobile route across the dunes (Fig. 7-30). Shifting sand often made maintenance of the road difficult and costly. When parts were buried by sand, either the sections were excavated or new sections were built.

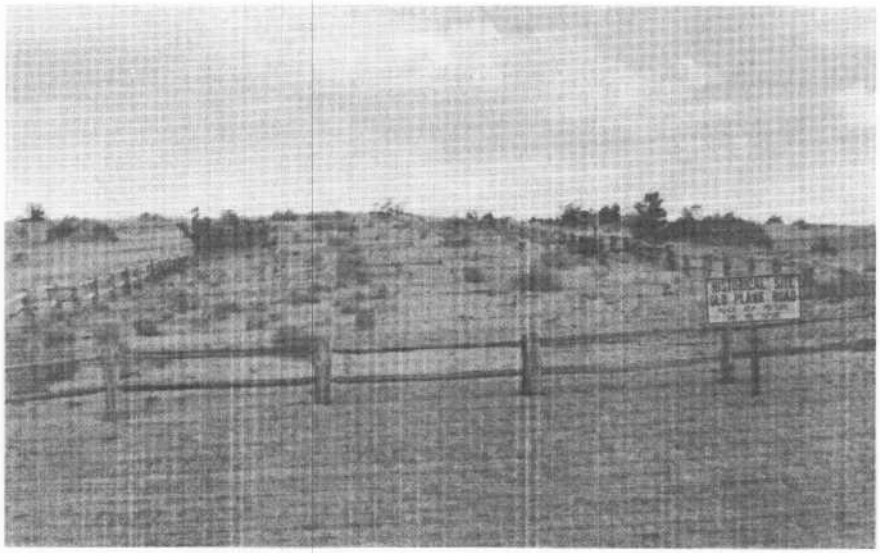

FIGURE 7-30. Remnants of the plank road which was the first automobile route across Algodones dunes. (Photograph by Ronald Greeley, University of Santa Clara, January, 1977.)

STOP 8. ALGODONES DUNES, also known as Sand Hills, extend 64 km in a northwesterly direction. The field is 5 to 10 km wide and contains dunes up to 91 m high. To the south the dunes end abruptly where the sand is removed by the Colorado River. From the ground, the dunes appear to be an unsystematic mass of peaks and valleys (Fig. 7-31), in which the only discernible order is the local consistency of slip face orientation. Aerial photos, however, reveal a series of large ridges in the western part of the field which curve eastward and disappear in a complex of prominent southward facing slip faces. Norris and Norris (1961) believe Algodones Dunes to be a chain of barchan dunes.

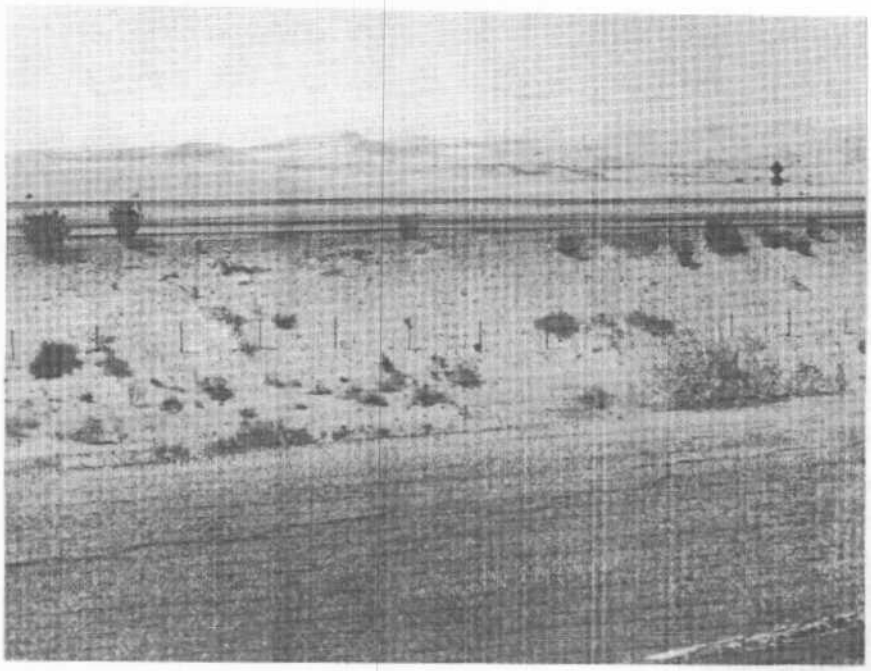

FIGURE 7-31. Aerial view looking northward across the southern Algodones dunes. The highway passes through one of the almost sand-free intradune areas. From the ground, no consistent pattern within the dune field can be seen. (Photograph by John S. Shelton.)

Mileage
Cumulative Difference

The most distinctive features of the southern portion of the dunes are flat-floored, sand free, irregular depressions (Fig. 7-32). These depressions are roughly triangular in plan view with the base, generally about 1.5 km long, transverse to the main dunes trend, with an apex to base distance of approximately 0.8 km. Slip faces 46 m to 61 m high bound the depressions to the north and west while gentle slopes form the southern border. Parallel sand ridges and small barchan dunes indicate active sand encroachment; completely sand free depressions are found only in the southern dunes.

Norris and Norris (1961) believe that the intradune areas have been left uncovered by the dune mass and may be analogous to sand free areas enclosed by merging barchans. An alternative origin is deflation; however, deflation would be unable to account for the ridges which cross the sand free area. The northern slip faces that border the areas are advancing and are clearly constructional forms.

54.7 2.2 Turn back onto Interstate Highway 8 East.

FIGURE 7-32. Oblique eastward aerial view of the almost sand-free intradune areas in the southern Algodones dunes, with the All-American canal on the right. The Cargo Muchacho Mountains are visible in the background. (Photograph by John S. Shelton.)

Mileage		
Cumulative	Difference	
57.7	3.0	All-American Canal. The dunes have decreased in height and form an undulating surface.
59.8	2.1	Turn onto Ogilby Road going north.
60.5	0.7	To the right Ogilby Hills appear in the foreground with the Cargo Muchacho Mountains in the background. Ogilby Hills are composed of a dark gray, fine-grained Pleistocene olivine basalt overlying Mesozoic quartz monzonite.
63.8	3.3	Southern Pacific Railroad. Ogilby Station once existed here as a flag stop; all that remains is the cemetery to the left.

Mileage Cumulative	Difference	
64.0	0.2	Junction Ted Kipf Road and S 34 (Ogilby Road). Remain on S 34.
65.7	1.7	Cargo Muchacho Mountains to the right. The southern Cargo Muchacho Mountains are primarily composed of Mesozoic quartz monzonite and quartz diorite. The quartz monzonite contains clusters of biotite and hornblende crystals and is locally gneissic, aplitic, or porphyritic. The quartz diorite is a dark-colored granitoid rock consisting of gray feldspar and quartz with abundant biotite and hornblende (Strand, 1962). The northwest section of the southern Cargo Muchacho Mountains is composed of the Vitrefrax Formation, a complex of pre-Cretaceous schists. On the outer margin of the Vitrefrax Formation is a small Tertiary andesitic intrusive.
67.0	1.3	Pleistocene volcanic basalt can be seen in hill to the right. These basalts become highly vesicular at both the upper and lower margins. The Cargo Muchacho Mountains behind this knob consist of Mesozoic biotite granite, a variably colored granite characterized by abundant coarse pink to gray feldspar and biotite. The granite is ringed by the Tumco Formation, a gray to pinkish gray, massive, fine-grained, quartzite, with minor gray-green hornblende schist. North of the Tumco Formation, the mountains are composed of leucogranite (Strand, 1962).
68.4	1.4	Knobs of Tumco Formation to the right, with prospect pits. This is the Tumco mining district which operated steadily between 1892 and 1900 and then from 1913 to 1916.
69.0	0.6	To the left is the turnoff to Gold Rock Ranch, a local trading post.
70.9	1.9	Knobs of Tumco Formation and leucogranite on both sides of road.
72.0	1.1	Black Mountain in the distance (Fig. 7-33) consists of vesicular basalt flows. The mountain center is composed of pyroclastic tuff, welded tuff, tuff breccia, agglomerate, and minor interbedded flows (Jennings, 1967).
73.8	1.8	Indian Pass Road is a partially improved dirt trail connecting Ogilby Road and the Colorado River. Along this road are old prospect holes, Indian sites, former Mexican "wetback" camps, and fisherman landings behind Imperial Dam.
81.7	7.9	Road passes through fanglomerate composed of brown to reddish brown cemented gravel from Black Mountain (Jennings, 1967).
85.3	3.6	Junction S34 (Ogilby Road) and State Highway 78 (Ben Hulse Highway). Turn left onto State Highway 78.

FIGURE 7-33. Black Mountain, composed of vesicular basalt flows and tuffs. (Photograph by Ronald Papson, University of Santa Clara, May, 1977.)

Mileage		
Cumulative	Difference	
85.7	0.4	Tertiary hypabyssal andesitic and rhyolitic intrusives on both sides of road. Larger hills in distance to the right are composed of pre-Cretaceous metasedimentary schists.
86.6	0.9	Pre-Columbian Indian Trail historical marker to the left. This well worn trail once connected the Colorado River with ancient Lake Cahuilla.
87.4	0.8	Fault bounded Tertiary andesitic volcanics on the right. The eastern margin of Algodones dunes visible ahead.
90.5	3.1	Dissected fanglomerate of possible Miocene age on the right. Tertiary basalt on the left.
91.9	1.4	Tertiary volcanic basalt knob on the right.
96.7	4.8	Town of Glamis.
100.6	3.9	STOP 9. HUGH T. OSBORN OVERLOOK provides a view of the central portion of Algodones dunes (Figs. 7-34a,b,c). The dune field, which trends northwest-southeast, is 64 km long and 5 to 10 km wide and is located on

Mileage
Cumulative Difference

the southeastern margin of Salton Basin. The northern third of the dune field is composed of a simple undulating ridge, along which the highest peaks lie, and grades southward into a series of parallel ridges on the western margin of the field (see Smith, Chapter 6).

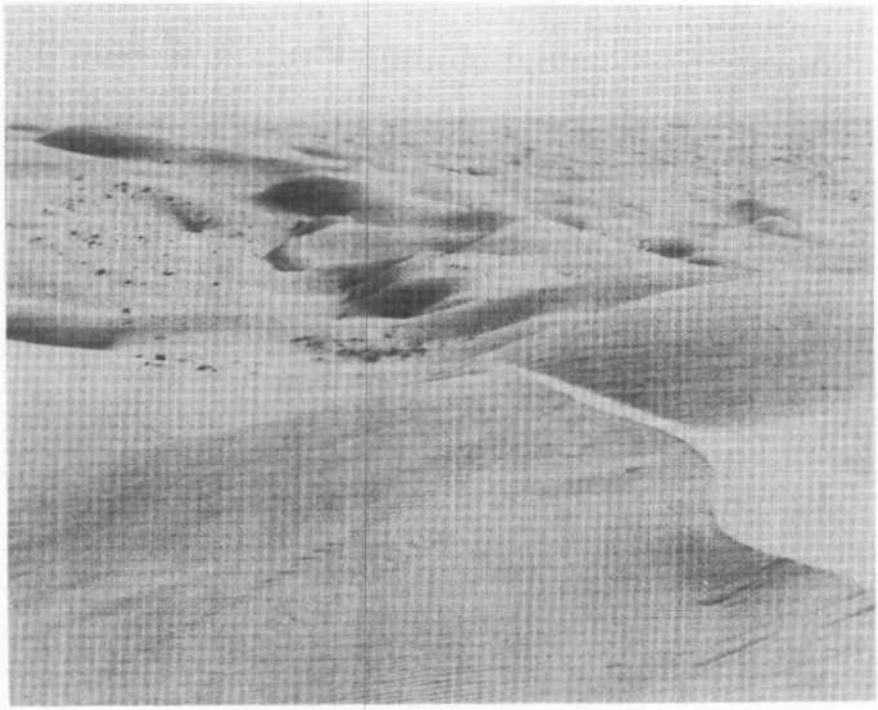

FIGURE 7-34a. Southward view of the central Algodones dunes. Note the unsystematic appearance of the dunes. (Photograph by Ronald Greeley, University of Santa Clara, January, 1977.)

The northeastern margin consists of a sand apron divided into low hook-shaped features extending east and northeast, some of which recurve and point slightly west of north. To the south, the apron extends eastward from the dune mass and thins out against the alluvial fans. The apron and hook features are thin, rarely exceeding 4.6 m in thickness. Vague ridges are found on the sand apron but are less than 3 m high and rarely more than 183 m to 244 m long. They are parallel to the main dune mass and are 30 m to 91 m apart (Fig. 7-35).

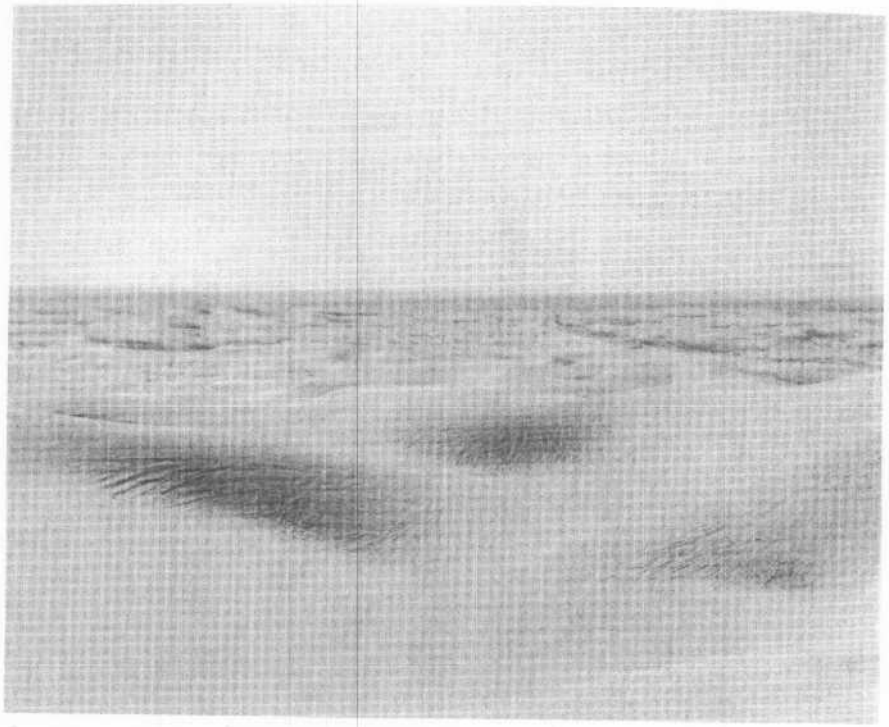

FIGURE 7-34b. Westward view of the central Algodones dunes. (Photograph by Ronald Greeley, University of Santa Clara, January, 1977.)

Mileage		
Cumulative	Difference	
		Characteristics of the Algodones sand are: 1) more potassium-feldspar than plagioclase, 2) fine-grained lithic fragments consisting of volcanics and subordinate chert, 3) detrital foraminifera identical to those of the Upper Cretaceous Mancos Shale of the Colorado Plateau, 4) about 5 percent carbonates, including detrital calcite, dolomite and minor amounts of foraminifera, and 5) very uniform sorting. Since the first four characteristics also apply to all of the Cenozoic Colorado River sediments in the area, it is concluded that the sand of Algodones dunes originated from the Colorado River sediments (Merriam, 1969), instead of from the Whitewater River and locally derived sediments, as postulated by Norris and Norris (1961).
103.0	2.4	Road to left goes to Gekco Campsite, about 5 km south of here. Cross the trace of the San Andreas fault and leave Algodones dunes.
103.8	0.8	Coachella Canal.

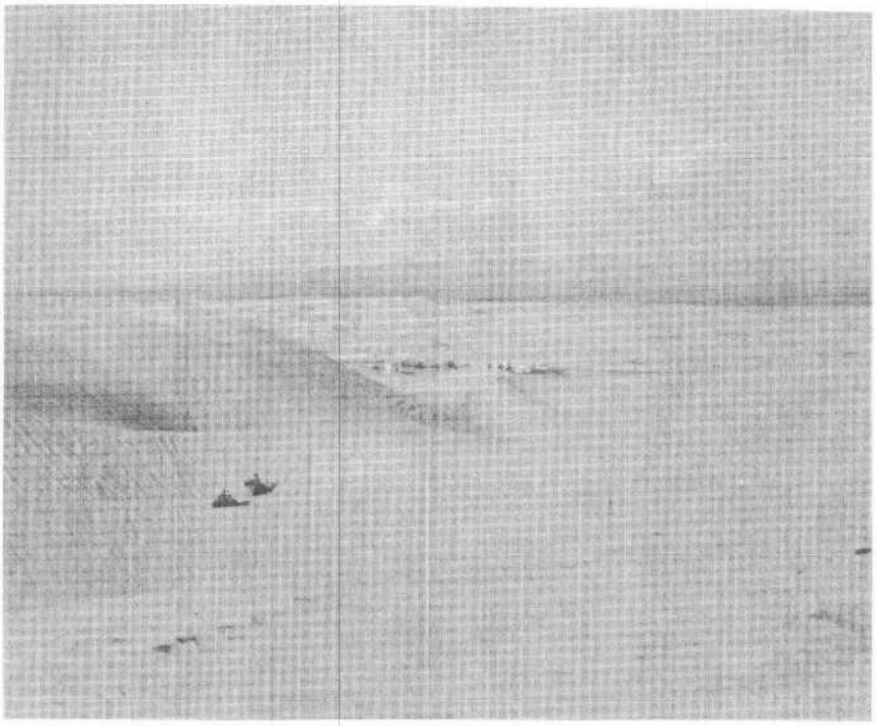

FIGURE 7-34c. Northward view of the central Algodones dunes, with the Chocolate Mountains in the background. (Photograph by Ronald Greeley, University of Santa Clara, January, 1977.)

Mileage		
Cumulative	Difference	
110.1	6.3	Pass sand ridge marking the shoreline of Lake Cahuilla.
110.4	0.3	East Highline Canal of the All-American Canal System.
120.4	10.0	Alamo River.
123.3	2.9	Brawley city limit.
123.8	0.5	Junction State Highway 78 and State Highway 111. Turn right onto State Highway 111.
125.8	2.0	New River. The first canal system for Imperial Valley incorporated the New River. During the floods of 1905 through 1907, the Colorado River widened the river banks which remain today as testimony of the power of the raging river. Today the New and Alamo Rivers serve as drainage channels for the irrigated fields.

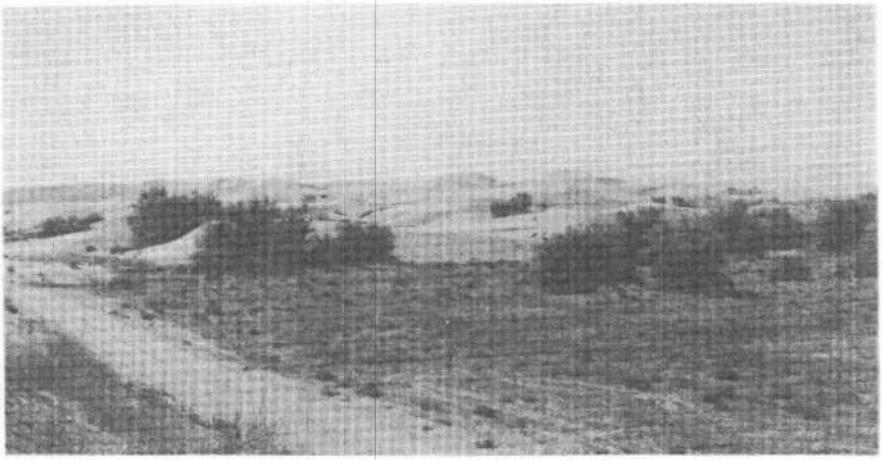

FIGURE 7-35. Relatively dense vegetation along the eastern margin of Algodones dunes. The edge of the dune field here is sharply defined. (Photograph by Eilene Theilig, University of Santa Clara, May, 1977.)

Mileage		
Cumulative	Difference	
128.9	3.1	New River.
131.2	2.3	Two Rivers Rest Area.
134.3	3.1	Junction State Highway 111 and State Highway 115 in Calipatria (elevation 56 m), which is known as the "lowest down city in the Western Hemisphere." Turn left onto State Highway 115 (dirt road).
137.3	3.0	Alamo River.
139.9	2.6	Turn right onto Gentry Road.
142.9	3.0	Turn left onto road to Obsidian Butte.
143.9	1.0	STOP 10. OBSIDIAN BUTTE is the southernmost member of the Salton Domes. Obsidian Butte consists of a central pumice dome which is ringed by several flow-banded obsidian outcrops. Obsidian Buttes originated as magma encountered a previously emplaced resistant pumice cap and flowed laterally towards the margin, where it chilled quickly into preferential obsidian domes (Fig. 7-36) (Kelley and Soske, 1936).

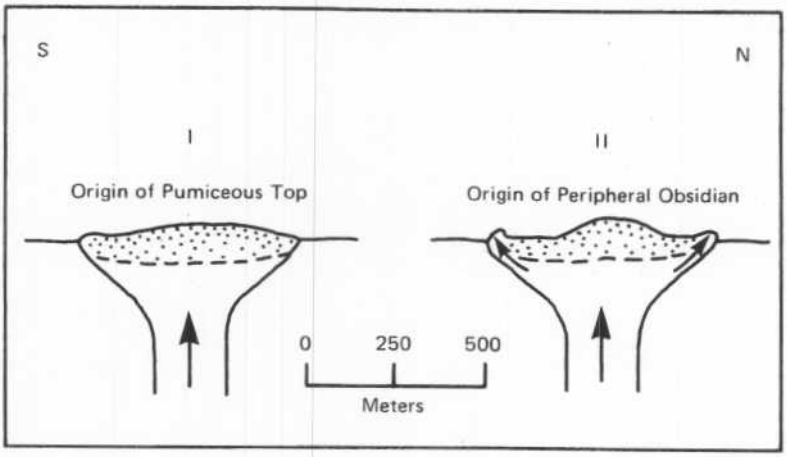

FIGURE 7-36. Schematic diagram of the formation of Obsidian Butte (from Kelley and Soske, 1936).

Mileage		
Cumulative	Difference	
144.9	1.0	Return to Gentry Road, turn left.
145.4	0.5	Turn left onto Sinclair Road.
145.9	0.5	STOP 11. SALTON DOME. Park here and walk to Salton Dome Observation Point along the trail on the east side of the dome. From this vantage point, the other rhyolitic Salton Domes can be seen – Obsidian Butte to the south and Pumice Buttes and Mullet Island to the north. Salton Domes are arranged roughly parallel to the southeastern shore of Salton Sea (Fig. 7-37), lie perpendicular to the trace of the San Andreas fault, and are dated at 16,000 years B.P. (Muffler and White, 1969). The mud pots associated with the domes are now inactive and partially submerged by the Salton Sea.

Xenoliths include mudstone, sandstone, basalt, and leucocratic granite (Robinson and Elders, 1970). The mudstone and sandstone xenoliths originated from deltaic sediments while the basaltic xenoliths were derived from either the basement or, more probably, numerous basaltic intrusions within the deltaic sediments (Robinson and Elders, 1970). Compositional similarities between the rhyolites and granitic xenoliths indicate that the magma was partially generated by melting of the continental crust (Elders and Robinson, 1970). Hail and others (1970) proposed that the East Pacific Rise extends beneath the sediments of Imperial Valley to approximately the Salton Sea. These rhyolites would, therefore, be the first surficial magmatic episodes in the generation of a "proto-ocean" (Elders and Robinson, 1970).

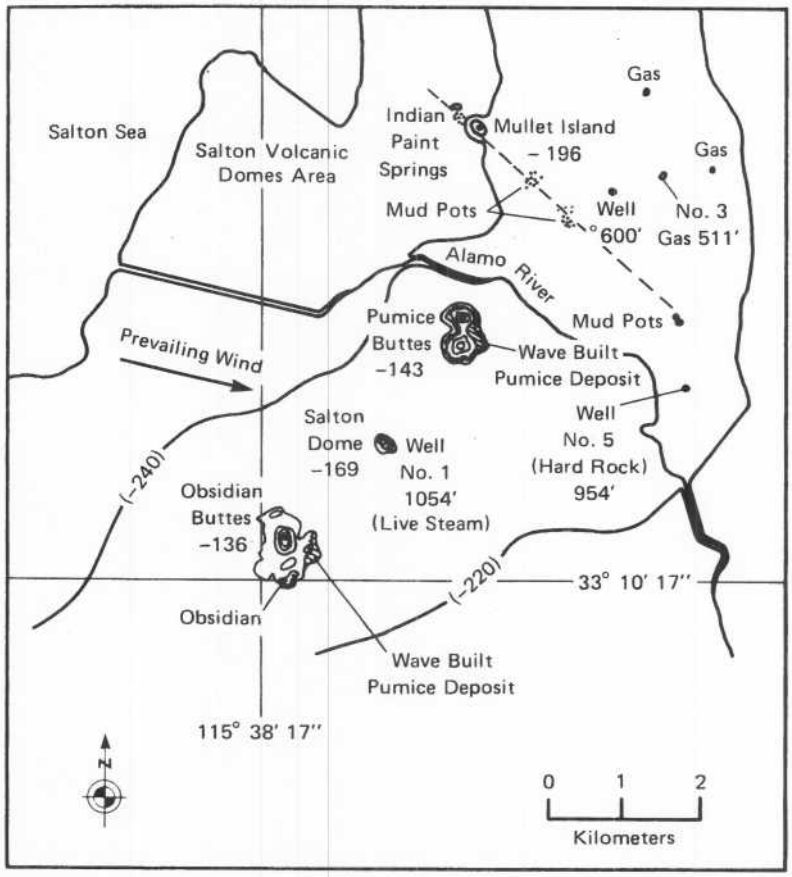

FIGURE 7-37. Map of Salton Domes showing the location of the mud pots and the wave-built pumice deposits on the east side of Obsidian and Pumice Buttes (from Kelley and Soske, 1936).

Mileage
Cumulative Difference

A region of high heat flow and thermal spring activity covers 31 km^2 near Salton Domes. Early descriptions of the area (Blake, 1855) indicate abundant thermal activity in the past, but today activity is limited to a few passive CO_2 rich hot springs and cool mudpots.

This area first attracted commercial interest in 1927 when three exploratory steam wells were drilled; however, heat production was insufficient to generate power (Rook and Williams, 1942). In 1957 large amounts of hot brine encountered in a deep discovery well renewed interest in geothermal production.

Mileage
Cumulative Difference

One of the unique characteristics of this field is the high concentration of dissolved elements in the brines. The brine composition is a result of high temperature reactions between pore fluids and deep sediments (Helgeson, 1968). The geothermal field is localized by the low thermal conductivity of upper lacustrine shales. Heat may be generated by: 1) a cooling intrusive body at depth, or 2) conduction from the mantle. Geophysical studies reveal no deep intrusions at depth; however, numerous dikes and sills within the sediments do give evidence of local Plio-Pleistocene volcanism. Koenig (1967) favors a heat transfer system of convection in the mantle, conduction through a thinned continental crust, and convection in the overlying water saturated sediments (Fig. 7-38). Two possible origins for the brines are: 1) local runoff from surrounding mountains, and 2) connate water from the Colorado River sediments.

A quarry wall (Fig. 7-39) on the west side of Salton Dome reveals nearly vertical flow structures on the flanks, which indicate a plug-like emplacement. In 1936 Kelly and Soske observed numerous small vents from which steam escaped but are not visible today.

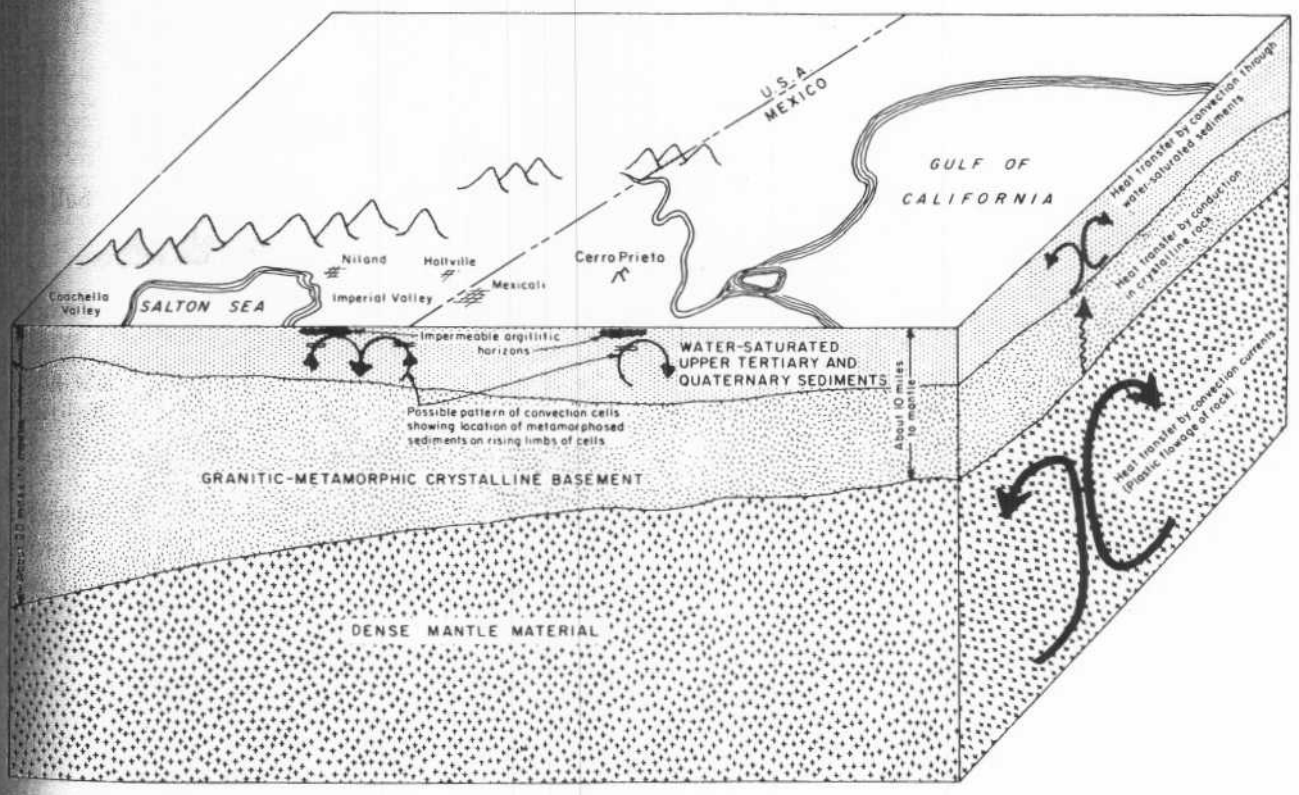

FIGURE 7-38. Schematic block diagram northwest-southeast along Salton-Mexicali trough, showing possible methods of heat transfer and development of geothermal fields (from Koenig, 1967).

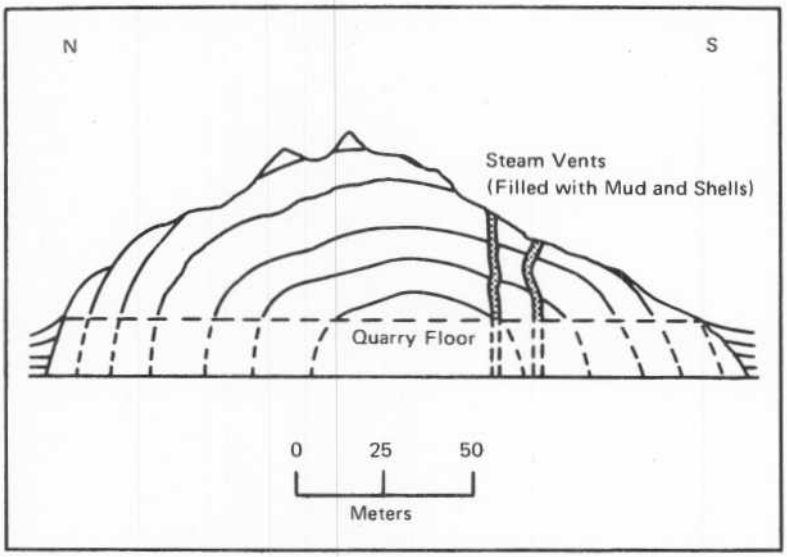

FIGURE 7-39. Schematic diagram of quarry face at Salton Dome in 1936, showing approximately vertical steam vents. The vents were subsequently filled by material from Lake Cahuilla (from Kelley and Soske, 1936).

Mileage		
Cumulative	Difference	
148.4	2.0	Turn left on Garst Road.
149.9	1.5	Turn left onto road to Red Hill Marina and Campground, part of the Salton Sea National Wildlife Refuge.
150.9	1.0	STOP 12. PUMICE BUTTES consist of two small coalesced volcanic domes of rhyolitic pumice with subordinate amounts of obsidian (Fig. 7-40). Wind and waves have exhumed an extensive mudflow on the southern dome and have revealed textures and crude bedding typical of consolidated mudflows (Fig. 7-41). A wave-built terrace on the eastern side contains a high grade pumice which has been extensively quarried. One such quarry at Pumice Buttes has provided excellent cross sections of the terrace material (Fig. 7-42). The cross sections reveal clay and silt interbedded with coarse sandstone and conglomeratic layers (Fig. 7-43a,b) that are composed of pebbles and cobbles of pumice and obsidian. Finer grained beds often contain pebbles of volcanic rocks and shells. Some cross-bedding is visible (Fig. 7-44).
153.4	2.5	Return to Sinclair Road; turn left.
157.9	4.5	Junction Sinclair Road and State Highway 111. Turn left onto State Highway 111.

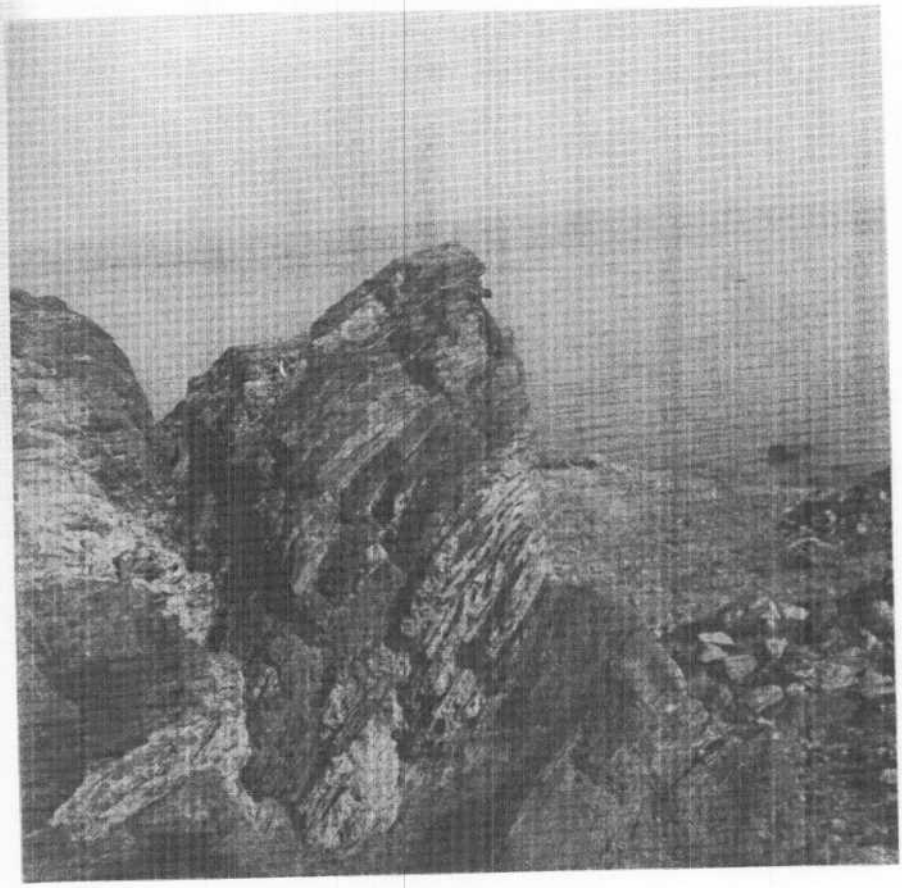

FIGURE 7-40. Pumice and obsidian outcrop of Pumice Buttes. Salton Sea is in the background. (Photograph by Ronald Papson, University of Santa Clara, May, 1977.)

Mileage		
Cumulative	Difference	
162.3	4.4	Turn right onto Beal Road in Niland.
164.5	2.2	East Highline Canal.
165.1	0.6	Sand ridge represents the high shoreline of Lake Cahuilla. Shoreline features are generally more persistent on the eastern side of the basin; however, in this area, beach deposits are only found as remnants between present day drainage channels (Norris and Norris, 1961).
167.9	2.8	Return to State Highway 111; turn right.
174.2	6.3	Chocolate Mountains to the right are composed of Precambrian igneous and metamorphic rocks, pre-Cretaceous metasedimentary schists, and Tertiary volcanics and hypabyssal intrusives.

Mileage		
Cumulative	Difference	
25.8	1.0	Whitewater River is an intermittent braided stream with a watersh rea of 3100 km² (which includes northeastern Coachella Valley) and ately drains into the Salton Sea. The river originates in the San Bernar Moun- tains and has an average gradient of 9.5 to 19 m/km.

San Gorgonio Pass to the left, discovered in 1853 by R. S. Willia , pro- vides the best route across the mountains to the Pacific coast. It arates the San Bernardino Mountains of the Transverse Range province n the San Jacinto Mountains of the Peninsular Range province. The Salto ough, an extension of the Gulf of California structural province, narrow and ter- minates at the pass (Fig. 8-1). Truncation of the Salton Trough and iated complex structure is caused by interaction between the east trend aults of the Transverse Ranges and the northwest trending faults of th alton Trough (Biehler and others, 1964). San Jacinto Peak (elevation 33 and San Gorgonio Mountain (elevation 3506 m) rise steeply at the stern entrance to San Gorgonio Pass (Fig. 8-7).

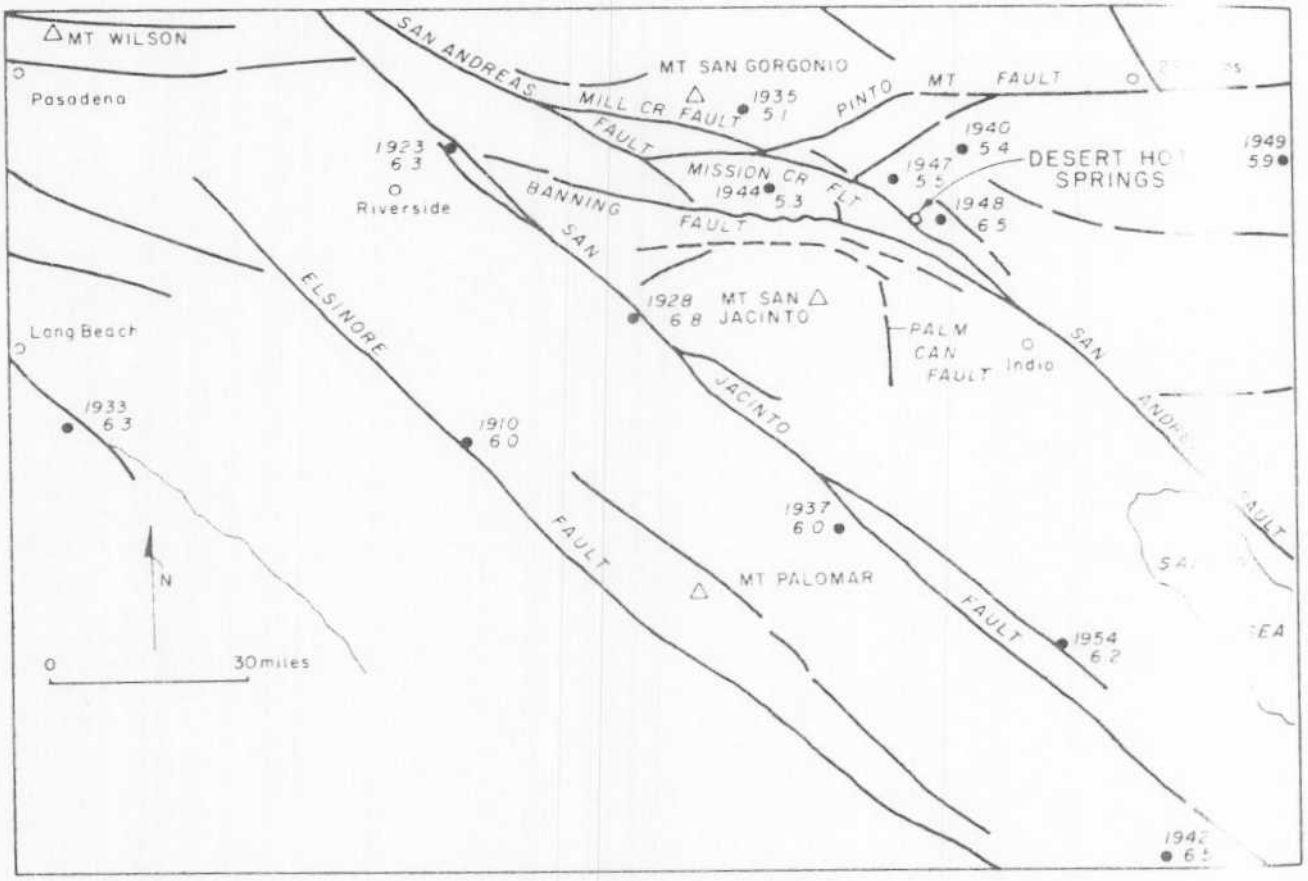

FIGURE 8-7. Major faults of southern California where the east trending faults of the Transverse Ranges m the northwest trending faults of the Salton Trough meet, resulting in complex structures. Also indicat re epicenters of earthquakes 5.9 or greater (Richter scale) that have occurred within the past 50 years ir additional earthquakes of lesser magnitude around Desert Hot Springs are shown (from Proctor, 1968).

Mileage		
Cumulative	Difference	
27.8	2.0	STOP 2. GARNET HILL (see Sharp and Saunders, Chapter 2) is a low anticline associated with the buried Garnet Hill fault (evidence by a trough defined by gravity low contours) located immediately to the south (Fig. 8-8).

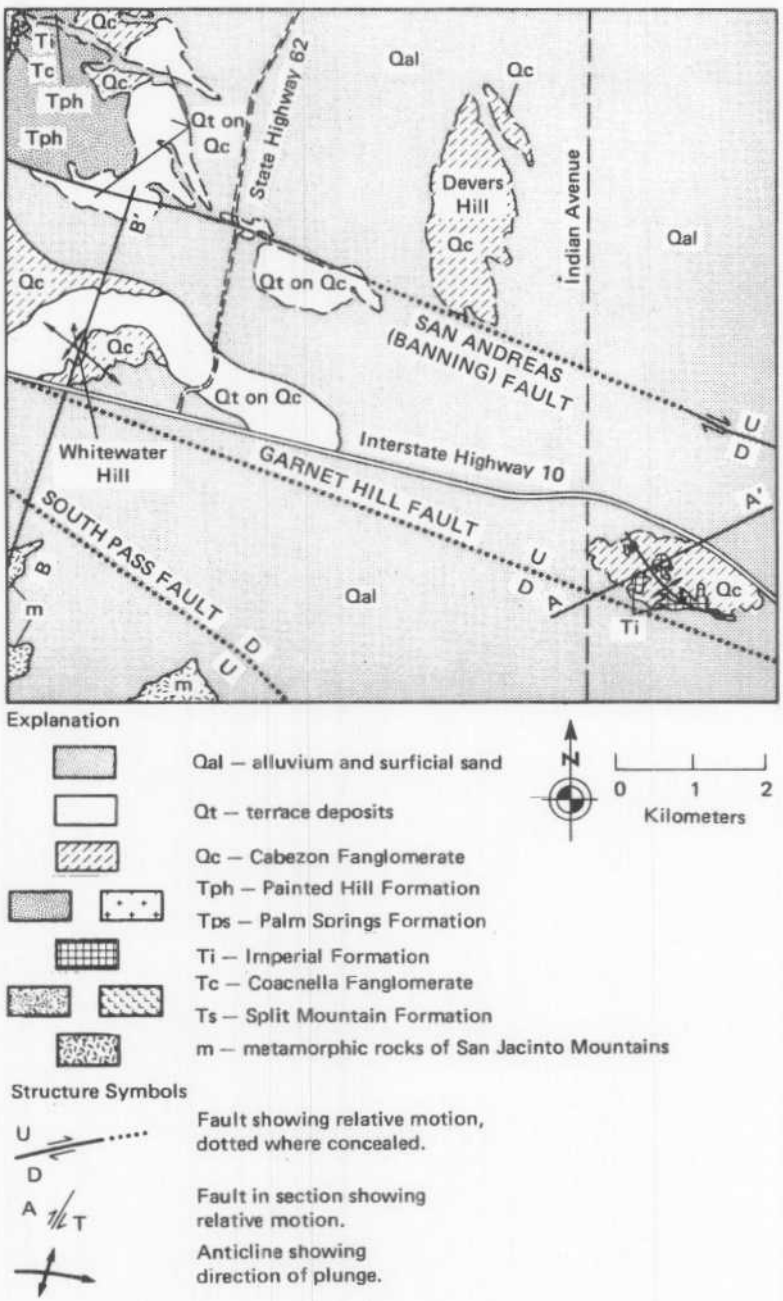

FIGURE 8-8. Geological map of Garnet, Whitewater, and Devers Hills. These hills consist of Cenozoic sediments deformed along faults associated with the San Andreas fault system. Cross sections of Garnet and Whitewater Hills are also shown (modified after Proctor, 1968).

Mileage
Cumulative Difference

Garnet Hill fault parallels the San Andreas fault system 2.4 km to the north, and is probably an ancestral branch of the system. Garnet Hill is composed of fossiliferous marine sandstone and shale of the Imperial Formation, overlain by the Cabezon Fanglomerate. At depth the Imperial Formation is underlain by the Split Mountain Formation (Fig. 8-8). Garnet Hill is situated within the path of prevailing winds from San Gorgonio Pass which have wind speeds high enough to move sand and capable of sand-blasting resistant surfaces. Evidence of the scouring action by wind is seen on many boulders at Garnet Hill (Fig. 8-9A, -9B, -10, -11); however, most of the flutes and pits seen here are the result of wind action several thousand years ago. Vegetation on the hill has been affected by the wind and commonly grows in the downwind direction.

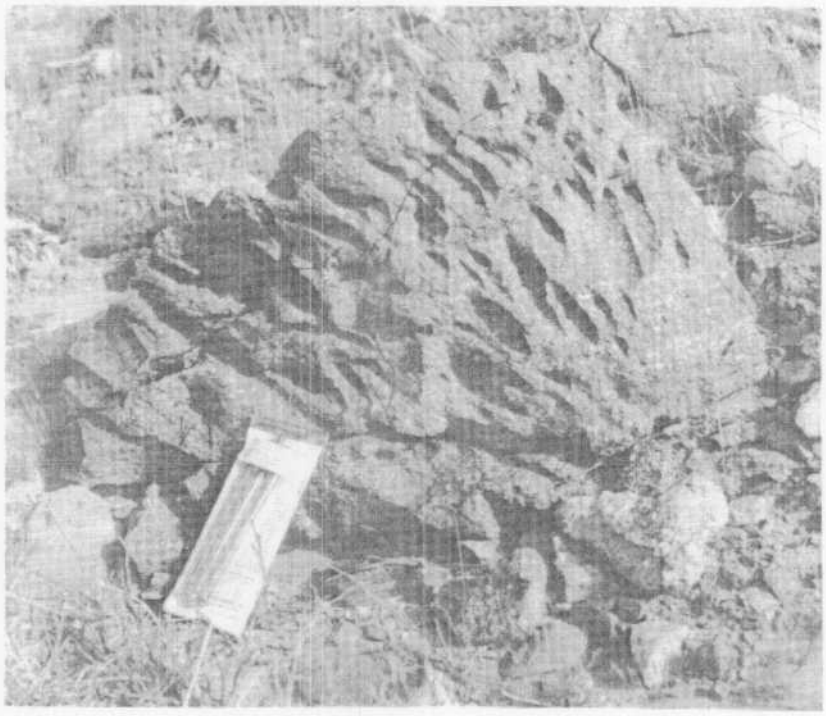

FIGURE 8-9A. Boulders on Garnet Hill exhibiting flutes formed by wind action. Fractures cross-cutting the flutes indicate that they are very old (several thousand years) and not a result of current wind action (photograph by Ronald Papson, University of Santa Clara, May, 1977).

FIGURE 8-9B. (Photograph by Ronald Greeley, January, 1977).

Mileage		
Cumulative	Difference	
		From here, Whitewater Hill, at the junction of State Highway 62 (Twenty-nine Palms Highway) and Interstate Highway 10, is visible to the west northwest. Whitewater Hill is a domical anticline formed by recent warping (Proctor, 1968) possibly associated with activity along the Garnet Hill fault (Fig. 8-8). Surficial material on the hill consists of Cabezon Fanglomerate and a thin orange mantling of terrace deposits. A superposed radial drainage pattern (Fig. 8-12) and an undulating surface indicate that deformation may still be occurring (Proctor, 1968).
28.0	0.2	Junction Indian Avenue and Interstate Highway 10; continue northward on Indian Avenue.
29.9	1.9	Devers Hill, an inlier of Cabezon Fanglomerate (now being buried by recent aggradation) can be seen to the left (Fig. 8-8). In the distance to the left, are the foothills of the San Bernardino Mountains which are composed primarily of Cenozoic sediments.

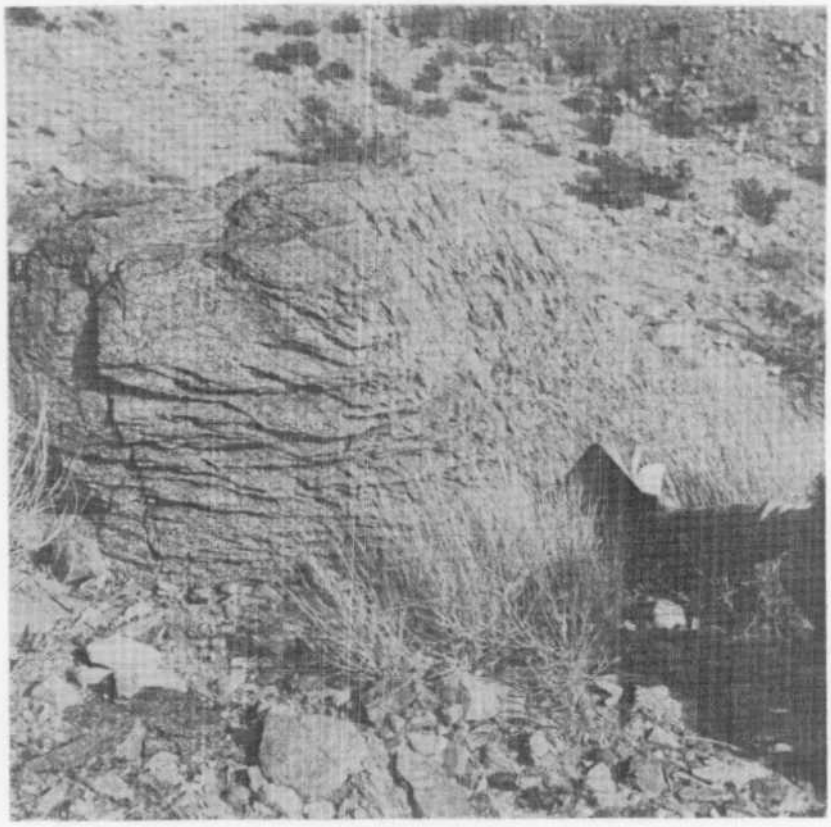

FIGURE 8-10. Boulder on Garnet Hill eroded by wind. To the right, flutes and pits predominate, whereas on the left, erosion has occurred along foliation planes (photograph by Ronald Papson, University of Santa Clara, May, 1977).

Mileage		
Cumulative	Difference	
31.9	2.0	Pierson Boulevard, continue straight. Ahead are the Little San Bernardino Mountains, bounded on the south by the Mission Creek fault: a reverse, right lateral fault. To the east, the base of the mountain front extends beneath the alluvium. Fault planes of the Mission Creek fault zone dip more steeply to the east (as the zone curves southeastward) until they are nearly vertical in Indio Hills. Along the valley margin the fault traces are marked by disrupted alluvium, truncated older fans, and heavy vegetation where ground water, dammed on the north side of the fault, supports plant growth. In this area the Little San Bernardino Mountains are composed of the Precambrian San Gorgonio Complex, a mixture of igneous and metamorphic rocks.
36.1	4.2	Junction Indian Avenue and State Highway 62. Turn onto State Highway 62 north to Twentynine Palms. Here, the Mission Creek fault zone forms scarps in the green amphibolite gneiss of the San Gorgonio Complex. The main fault is considered to be located along the southernmost scarp.

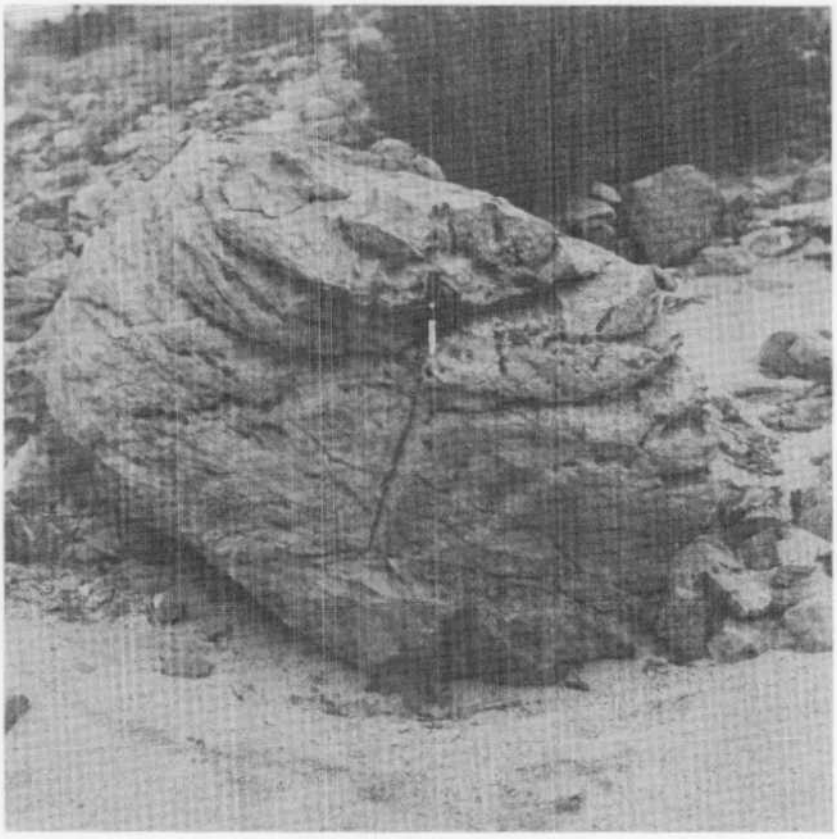

FIGURE 8-11. Boulder on Garnet Hill exhibiting pits and flutes formed by sand blasting several thousand years ago (photograph by Ronald Greeley, University of Santa Clara, May, 1977).

Mileage		
Cumulative	Difference	
		The highway enters Morongo Valley Canyon (Dry Morongo Canyon) which cuts through rocks of the San Gorgonio Complex in the Little San Bernardino Mountains. The San Gorgonio Igneous Metamoprhic Complex is equivalent to the Chuckwalla Complex of Miller (1964) and consists of a heterogeneous assemblage of intermediate to basic gneisses locally injected by quartz monzonitic intrusives.
38.8	2.7	Enter Morongo Valley which is interpreted as a wedge shaped graben dividing the San Bernardino and Little San Bernardino Mountains. The valley is bounded to the southeast by the Morongo Valley fault zone and to the southwest by the Dry Morongo fault (Fig. 8-2). To the northwest there is no direct evidence of a fault; however, the Pinto Mountain fault, 3 km to the north, exhibits relative vertical displacement and supports the graben theory. Relative motion along the Morongo Valley fault is left lateral.

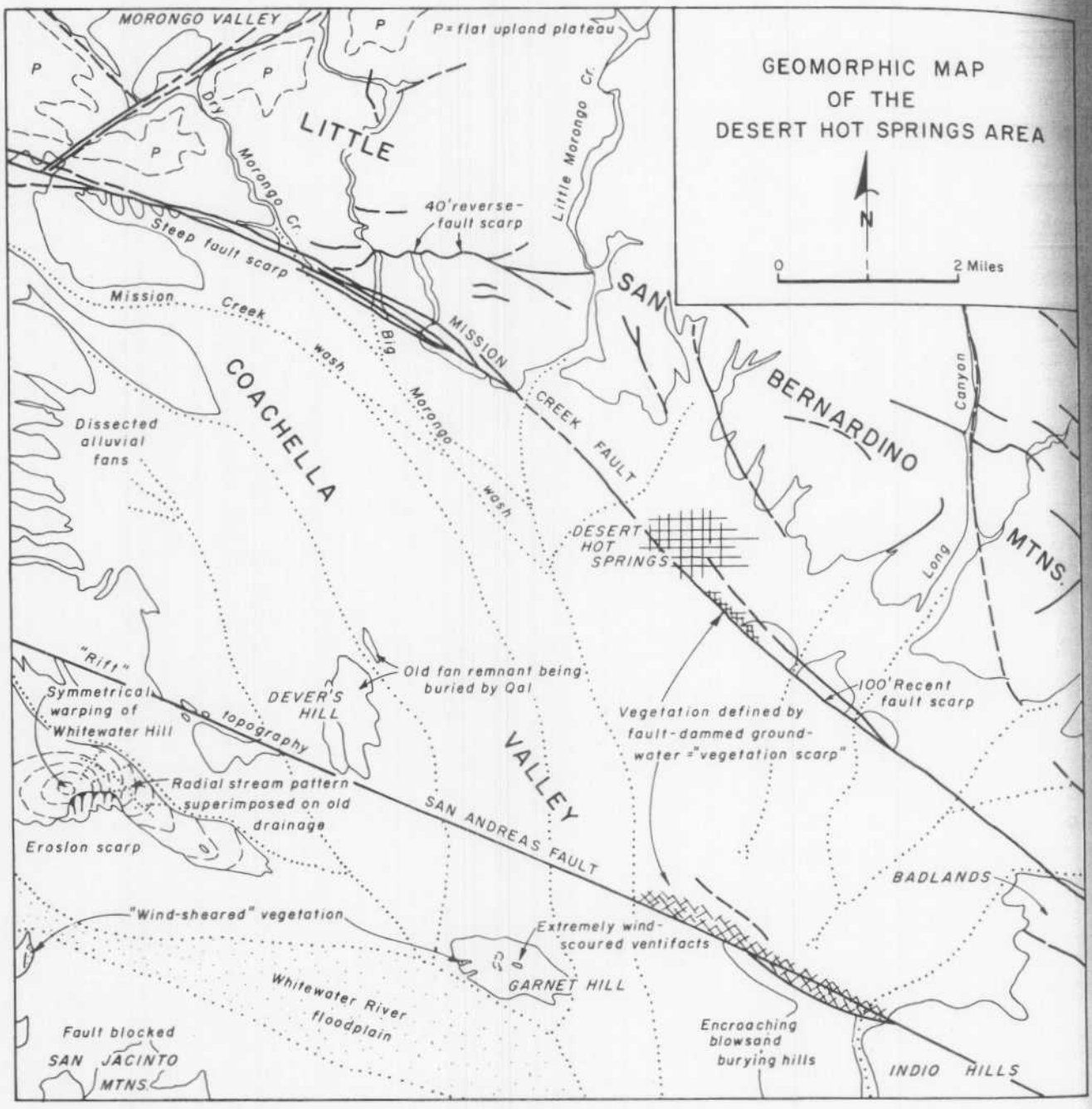

FIGURE 8-12. Geomorphic map of the Desert Hot Springs area (from Proctor, 1968).

Mileage		
Cumulative	Difference	
41.6	2.8	Dry Morongo, Big Morongo, and Little Morongo Creeks flow across Morongo Valley and then pass southward through the Little San Bernardino Mountains, bypassing an easier route through the valley. During the Pleistocene, wet climates causing torrential runoff from the eastern slopes of the San Bernardino Mountains and uplift of the surrounding mountains incised the present-day stream channels (Proctor, 1968). Vaughn (1922) believed that Dry, Big, and Little Morongo Creeks captured an ancestral east flowing Morongo Valley stream; however, no evidence of such an ancestral stream is seen.
42.3	0.7	To the left, the San Bernardino Mountains rock type changes from San Gorgonio Complex in the south, to Cactus Quartz Monzonite in the north. The latter formation is a gray-buff biotite quartz monzonite with subordinate granite.
45.9	3.6	As the highway climbs out of Morongo Valley it passes between the Pinto Mountain fault and the Morongo Valley fault. The Pinto Mountain fault is the most physiographically prominent east trending fault zone in the southern Mojave Desert and extends eastward from the San Andreas fault near San Gorgonio Peak along the northern edge of the Little San Bernardino and Pinto Mountains (Allen, 1957). Motion along the fault appears to be left lateral along the western portion and vertical in the central and eastern portions.
49.1	3.2	Yucca Valley. To the south are the western Little San Bernardino Mountains composed of gneiss with subordinate quartz monzonite and granodiorite intrusives. The gneiss is medium to coarsely crystalline and ranges from dark gray, prominently laminated quartz diorite gneiss, to light gray to buff white, faintly laminated quartz monzonite gneiss. The gneiss has been mapped as San Gorgonio Complex (Rogers, 1967) and as Pinto Gneiss (Rogers, 1961). To the north, Water Canyon provides excellent exposures through the monzonite of the San Bernardino Mountains. This unit is white to light gray, massive and medium to coarse grained and is part of the Southern California batholith. Pinto Mountain fault is located at the base of the mountain front.
51.0	1.9	Junction State Highway 62 and State Highway 247. Continue on State Highway 62. Burnt Mountain, to the right, is a remnant of Pleistocene fanglomerate composed mainly of detrital gneiss with granodiorite cobbles and pebbles.
52.9	1.9	Hill to the left is composed of quartz monzonite, surrounded on the east, north, and west by Pinto Gneiss; a dark-colored strongly foliated, quartz biotite gneiss.
		To the south, rock types in the Little San Bernardino Mountains change from gneiss to a light gray to buff, massive to somewhat gneissoid, fine to medium grained granodiorite. In some places it is slightly porphyritic with

Mileage Cumulative	Difference.	
		phenocrysts of potassic feldspar. Several hornblende diorite or gabbro intrusives are found within this unit. The stream near the contact of the two units provides drainage for Lower Covington Flat within Joshua Tree National Monument.
54.6	1.7	Narrow bands of gneiss within leucocratic quartz monzonite compose the mountain to the left. The quartz monzonite is similar to Palms Quartz Monzonite within Joshua Tree National Monument (Dibblee, 1967).
57.0	2.4	Road to the northwest entrance of Joshua Tree National Monument junctions from the right and follows Quail Wash into the mountains. To the east of Quail Wash the predominant rock type is quartz monzonite. Continue on State Highway 62.
60.1	3.1	Hill to the left is composed of leucocratic quartz monzonite intruded by several mafic dikes. The slight rise to the north is Pleistocene alluvial fan material that is presently being dissected.
62.5	2.4	Dry Lake at base of Copper Mountain to the left.
63.3	0.8	Copper Mountain is divided into two distinct areas; the northern portion is bounded on the southwest by a fault that continues through the southern portion of the mountain. The southwest block is downdropped and rock types include quartz monzonite and gabbro. North of the fault, the mountain is composed of quartz monzonite, gabbro, and Pinto Gneiss. The Pinto Mountain fault is located at the southern base of Copper Mountain.
66.1	2.8	To the north, sand has accumulated around a knob of Pinto Gneiss. On the right, Rattlesnake Canyon divides two types of granitic intrusives: quartz monzonite on the west and a quartz monzonite porphyry containing large phenocrysts of potassic feldspar on the east.
67.7	1.6	Pleistocene alluvial fan material forms rolling hills to the left. Sand accumulating along the base of the Bullion Mountains can be seen.
68.7	1.0	Small rise of Pleistocene alluvial deposits.
69.5	0.8	Highway crosses the trace of Pinto Mountain fault; however, there is no observable evidence for its location.
72.1	2.6	Junction State Highway 62 and Adobe Road in Twentynine Palms. Turn left onto Adobe Road. Twentynine Palms served as a base camp for the Palms Mining District in the late 1800's. An oasis is located on the Pinto Mountain fault and can be seen at the Joshua Tree National Monument Visitors Center. Twentynine Palms served as a base camp for the Palms Mining District in the

Mileage Cumulative	Difference	
		late 1800's. Although the first claims in the district were filed in 1873, by 1883 the miners had moved farther into the hills and Twentynine Palms had become quiet and inactive (Miller, 1968).
74.1	2.0	Turn right onto Amboy Road.
74.6	0.5	Sand mounds to the left. Pinto Mountains are visible to the right and are composed of quartz monzonite, quartz diorite, diorite, Pinto Gneiss, and a Precambrian igneous and metamorphic complex.
75.7	1.1	Mesquite Dry Lake fault extends N30°W from Twentynine Palms to Gypsum Ridge, a distance of about 25 km, and is delineated on aerial photographs by a relative abundance of vegetation. Probable right lateral motion is indicated by WNW trending fold axes in Gypsum Ridge, which is adjacent to and associated with the fault. The fault has also caused local folding in the Pleistocene alluvial fan material east of Twentynine Palms. A typical section of these hills (on the right) consist of coarse sands and gravels near the top and finer sand and silt below. A graben exists eastward from Mesquite Dry Lake fault to Bullion fault (Bassett and Kupfer, 1964). The east trending Pinto Mountain fault is intersected and disrupted by the Mesquite Dry Lake fault slightly south of here and has resulted in complex structures and a possible offset of the Pinto Mountain fault.
81.5	5.8	Valley Mountain to the left consists of two hills connected by a low saddle. The western hill is composed of pre-Cretaceous metasediments and metavolcanics, along with Cretaceous granitic intrusives, and is bounded on the southwest by the Bullion fault. The eastern hill is also fault bounded to the southwest but consists primarily of Cretaceous granitic intrusives and a small outcrop of Tertiary volcanics (Bishop, 1963). Faults passing through Valley Mountain may be part of the Bullion fault zone.
85.1	3.6	Region of vegetation shadow dunes and sand sheets.
88.1	3.0	On the left, fault contact between granitic rocks (northwest) and granitic metamorphic complex rocks (southeast) in the Bullion Mountains. To the east, the Bullion Mountains consist primarily of metasediments.
90.0	1.9	Large bajada from Bullion Mountains is composed of Pleistocene sediments to the west and recent alluvial fans to the east. The Dale Mining district (Fig. 8-13), which became an active mining center as the activity around Twentynine Palms decreased, is located in the Pinto Mountains to the right. The town of New Dale was located near the Supply Mine which produced $1 million in gold until 1917. The mine has been inactive since World War II. At one time New Dale had a population of 3,000 but very little remains of the town today.

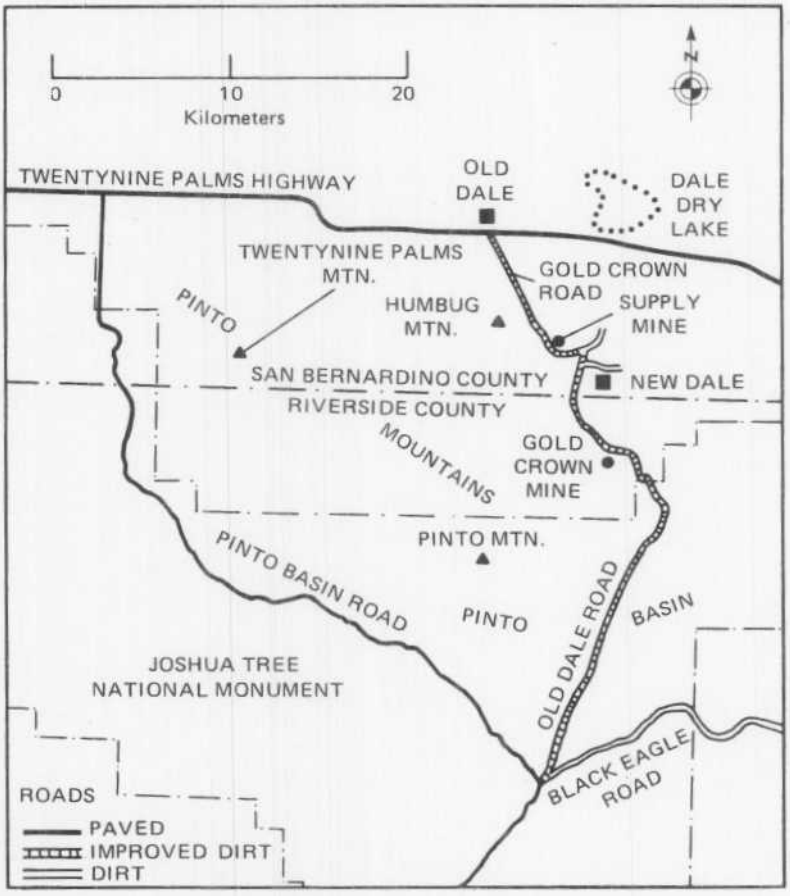

FIGURE 8-13. Location map of the Dale mining district (from Leadabrand, 1972).

Mileage

Cumulative Difference

91.7 1.7 Barnett. Dale Dry Lake, to the right, is a moist type of playa that has formed where the water table is located at or near the surface (Bassett and Kupfer, 1964) (Fig. 8-14). Part of the playa is covered by a brine or consists of a perennially brine soaked clay. Elsewhere the surface consists of a crust of puffy, loosely packed salt mixed with clay and silt deposits. This type of deposit forms by evaporation of ground water drawn to the surface by capillary action. Around the edge of Dale Dry Lake, alluvial sand has mixed with playa materials forming a transition zone between the two. Sand features seen around Dale Dry Lake include fixed and shadow dunes and sand sheets.

Playas occupy the flat central basin of a desert plain and require interior drainage, with evaporation exceeding precipitation. Present-day playas of the Basin and Range province and associated areas are remnants of semi-permanent water bodies created in the cooler, moist, "pluvial climates" of previous glacial epochs (Fig. 8-15). Extended periods of moist climates in recent times have reverted some playas to lakes, indicating that they are sensitive to climatic fluctuations (Neal, 1965).

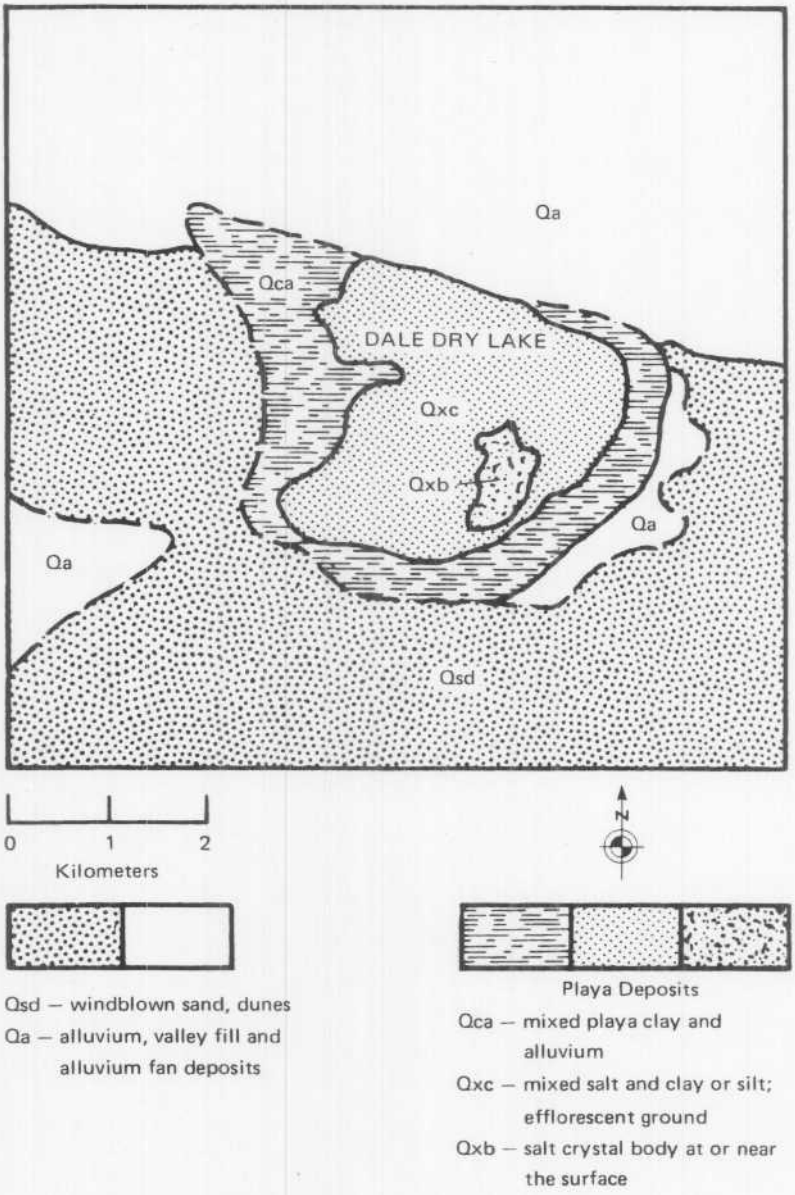

FIGURE 8-14. Geological sketch map of Dale Dry Lake showing playa surface deposits (after Bassett and Kupfer, 1964).

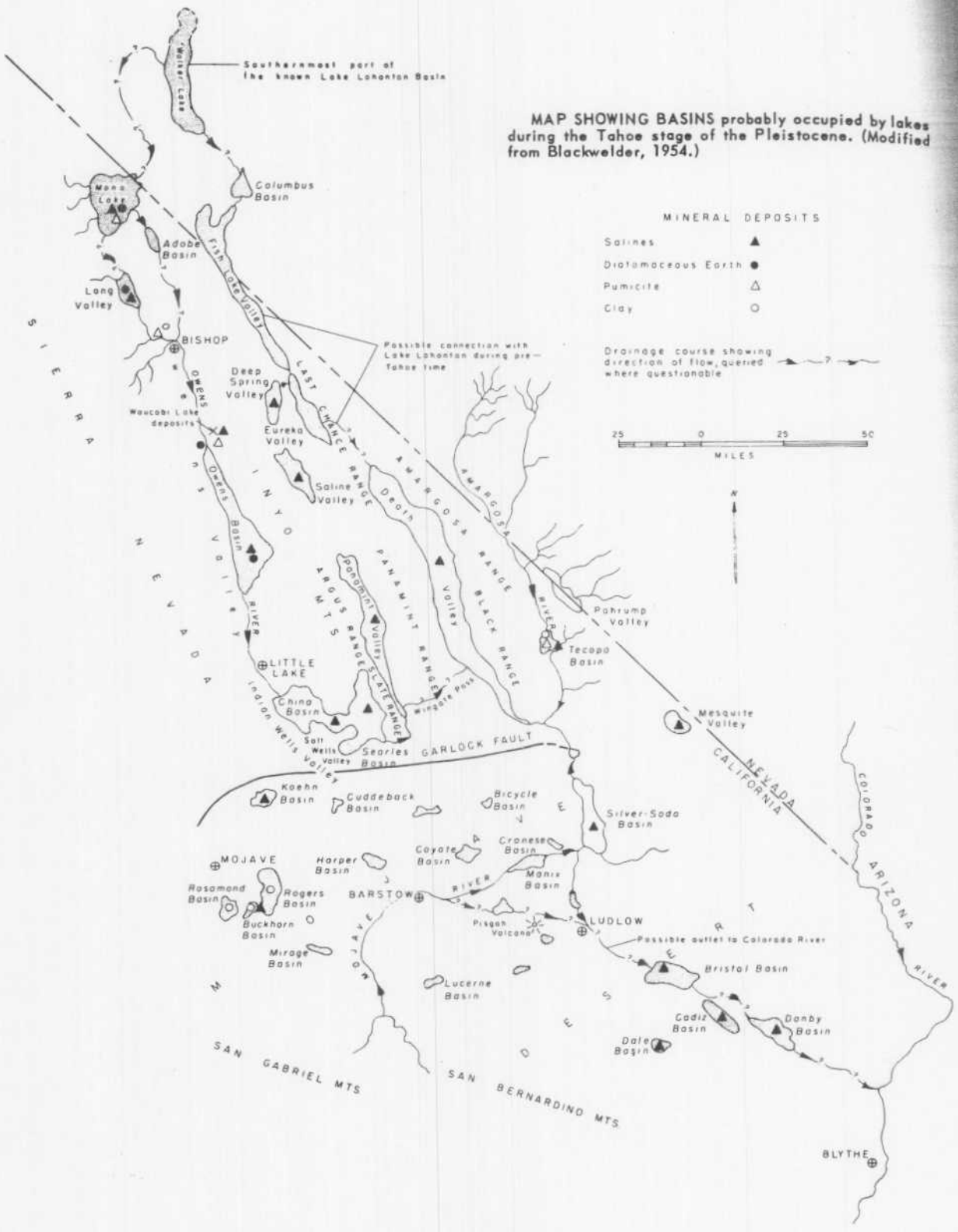

FIGURE 8-15. Late Pleistocene freshwater lakes and rivers in the Great Basin and Mojave Desert (California Division of Mines and Geology, Mineral Information Service, April, 1961.)

Mileage
Cumulative Difference

Playas are among the flattest landforms known and often have slopes of .2m/km or less. They have proved to be useful as sites for large antenna arrays (e.g. Clark Dry Lake) and sources of potash and salt (e.g. Bristol Dry Lake).

96.1 4.4 STOP 3. TWENTYNINE PALMS VALLEY. This stop provides an overall view of the eastern portion of the valley between the Bullion and Pinto Mountains. This valley is part of a trough that parallels the larger Bristol-Cadiz-Danby trough to the north. To the south are the Pinto Mountains which have been mapped as granitic intrusives by Bishop (1963) and as foliated metamorphics by Bassett and Kupfer (1964). The Sheep Hole Mountains bound the valley on the east. On the right, looking southward, a fault bounds the western side of the Sheep Hole Mountains and forms a steep face with 610 m of relief. The fault trends northwest and distinctly separates the mountain front from the Pleistocene dissected alluvium. It continues through the Bullion Mountains to form the valley containing Cleghorn Lakes (a series of playas).

The Pleistocene dissected alluvium is above the present alluvial level and unrelated to the present drainage systems. It is typically composed of coarse unconsolidated, unsorted alluvial fan material. To the southeast, sand sheets and dunes can be seen extending to the base of the Sheep Hole Mountains (Fig. 8-16). In the Mojave Desert, prevailing westerly winds carry large amounts of sand which is generally deposited upwind of large structural obstacles. Dunes form against hills and ridges in this area and along the eastern edge of the trough. To the south, an inlier of the Pinto Mountains appears to have a dissected alluvial fan west of it; however, the slope is actually the windward surface of a large sand dune which formed against the knob (Fig. 8-17).

FIGURE 8-16. Sand (light areas) accumulating on the west side of the southern Sheep Hole Mountains. Westerly winds predominate in the Mojave Desert and typically deposit sand on the windward side of obstacles such as hills and ridges. The Sheep Hole Mountains form the western border of the valley around Twentynine Palms and block the westerly winds. Part of the sand has formed climbing dunes up the side of the mountains (photograph by Ronald Papson, University of Santa Clara, May, 1977).

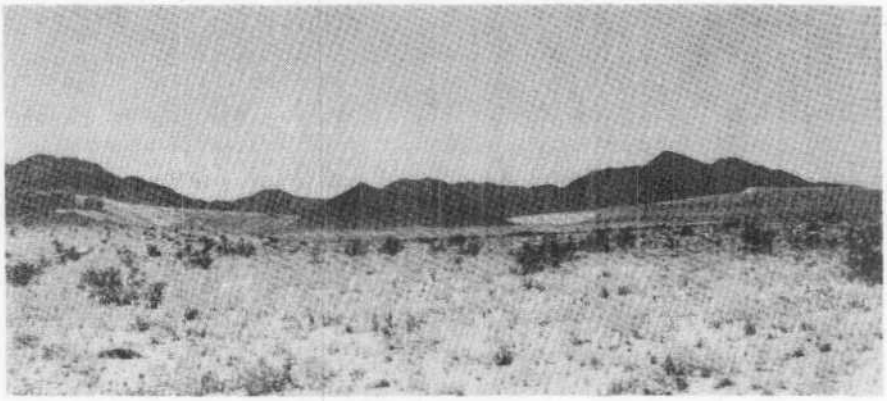

FIGURE 8-17. Sand accumulations on west side of knob in the Pinto Mountains. Note slip face of the dune form in central foreground (photograph by Ronald Papson, University of Santa Clara, May 1977).

Mileage		
Cumulative	Difference	
97.7	1.6	Sheep Hole Microwave Relay Station. Rocks to the left are granitic Mesozoic intrusives of the Bullion Mountains and to the right are pre-Cenozoic granites and metamorphics of the Sheep Hole Mountains.
100.1	2.4	Granitic inlier to the left. The road descends a large recent bajada into the Bristol-Cadiz-Danby trough which is transverse to the dominant northwest structural trend of this region. The trough is partially of structural origin and may have at one time contained an integrated drainage system that connected the western Mojave Desert or Death Valley to the Colorado River (Bassett and Kupfer, 1964). Drill holes around Bristol Dry Lake provide some data on the thickness of alluvial fill within the basins along the trough. Well-drilling operations near Bagdad and Amboy struck bedrock at 245 m and 460 m respectively. Recent holes about 335 m deep drilled at Bristol Dry Lake did not reach bedrock.
106.5	6.4	STOP 4. VALLEY OF AMBOY. In the distance on the right are the Calumet Mountains, predominantly composed of gneissic and granitic rocks. The dark areas in front of the mountains are silicic volcanics. Like the Sheep Hole Mountains to the southeast, these mountains act as obstacles to the westerly sand-laden winds and large amounts of sand have been deposited on the alluvial fan west of the Calumets. Amboy Crater, with its associated lava flow, and Bristol Dry Lake can be seen from here. Bristol Dry Lake, like Dale Dry Lake, is a moist playa. It has been subdivided by Bassett and Kupfer (1964) on the basis of the groundwater level (Fig. 8-18). Some of the playa clay is perennially brine soaked (Qxb); however, most of the playa exhibits a crust of puffy, loosely packed salt mixed with clay or silt (Qxc). Along the northwestern edge of Bristol Dry

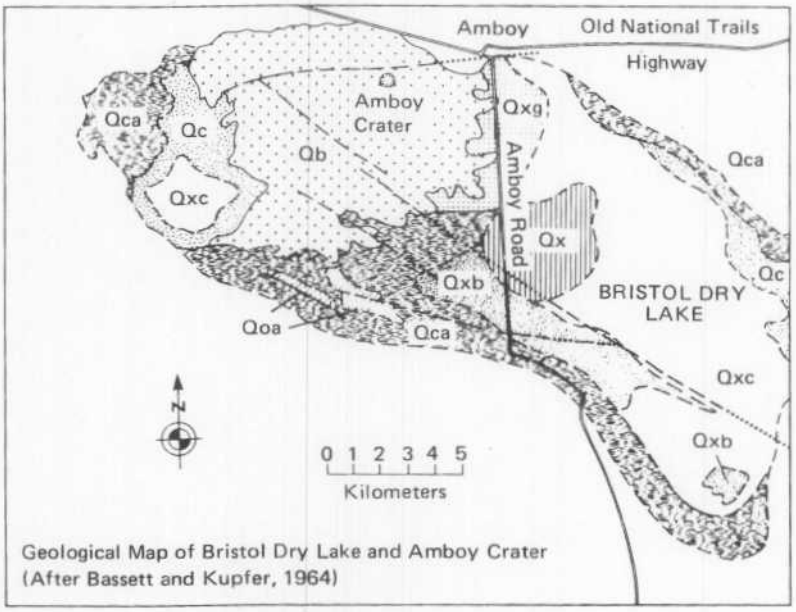

Geological Map of Bristol Dry Lake and Amboy Crater
(After Bassett and Kupfer, 1964)

Playa Deposits

Qca — mixed playa clay and alluvium

Qc — hard-packed clay

Qxc — mixed salt and clay or silt; efflorescent ground

Qx — salt crystal body at or near surface

Qxb — mud, salt, and brine in perennially wet sink areas

Qxg — gypsum-capped pedestals on Cadiz and Danby Dry Lakes, mixed gypsum and silt on Bristol Dry Lake

Qb — Quaternary basalt flows and cones
Undissected cinder cones and associated flows; some rest on playa surfaces

Qoa — Older alluvium
Dissected alluvium related to present drainage pattern; usually dark with desert varnish

Cinder Cone

Fault, dashed where approximate, dotted where inferred.

NOTE: No age relationship implied.

FIGURE 8-18. Geological map of Bristol Dry Lake and Amboy lava field showing different types of playa surfaces as related to groundwater (after Bassett and Kupfer, 1964).

Mileage
Cumulative Difference

Lake, gypsum crystals are found within the silt (Qxg). In the southwestern corner of the playa, oblong concretions of celestite can be found about .3 m below the surface in gypsiferous sandy clay. A transition zone of mixed alluvial sands and playa deposits occurs on all margins of Bristol Dry Lake except along the Amboy lava field. Amboy crater, rising 61 m above its associated flows, is a breached cinder cone.

Mileage		
Cumulative	Difference	
		The Bristol Mountains can be seen north of Amboy. The southeastern portion of these mountains is composed of granitic intrusives ranging in composition from quartz monzonite to granodiorite, and a Precambrian igneous-metamorphic complex of plutonic rocks (diorites and granites) and metamorphic rocks, including migmatites. Elsewhere, the Bristol Mountains consist of a complex suite of volcanic and clastic rocks.
		Southwest of Amboy lava field is Lead Mountain which is composed primarily of Miocene andesitic volcanics. This mountain is highly deformed by the still active Ludlow fault zone which strikes N40°W and extends about 65 km from the Cady Mountains through Ludlow to Lead Mountain (Bassett and Kupfer, 1964). On the southwest margin of Lead Mountain is a well preserved cinder cone and associated basalt flow. The lava spread south and east 8 km toward Bristol Dry Lake.
112.9	6.4	A Tertiary hypabyssal andesitic intrusion forms a dark knob in front of the granitic Bullion Mountains to the left.
115.1	2.2	National Chloride Company mining site in an area of Bristol Dry Lake covered by crystalline salts (Fig. 8-19).
118.1	3.0	Flow front of Amboy lava to the left. Dark low mounds of older flows can be seen rising up from the playa deposits.
121.3	3.2	Junction Amboy Road and Old National Trail Highway; turn left.
122.2	0.9	Turn off on left to Amboy lava flow.
		STOP 5. AMBOY CRATER (Fig. 8-20) is a complex basaltic cinder cone about 460 m in diameter and 76 m high. It is considered to be approximately 6000 years old and is composed of an accumulation of volcanic ejecta with subordinate amounts of agglutinated ejecta and flows. Ejecta material varies but angular scoriaceous cinders predominate over ropy, ribbon, and almond shaped bombs. Amboy Crater consists of at least four almost coaxial cones (Fig. 8-20). The major cone has an irregular summit crater, about 200 m in diameter and 30 m deep, in which the other cones are located. Most of the outer slopes of the cone are gullied except near the crater crest and on the western flank where the gullies disappear under an agglutinated surface (Fig. 8-21). A remnant of a second cone is present on the western slope inside the crater. The lava field surrounding Amboy Crater covers about 70 km^2. Thicknesses of individual flows range from .3 to 4 m. Most of the lava is "degassed", slightly vesicular pahoehoe, but aa is present at the toes of some flows.

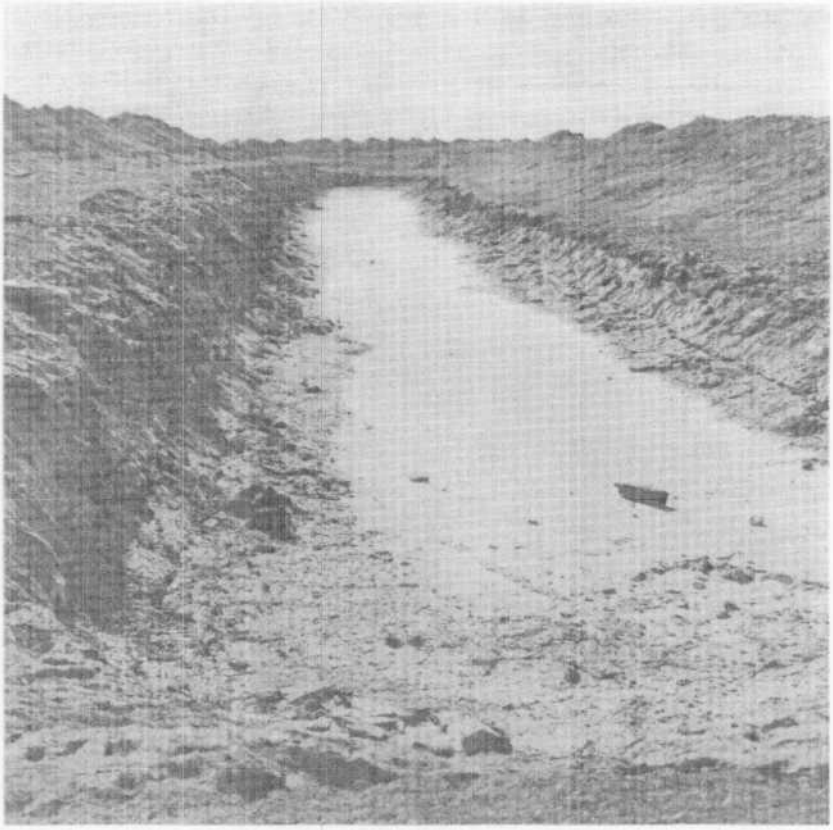

FIGURE 8-19. Trench of the National Chloride Company on Bristol Dry Lake. The floor of the trench is encrusted by salt, and salt crystals may be found in the trench walls (photograph by Ronald Papson, University of Santa Clara, May, 1977).

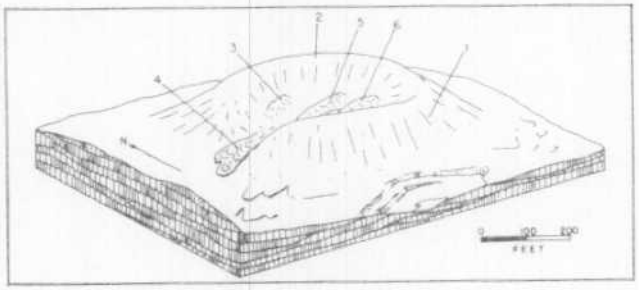

FIGURE 8-20. Schematic block diagram of Amboy Crater showing major features and eruptive events: (1) formation of main cone; later erosion of outer slopes, (2) eruption and deposition of agglutinate material on the western side and upper slopes of the major cone, (3) formation of the outermost conelet within the crater, (4) both cone walls were breached on the western side, (5) formation of a second cone within the crater, and (6) formation of innermost cone (from Parker, 1963).

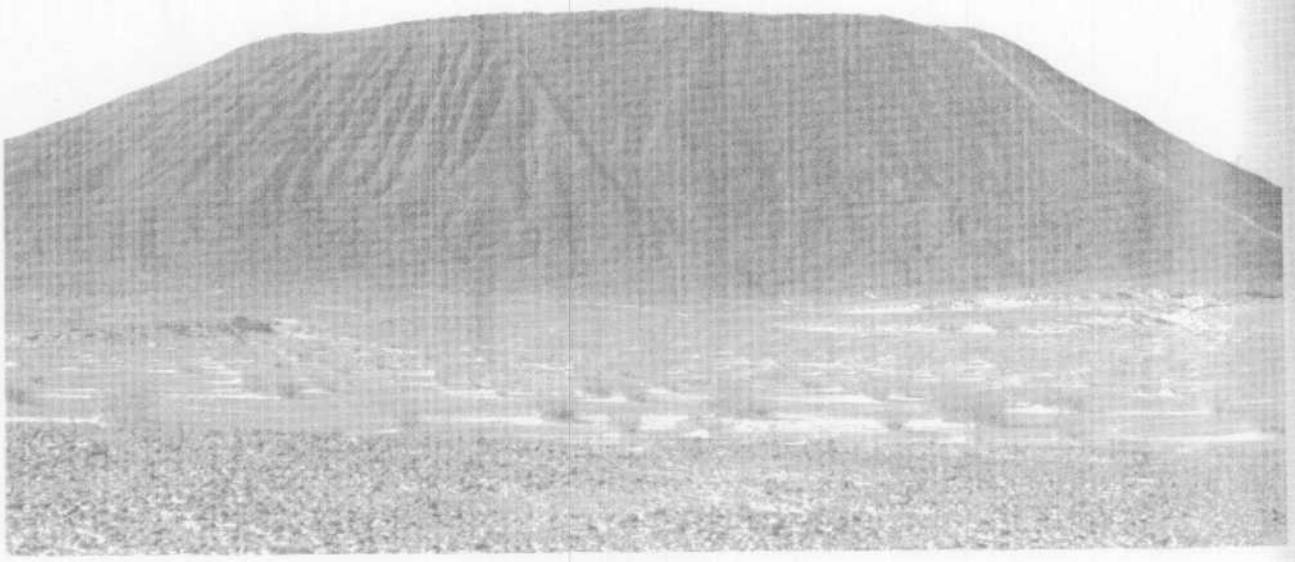

FIGURE 8-21. Amboy Crater. To the left, gullies developed on the cinder cone can clearly be seen, however, to the right these features have been covered by agglutinate from the second eruptive event. The white line on the right is a path to the top of the cone. In the foreground the weathered surface of the lava flow can be seen. Most of the basalt pebbles and cobbles have formed in place. The light material blanketing the surface is aeolian sand deposited on the flow (photograph by Ronald Greeley, University of Santa Clara).

Mileage
Cumulative Difference

Lava flows in the field have been divided by Hatheway (1971) into 3 basic units: platform lavas, vent lavas, and undifferentiated flows (Fig. 8-22). Platform lavas are isolated, relatively flat surfaced zones of uniform basalt that solidified in place (Fig. 8-23). Vent lavas are topographically higher areas of relatively dense pahoehoe and may be over 10 m thick. Most of the Amboy lava field consists of hummocky undifferentiated flows that are characterized by randomly arranged tumuli and pressure ridges (Fig. 8-23).

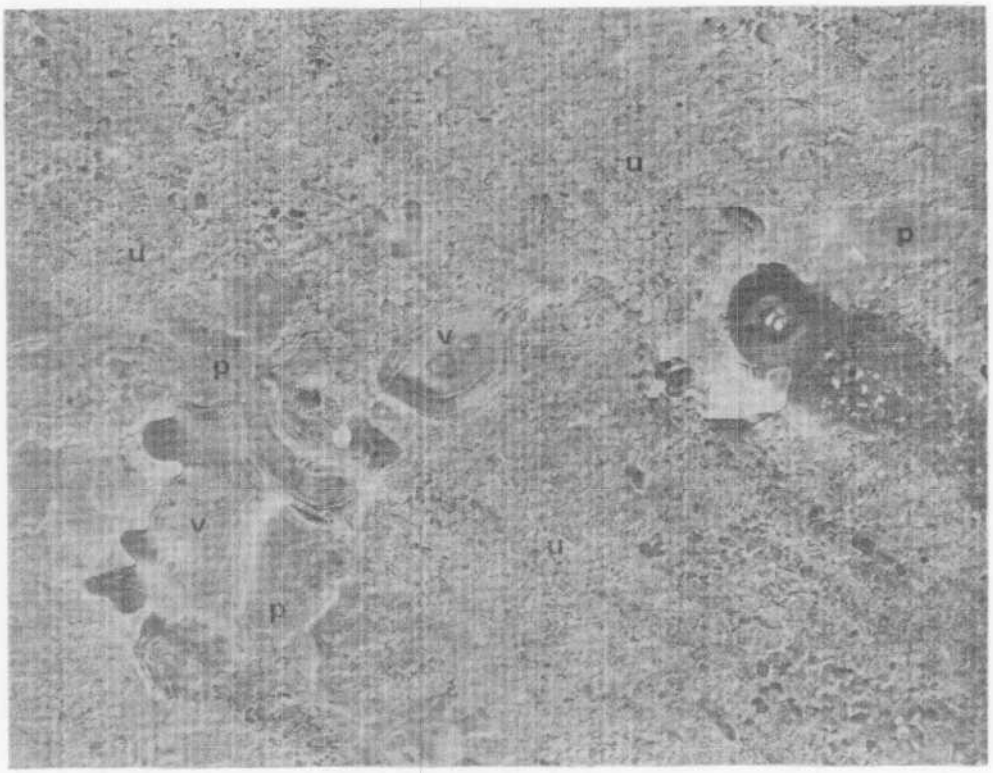

FIGURE 8-22. Vertical aerial photograph showing the three divisions of lava flows by Hatheway (1971): vent lava (v), platform lava (p), and undifferentiated flows (u) (U.S. Department of Agriculture photograph, AXL-1K-73, October 1952).

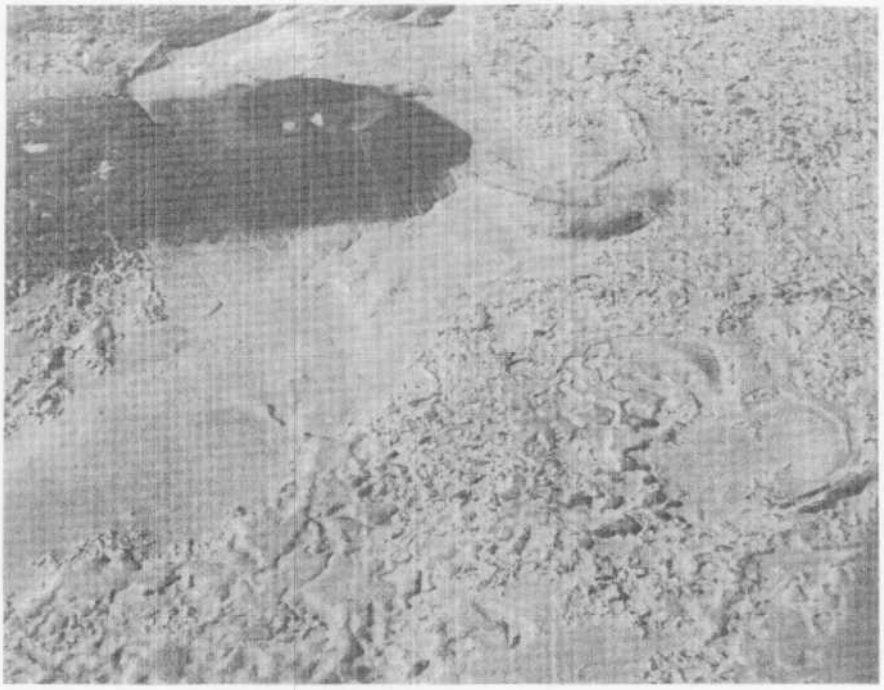

FIGURE 8-23. Oblique view of Amboy Crater and lava field to the south-southwest. The hummocky areas are part of the undifferentiated flows. Isolated, relatively smooth areas near the cone and in the lower central platform remnant. Aeolian deposits cover much of the flow and are especially evident in the numerous depressions. The dark area to the left (east) of Amboy Crater is also the result of aeolian activity; however, the surface in the lee of the cone is devoid of aeolian sand (photograph by Ronald Greeley, University of Santa Clara).

Mileage
Cumulative Difference

Other features associated with the field are circular depressions, domal folds, block mounds, and bowl-shaped depressions. Circular and oval depressions, 1 to 45 m in mean diameter, are abundant on the flows and are interpreted as collapsed depressions created by the withdrawal of lava from beneath a cooled crust (Fig. 8-23). Domal folds, approximately 30 m in diameter and reaching 9 m in height, are characterized by summit depressions .9 to 1.2 m wide with associated radial fractures. The two features unique to the plateau are mounds of chaotically arranged blocks, confined to the northern half, and bowl-shaped depressions, confined to the southern half. They tend to have a linear arrangement and have been interpreted by Parker (1963) to be explosive centers. An interesting feature associated with Amboy Crater is a dark streak east-southeast of the cone. Much of the lava surface has been obscured by aeolian sand carried into the area by the prevailing westerly winds. Within the dark streak area, however, the surface is relatively free of sand, resulting in the low albedo observed (see Greeley and Iversen, Chapter 3).

AMBOY TO KELSO DUNES

This trip proceeds northward from Amboy and passes between several northwest trending mountain ranges typical of the Mojave Desert. Geologic summaries of the area were obtained from Bishop (1963) and Bassett and Kupfer (1964). Most of the mountain ranges are formed by northwest trending faults, and are composed of Precambrian and Paleozoic metamorphics intruded by Mesozoic granites; however, the Bristol, Old Dad and Marble Mountains are predominantly composed of Cenozoic sediments intercalated with volcanics. These rocks were apparently deposited in a series of local basins which may have had somewhat different histories.

In the valley north of the Granite Mountains is a large accumulation of sand called Kelso Dunes (Sharp, 1966). This field is part of the Devil's Playground and derives its sand from the Mojave River sediments deposited below Afton Canyon. The field consists of a series of transverse dunes superposed on several large sand ridges and may be the product of a different climate several thousand years ago.

ROAD LOG

Mileage		
Cumulative	Difference	
0.0	0.0	Amboy. Proceed east on Old National Trails Highway. On the left is the southeastern extension of the Bristol Mountains. This arm is composed of a mixture of Precambrian plutonic (diorites to granites) and metamorphic rocks, including migmatites in the southwestern portion, and of Mesozoic granite intrusives and metasediments generally in the eastern and northeastern portion.
6.0	6.0	Small metamorphic knob on right. Turn left onto Kelbaker Road which proceeds up the alluvial fan between Bristol Mountains (left) and Marble Mountains (right). The southwest portion of the Marble Mountains consists of Precambrian plutonic rocks, varying from granites to gabbros; Cambrian and Devonian marine sediments and metasediments, consisting chiefly of limestones, dolomites, and shales; Paleozoic marble; and Mesozoic granitic intrusives. The northern and northeastern portion of the Marble Mountains consists of Tertiary volcanic and hypabyssal intrusive rocks.
7.8	1.8	Both metamorphic and granitic rocks of the Bristol Mountains can be seen on the left.
9.6	1.8	To the left is the uranium Hope'n Mine. Several other uranium mines are located in the Precambrian plutonic rocks in the southern portion of the Marble Mountains.
13.3	3.7	To the right are layered flows and pyroclastics in the Tertiary volcanic rocks of Marble Mountains. Rhyolitic intrusions in contact with granite are visible near the summit of the mountains.

Mileage		
Cumulative	Difference	
16.4	3.1	STOP 6. TERTIARY VOLCANICS. This stop provides the opportunity to easily sample some of the rhyolitic volcanics we have been passing. Most of the rocks at this stop are covered with desert varnish composed of complex manganese-iron oxides. This outcrop consists of light pink rhyolite. Volcanic material also occurs in patches west of the road.

This stop also affords the opportunity to view and discuss the surrounding mountains (Fig. 8-24). To the north are the Granite Mountains composed of granitic and metamorphic rocks. The southeastern portion of these mountains exhibits the typical weathering features associated with granite in this area. The rocks are usually light-toned and weather to large bare boulders and faces (Fig. 8-25). Weathering and erosion has also accentuated joints within the granitic mass.

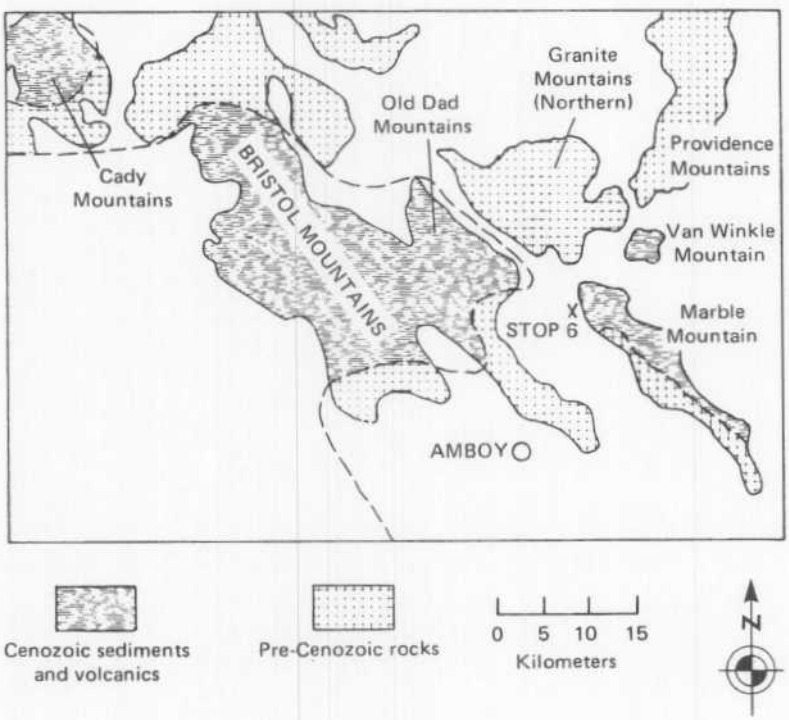

FIGURE 8-24. Location map of mountains around STOP 6. Pre-Cenozoic rocks are composed of granites and metamorphics. Cenozoic rocks are primarily volcanics and sediments. The dashed line around Bristol and Old Dad Mountains indicates the approximate extent of an old basin into which a series of sediments intercalated with volcanics was deposited (from Bassett and Kupfer, 1964).

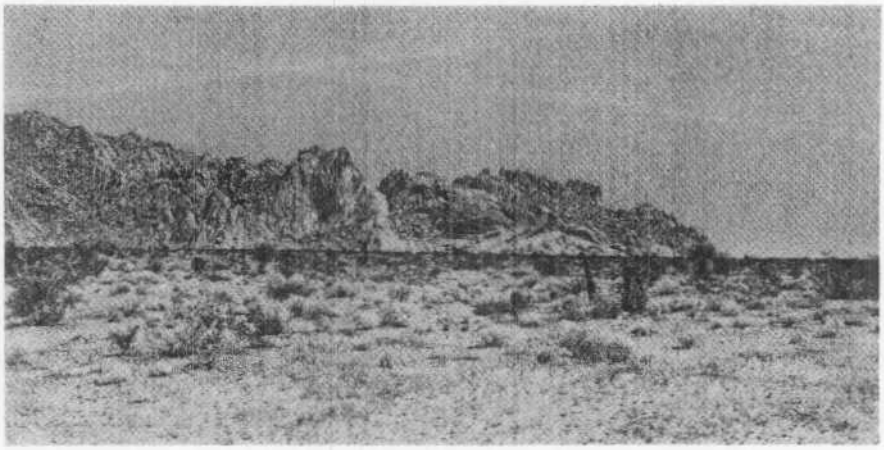

FIGURE 8-25. Typical spheroidal weathering of granitic rocks in the Mojave Desert as seen in the Granite Mountains. The granitic material weathers to bare rounded boulders or steep faces (photograph by Ronald Papson, University of Santa Clara, May, 1977).

Mileage		
Cumulative	Difference	
		The Old Dad Mountains are southwest of the Granite Mountains and are separated from them by a concealed fault which may be the southern extension of the Death Valley fault zone (Bassett and Kupfer, 1964). The southern Old Dad Mountains are composed of granitic and metamorphic rocks that extend northward from the Bristol Mountains. The majority of the Old Dad Mountains, like the Bristol Mountains, are composed of a complex suite of Cenozoic volcanic and clastic rocks. These rocks were probably deposited in several local basins each with a slightly different history, and are therefore difficult to correlate (Bassett and Kupfer, 1964). Most of the surface rocks of the mountains consist of tuff, tuff breccia and welded tuff with subordinate amounts of perlite, perlitic rhyolite, and conglomerate (Bishop, 1963).
17.6	1.2	Junction Kelbaker Road and Interstate Highway 40. Pass under the highway and continue on Kelbaker Road.
19.8	2.2	The road passes between the Marble and Granite Mountains. Contact between Tertiary volcanics and Mesozoic granite can be seen to the right. Several granitic outcrops above the thin alluvial cover dot the valley floor.
24.0	4.2	Clipper Mountains composed of Precambrian gneiss and Tertiary basalts and pyroclastics are visible in the distance on the right. Granitic intrusives are located around the northwestern base of Van Winkle Mountain.
25.0	1.0	View of typical granitic type weathering (Fig. 8-26).
25.6	1.0	Granite Pass and Microwave Relay Station.

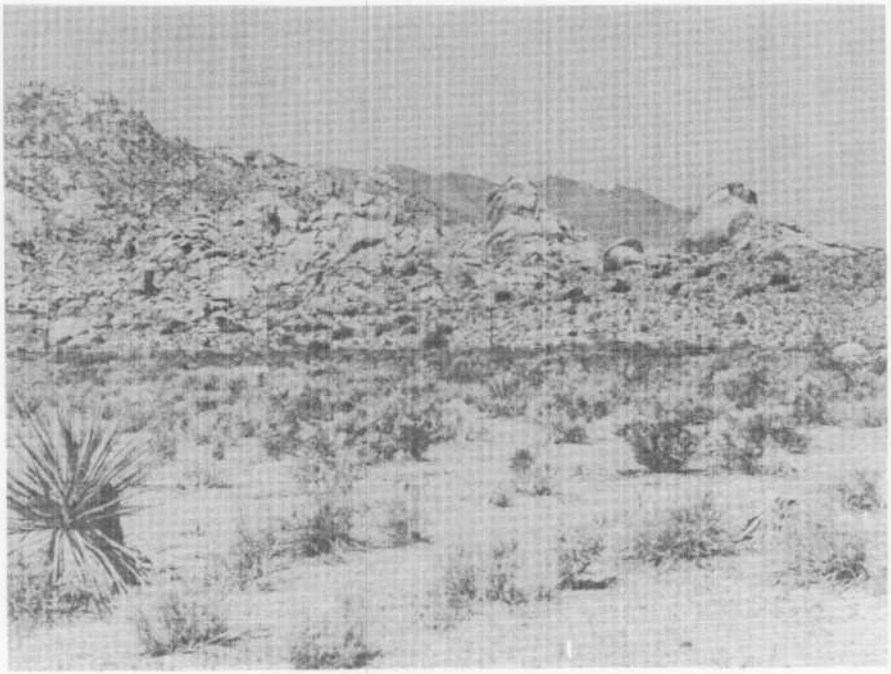

FIGURE 8-26. Typical spheroidal weathering of granitic rocks in the Mojave Desert as seen in the Granite Mountains west of Granite Pass (photograph by Ronald Papson, University of Santa Clara, May, 1977).

Mileage		
Cumulative	Difference	
27.2	1.6	In the canyon to the left, the alluvial fan material consists of Tertiary fanglomerates. North of the canyon is a spur of Precambrian metamorphic and igneous-metamorphic complex rocks.
29.6	2.4	Note the different weathering characteristics of the granitic rocks in the Providence Mountains on the right. Some of the rocks appear to have a colluvial gruss covering while others are bare. Gruss forms as grain interfaces and fractures of a granitic rock are weathered, leaving an accumulation of unconsolidated mineral grains in place of the original rock. The southern half of the Providence Mountains is predominantly granitic intrusives although minor amounts of igneous-metamorphic mixed rocks also occur.
31.0	1.4	Dissected older alluvium on the left.
32.2	1.2	Kelso Station of the Southern California Gas Company.
32.8	0.1	Turn left onto graded dirt road to Kelso Dunes. The heavily faulted northern portion of the Providence Mountains is visible from here. This portion of the mountains is composed of predominantly Paleozoic limestones around a Tertiary hypabyssal rhyolitic intrusion and minor amounts of Precambrian metamorphic rocks.

Mileage		
Cumulative	Difference	
36.1	3.8	STOP 7. KELSO DUNES (see Sharp, Chapter 4) are part of the Devil's Playground, a 56 km long and 3 to 6 km wide sand area (Fig. 8-27). The dunes sit on the alluvial apron of the Granite Mountains in a valley bounded on the north by Kelso Mountains, on the east by Providence Mountains, and on the south by Granite Mountains. The western side is only partially blocked by the Bristol Mountains and windblown sand enters through the gap to the northwest. Kelso dunes cover an elongate area of about 111 km^2 with the long axis striking N55°E. Borders of the dune field are sharp. The highest elevation within the dunes is 949 m while maximum dune sand thickness is 213 m.

The sand source for this area is the Mojave River sediments and is renewed by floods. Originally derived from sedimentary, metamorphic, volcanic and plutonic terrains, it is deposited as a broad alluvial apron at the mouth of Afton Canyon.

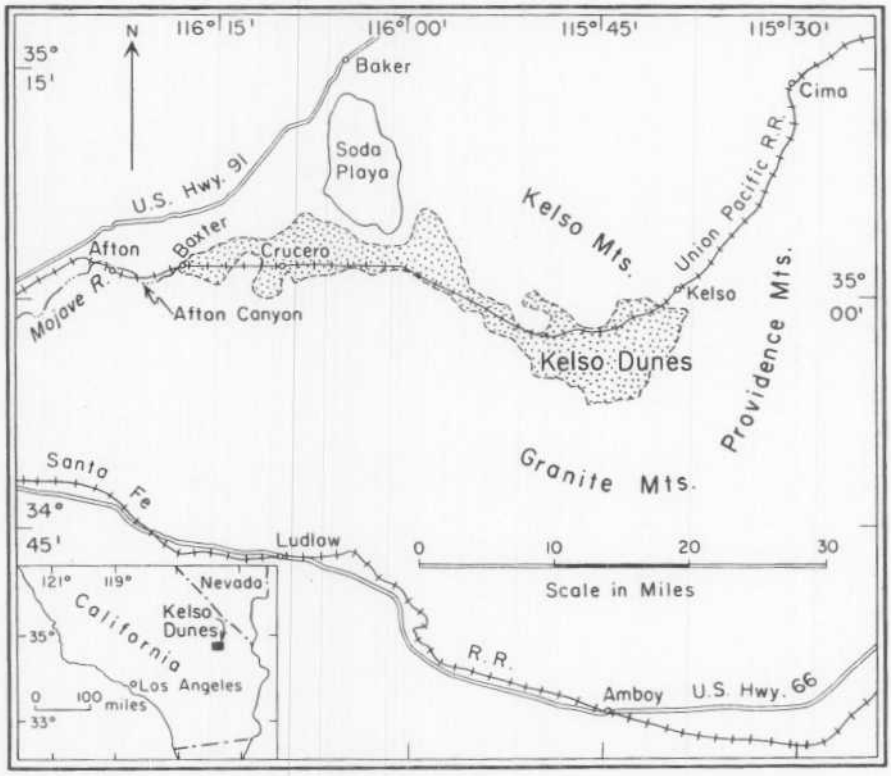

FIGURE 8-27. Location map for Kelso Dunes, Mojave Desert, California (after Sharp, 1966).

Mileage
Cumulative Difference

Localization of Kelso dunes appears to have been the result of crosswinds achieving a net effect of nearly zero. Prominent westerly winds are counterbalanced by strong, orographically controlled winds from different directions. Winds from these directions are less frequent and of shorter duration but they tend to have higher velocities.

The Kelso Dunes have existed for several thousands of years and may have formed 20,000 years B.P.. Four almost parallel ridges trending about N65°E form the largest dunes within the field (Fig. 8-28) and are being modified by current winds. Classical transverse dunes are uncommon in Kelso dunes. On most dunes in the area, slip faces attain heights of less than 7 m and form only the upper portion of the lee slope. Lower lee surfaces have gentle slopes generally inclined less than 20 degrees. Slip faces are occasionally smoothed

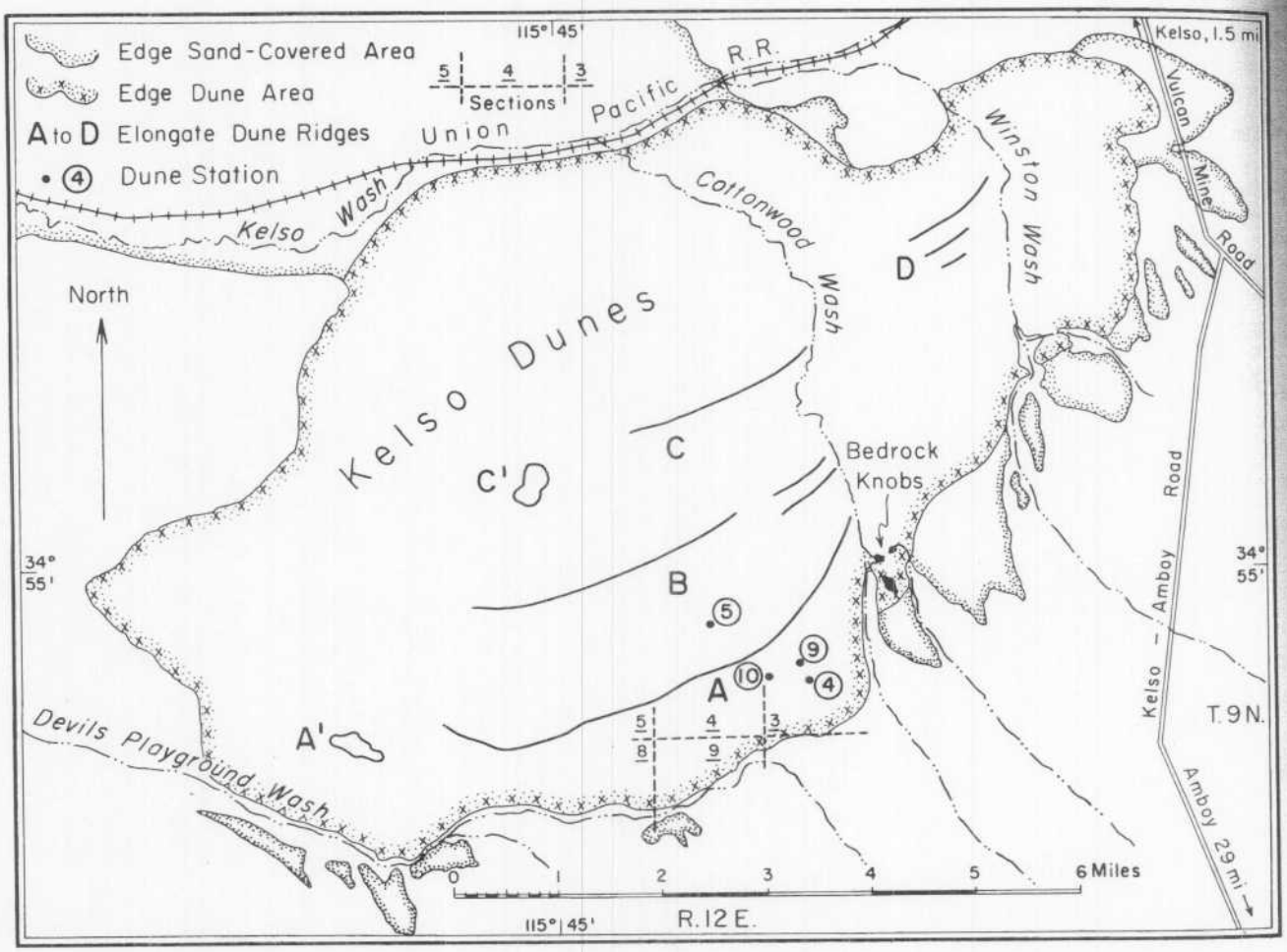

FIGURE 8-28. Schematic map of Kelso Dunes showing elongate ridges (after Sharp, 1966).

Mileage
Cumulative Difference

by longitudinal winds which also destroy the brink. Reversal of slip face orientation may leave residual forms, and truncated dune crests formed by strong reverse winds are also seen (Fig. 8-29).

Material within the dunes consists of local concentrations of coarse grains and typical aeolian sand with about 90% of grain diameters between 0.25 and 0.50 mm. A large mineral assemblage, with fine granitic and volcanic rock fragments, is found in the dune sand. Dark heavy minerals are concentrated throughout the dunes by selective deflation and by slumping on slip faces (Sharp, 1966).

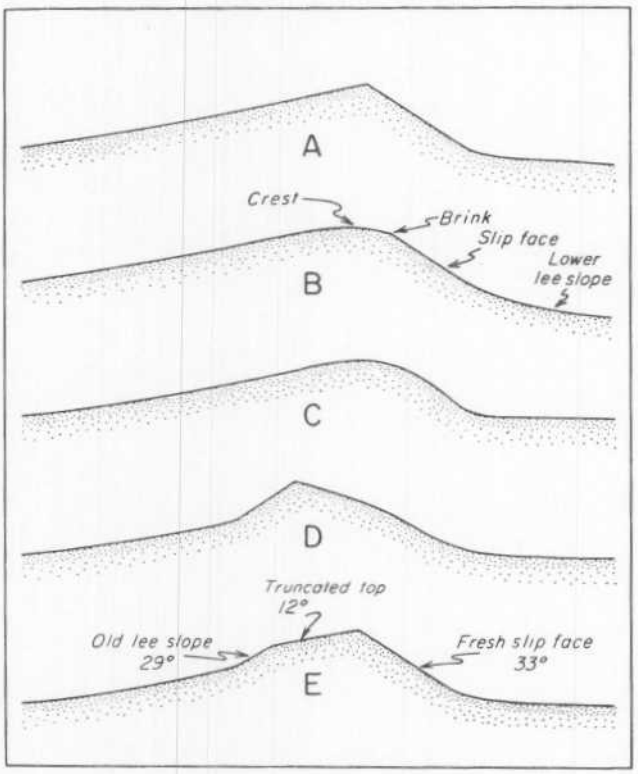

FIGURE 8-29. Schematic cross sections of transverse dune ridges (from Sharp, 1966).

JOSHUA TREE NATIONAL MONUMENT VISITORS CENTER IN TWENTYNINE PALMS TO INDIO

This segment may be used as an alternate route for a return trip from Amboy to Palm Desert. The route from Indio to Palm Desert is covered in the southern roadlog. Joshua Tree National Monument, south of Twentynine Palms, is located within the Little San Bernardino Mountains, a portion of the Transverse Range province. The mountains are composed predominantly of Precambrian metamorphics and Mesozoic granitic intrusives described by Rogers (1961), Bishop (1963), Rogers (1965, 1967), and Jennings (1967). Intrusive contacts between the general units are easily discernible along the road and interesting features formed by weathering of the granites may also be seen. A large east-west trending valley, Pinto Basin, between the Pinto and Eagle Mountains formed by faulting typical of the Transverse Range province. In the Cenozoic, the basin was filled by basalt flows intercalated with lacustrine and alluvial fan deposits (Scharf, 1935).

South of the Little San Bernardino Mountains are the Orocopia Mountains. These mountains are described by Crowell (1975) and consist of Precambrian metasediments intruded by Mesozoic granites, both overlain by marine and nonmarine Cenozoic sediments. The Orocopia thrust fault, a regional overthrust of unknown displacement, has faulted and deformed all geologic units; however, it has itself been folded and faulted.

Upon entering Coachella Valley from the west, the route passes north of Mecca Hills, which formed along the San Andreas fault zone. This area lies within the Salton Trough province of which Coachella Valley is the northwesternmost extension.

Cultural and natural history was obtained from Campbell and Campbell (1935) and numerous pamphlets published by the Joshua Tree Natural History Association.

Mileage		
Cumulative	Difference	
0.0	0.0	STOP 8. JOSHUA TREE NATIONAL MONUMENT VISITORS CENTER is located at Twentynine Palms oasis. Like many other desert oases in this area, it formed where groundwater circulation is restricted along a fault; in this case, the Pinto Mountain fault. About 200 years ago the oasis was occupied by two clans of the Serrano Indians who, like the Cahuilla Indians to the south, belong to the Uto-Aztecan family. Settlement of the area in 1873 by white men began with the discovery of gold. The oasis became the center of mining activity until 1935.
3.5	3.5	Entrance to Joshua Tree National Monument. Established by President Roosevelt in 1936, it covers an area of approximately 2,253 km^2 and is administered by the National Park Service, U.S. Department of the Interior. The Monument lies in the transition zone between the high Mojave Desert and the low Colorado Desert with altitudes which range from 304 m in Pinto Basin to 1800 m in the Little San Bernardino Mountains. Rainfall averages less than 12 cm a year; however, during sudden rain storms flash-flooding is common.

Mileage		
Cumulative	Difference	
4.2	0.7	The mountains to the right consist mainly of Palms Quartz Monzonite which is typically a gray to brown, coarse to medium grained, massive rock. A monzonitic porphyry occurs in the northwestern corner of these mountains and consists of brown to gray, coarse grained rock characterized by potassium feldspar phenocrysts. The darker rocks to the right are basic intrusives of Gold Park Gabbro Diorite. This unit is massive, coarse to fine grained, and varies in texture and composition (Rogers, 1961). The Pinto Gneiss, formed by medium grade metamorphism of sedimentary or volcanic rocks, constitutes the Pinto Mountains to the left. To the north the mountains are bounded by the Pinto Mountain fault, a prominent fault that extends eastward to the San Andreas fault zone near San Gorgonio Pass.
6.5	2.3	To the right is an intrusive contact between White Tank Quartz Monzonite and Pinto Gneiss. The White Tank Quartz Monzonite is of probable Jurassic age and consists of light brown to gray, massive, coarse to medium grained rocks with slight textural and compositional variations (Rogers, 1961).
8.2	1.7	Road from Joshua Tree intersects from the right. Continue straight on Pinto Basin Road.
8.5	0.3	Intrusive contact between White Tank Quartz Monzonite and Pinto Gneiss on the left.
9.5	1.0	Belle Campground.
11.9	0.9	Hexie Mountains to the right are primarily composed of Pinto Gneiss.
14.3	2.4	The road passes between Pinto Mountains and Hexie Mountains.
17.6	3.3	To the right the Hexie Mountains are bounded by the eastwest trending Precambrian Eagle Mountain-Blue Cut fault zone. In this area, Hexie Mountains consist of predominantly Precambrian foliated granitic rocks.
18.2	0.6	Cholla Cactus Garden.
19.7	1.5	STOP 9. OCOTILLO PATCH. The Pinto Basin to the east is a large desert drainage system bounded by the Pinto Mountains on the north, the Little San Bernardino Mountains on the west, the Eagle Mountains on the south, and the Coxcomb Mountains on the east (Fig. 8-30).

FIGURE 8-30. Pinto Basin as viewed to the east. The basin is a fult bounded valley bordered on the north (left) by the Pinto Mountains, on the south (right) by the Eagle Mountains, and on the east (not seen) by the Coxcomb Mountains. During the Pleistocene the basin was inundated by a lake which, after breaching a dam to the southeast, formed a slow moving river approximately along the same course as Pinto Wash. The climate subsequently became arid and the river disappeared (photograph by Ronald Papson, University of Santa Clara, May, 1977).

Mileage
Cumulative Difference

Four stages of Quarternary deposition are represented within the basin. The folded basal Pinto Formation consists of lacustrine clays, sandstones, and gravels, intercalated with basalts flows. Overlain on these are tilled intermediate gravels of reworked Pinto Formation. Later gravels formed a fanglomerate from the Coxcomb Mountains and are dissected but undeformed. Recent deposits in the basin includes sand dunes, alluvial fans, and material in wash beds.

Subsequent to the last glacial period, runoff from the western highlands was sufficient to support an extensive shallow lake within the basin. This lake eventually breached a natural dam to the southeast leaving a broad meandering river which flowed eastward across the length of the basin. Campsites of pre-pottery and pre-arrowpoint Indians found along the banks of the wide channel indicate that enough water flowed to make it a favorable site for early human occupation (Campbell and Campbell, 1935). During this time uplift of the Pinto Formation and intermediate gravels occurred. Eventually, the moist climate disappeared and the Pinto River dried up. Today, Pinto Wash is subject to infrequent flash-flooding.

23.4 3.7 Pinto Mountain Peak in the distance to the left. Hexie Mountains to the right are predominantly composed of Pinto Gneiss.

Mileage Cumulative	Difference	
27.0	3.6	Dark material in a spur of the Eagle Mountains (to the left) is a Pleistocene, highly vesicular olivine basalt. Hexie Mountains to the right have changed from Pinto Gneiss to Coxcomb Granodiorite: a very light pinkish gray, medium-grained, massive rock with a faintly developed primary foliation.
29.7	2.7	Porcupine Wash. Road passes across Coxcomb Granodiorite of the Hexie Mountains.
31.4	1.7	Junction Pinto Basin Road with Old Dale Road which leads to the Old Dale Mining District in San Bernardino County.
33.3	1.9	Road passes between Coxcomb Granodiorite of the Eagle Mountains on the left, and Hexie Mountains on the right.
33.7	0.4	Smoketree Wash.
34.5	0.8	Intrusive contact between Coxcomb Granodiorite and Pinto Gneiss is on the right.
36.8	2.3	Pinto Gneiss to the right. The Cottonwood Mountains to the south are primarily the Coxcomb Granodiorite as well as the Eagle Mountains to the left.
40.3	1.5	Cottonwood Springs Visitor Center. During the mining activity between 1870 and 1910, Cottonwood Springs served as one of the two water holes between Mecca and the Dale Mining district. Output of the spring had fallen from 11,356 lt/day in the early 1900's to just a few lt/day in recent times. Since the San Fernando earthquake in 1971, however, output has increased to 2736 lt/day.
40.9	0.6	Cottonwood Pass. Road passes between Coxcomb Granodiorite of the Cottonwood Mountains to the right and Eagle Mountains to the left.
42.5	1.6	Patch of dark and light banded Pinto Gneiss on the left.
43.9	1.4	Road descends an alluvial fan from the Cottonwood and Eagle Mountains. The structurally complex Orocopia Mountains are across the valley. Basement rocks consist of Precambrian augen gneiss and migmatite of the Chuckwalla Complex (Miller, 1944), gneiss, and anorthosite-syenite complex with Mesozoic granodiorite, granite, and quartz monzonite. Cenozoic sediments of the mountains include beds of the Maniobra Formation, early Miocene nonmarine sediments of the Diligencia Formation to the northeast, nonmarine Plio-Pleistocene Mecca and Palm Spring Formations, and the Pleistocene Ocotillo Formation to the southwest.

Mileage		
Cumulative	Difference	
		Tertiary volcanics also occur in the mountains. The central portion of the mountains consists of the Orocopia Schist, a sequence of greenschists developed from graywacke and mudstone with subordinate amounts of chert and basic volcanic rocks. Structural evolution of the Orocopia Mountains began with multiple events of intrusion and metamorphism in the Precambrian and Mesozoic basement rocks. The Orocopia thrust fault, a major regional overthrust of unknown displacement, is of probable late Cretaceous-early Tertiary age. It has subsequently been folded and faulted, deforming and fracturing the thrust plate. The underlying schist apparently responded to the later folding by flexural slip along foliation surfaces resulting in an antiform (Crowell, 1935). Many of the later faults occur in the northern portion of the mountains, and divide the mountain face into three basic rock units: Mesozoic granites near the base, Precambrian Chuckwalla Complex rocks in the central portion, and Orocopia Schist near the top.
46.2	2.3	Leave Joshua Tree National Monument.
47.3	1.1	Turn right on Interstate Highway 10 West to Indio. To the west are Mecca Hills with the San Jacinto and Santa Rosa Mountains in the distance. Mecca Hills are composed of Cenozoic sediments that have been highly deformed by the San Andreas fault system.
49.7	2.4	Small hills on the left are composed of granite and the Eocene Maniobra Formation, a marine siltstone, sandstone, conglomerate and breccia with sandy limestone (Jennings, 1967).
50.5	0.8	Cottonwood Mountains on the right.
52.0	1.5	Highway passes through hill of an old fanglomerate.
53.9	1.9	Lowland on the right between the Orocopia Mountains and Mecca Hills is formed by the still active Hidden Springs fault. To the south it trends toward the San Andreas fault (Crowell, 1975).
55.6	1.7	Rest area. Highway crosses the Ocotillo Conglomerate, a gray boulder fanglomerate.
59.3	2.6	Highway passes through heavily dissected, steeply dipping Ocotillo Conglomerate which forms the Dillon Road Piedmont Slope, a narrow lowland which extends from Desert Hot Springs to the Mecca Hills. It consists of a series of coalescing alluvial fans which terminate or merge with Indio and Mecca Hills. Coarse material of the fans was deposited behind the hills while the fine material was transported beyond and deposited in Coachella Valley.

Mileage		
Cumulative	Difference	
60.2	0.9	Hill to the left is composed of a granitic and metamorphic complex with Pliocene nonmarine sediments.
64.6	4.4	To the right, the Little San Bernardino Mountains change composition from Mesozoic Fargo Canyon Diorite (Miller, 1944), a medium gray, locally foliated quartz diorite, to Precambrian Chuckwalla Complex, a dark-colored strongly foliate quartz-biotite gneiss and biotite schist (Rogers, 1965).
65.9	1.3	Highway enters Coachella Valley, the northernmost extension of the Salton Trough. The valley is bounded on the northeast by the Little San Bernardino and Orocopia Mountains and on the southwest by the San Jacinto and Santa Rosa Mountains. It has an average width of less than 24 km and extends from San Gorgonio Pass to the Salton Sea.
67.8	1.9	Sand sheets are on both sides of the highway.
68.1	0.3	All-American Canal in this area lies within and parallel to the Banning-Mission Creek fault zone.
		The high shoreline of ancient Lake Cahuilla is crossed at this point. Remnants of the lake were first recognized by Blake (1856) while he and others searched for an easy route from the interior of the continent to the Pacific Ocean. It is estimated that at one time Lake Cahuilla had a maximum length of 160 km, a width of 56 km, and covered an area of about 5450 km^2. The lake was formed by a channel shift of the Colorado River which allowed water to flow northward into the Salton basin. After the river regained its original channel to the Gulf of California, Lake Cahuilla gradually disappeared by evaporation.
69.5	1.4	Indio. Turn off onto State Highway 111 west to Palm Desert.

JOSHUA TREE TO PINTO BASIN ROAD

This portion of Joshua Tree National Monument consists of Precambrian metamorphics that have been repeatedly intruded by Mesozoic granitic rocks of the Southern California Batholith. The Pinto Gneiss is the dominant Precambrian unit; however, Chuckwalla Complex also occurs within this area. Rogers (1961) believes the two units may be correlated. The Pinto Gneiss is a medium grade metamorphic rock consisting of metasediments and metavolcanics. Chuckwalla Complex is an igneous-metamorphic complex of diorites, granodiorites, and metasediments. These Precambrian units have been intruded by Mesozoic Palms Quartz Monzonite and White Tank Quartz Monzonite. Basaltic Tertiary hypabyssal intrusives mark the latest igneous activity of the area.

Most of the valleys within this portion of the Monument are underlain by White Tank Quartz Monzonite, which is the least resistant rock type. Within the valleys, quartz monzonite monoliths separated by areas of loose sand derived from the monzonite are frequently seen (Fig. 8-31). Quartz monzonites throughout this area exhibit the typical joint controlled "sack" weathering pattern. Aplitic dikes within the quartz monzonite are distinct and stand out due to differential weathering. The change in slope between valley floors and mountain faces is usually abrupt; however, small fans and pediments have locally formed.

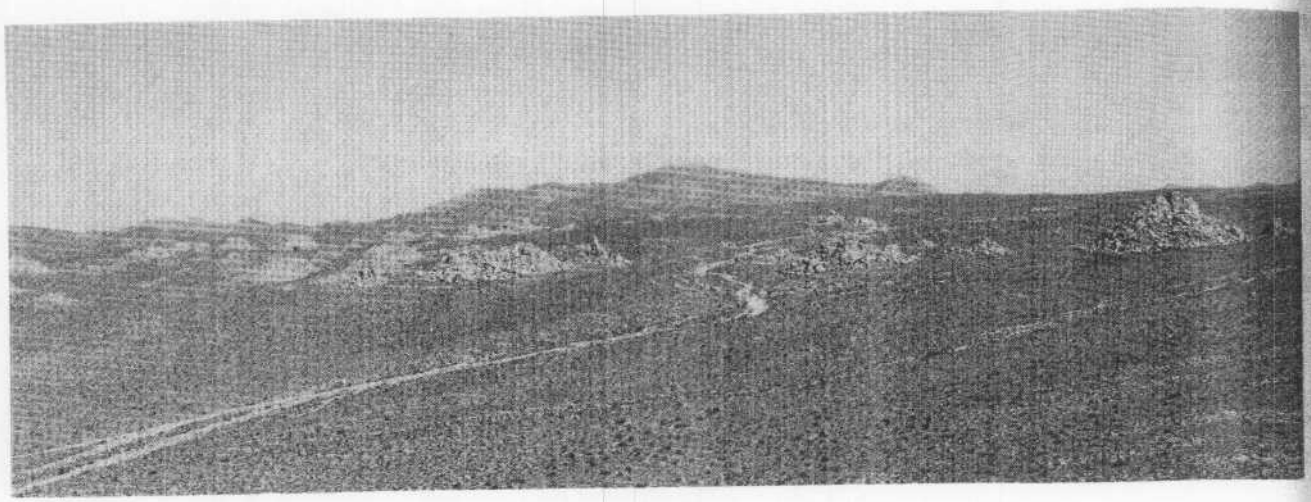

FIGURE 8-31. Photograph looking northward through Queen Valley. Queen Valley has formed by the weathering of the moderately resistant White Tank and Palms Quartz Monzonites. Mounds on the valley floor are resistant remanants of these formations. Lost Horse Mountain is in the background (photograph by Ronald Papson, University of Santa Clara, April, 1977).

ROAD LOG

Mileage		
Cumulative	Difference	
0.0	0.0	Joshua Tree. Turn off of State Highway 62 onto road to Joshua Tree National Monument.
0.6	0.6	To the left the rocks consist of a fine grained light brown and generally massive member of the Palms Quartz Monzonite. Pinto Gneiss, characterized by sodic plagioclase, quartz, and biotite, is on the right.
4.2	3.6	Quail Creek Canyon. The mountain within the canyon consists of Pinto Gneiss.

Mileage		
Cumulative	Difference	
5.2	1.0	Enter Joshua Tree National Monument, which derives its name from the large yucca Joshua Tree, a member of the lily family. These plants reach heights of 12 m and have leaves about 25 cm long with fine teeth along the edges. Creamy white blossom clusters adorn the ends of the branches in March and April. Joshua Trees are usually found at elevations above 900 m and are therefore found mainly in the western, higher portion of the Monument.
7.6	2.4	Pinto Gneiss on the right.
10.9	2.9	Differential weathering of Pinto Gneiss and Palms Quartz Monzonite visible to the right.
12.8	1.9	Road to Lost Horse Ranger Station. Continue straight.
14.4	1.6	Lost Horse Valley. On two hills to the left is the intrusive contact between Pinto Gneiss and Palms Quartz Monzonite. Within the hills to the right is Hidden Valley, a base camp once used by a group of cattle rustlers and horse thieves, known as the McHaney gang. Lost Horse and Queen Valleys provided excellent areas to hide and rebrand livestock until it could be sold in southern California markets, including Los Angeles and San Diego.
16.0	1.6	This portion of the valley floor is composed of Mesozoic White Tank Quartz Monzonite intrusive (Rogers, 1961). Road to Key's View is to the right. Key's View, 9 km down the road, provides an excellent overview of the Salton Basin. On a very clear day, Signal Mountain in Mexico, 153 km distant, may be seen. Cap Rock composed of White Tank Quartz Monzonite is on the right.
16.6	0.6	Ryan Campground turnoff. Continue on main road. The Lost Horse Mountains ahead extend northward from the Little San Bernardino Mountains and form the eastern border of Lost Horse Valley. These mountains are composed of Pinto Gneiss and may be the topographic expression of a gneissic screen between two intrusive bodies of White Tank Quartz Monzonite.
18.1	1.5	Ryan Mountain parking area. Intrusive contact of White Tank Quartz Monzonite and Pinto Gneiss is visible on Ryan Mountain to the right.
18.9	0.8	Sheep Pass Group Campground.
19.9	1.0	Queen Valley, like Lost Horse, formed by erosion of the less resistant quartz monzonites. Queen Mountain, forming the northern border of the valley, is composed of Palms Quartz Monzonite.

Mileage		
Cumulative	Difference	
		Located within the valley are several knobs of Gold Park Gabbro-Diorite, a dark gray, massive, coarse to fine grained rock with extreme variations of composition and texture (Rogers, 1961).
21.4	1.5	Road to Squaw Tank junctions from the right (see side-trip to Pleasant Valley).
22.3	0.9	Once wedging along the joints sufficiently separates different blocks, chemical weathering erodes quartz monzonite along grain boundaries. This action results in a rounding of the boulders and has produced interesting rock forms such as Jumbo Rocks and Skull Rock.
23.1	0.8	Jumbo Rocks.
23.7	0.6	Skull Rocks.
24.3	0.6	Live Oak and Split Rock picnic areas.
26.5	2.2	Junction with Pinto Basin Road.

SIDE TRIP TO PLEASANT VALLEY

This side trip is a modified version of the "Geology and Man" self guide tour by Elden K. Wanrow (1975) published by the Joshua Tree Natural History Association. The trip extends through southern Queen Valley and into Pleasant Valley. Queen Valley formed by differential erosion whereas Pleasant Valley formed by faulting.

ROAD LOG

Mileage		
Cumulative	Difference	
0.0	0.0	Junction of road to Squaw Tank and Park Boulevard.
1.2	1.2	Lost Horse Mountains, composed predominantly of Pinto Gneiss, form the western boundary of Queen Valley. The Little San Bernardino and Hexie Mountains border the valley to the south. This point marks the north-south drainage divide of this area. From here, water flows either northwest via Quail Springs Wash or southeast via Fried Liver Wash. It is interesting that this divide occurs within a valley and not along a mountain crest.

Mileage		
Cumulative	Difference	
2.9	1.7	Road crosses a typical desert wash. Malapai Hill, a Tertiary basalt intrusive, appears at 1 o'clock.
3.2	0.3	Distinctive 10 to 15 cm benches occur on the White Tank Quartz Monzonite boulders to the left (Fig. 8-32). The benches occur about 2 m above the ground and may indicate an old erosional surface level. Evidence of this level may also be seen on the boulders to the right; however, benches are faint.

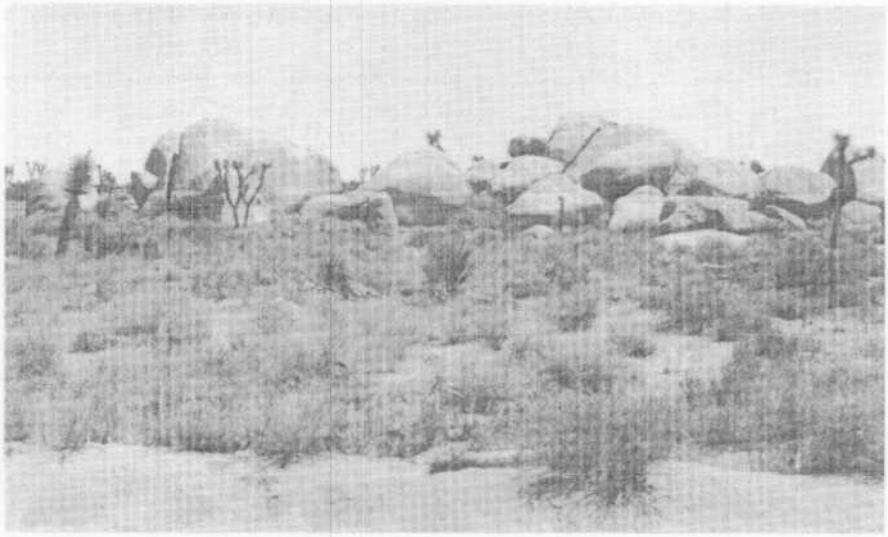

FIGURE 8-32. Distinctive 10 to 15 cm bench in White Tank Quartz Monzonite. This bench may mark an old stable erosional surface level (photograph by Ronald Papson, University of Santa Clara, May, 1977).

3.7	0.5	Many outcrops of weathered quartz monzonites.
4.8	1.1	Malapai Hill (Fig. 8-33) to the right, is dominantly composed of a Tertiary black aphanitic, olivine basalt with no associated flows, apparently an hypabyssal intrusion into the White Tank Quartz Monzonite. Crude columnar jointing is present in the steep faces near the summit (Fig. 8-34).
5.5	0.7	Squaw Tank was often used as a campsite for the nomadic Indians who occupied this area from about 1000 A.D. to the early 1900's. Several bowl-like mortars had been cut into the quartz monzonite around this site (Fig. 8-35) and were used in food preparation.

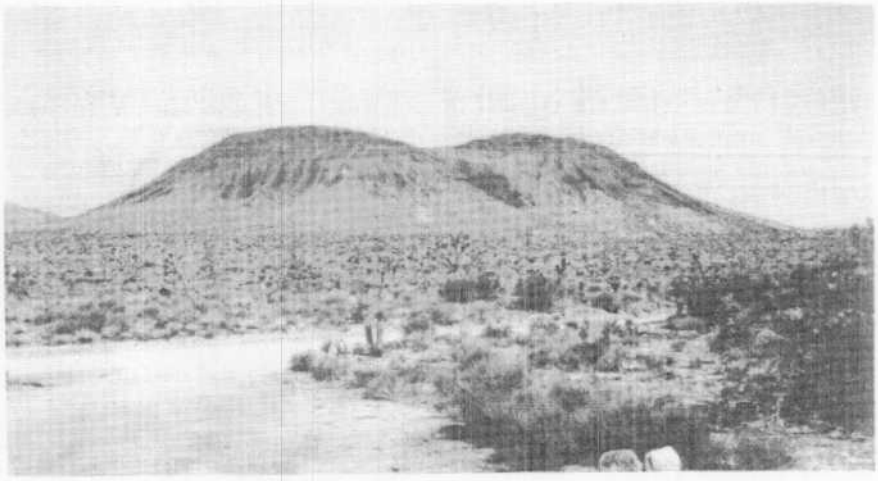

FIGURE 8-33. Malapai Hill, consisting primarily of Tertiary hypabyssal basalt intruded into White Tank Quartz Monzonite, forms a prominent butte in Queen Valley (photograph by Ronald Papson, University of Santa Clara, May, 1977).

FIGURE 8-34. Columnar jointing in the basalt at Malapai Hill (photograph by Ronald Papson, University of Santa Clara, May, 1977).

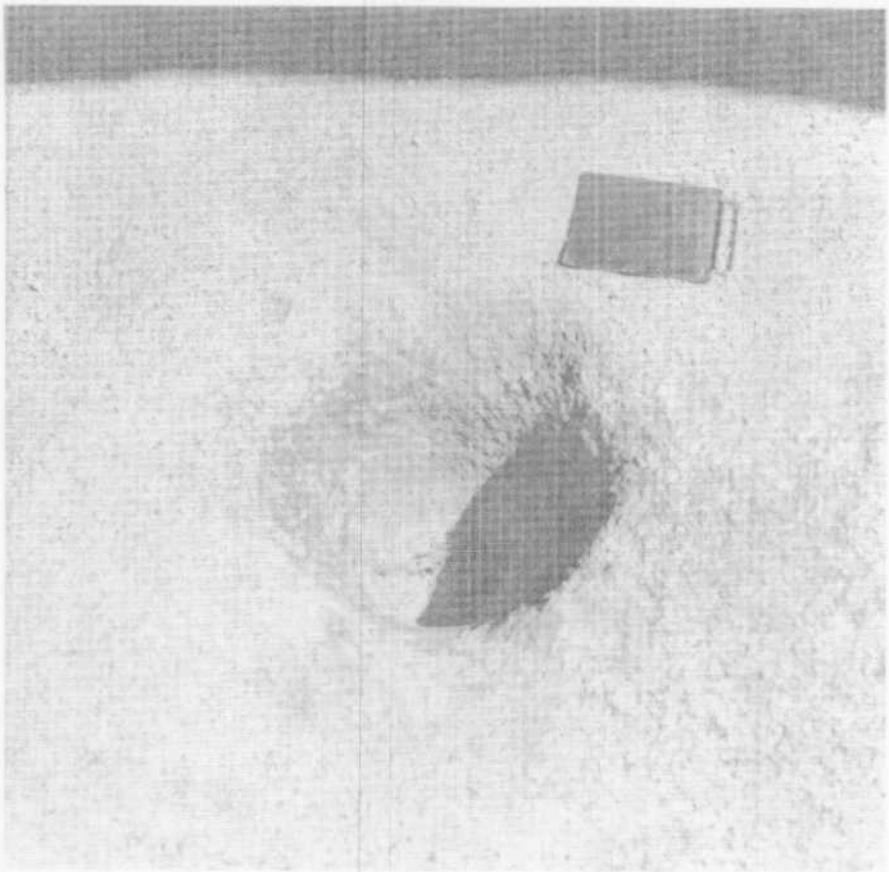

FIGURE 8-35. Mortar used by Indians who often camped at Squaw Tank (photograph by Eilene Theilig, University of Santa Clara, May, 1977).

Mileage
Cumulative Difference

In the early 1900's cattlemen were drawn to this area in search of good grazing land. Small dams such as Squaw Tank (Fig. 8-36) were built to contain runoff from the surrounding highlands. Many were built at natural pools or "tanks" that had previously been used by the Indians. Quartz monzonite boulders here contain several aplitic dikes (Fig. 8-37).

DO NOT PROCEED BEYOND THIS POINT IN WET WEATHER.

5.7 0.2 Pleasant Valley is bounded to the north by the Blue Cut fault and partially to the south by the Eagle Mountain fault. These two fault zones merge eastward and extend to the eastern portion of the Pinto Basin. On the left the Blue Cut fault forms the southern linear scarp of the Hexie Mountains which were uplifted by the fault (Fig. 8-38). The fault is named for the blue granodiorite found within the fault zone.

FIGURE 8-36. Small dam built by the cattlemen in the area to hold runoff and spring water (photograph by Ronald Papson, University of Santa Clara, May, 1977).

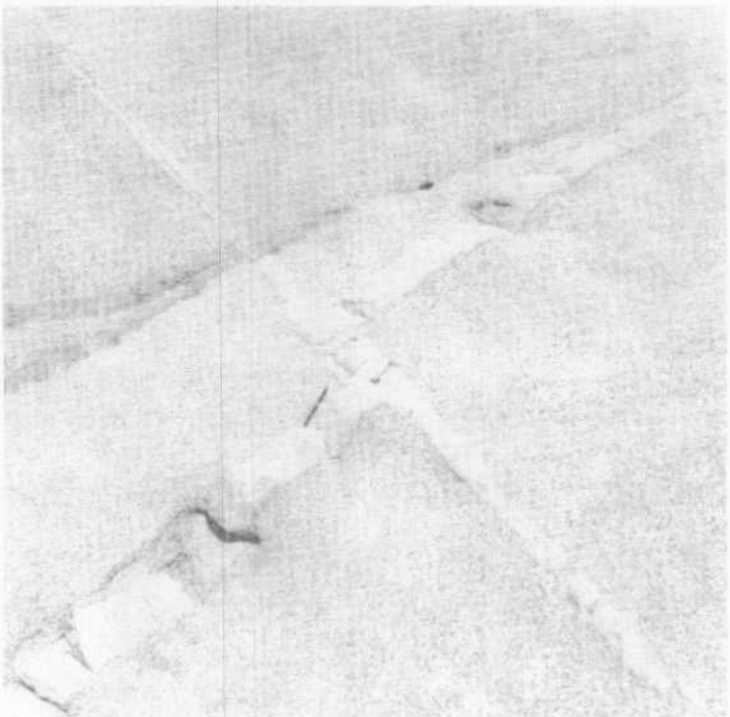

FIGURE 8-37. Cross-cutting aplite dikes in White Tank Quartz Monzonite near Squaw Tank (photograph by Ronald Papson, University of Santa Clara, May, 1977).

FIGURE 8-38. Linear southern face of the Hexie Mountains looking eastward in Pleasant Valley. This face is formed by the Blue Cut fault which merges with the Eagle Mountain fault and cuts through the Hexie Mountains (photograph by Ronald Papson, University of Santa Clara, May, 1977).

Mileage		
Cumulative	Difference	
		To the left is an intrusive contact between White Tank Quartz Monzonite and Pinto Gneiss (Fig. 8-39).
		Indian petroglyphs are found on several rocks here. These "rock carvings" were created by chipping away part of the desert varnish which coats the rocks.
6.8	1.1	Playa and small partially vegetated sand mounds on the left.
7.1	0.3	Tunnels and shafts associated with gold mines of the Hexahedron Mining Company. This company operated from about 1900 to World War I but with little productivity.
9.0	1.9	Pleasant Valley, like many valleys within the Monument, was at one time a grassland sustained by runoff stored within the deep soil. Overgrazing and prolonged drought caused the grasses to decline while cacti and shrub bushes became the dominant vegetation. Since the establishment of the National Monument, however, grassland vegetation has regained dominance.
9.8	0.8	Outcrop of Pinto Gneiss to the left. Note abundant lichen covering the surface.
10.0	0.2	Excellent panoramic view to the north.

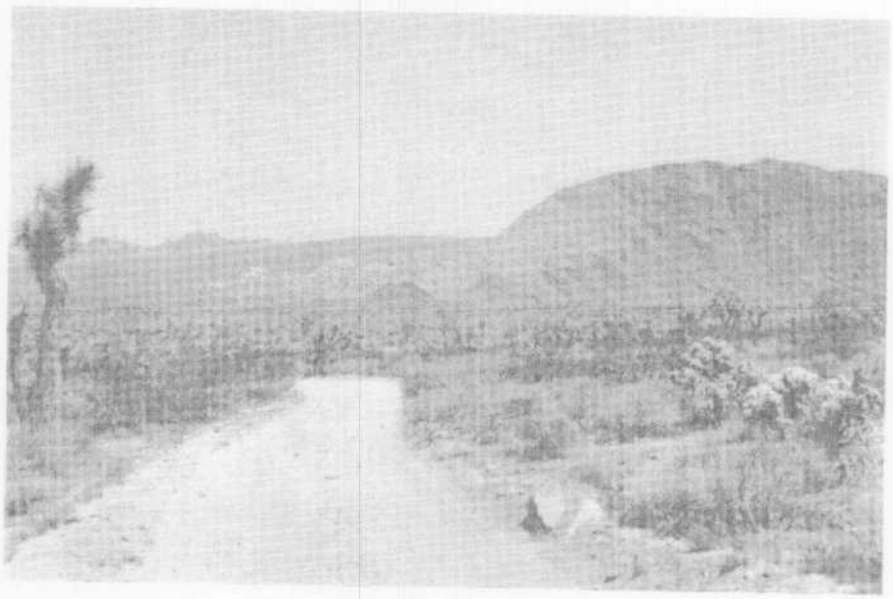

FIGURE 8-39. Intrusive contact between Mesozoic White Tank Quartz Monzonite (light) and Precambrian Pinto Gneiss (dark) on a spur of the Hexie Mountains (photograph by Ronald Papson, University of Santa Clara, May 1977).

REFERENCES

Allen, C. R., 1957. San Andreas fault zone in San Gorgonio Pass, Southern California: Geol. Soc. Am. Bull., v. 68, p. 315-350.

Bassett, M., and H. Kupfer, 1964. A geologic reconnaissance in the southeastern Mojave Desert, California: Cal. Div. of Mines and Geol. Spec. Report 83, 43p.

Biehler, S., R. Korach, and C. R. Allen, 1964. Geophysical framework of the northern end of the Gulf of California structural province: Am. Assoc. Petroleum Geologists Mem. 3, p. 126-143.

Bishop, C., 1963. Geological Map of California, Needles Sheet: Cal. Div. of Mines and Geol.

Blake, W. P., 1856. Ancient Lake in the Colorado Desert: Amer. Jour. Sci., 2nd Series, XVII, p. 435-438.

Campbell, E.W.C. and W.H. Campbell, 1935. The Pinto Basin Site: Southwest Museum Papers #9, Southwest Museum, Los Angeles.

Crowell, J.C. 1935. Geologic sketch of the Orocopia Mountains, southeastern California: Calif. Div. of Mines and Geol. Special Report 18, p. 99-110.

Dibblee, T.W., Jr., 1967. Geologic map of the Joshua Tree quadrangle, San Bernardino and Riverside Counties, California: U.S. Geol. Survey Misc. Geol. Inv. Map I-516.

Dutcher, L.C. and J.S. Bader, 1963. Geology and hydrology of Aqua Caliente Spring, Palm Springs California: U.S. Geol. Survey Water Supply Paper 1605, 44 p.

Fraser, Donald M., 1931. Geology of San Jacinto quadrangle south of San Gorgonio Pass, California: Calif. Div. of Mines and Geol. Report 27, p. 494-540.

Greeley, R. and T.E. Bunch, 1976. Basalt models for the Mars penetrator mission: Geology of Amboy Lava Field, California: NASA Technical Memorandum TMX-73, 125, 53 p.

Hatheway, A.W., 1971. Lava tubes and collapse depressions: Ph.D. Thesis, Univ. of Arizona (unpublished).

Jennings, C.M.V., 1967. Geol. Map of California, Salton Sea Sheet: Cal. Div. of Mines and Geol.

Leadabrand, R., 1972. *Exploring California Byways III: Desert Country*: Ward Ritchie Press, Los Angeles, 154 p.

Miller, R. D., 1968. *Mines of the High Desert*: La Siesta Press, Glendale, California, 71 p.

Miller, W.J., 1944. Geology of Palms Springs-Blythe Strip, Riverside County, California: Calif. Div. Mines and Geology Rep. 40, p. 11-72.

Neal, J.T., 1965. Geology, mineralogy, and hydrology of U.S. Playas: Air Force Cambridge Research Laboratories, Envir. Res. Papers #96 (AFCRL 65-266).

Oakshott, G.B., 1971. *California's Changing Landscapes, A guide to the geology of the state*: McGraw-Hill Book Co., San Francisco, 388 p.

Parker, B., 1963. Recent volcanism at Amboy Crater, San Bernardino County, California: Calif. Div. Mines and Geol. Spec. Rept. 76, 23 p.

Peterson, G.L., R.G. Gastil, and E.C. Allison, 1966. Geology of the Peninsular Ranges *in* Mineral resources of California: U.S. Cong., 89th, 2nd Sess., Comm. Interior and Insular Affairs, Comm. Print: Calif. Div. of Mines and Geology, Bull. 191, p. 70-73.

Proctor, J., 1968. Geology of the Desert Hot Springs-Upper Coachella Valley area, California: Calif. Div. of Mines and Geol. Spec. Rept. 94, 43 p.

Rogers, J., 1961. Igneous and metamorphic rocks of the western portion of Joshua Tree National Monument, Riverside and San Bernardino Counties, California: Calif. Div. of Mines and Geol. Spec. Rept. 68, 26 p.

Rogers, T.H., 1965. Geol. Map of California, Santa Ana Sheet, Calif. Div. of Mines and Geol.

Rogers, T.H., 1967. Geol. Map of California, San Bernardino Sheet, Calif. Div. of Mines and Geol.

Scharf, D.W., 1935. The Pinto Basin Site, an ancient aboriginal camping ground in the California desert: Southwest Museum paper 9, 51 p.

Sharp, R.P., 1966. Kelso Dunes, Mojave Desert, California: Geol. Soc. Amer. Bull., v. 77, p. 1045-1074.

Vaughan, F.E., 1922. Geology of the San Bernardino Mountains north of San Gorgonio Pass: Univ. of California, Dept. Geol. Sci. Bull., v. 13, p. 319-411.

Wanrow, E.K., 1975. Geology and Man: An 18 mile self-guiding motor nature trail: Joshua Tree Natural History Association.

9. AERIAL GUIDE TO GEOLOGICAL FEATURES OF SOUTHERN CALIFORNIA

John S. Shelton
P. O. Box 48
La Jolla, California 92038

Ronald P. Papson
Department of Geology and
Center for Meteorite Studies
Arizona State University
Tempe, Arizona 85281

Michael Womer
Department of Geology and
Center for Meteorite Studies
Arizona State University
Tempe, Arizona 85281

9. AERIAL GUIDE TO GEOLOGICAL FEATURES OF SOUTHERN CALIFORNIA

John S. Shelton
P. O. Box 48
La Jolla, California 92038

Ronald P. Papson
Department of Geology and
Center for Meteorite Studies
Arizona State University
Tempe, Arizona 85281

Michael Womer
Department of Geology and
Center for Meteorite Studies
Arizona State University
Tempe, Arizona 85281

The study of aeolian features in southern California is the primary objective of this field conference. Planetary geological investigations involve the use of photography covering a wide variety of scales and viewing angles. This flight guide will cover the major geological features in the Salton Trough and southeastern Mojave Desert. Low altitude aerial photographs of terrestrial features will give insight into the processes operating on other planetary surfaces.

The air tour will be approximately three and one-half hours in duration. Figure 9-1 shows the general flight path, which is broken into three "legs". The tour begins at the Palm Springs airport and continues southward to Algodones dunes at the international border with Mexico. The flight then heads northward to Kelso Dunes and then returns to Palm Springs.

The following features will be of interest during the flight; they are listed in their order of appearance.

LEG 1

- Sand flow around obstructions
- Martinez rock slide
- Cahuilla shorelines
- Barchan dune field
- Tertiary structures
- Longitudinal dunes
- Algodones dune complex
- San Andreas fault trace

LEG 2

- Climbing dunes and sand sheets
- Amboy cinder cone
- Kelso dunes
- Volcanic field
- Longitudinal dunes

LEG 3

- Falling dunes
- Volcanic field, overblown with sand
- Giant mud cracks
- Blackhawk slide
- San Andreas fault system

FIGURE 9-1. ERTS mosaic overlain with flight path for southern California flight.

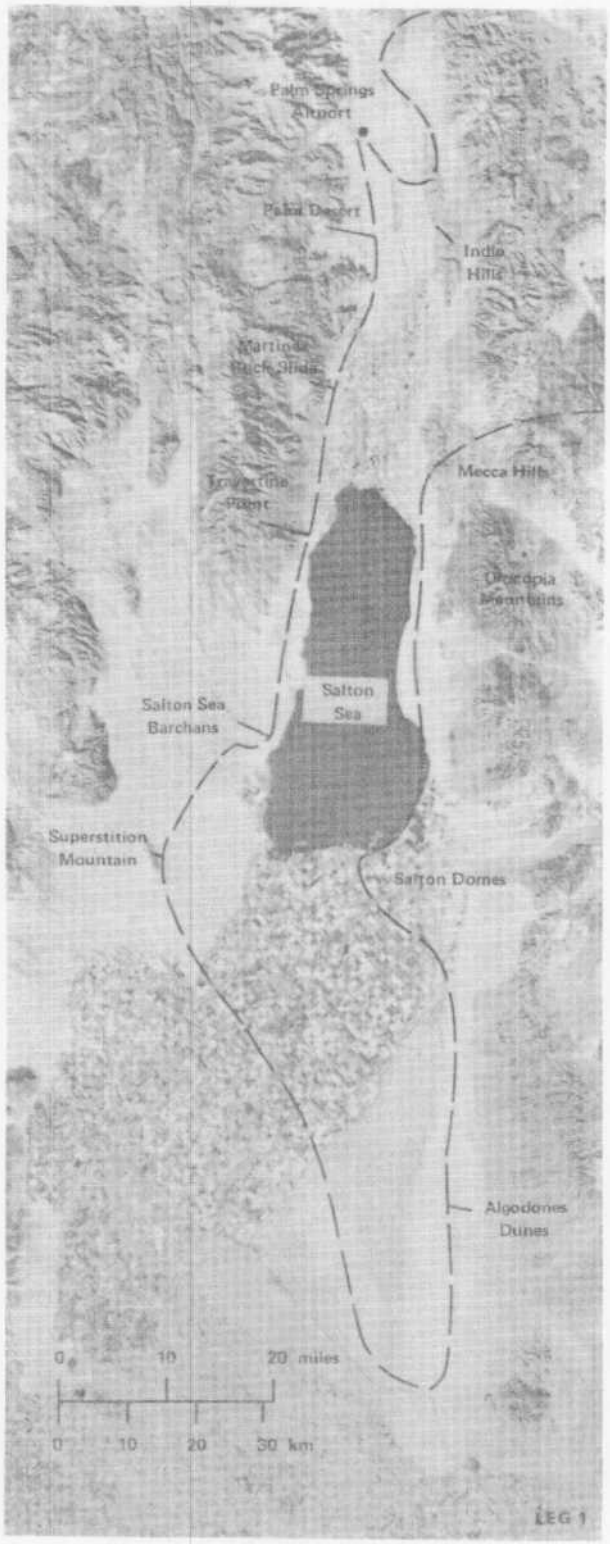

FIGURE 9-2. ERTS mosaic of Leg 1 for the flight path.

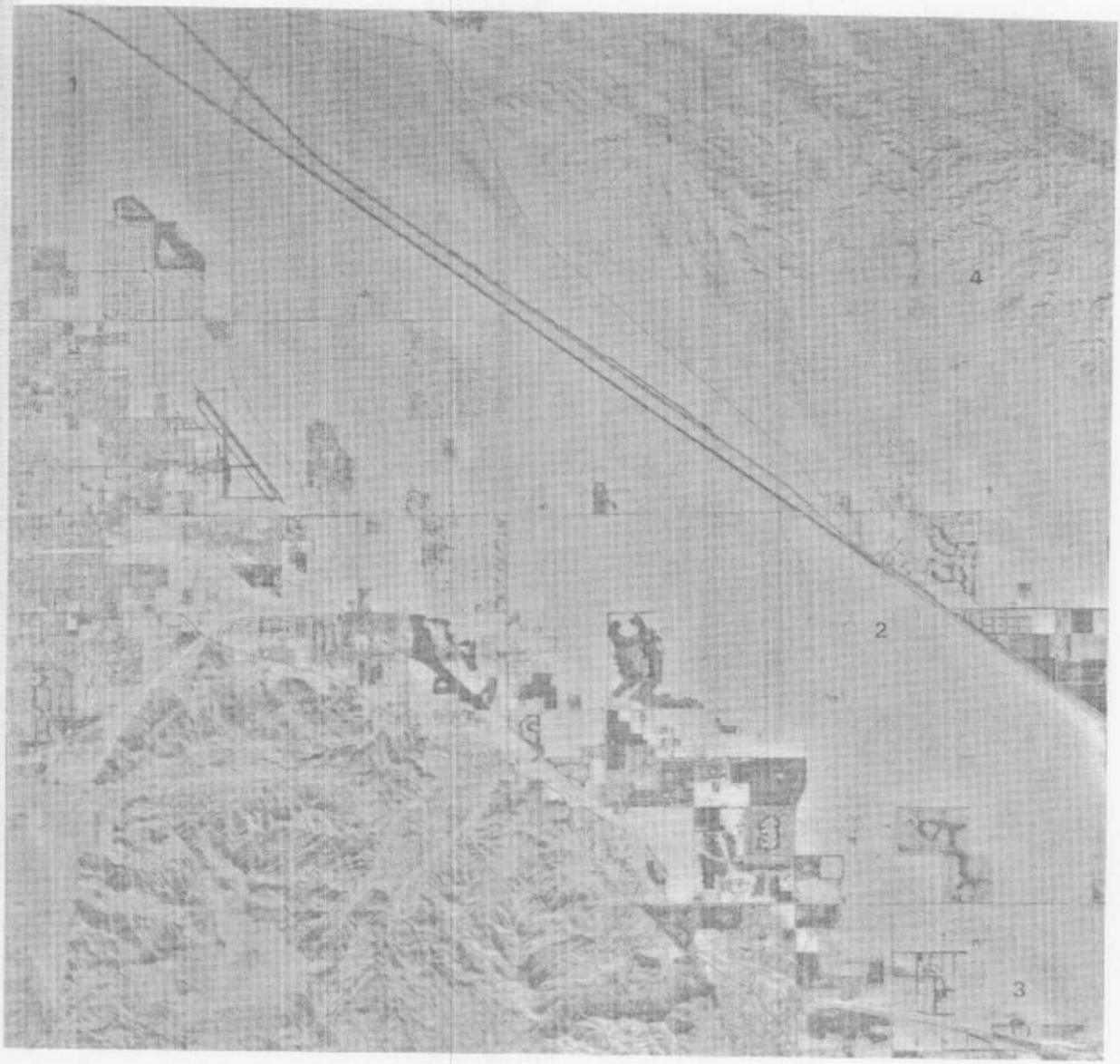

FIGURE 9-3. Vertical aerial photograph of the northern Coachella Valley. Prevailing winds enter from the northwest (upper left) near Palm Springs (1) and travel southeastward through the valley. Wind features such as lee depressions (2) and fields of modified barchans (3) occur north of Palm Desert. Indio Hills (4) are in the upper right. Photograph is approximately 18.5 km by 18.5 km. (U.S. Geological Survey Photograph GS-VDWU, 1-48, October, 1975.)

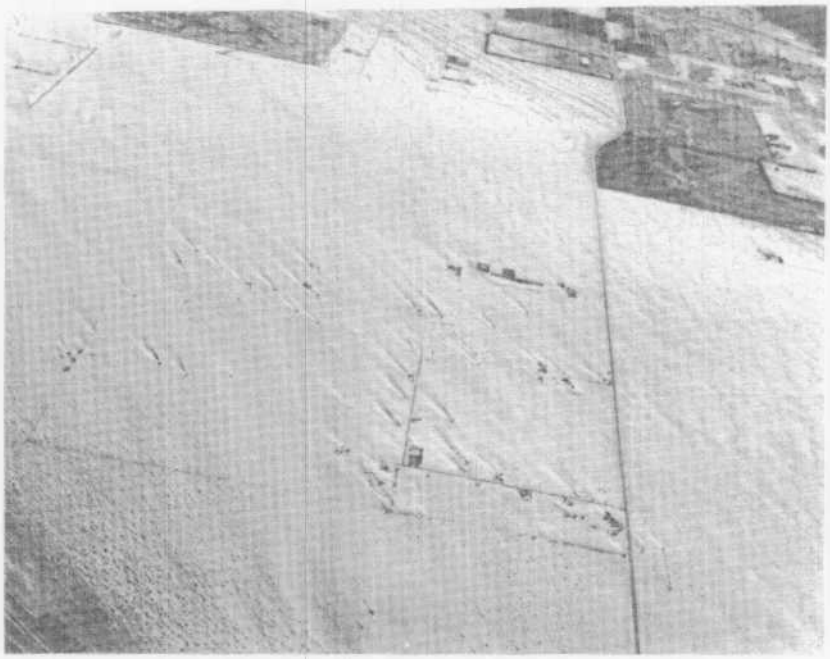

FIGURE 9-4. Southward view of lee depressions north of Palm Desert (see Fig. 9-3, no. 2). Influence of obstacles on flow of sand is well demonstrated. (Photograph 6829 by John S. Shelton.)

FIGURE 9-5. South-southwest view of field of barchanoid dunes north of Palm Desert (see Fig. 9-3, no. 3). Wind direction is from right to left. Dunes are partially stabilized by vegetation. (Photograph 67-236 by John S. Shelton.)

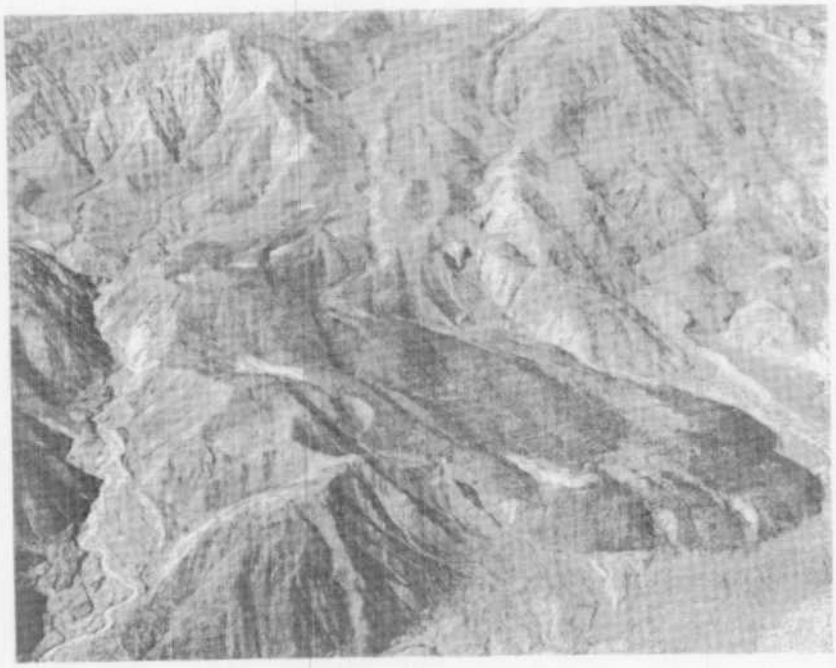

FIGURE 9-6. View westward of the Martinez rock slide. It averages 8 km long and 2 km wide with blocks up to 10 m in diameter in distal areas. (Photograph 2386 by John S. Shelton.)

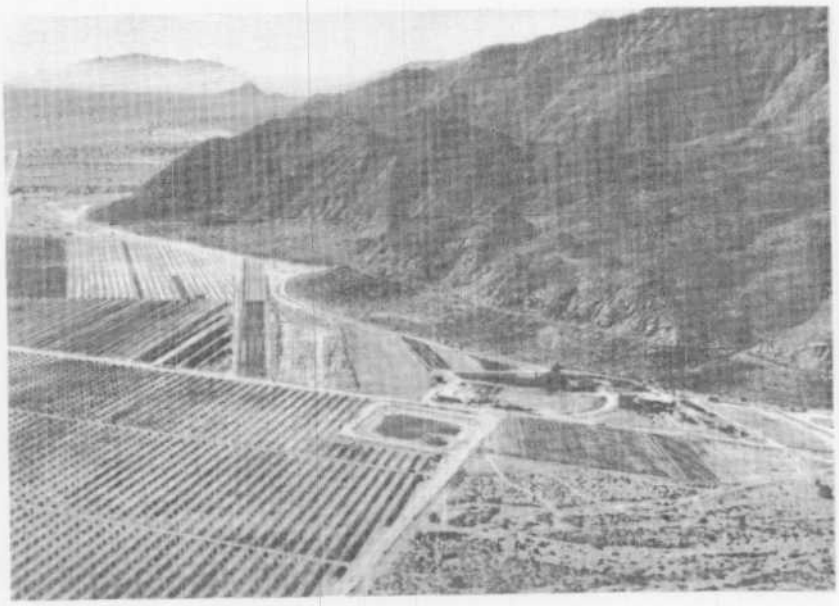

FIGURE 9-7. Ancient shoreline of Pleistocene Lake Cahuilla west of Mecca. Lake Cahuilla occupied up to 5400 km^2 of the Salton Trough, perhaps as recently as 300 years B.P., and had a maximum surface elevation of about 13 m above sea level. (Photograph 3600 by John S. Shelton.)

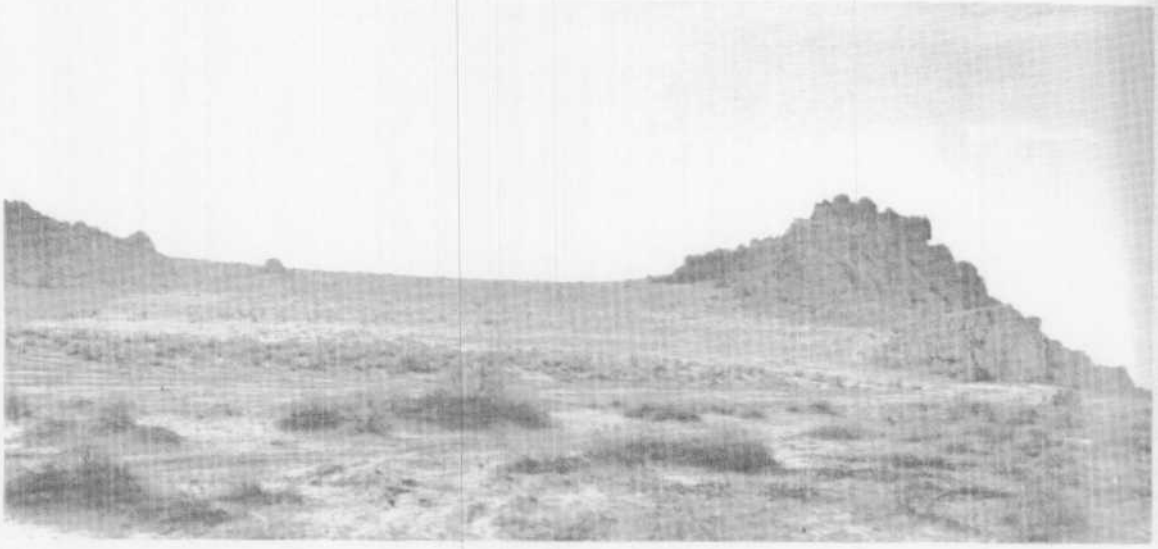

FIGURE 9-8. Travertine Point connected by a tombolo to the base of the Santa Rosa Mountains. The dark upper portion of Travertine Rock (center right) remained above the high water line of Lake Cahuilla. Below this line, the boulders are covered by thick tufa deposits. Successive Lake Cahuilla shorelines are visible on the tombolo. (Photograph 4220 by John S. Shelton.)

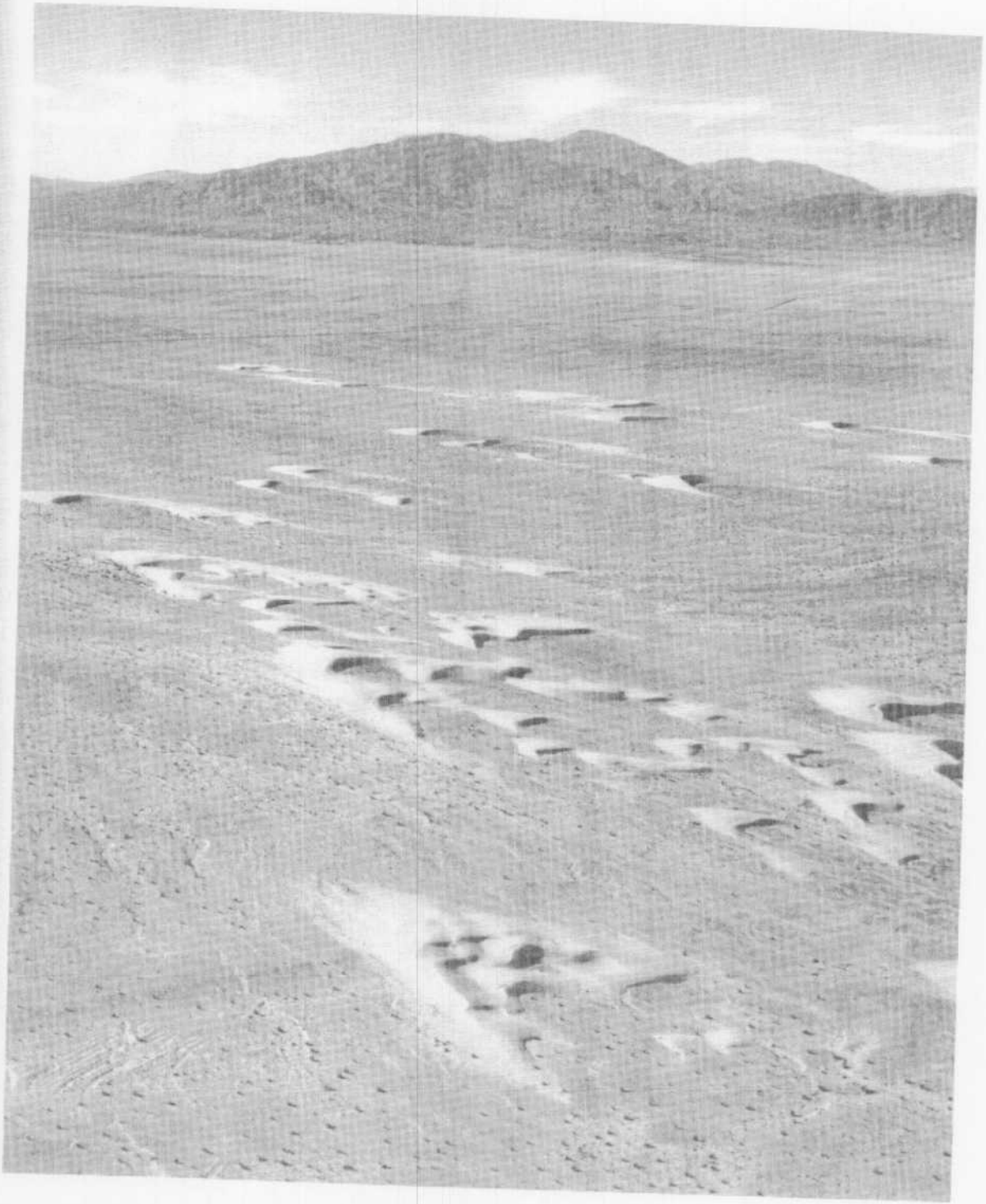

FIGURE 9-9. Salton Sea barchans looking northwest toward the Santa Rosa Mountains. The dunes migrate eastward approximately 18 m/yr. Note the tendency for individual barchans to be "shed" from the horns of others upwind. Dune sand is derived from Borrego Valley and dry washes to the west. (Photograph 5461cr by John S. Shelton.)

FIGURE 9-10. Closer upwind view of members of the Salton Sea barchan field. There is some sand in interdune areas, but almost none downwind from slip faces. Note small dune overtaking larger one in foreground. (Photograph 5465cr by John S. Shelton.)

FIGURE 9-11. Two eroded domes in Quaternary sedimentary strata west of the Salton Sea; Vallecito Mountains in the distance. (Photograph 5897 by John S. Shelton.)

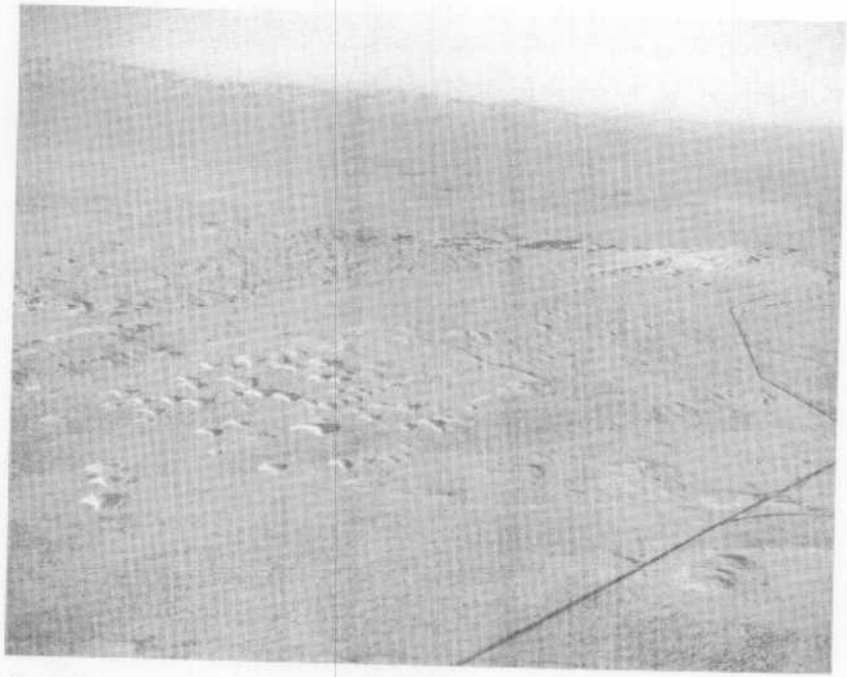

FIGURE 9-12. View southwestward of longitudinal dunes extending from Superstition Mountain (see Chapter 5). The longitudinal ridges spawn barchanoid dunes downwind (toward lower left). (Photograph 67-203 by John S. Shelton.)

FIGURE 9-13. View north of sand free intradune areas with exposed desert floor in southern Algodones dunes (see Chapter 6). Long linear slip faces are an average of 50 m high and 1.5 km long. (Photograph 1815 by John S. Shelton.)

FIGURE 9-14. Low oblique view north-northwest along the central Algodones dune field. Note the predominantly southeast-facing lee slopes in the main mass of coalesced dunes in the foreground. (Photograph 67-208 by John S. Shelton.)

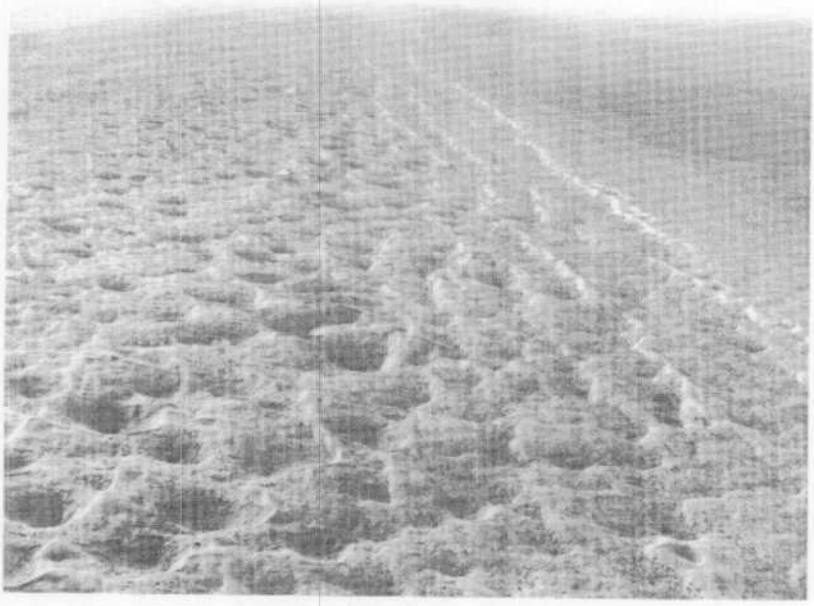

FIGURE 9-15. View southeast of linear dunes parallel to the western edge of the Algodones dune field. Sand in this area has been partially stabilized by vegetation. (Photograph 67-216 by John S. Shelton.)

FIGURE 9-16. Looking eastward at the northern end of Algodones dune field. The scene suggests that the dry wash may be a local source of sand and that there have been minor reversals of wind direction. Note how dune character changes downwind. (Photograph 67-226 by John S. Shelton.)

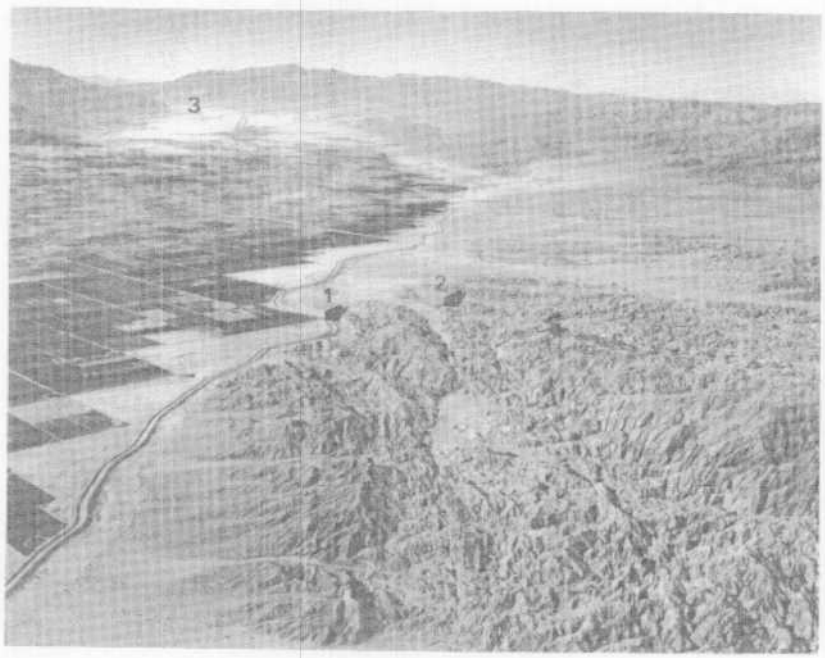

FIGURE 9-17. View northwest of highly folded and faulted beds of Cenozoic sedimentary rocks in the Mecca Hills. Several branches of the San Andreas fault (1 and 2) can be traced through this area. San Gorgonio Pass (3) is in the upper left corner. (Photograph 6817 by John S. Shelton.)

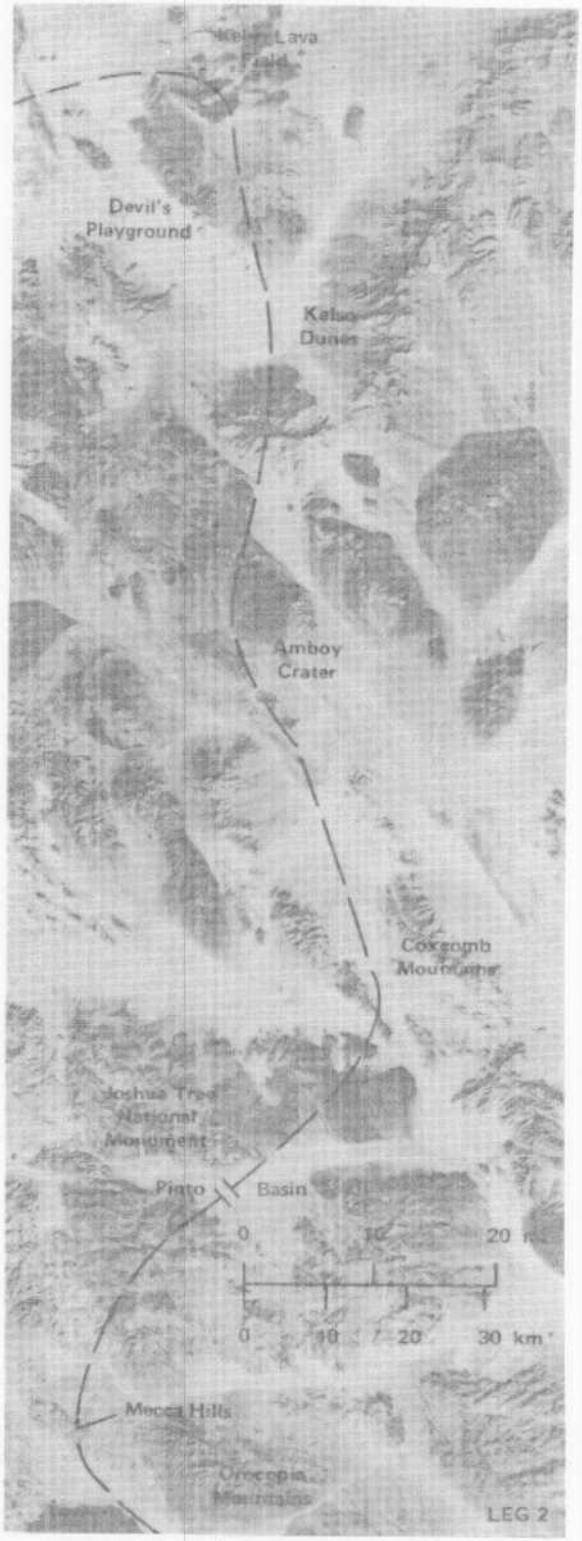

FIGURE 9-18. ERTS mosaic of Leg 2.

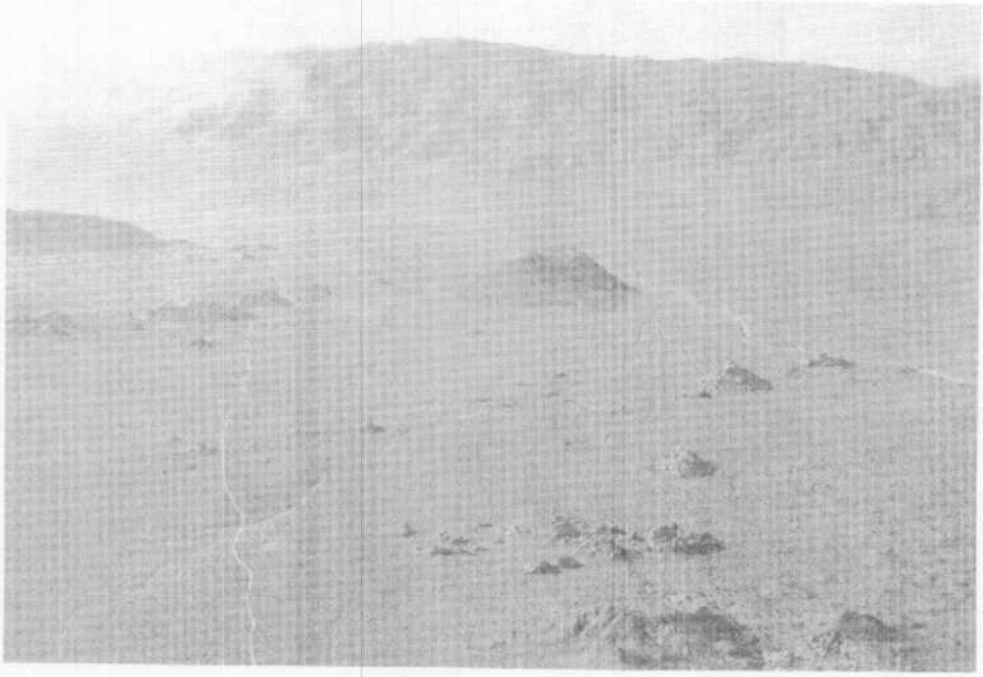

FIGURE 9-19. Low oblique southerly view of Southern Queen in Joshua Tree National Monument. Note small plutonic knobs on the valley floor. The large dark hill (center) is Malapai Hill, a Tertiary basaltic intrusion. (Photograph by Ronald Papson, September, 1977.)

FIGURE 9-20. View east-northeast of climbing dunes at the eastern end of Twentynine Palms valley. Westerly winds through the valley deposit sand on the windward slopes of large obstacles. (Photograph 67-245 by John S. Shelton.)

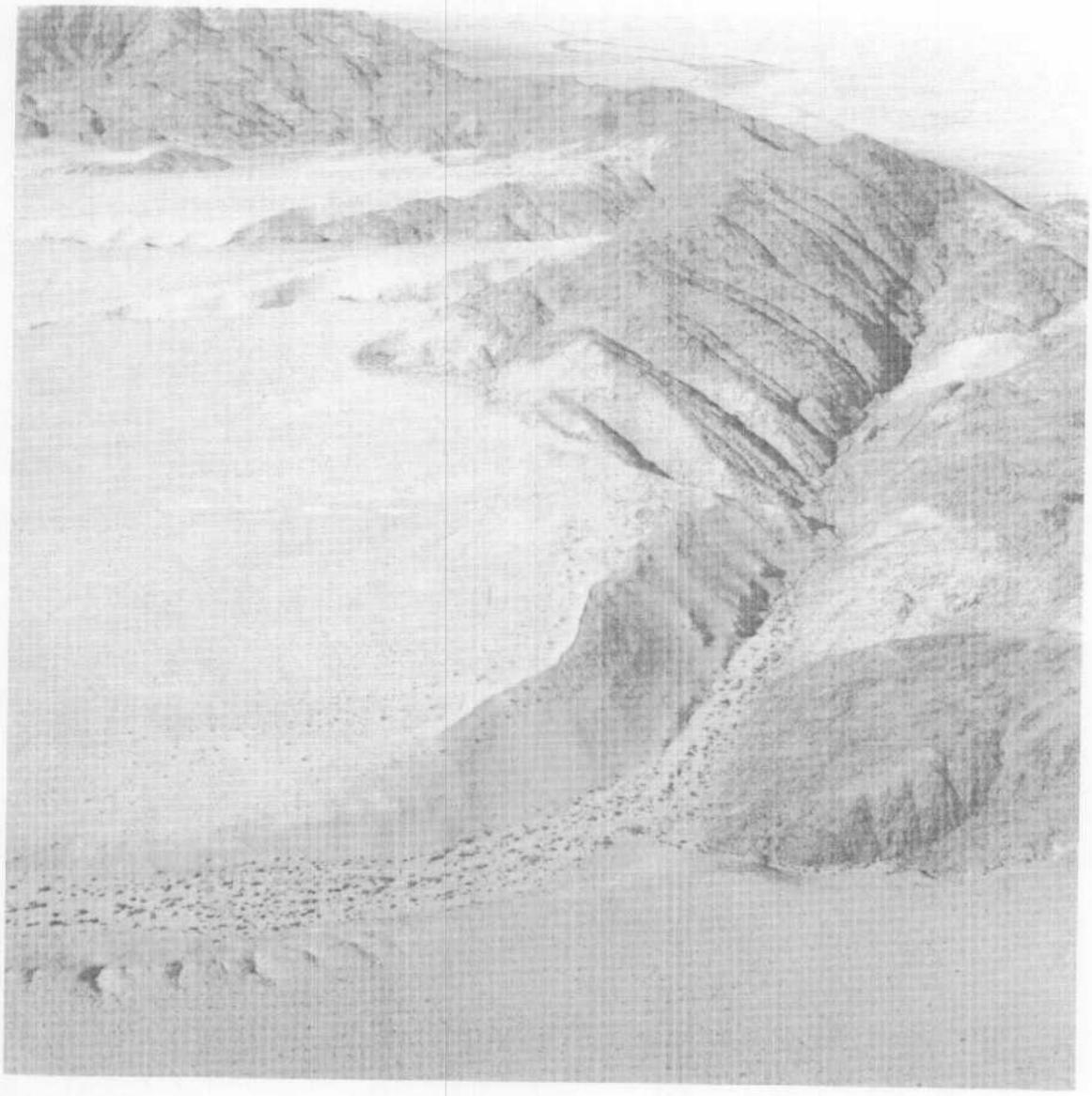

FIGURE 9-21. View north-northwest of climbing dunes (Fig. 9-20, no. 1) on the western side of the Sheep Hole Mountains at east end of Twenty-nine Palms Valley. (Photograph by Ronald Greeley, University of Santa Clara, 1977.)

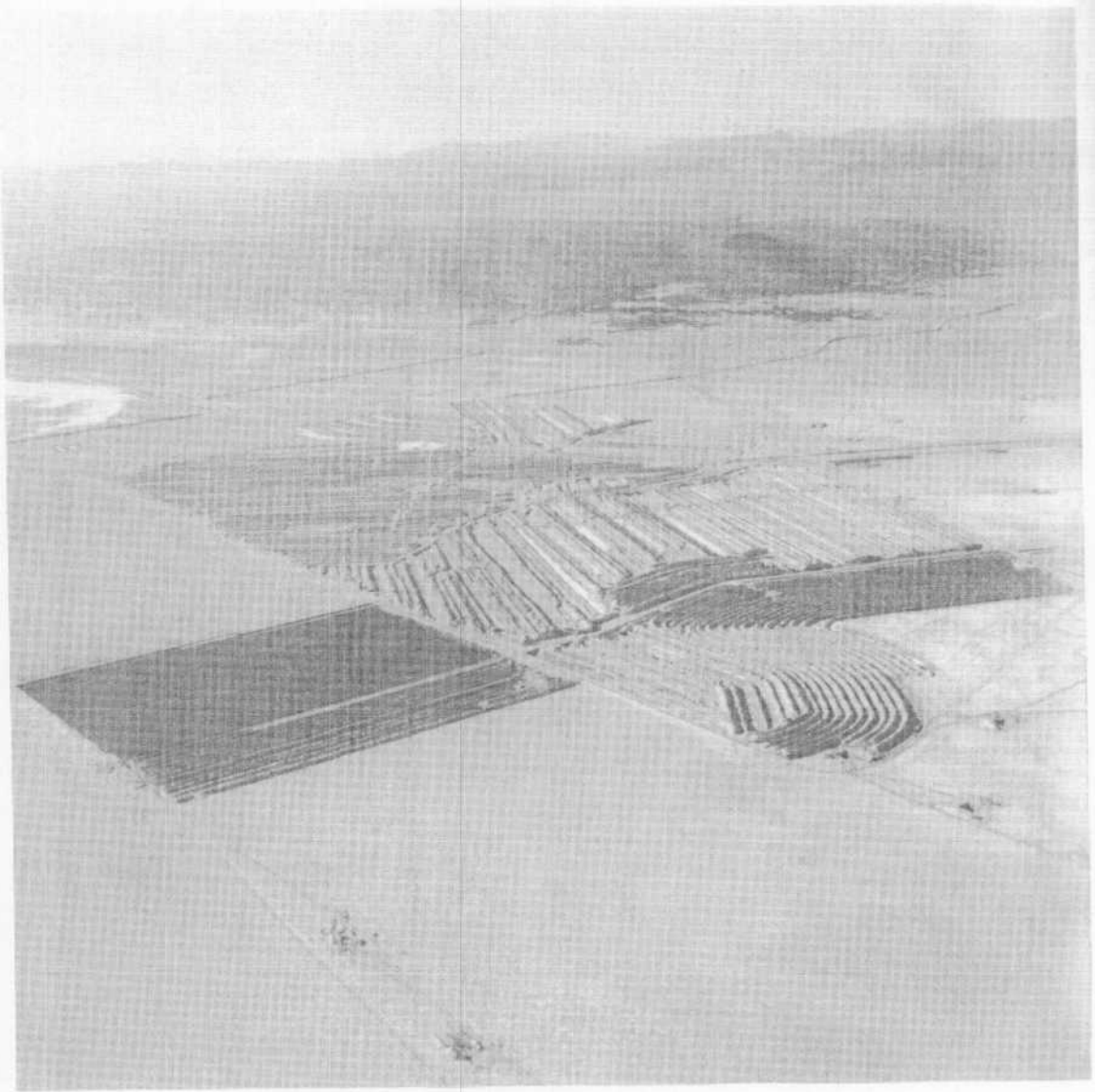

FIGURE 9-22. Salt evaporators of the National Chloride Company on Bristol Dry Lake. Amboy lava field is in the distance with its single, distinctive cinder cone (upper right). (Photograph by Ronald Greeley, University of Santa Clara, 1977.)

FIGURE 9-23. Amboy Crater and associated basalt flows viewed toward the south. The dark "plume" downwind of the cinder cone is an area devoid by surficial sand, caused by air turbulence in the wake of the crater (see Chapter 31). (Photograph 67-248 by John S. Shelton.)

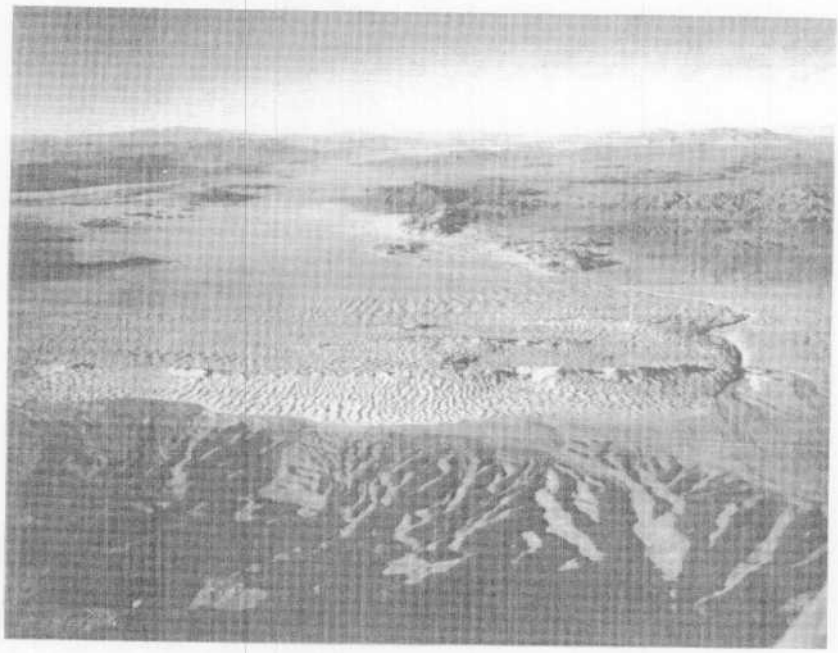

FIGURE 9-24. Kelso Dunes, viewed northward, is the southernmost extension of Devil's Playground, a vast area of sand deposits fed by sand transported from the Mojave River Sink (upper left). The unnamed lava field visible in the upper right consists of numerous basaltic vents. (Photograph 5745 by John S. Shelton.)

FIGURE 9-25. Low oblique view of Kelso Dunes. This transverse linear ridge on the southeastern edge of the dune field attains a maximum height of approximately 200 m above the underlying valley floor (see Chapter 4). (Photograph by Ronald Greeley, University of Santa Clara, 1977.)

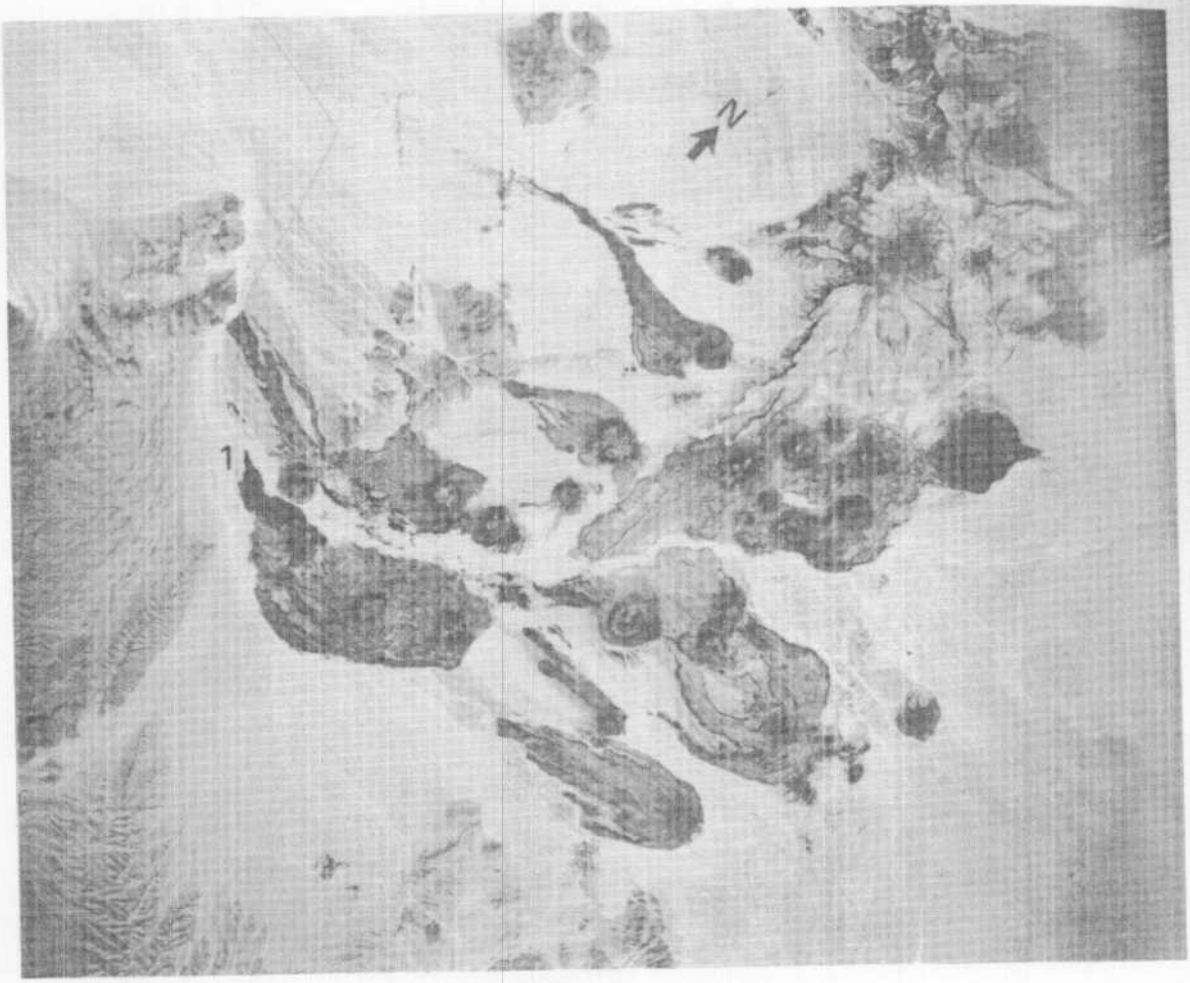

FIGURE 9-26. High altitude (U-2 aircraft) vertical aerial view of the lava field between Baker and Kelso Dunes. The Pleistocene basalt flows are elongate down the alluvial fan slope. Photograph is approximately 25 km by 23 km. (NASA-Ames Photograph 1278, frame 2849.)

FIGURE 9-27. Low oblique view of recent lava flow issued from breached cinder cone (Fig. 9-26, no. 1) in unnamed lava field. (Photograph by Ronald Greeley, University of Santa Clara, 1977.)

FIGURE 9-28. Northwesterly low oblique view of linear ridges and barchanoid dunes (foreground) in the Devil's Playground. (Photograph by Ronald Greeley, University of Santa Clara, 1977.)

FIGURE 9-29. Sand features northwest of Kelso Dunes (upper left). Sand derived from the Mojave River sink is carried by the wind and deposited around large obstacles. (Photograph by Ronald Greeley, University of Santa Clara, 1977.)

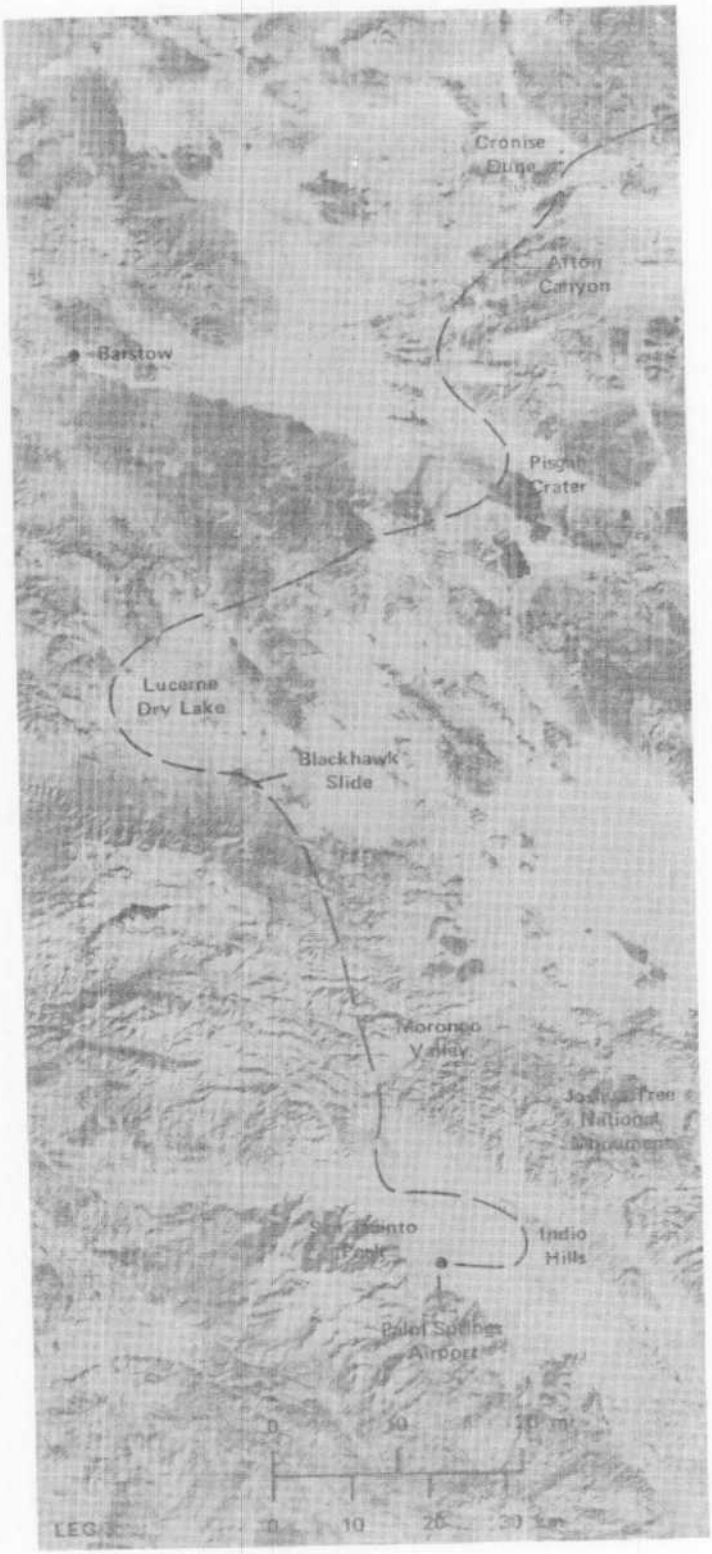

FIGURE 9-30. ERTS mosaic of Leg 3.

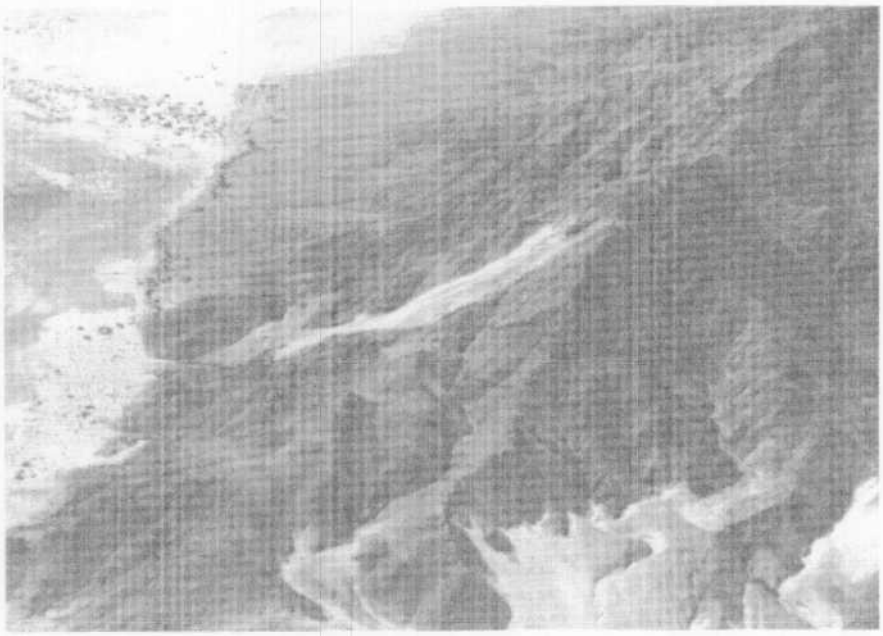

FIGURE 9-31. Cronese Dune, a large falling dune north of Cave Mountain, is visible as the elongate sand strip in the upper center. (Photograph 27-264 by John S. Shelton.)

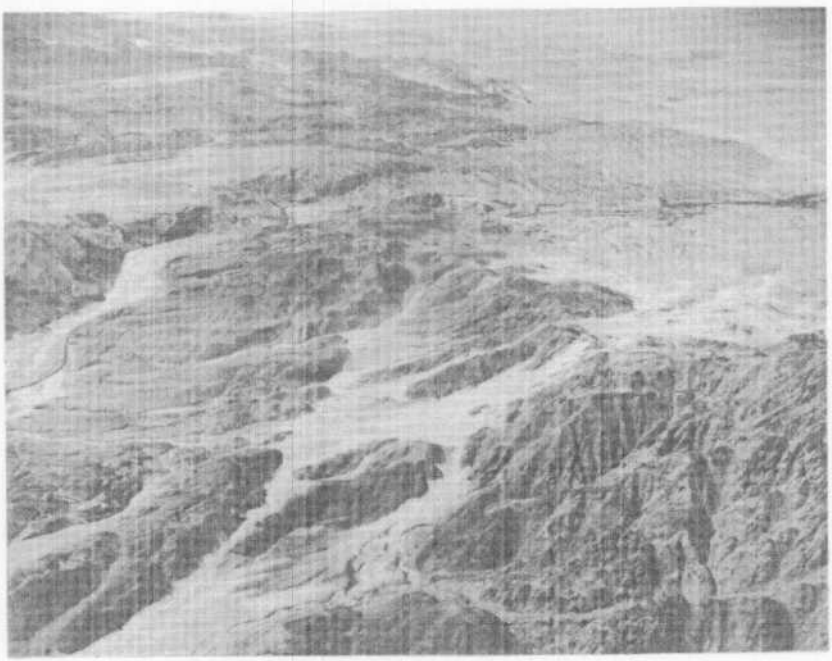

FIGURE 9-32. Southwest end of Cave Mountain (lower right) and Afton Canyon (upper center). The Mojave River flows eastward (left) through this canyon during peak flow and debauches into the Mojave River sink farther east. As the deposits dry, wind transports the sediments towards the Devil's Playground. (Photograph 67-266 by John S. Shelton.)

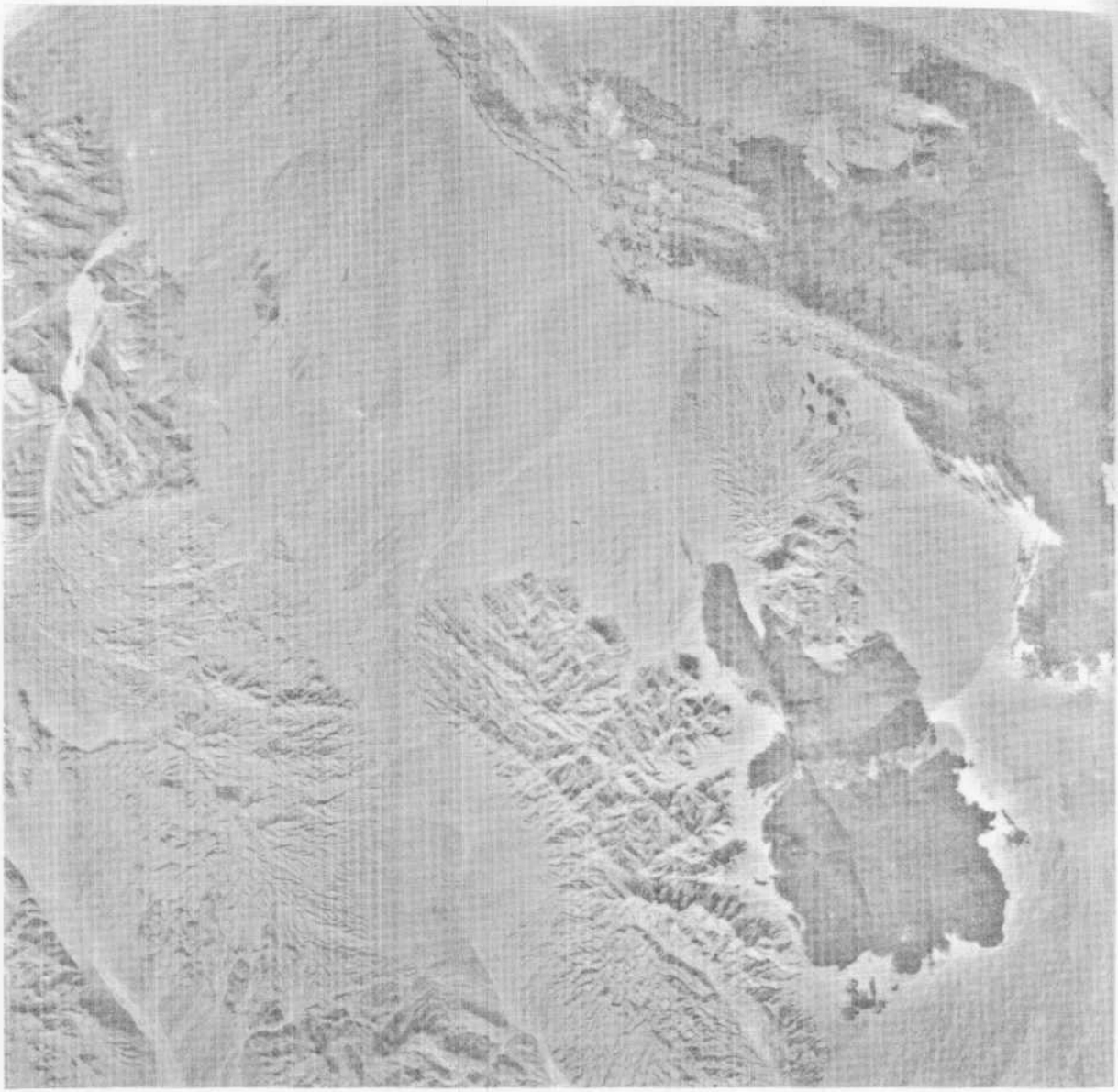

FIGURE 9-33. Vertical aerial photograph of Pisgah lava field. Fresh basalt surfaces are being partially covered by a veneer of windblown sand (light linear features, upper right). Lavic Lake (L, lower right) exhibits large desiccation features. (U.S. Geological Survey Photograph, GS-VDQM, 1-45, November, 1974.)

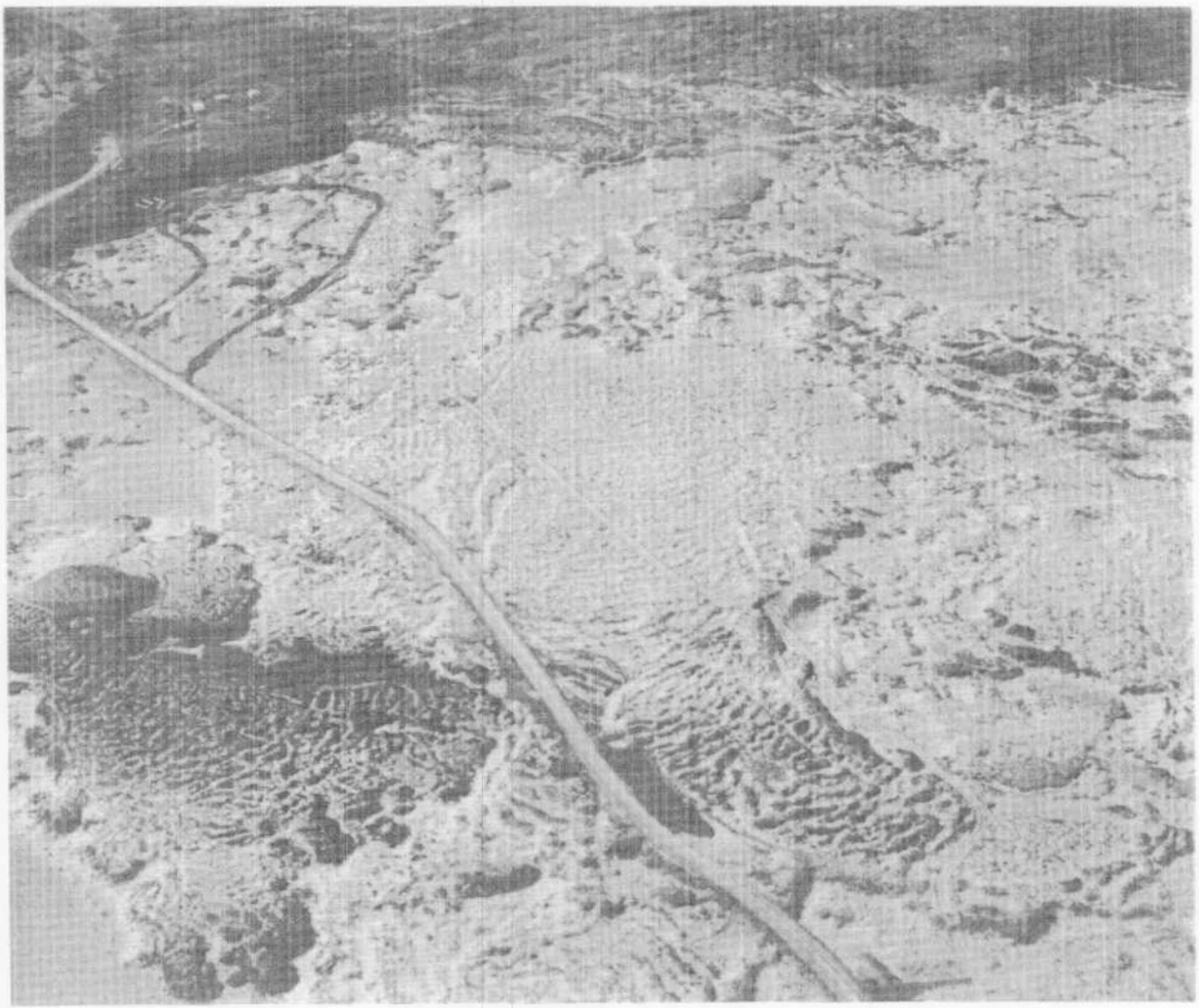

FIGURE 9-34. Low oblique view southwest toward Pisgah Crater (upper left). Aeolian sand covers much of the basalt surface. Note the contrasting high and low albedo areas. (Photograph by Ronald Greeley, University of Santa Clara, 1976.)

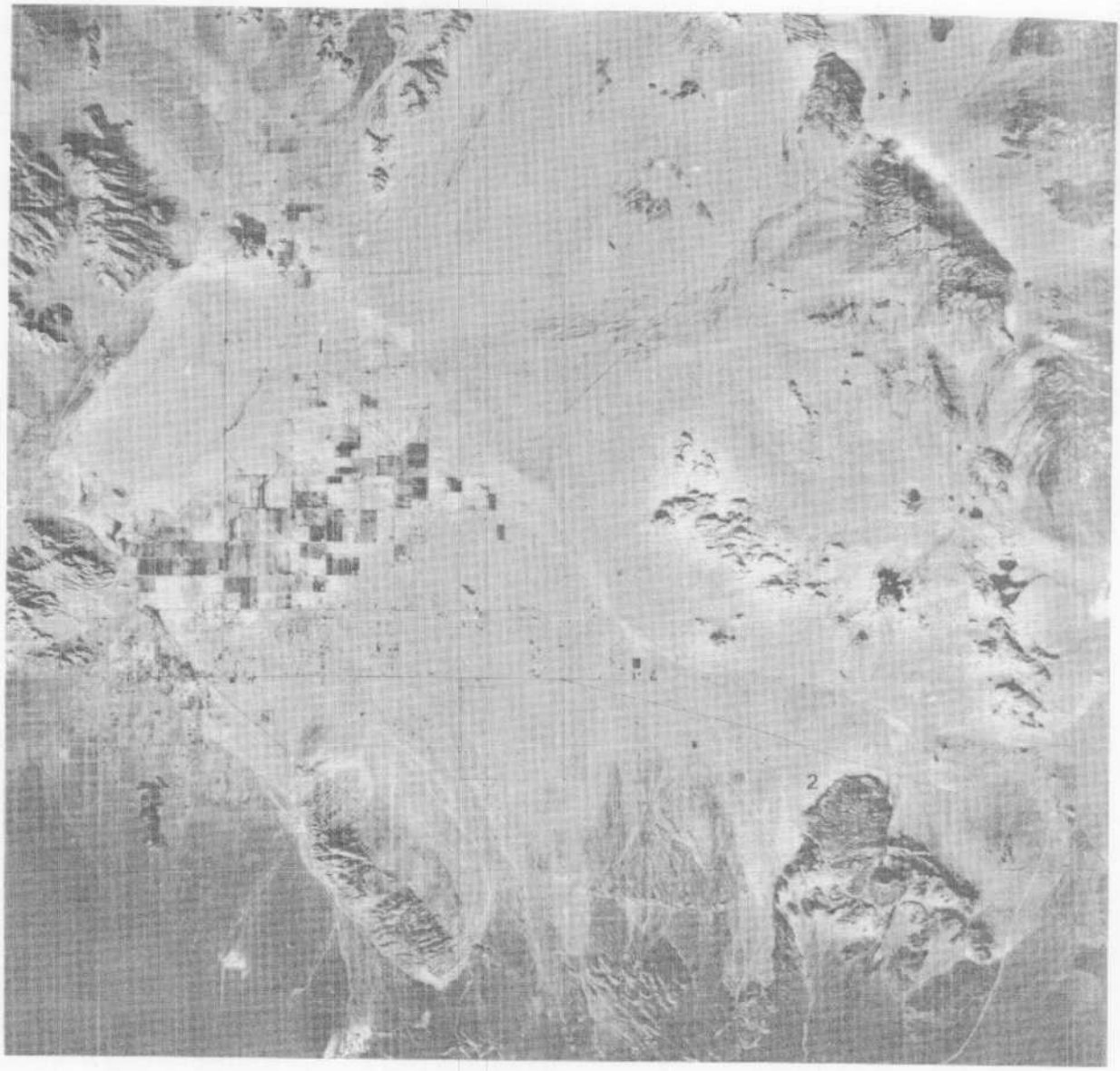

FIGURE 9-35. High altitude (U-2) vertical photograph of area around Lucerne Dry Lake (1) exhibits large desiccation cracks on its surface (see Figs. 9-36 and 9-37). Blackhawk Slide (2) covers approximately 24 km^2. Photograph covers approximately 26 km by 26 km.

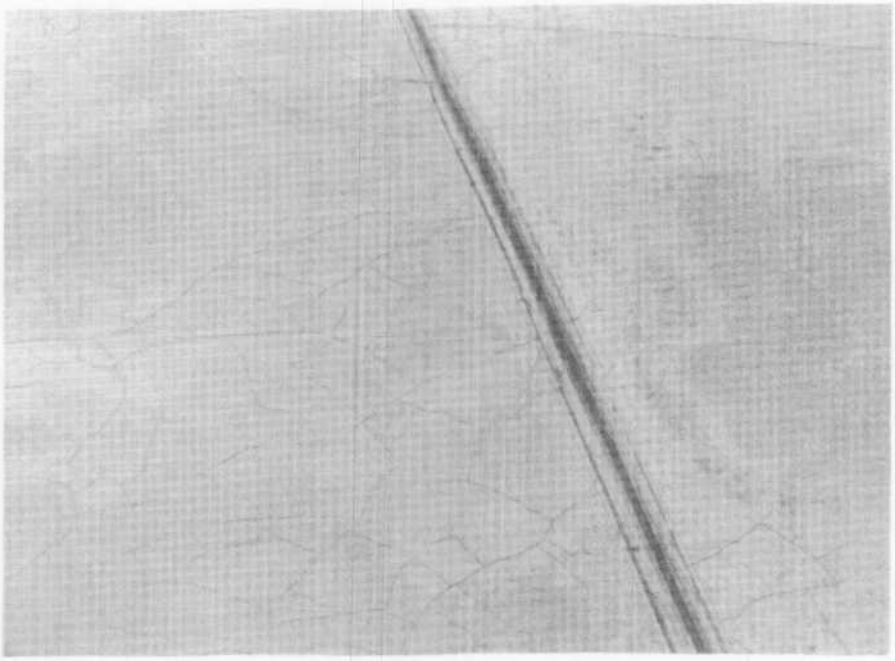

FIGURE 9-36. Giant desiccation cracks on Lucerne Dry Lake. Recent growth is evidenced by disruption of the road embankment where cracks cross the road (center and lower right). (Photograph 67-275 by John S. Shelton.)

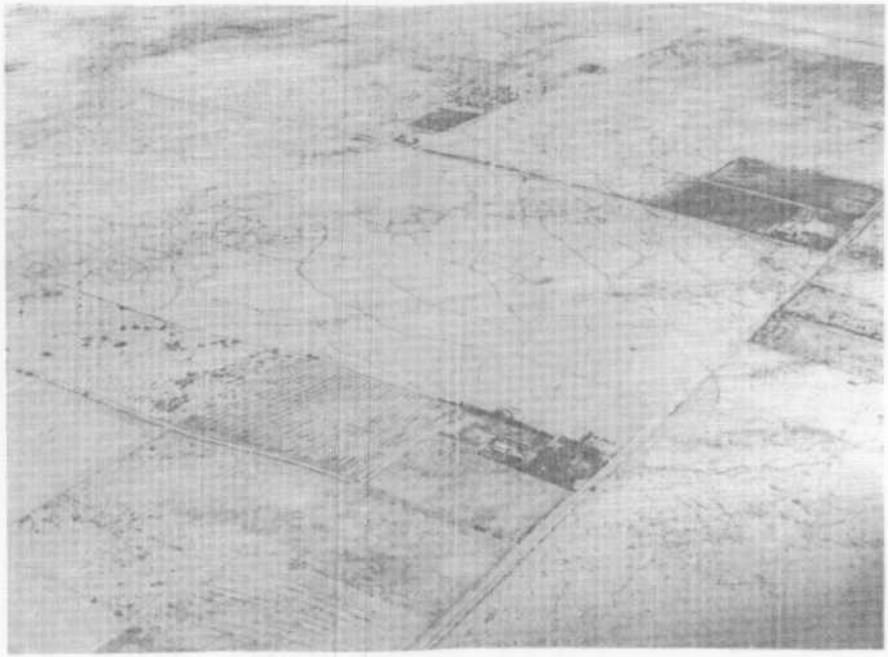

FIGURE 9-37. Low oblique view of giant desiccation cracks on Lucerne Dry Lake. In this part of the lake, cracks are vegetated, probably an indication of greater age. Little is known concerning how these large-scale features form. (Photograph 67-274 by John S. Shelton.)

FIGURE 9-38. Blackhawk landslide viewed southward toward the San Bernardino Mountains. It consists of approximately 3 x $10^8 m^3$ of crushed marble and is 3 km wide, 8 km long and from 9 to 30 m thick. (Photograph 2459cr by John S. Shelton.)

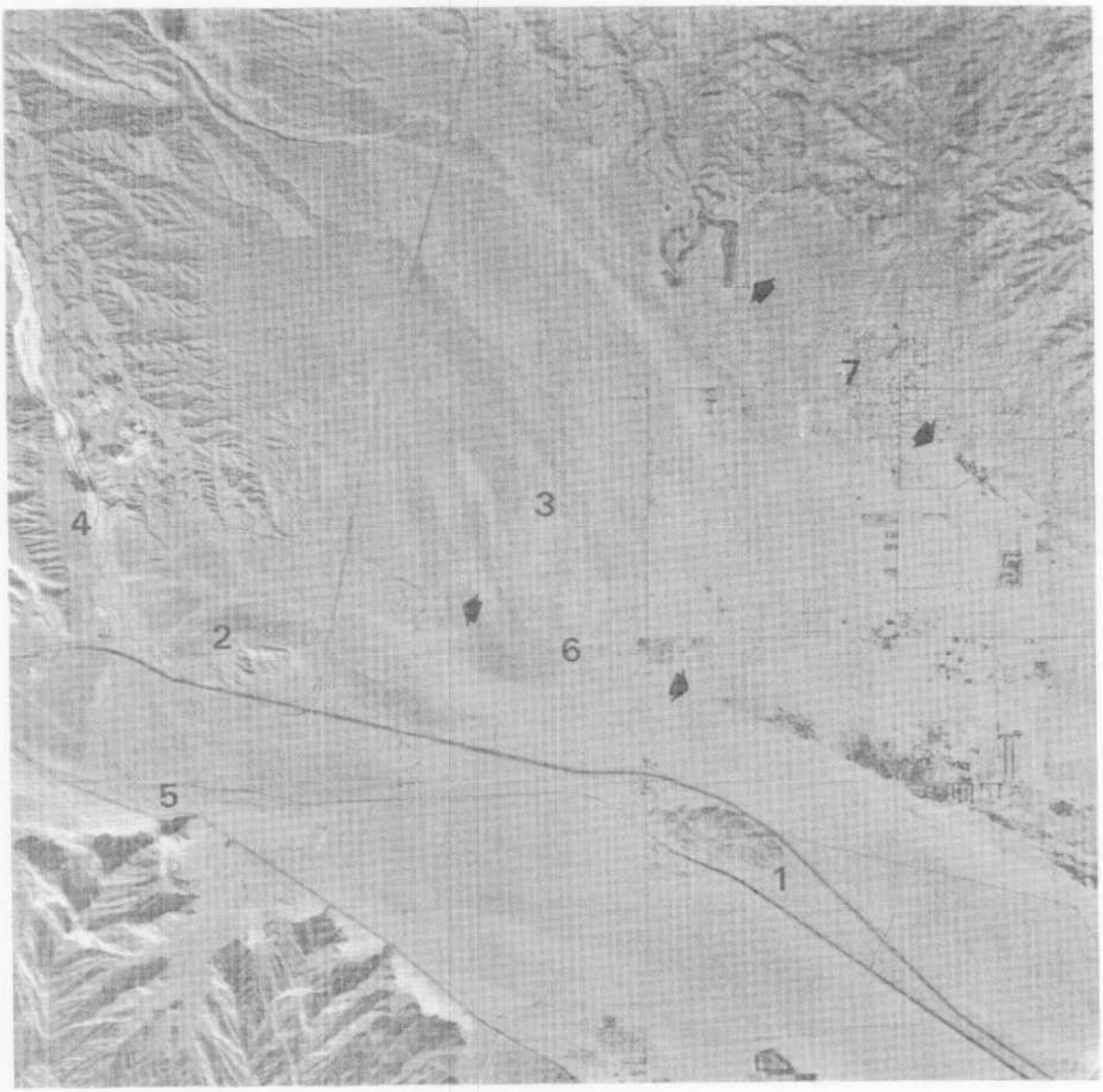

FIGURE 9-39. Vertical aerial photograph showing features northwest of Palm Springs: (1) Garnet Hill with abundant ventifacts and wind scour features, (2) Whitewater Hill, (3) Devers Hill, (4) Whitewater River, (5) Windy Point, (6) Banning fault trace, and (7) Mission Creek fault trace. Photograph covers an area approximately 21 km by 21 km. (U.S. Geological Survey Photograph, GS-VDWU, 1-59, October, 1975.)

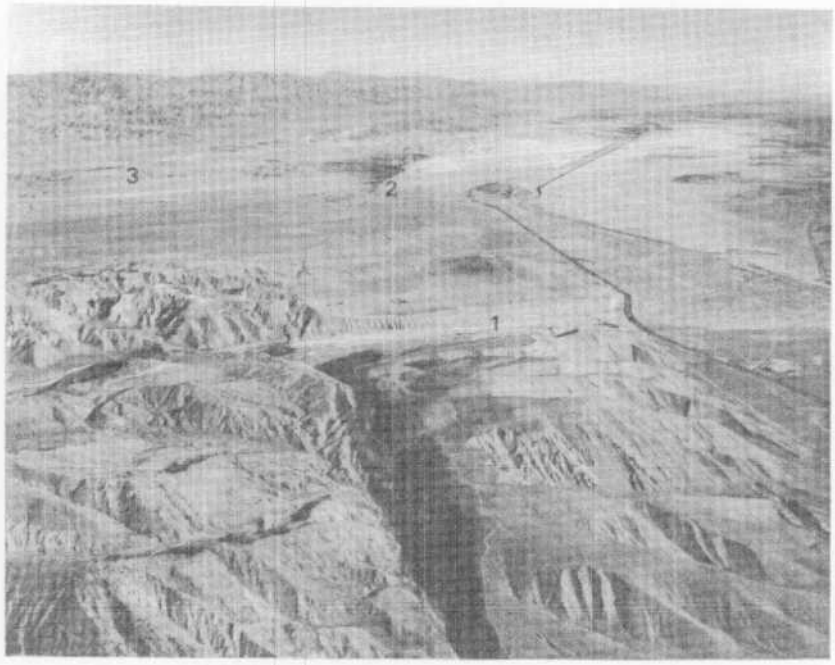

FIGURE 9-40. View southeastward through Coachella valley. In foreground is Whitewater Canyon (1). The Banning fault (2) can be clearly traced on the photograph; the Mission Creek fault trace (3) in the upper left is more obscure. Palm Springs is in the upper right. (Photograph 6837 by John S. Shelton.)

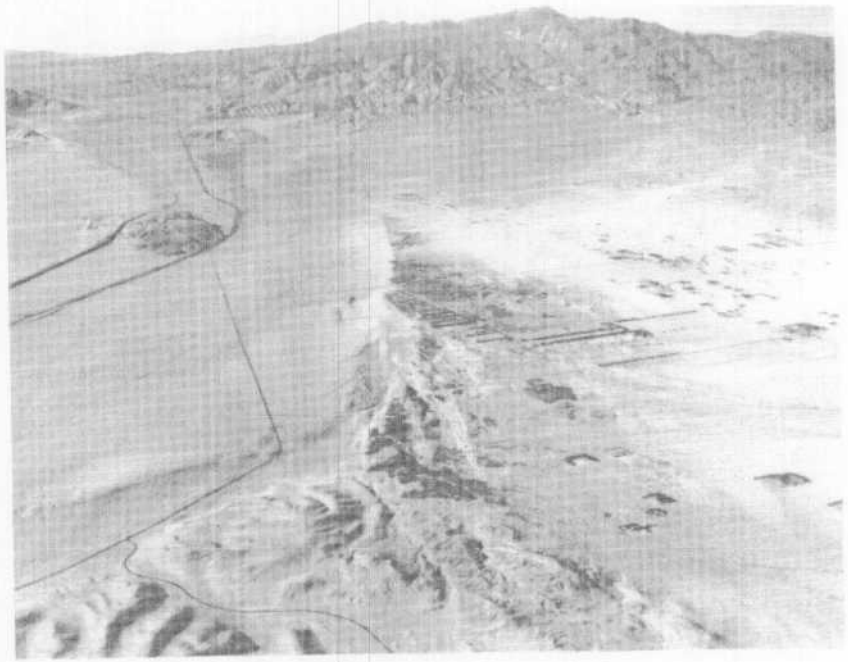

FIGURE 9-41. View northwest along trace of the San Andreas fault zone. Being less permeable, the fault zone impedes ground water movement, causing the water table to rise along the north side of the fault. Garnet Hill (center left) is in direct line with the winds from San Gorgonio Pass (upper left) (see Chapter 2). The San Bernardino Mountains are in the background. (Photograph 6832 by John S. Shelton.)

10. COACHELLA VALLEY AREA GENERAL GEOLOGY FIELD TRIP

George L. Meyer
College of the Desert
Palm Desert, CA 92260

10. COACHELLA VALLEY AREA GENERAL GEOLOGY FIELD TRIP

George L. Meyer
College of the Desert
Palm Desert, CA 92260

The Coachella Valley is a structural extension of the Gulf of California Rift which began to form in the late Pliocene. That part of the rift lying north of the present gulf is referred to as the Salton Trough. With rifting, the valley floor subsided and mountain roots on the sides were re-elevated to form the mountains that bound the present valley.

Alluvial fan deposition occurred on valley margins as it does now. The valley floor was physically as well as structurally part of the Gulf of California until such time as the Colorado River constructed its delta across the lower part of what is now the Imperial Valley. Once the lowest part of the delta was above sea level, the history of the valley diverged from that of the gulf, being the site of fresh-water lakes when the Colorado River flowed northward, or of saline lakes and salt flats when the river flowed southward into the gulf.

The San Andreas fault is related to the rift as the rift structure (East Pacific Rise) is offset by it from the Salton Sea area to a point off Cape Mendocino. The northern part of the San Andreas fault is considerably older than that portion in the Coachella Valley; structure on the northeastern valley margin is closely tied to the San Andreas fault. Its movement is dominantly right lateral and is shown by local stream valley offsets.

The rifting that produced the valley depression created a pronounced rain shadow environment for the valley as a result of mountain uplift. Also, a "wind channel" was formed from the San Gorgonio Pass area onto the valley floor. Thus the wind, aided by the arid climate, is a dominant transportational and depositional agent on the central part of the valley floor.

FIELD TRIP

The following field trip itinerary includes special points of interest in the Coachella Valley. Although a full day is required for the entire field trip, individual segments may be visited separately.

Mileage		
Cumulative	Difference	
0.0	0.0	Start at College of the Desert, in Palm Desert; go to west entrance.
0.5	0.5	Turn right on Monterey Avenue at west entrance.
1.1	0.6	Monterey Avenue crosses Whitewater Wash. It is fed by San Gorgonio and Whitewater rivers and flows only with major runoff.
2.2	1.1	Turn west (left) on Country Club Drive from Monterey Avenue. Note the "sandbelt": irregular dunes and sand shadows largely stabilized by vegetation. (Much Russian thistle has been present since the heavy rains of September 1976).

Mileage		
Cumulative	Difference	
3.2	1.0	Turn right (north) from Country Club Drive onto Bob Hope Drive.
3.9	0.7	This is an area of formerly actively moving sand (left) stabilized by windbreaks and golf courses.
4.8	0.9	Unmodified sandsheet area on sand tongue extending towards southeast. Sand is poorly sorted, accumulations with any relief being sand shadows downwind (southeast) of creosote bushes and scattered dwellings. Note the particularly large shadow downwind of the house on the right.
5.2	0.4	High point of sand tongue. The elevation here is 30–40 m higher than that on the distal margins of the alluvial fans on the margins of the valley, attesting to active aeolian deposition. This area is particularly good for observation of migrating ripples during frequently-occuring sandstorms.
6.3	1.1	Turn right (east) from Bob Hope Drive onto Ramon Road. Note the very numerous sand shadows on downwind sides of creosote bushes.
6.5	0.2	Overpass over railroad. Tamarisk trees planted to either side of railroad make an effective windbreak.
9.6	3.1	Turn left (north) from Ramon Road onto dirt road and proceed as far as power lines (or you can stop on Ramon Road at this point if the dirt road is impassable). Note palm oasis to the north (Willis Palms) marking the trace of the Banning fault along the base of the Indio Hills. Also note the straightness of the base of the hills to the northwest.

The Banning fault is the southern branch of the San Andreas fault system in this area. The Mission Creek fault (northern branch of San Andreas fault system) forms the northern boundary of the Indio Hills in this area. Both faults converge at the southern margin of the Indio Hills several kilometers to the east near Biskra Palms oasis, where the single fault is again referred to as the San Andreas fault. It can be traced to the southeast as far as the south end of the eastern shoreline of the Salton Sea.

Willis Palms oasis and others in the area have apparently been formed by fault-damming of groundwater. The water-table surface slopes south from the Little San Bernardino Mountains (the range to the north) and pulverized rock along fault traces dams water to the extent that the ground on the north side is moistened; often there are active springs. The moisture-loving native California fan palm *Washingtonia filifera* is a "trademark" of these oases.

Mileage Cumulative	Difference	
		The light-colored material to the west of Willis Palms is marine Imperial Formation uplifted 1000 m or more in a fault slice within the Banning fault zone. The Imperial Formation here is clay to siltsone containing oyster beds. It dates from the late Pliocene, when the Coachella Valley was physically part of the Gulf of California (nearly as far northwest as Banning).
10.1	0.5	Return to Ramon Road; turn left (east).
10.6	0.5	Turn left (north) from Ramon Road onto Thousand Palms Canyon Road.
11.0	0.4	Crossing Banning fault.
11.4	0.4	Note badlands erosion to right (east) and gentle tilt of the rock layers (alluvial fan deposits of late Pleistocene Ocotillo Formation) towards the north (up-canyon). The upper surface which is parallel to underlying layers is a former alluvial fan surface tilted northward by uplift along the Banning fault. Similar southward tilting occurs to the northwest on the south side of the Mission Creek fault. Note desert-varnished lag materials to the north. Wind and running water have removed fines from the old alluvial fan deposits, leaving pebbles to boulders on the surface.
12.0	0.6	Cross-section of alluvial fan deposits in cliff to left illustrates contrast with surface concentration of the coarse fraction. Thousand Palms Canyon here clearly shows the effects of the September 1977 flash flood which caused extensive change to the alluvial fan surfaces and resulted in property damage between the Indio Hills and the Little San Bernardino Mountains. This included filling of the Colorado River aqueduct with boulders and other debris when a hatch cover was carried away. Most of the runoff in the area converged towards Thousand Palms Canyon, deepening and widening its floor considerably and removing numerous palms.
12.4	0.4	Crossing main trace of Mission Creek fault zone. Note palm oases and scarp to the northwest, and mesquite scrub adjacent to the road. In this immediate area, five more traces of the Mission Creek fault have been mapped (Popenoe, 1959), which, in conjunction with the low elevations along the canyon floor, account for considerable surface water and vegetation in the area.
13.4	1.0	Turn around. (You can pull into dirt road to left for this). Older (elevated) alluvial fan deposits here are also of the Ocotillo Formation. The difference in surface elevation and tilt of these deposits compared to those in the canyon area attest to considerable faulting activity in the canyon area in comparatively recent times. Silts capping the Ocotillo Formation here may be from a lake formed by damming of the local drainage by a particularly rapid phase of uplift in the Indio Hills.

Mileage Cumulative	Difference	
16.1	2.7	Return to intersection of Thousand Palms Canyon Road and Ramon Road. Turn left (east) on Ramon Road. Thousand Palms Canyon alluvial fan here received a thick layer of deposits as a result of the previously mentioned storm.
17.7	1.6	Turn left from Ramon Road onto a dirt road leading into "old" Pushawalla Canyon. Be extremely cautious in negotiating this road as there is a possibility of getting stuck and "high-centering" on boulders.
18.0	0.3	Crossing Banning fault.
18.4	0.4	Hidden Palms oasis on a short fault (Hidden Palms fault). Note that numerous palms have sprouted since a fire charred the trunks of the larger palms.
19.1	0.7	Major trace of Mission Creek fault marked by linear oasis on northeast side of southeast-trending canyon. Note that canyon has made a right-angle turn and remains parallel to the fault for approximately 1 km.
19.4	0.3	Turn around and park vehicle at end of passable road (just south of southeast end of linear oasis). In this area, pits and trenches have been dug. These should be dry, whereas amongst the palms the soil is very moist and just behind the southeasternmost palms is a small pond of standing water.

The oasis ends rather abruptly at its southeast end. Continue walking southeast to the edge of present Pushawalla Canyon; the canyon floor has been cut considerably below the floor of the captured canyon that you have been travelling along.

Observe the thin layer of alluvium (mostly granitic and gneissic rock from the Little San Bernardino Mountains) on which you are standing, overlying truncated steeply-dipping layers of lower Ocotillo Formation. These layers may also be seen in the opposite wall of the canyon to the southeast. To the southwest and on the same side of the canyon on which you are standing, nearly horizontal layers of upper Ocotillo Formation overlie lower Ocotillo Formation with angular unconformity.

Just up the canyon on its northwest side, two erosional/depositional terraces may be seen. They are separated in elevation by about 10 m, with the upper terrace alluvium clearly showing a greater amount of weathering than the lower. These terraces continue down the northwest-trending older portion of Pushawalla Canyon.

Mileage		
Cumulative	Difference	
		It should be clear that this older portion of Pushawalla Canyon parallel to the Mission Creek fault was a progressively lengthened dogleg offset as the right-lateral movement on the Mission Creek fault continued. However, at some time in the past few thousand years, its course was captured by another canyon moving northwest with the southwestern block. With capture, the offset portion of Pushawalla Canyon became abandoned and that portion above became rejuvenated, as the new route presented a more direct, steeper path to the desert floor.
21.1	1.7	Return to the intersection of dirt road and Ramon Road; turn left (southeast).
24.4	3.3	Turn left (east) on freeway frontage road from Ramon Road. Turn right (south) after about 100 m onto overpass (Washington Avenue).
24.8	0.4	Turn right (west) from Washington Avenue onto Country Club Drive.
25.8	1.0	Stop on Country Club Drive to look at barchan dunes to right (north). These are some of the best dunes of this type in the Coachella Valley. Concave slip faces are well-defined, there is little binding by vegetation, and the sand is well sorted. You may wish to walk over for a closer look. Turn around and go east back to Washington Avenue.
26.8	1.0	Turn right (south) from Country Club Drive onto Washington Avenue.
29.3	2.5	Cross Highway 111 on Washington Avenue. Continue south on Washington Avenue. Much of this area is at about the surface level (+44 ft. = 13.4m) of Lake Cahuilla, which occupied all of the Imperial Valley and part of the Coachella for ten thousand years or more prior to its evaporation several hundred years ago. Shoreline features become obvious farther to the south and east along the base of the Santa Rosa Mountains.
32.2	2.9	Turn left (east) from Washington Avenue onto Avenue 52. Shoreline features to the right (south) are visible in a mile or so. The very flat valley floor here consists dominantly of silt-sized lake deposits in which can be found numerous small freshwater bivalves and gastropods. In many places where alluvial fans are absent, the lake deposits extend directly to the mountain front with no transition.
33.7	1.5	Turn right (south) from Avenue 52 onto Jefferson Avenue.
34.7	1.0	Turn right (west) from Jefferson onto Avenue 54. Large cottonwood trees mark intersection.

Mileage		
Cumulative	Difference	
35.3	0.6	Stop at or near canal. The canal is the Coachella Valley Canal which runs north on the east side of the valley, crosses the valley to the north, and runs south along the west side of the valley. Its terminus is Lake Cahuilla, two miles to the south – named after the "ancient" lake.

Two shoreline types are evident here: 1) a pre-existing cliffed shoreline with little or no transition between nearly vertical cliffs and the valley floor and 2) a slightly gentler sloping type often developed on talus slopes or cones or on sloping bedrock surfaces. In both cases, desert varnish is apparent above the shoreline and is essentially absent below. In addition, there is often a concentration of light gray-buff calcareous tufa below the shoreline level.

The first type of shoreline apparently developed as a result of sufficiently deep water adjacent to the cliff such that waves would not form, swells merely being reflected off the cliff face. In addition, nothing was available to act as an abrading tool.

On the other hand, with the second type of shoreline, swells "felt bottom" rather suddenly and formed waves which expended energy rapidly against talus or gently sloping bedrock. Abrading tools were available. Thus, along this type of shoreline, we find pronounced wave-cut notches and rounded talus-derived cobbles and boulders.

Desert varnish is observed here above the shoreline, but there is little below it. This fact can provide a rough age estimate for the shoreline, as dark desert varnish coatings probably take many hundreds of years to develop. Desert varnish coatings develop on exposed surfaces of iron-bearing rocks in hot, arid regions. It is thought that, in weathering, hydrolysis of ferrous iron (from biotite, amphiboles, pyroxenes, magnetite, pyrite, etc.) occurs, but with little migration in solution before oxidation and precipitation occur. With little moisture and high evaporation potential, this will occur directly on the rock surface. The heat, in addition to favoring evaporation, probably also accelerates the rate of oxidation.

Thicker coatings of calcareous tufa will be observed later, but an explanation should be advanced now for its occurrence. In saturated solutions of calcium and carbonate (or bicarbonate) ions, release or loss of carbon dioxide will tend to favor precipitation of calcium carbonate as calcite, as will evaporation. Carbon dioxide would be released by agitation of water along the shoreline or might be taken in by algae in photosynthesis. Either or both processes may operate to produce calcareous tufa deposits.

Turn around and return to Jefferson Avenue.

36.0	0.7	Turn right (south) from Avenue 54 onto Jefferson Avenue. Observe shoreline to the right (west) as you proceed south. Several "sea caves" are present.

Mileage		
Cumulative	Difference	
37.6	1.6	Lake Cahuilla (present) is to the right front behind the dike. You may be able to see a sandy beach from the earlier lake at the base of a cliff to the west.
38.0	0.4	Turn left (east) from Jefferson Avenue onto Avenue 58 and immediately make a 45 degree turn to the southeast on a dirt road. This road permits very close observation of shoreline features.
38.7	0.7	Observe thick calcareous tufa deposits to right. Wave-cut notches and pre-existing cliff shorelines may also be observed. You may wish to stop and look at the calcareous tufa. It reaches over one foot in thickness in some places. Its form inspired the name "coral reef" for this area.
39.0	0.3	Observe former stack to right (south).
40.9	1.9	Turn right (west) from dirt road onto Avenue 62 (also dirt). Drive onto dike.
41.1	0.2	Stop at top of dike. Dikes were constructed to protect farmlands. Material for dikes was excavated from alluvial fan and lake deposits on the "uphill" side as can be seen. The excavation trench serves as a settling basin. Exposed on its western side are alluvial fan and lake deposits, especially where the dirt road cuts the side of the trench. Thin, fine grained, light buff calcareous layers containing tiny gastropods alternate with coarser layers reminiscent of alluvial fan deposits. These, however, contain gastropods and bivalves, which implies deposition in the lake, but very close to the shoreline. where occasional floods on the alluvial fan would carry debris across the beach. The beach is visible as a faint grayish north-south trending band about 100 m west of the trench. It is a constructional feature built up by wave action from alluvial fan material on the gently-sloping alluvial fan surface. This is, then, the third type of shoreline observed. It is universal where the shoreline was on an alluvial fan surface. The persistence of the easily-erodable beach deposits cut only by occasional fan channels implies also a fairly recent age for the high-stand level of the lake. To the southwest, Martinez landslide can be recognized by the very coarse debris, hummocky topography, lobate toe, and "natural levees". The slide consists of granitic rock from the eastern side of Martinez Mountain (elevation 1996 m). The head of the slide is at 1900 m, and the toe lies at 60 to 100 m above sea level. The total vertical fall was thus about 1830 m. The horizontal distance travelled was about 7.5 km, of which about 5 km was nearly due east and then, after a nearly right angle turn to the north, another 2.5 km. The right angle bend was made immediately above a deep canyon (Toro Canyon) without any debris entering the canyon. The lower part of the slide has a width of about 1 km and the toe stands about 100 m higher

than the alluvial fan on which it rests. The slide volume is estimated to be 200,000,000 to 300,000,000 cubic meters, making it one of the largest slides in Southern California.

Closed depressions on the slide are filled. An alluvial fan lying on the toe of the slide contains dark, desert-varnished clasts; channels have developed across the slide, and the rocks in the slide are highly cracked, desert varnished, spheroidally weathered, and show granular disintegration. Granular disintegration also appears on the remnant of an old alluvial fan surface upon which the slide rests. Rocks in the slide were undoubtedly fresh when the slide occurred, so some antiquity is implied.

It is probable that the slide occurred during a moister climate phase in the past, probably correlating with the latter part of the last (Wisconsin) glacial. Radiocarbon dates on organic material associated with other slides in Southern California fall into the 16,000 to 20,000 year B. P. range correlating with this moister interval (Stout, 1977). Oversteepening of slopes due to more rapid erosion in this interval and jointing probably were contributors and an earthquake (from faulting on the San Jacinto or San Andreas faults) could have been a triggering mechanism.

Continue over the dike, across trench, up other side (noting lake deposits), and take dirt road bearing left (south). You will cross the beach and travel just west of and parallel to the beach.

42.2 1.1 Stop close to beach. The flat area on the west side of the beach is underlain by fine-grained lagoon deposits, cross-sections of which can be seen in washes cutting across the beach. The beach formed a low dam on the alluvial fan which trapped fine material either carried down the alluvial fan or over the beach during exceptional wave activity. No fresh-water mollusk shells have been found here, but they are found in a large lagoon deposit several miles to the southeast.

Where the beach trend changes from north-south to east-west, a considerable change in sedimentation is apparent. The east-west sand accumulation is immense in the immediate vicinity of the bend, much more sand being present than could have been derived locally, though there is some correlation between it and the large alluvial fan at the mouth of Toro Canyon, the western edge of which lies just to the east of the maximum sand accumulation. In any event, some longshore drifting was probably necessary for the sand accumulation. Convergent longshore drifting towards the bend would have occurred with the direction of wave approach from the northeast, which is the probable direction in this area given the prevailing winds.

Abundant vegetation south of the large beach and a palo verde "forest" to its north attest to a high water table. Numerous pottery shards have been

Mileage		
Cumulative	Difference	
		found on the beach and "bedrock" mortars are present in the wash between the beach and the slide. In addition, the lake plays an important role in legends of the local Indians.
		Drive toward the toe of the slide about 0.1 mile.
42.3	0.1	STOP. Allow about one-half hour for a walk to the slide and return. Estimate the size of the largest clasts in the slide before setting out. Hiking to the top of the toe and even farther allows good views of the valley and permits observations of details of the slide.
43.4	1.1	Return to top of dike. Head due east on Avenue 62.
45.2	1.8	Turn right (south) from Avenue 62 onto Jackson Street.
47.0	1.8	Turn right from Jackson Street onto dirt road on southeast side of citrus grove. Head towards "sea-cliff" and rounded talus slope.
47.1	0.1	Stop at base of slope. At this site there is an excellent wave-cut notch beneath which is an extensive slope of rounded talus boulders of granite porphyry. Calcareous tufa thickly mantles rocks just beneath the wave-cut notch. The notch lies at 13.4 m above sea level. About 20 m below the notch are three rows of pits excavated in the rounded talus. Each row consists of 40 or more pits and the rows are spaced between 1 and 2 m apart vertically. Individual pits are about 1 m deep and 3 to 4 m across.
		These pits are reputed to be fish traps. As they lie below the high-stand level of the lake, they were built when the lake level was actively dropping (no prominent shorelines exist below the high-stand level). At this time, the Colorado River was no longer entering the valley and the lake had fallen below its outlet level at 13.4 m above sea level. The river had shifted its course directly to the gulf. Considering the local evaporation, the lake level, with essentially no source, must have dropped between 1 and 2 m per year. If so, each row of fishtraps could only have been used one season (fall to spring).
		From the fishtraps, travel due east across the valley on Avenue 66.
55.2	8.1	Turn left (north) from Avenue 66 onto Highway 111 and almost immediately turn right (east) into Mecca. Proceed about three blocks south and then turn left (east) on Highway 195.
		The Salton Sea will become visible to the south and west as you ascend the slope east of Mecca. A salt flat existed at the site of the Salton Sea for several hundred years after the evaporation of Lake Cahuilla. However, by 1905, irrigation ditches without floodgates had been constructed from the Colorado

Mileage
Cumulative Difference

River into the Imperial Valley. And at this time, before dams were constructed along its length, the Colorado River was subject to radical fluctuations in discharge. The flood of 1905 was a case in point. At this time, the river changed its course as it had done numerous times before. This time the change was facilitated by the irrigation ditches, which became occupied and considerably enlarged. By 1907, when the flow was finally diverted back to the Gulf of California, an enlarged version of the present Salton Sea existed (salty because of dissolved salt from the salt flats) with a level at -60 m. Subsequently the level dropped with evaporation exceeding inflow to about -76 m in 1925. A steady rise began in 1935 (Sharp, 1975), continuing until 1975, when the level stood at -70 m. The average rate of rise was about 15 cm per year. Waste and leaching water from additional lands being brought under irrigated cultivation have been responsible for this. Theoretically, a balance would be eventually reached between evaporation and inflow preceded by a diminishing of the rate of rise as the lake area increased. However, the rate has accelerated since 1975 and the level as of September 1977 stood at -70 m. This has occurred because of increased irrigation wastes, decreased evaporation rates with cooler summers (down from the normal 2 m per year), and one tropical storm (Kathleen), in particular in September 1976, which was responsible for an instant 15 cm rise (Pers. comm., Coachella Valley County Water District, 1977). The result has been flooding of shoreline property.

In addition, the salinity of the Salton Sea has been increasing, which is to be expected as it occupies a closed depression in an arid region. This retards the reproductive capacity of the oceanic fish introduced to the sea, and is detrimental to the sportfishing-based local economy. Thus, various proposals have been advanced to stabilize both the salinity and level of the sea.

60.3 5.1 Crossing Coachella Valley canal. Construction of the canal and its protective dike destroyed shoreline features of Lake Cahuilla on this (northeast) side of the valley.

60.5 0.2 Turn left (northwest) from Highway 195 onto Painted Canyon Road (dirt). Here you are paralleling the San Andreas fault which is to your right (northeast) at the base of the steep slopes in the Mecca Hills. As you travel, its trace will be revealed by a reddish gouge zone in shales of the Palm Spring Formation. A steep gravity gradient across the San Andreas fault in this area probably indicates a near vertical step of the basement surface of at least 4000 m. Therefore, the San Andreas fault appears to be the major structural boundary between the Salton Trough and higher terrain to the northeast in which basement exposures occur (Sylvester and Smith, 1975). The Palm Spring Formation is of late Pliocene-early Pleistocene age and lies between the Imperial Formation/Mecca Conglomerate beneath and the Ocotillo Formation above, though it is believed that in its lowest part, it might be a lateral

equivalent of the upper part of the Imperial Formation. The lower part of the Palm Spring Formation consists of distal alluvial fan deposits which become finer upward and towards the valley. The upper portion consists of fluvial and alluvial sandstones and lacustrine shales. The proximal mountainward equivalent of the Palm Spring Formation is termed the Canebrake Conglomerate (Popenoe, 1959).

As the road turns northeast toward the mouth of Painted Canyon, the northwest-trending anticlinal structure of the Mecca Hills will be apparent to the north. On the southeast side of the mouth of the canyon, the reddish gouge zone marking the trace of the San Andreas fault is quite visible (Sylvester and Smith, 1975). The reddish gouge has washed down the slope over greenish shale, presenting a "spilled paint" appearance.

Entering the mouth of the canyon, small folds are visible. Then, steep southwesterly dips dominate as the major anticlinal structure is entered. The Palm Spring Formation progressively coarsens to conglomeratic sandstone upcanyon. Clasts are granitic with a probable source being the Little San Bernardino Mountains to the north and the Cottonwood Mountains to the northeast (Sylvester and Smith, 1975).

Thicknesses of individual layers may reach 3 to 4 m. Each of these layers represents a single depositional episode, probably the result of a single, major storm. Storm events even close to this magnitude occurring locally were not realized nor appreciated until just recently (tropical storm Kathleen of 1976 and the Thousand Palms Oasis event of 1977).

64.5 4.0 Small faulted anticline and syncline in Palm Spring Formation to left (northwest) adjacent to faulted contact with reddish Mecca Conglomerate (late Pliocene). At the faulted contact, the Palm Spring Formation is nearly vertical and the Mecca Conglomerate dips about 45 degrees southwest. However, on the southeast side of the canyon, no fault is visible and the contact between the Mecca Conglomerate and the Palm Spring Formation appears gradational. It is inconceivable that this fault could die out in such a short distance; thus, interception of this fault by another paralleling the canyon is proposed.

Imperial Formation is not present here. At least in part, the Mecca Conglomerate is a lateral facies equivalent of its lower portion. At the time of Imperial Formation/Mecca Conglomerate deposition, the shoreline, basinward of which the marine Imperial Formation was deposited, was farther to the southwest, perhaps immediately southwest of the San Andreas fault. The sea, since the origin of the Salton Trough, may never have extended this far northeast.

64.8 0.3 Nonconformity (low-angle buttressed). Mecca Conglomerate on Precambrian gneiss complex at the core of the Mecca Hills anticline.

Mileage		
Cumulative	Difference	

Note gneiss clasts in the Mecca Conglomerate, implying local derivation. Distinctive blue-gray clasts of Orocopia Schist also may be found, though they are quite rare compared to the gneiss. The thickness traversed in the Mecca Conglomerate here has been about 150 m.

The gneiss complex is intruded by small bodies of Mesozoic (?) granite and buff to light orange felsite dikes (K-Ar age about 24 m. y.) (Sylvester and Smith, 1975). The gneiss has been severely deformed at shallow levels and locally pulverized, as can be seen by local "badlands" topography on the left (north) as you proceed through the gneiss complex.

65.3 0.5 Painted Canyon fault zone. This is a somewhat complex fault zone truncating the eastern limb of the Mecca Hills anticline. It has been stated that this fault was probably a former active trace of the San Andreas fault and that it had topographic expression as a southwest-facing fault scarp (Sylvester and Smith, 1975). The topographic expression of this fault is apparent in that there is only a thin layer of Mecca Conglomerate (2 to 5 m) to the northeast of it. In addition, the Palm Spring Formation on the northeast never exceeds 100 m in thickness, while on the southwest side, its thickness is at least fifteen times as great. Also, the fault was active over a long time interval, as a scarp along it existed prior to Mecca Conglomerate deposition and Palm Spring Formation subsequent to deposition was highly deformed in the fault zone. In addition, there has been dip slip reversal, as the structural elevation on the southwest side of the fault is now higher than it is on the northeast side.

From here, the road continues up the broad canyon to the north. However, the steep-walled, narrow canyon to the northeast is of much greater interest. It is possible to drive up this canyon with a four-wheel drive vehicle. Up this canyon, the alluvial sandstones of the Palm Spring Formation soon assume an attitude approximating their original depositional slope. The canyon is very steep-sided and widening apparently occurs by undercutting and toppling of joint-bounded columns onto the canyon floor where they are gradually worn away. This is apparent in several places, particularly at the canyon-blocking rockfall. Incipient rockfalls may also be observed.

Just beyond the canyon-blocking rockfall, the gneiss complex gradually emerges. A thin layer of Mecca Conglomerate above the nonconformity contains only angular clasts of gneiss. A channel-filling of Mecca Conglomerate is also present. The nonconformity was a pediment surface left behind as the mountain front retreated to the northeast. As the surface was formed, it was covered by a thin layer of locally-derived alluvium (Mecca Conglomerate). Subsequently, up to 100 m of alluvial sandstone accumulated (Palm Spring Formation).

Farther up the canyon, more gneiss is exposed as the nonconformity rises high on the canyon walls. The gneiss shows deep-level plastic deformation in

Mileage
Cumulative Difference

its tight, small-scale folds and also shows shallow-level deformation in the form of low angle extensional fractures which truncate the banding and small-scale folds. Vertical west-trending faults are also present. Neither fault type displaces the Palm Spring Formation. An andesite which intruded the gneiss is not affected by the extensional fractures (it probably was guided by them and very likely is related to them), but has been displaced by the vertical faults. Granitic intrusive bodies are older and have been fractured with the gneiss.

Painted Canyon is an antecedent canyon as is Thousand Palms Canyon in the Indio Hills. The drainages of both predate the elevation of hills across their paths. In both bases, elevation of hills has been related to activity along the San Andreas fault.

End of Trip. Return to Palm Desert by way of Highway 111.

References Cited:

Popenoe, F. W., 1959. Geology of the southwestern portion of the Indio Hills, Riverside County, California: University of California, Los Angeles, unpublished M.A. thesis.

Sharp, R. P., 1976. Geology Field Guide to Southern California: Kendall/Hunt Publishing Co., Dubuque, Iowa, 208 p.

Stout, M. L., 1977. Radiocarbon dating of landslides in Southern California: California Geology, vol. 30, no. 5 pp. 99-105.

Sylvester, A. G. and R. R. Smith, 1975. Structure section across the San Andreas fault zone, Mecca Hills: *in* California Div. Mines and Geology Special Report 118, pp. 111-118.